Mapping above- and below-ground carbon stocks in the Sundarbans mangrove forest, Bangladesh

MD SAIDUR RAHMAN

Mapping above- and below-ground carbon stocks in the Sundarbans mangrove forest, Bangladesh

Md. Saidur Rahman

Thesis submitted for the Degree of Doctor of Philosophy

Department of Geography

Durham University

November 2022

Abstract

The study estimated ecosystem carbon stocks in the Bangladesh Sundarbans using field inventory data with species-specific allometric models, carbon fractions and remote sensing data. The plot level ecosystem carbon stocks were interpolated with regression kriging using a forest-type map developed from Sentinel-2 MSI satellite imagery and GEDI-based canopy height data in Google Earth Engine (GEE) platform. Error propagation from the field measurement and allometric models was estimated and interpolated. The study highlighted that both the above-ground carbon (AGC) and soil organic carbon (SOC) were significantly higher in the oligohaline zone, followed by the mesohaline and polyhaline zone. Multiple regression results indicated that soil salinity, organic C: N and tree diameter were the best predictor for the variability of the SOC in the Sundarbans. To understand how individual species affects biomass estimates in mangrove forests, five species-specific and four genus-specific allometric models were developed. At the individual tree level, the generic allometric models overestimated AGB from 22% to 167% compared to the species-specific models. At the plot level, mean AGB significantly differed in all generic models compared to the species-specific models. Using measured species wood density (WD) in the allometric model showed 4.5% to 9.7% less biomass than WD from a published database. When using plot top height and plot average height rather than measured individual tree height, the AGB was overestimated and underestimated by 19.5% and 8.3%, respectively. The total 1 m SOC in the Sundarbans was 21.37 Teragram (Tg) and the total AGC stocks comprised 23.91 Tg. On the other hand, the total ecosystem carbon (TEC) stocks were 62.70 Tg, which is comparatively lower than most mangrove forests in the world. The study demonstrated a methodology that could be used as an IPCC (Intergovernmental Panel on Climate Change) Tier 3 approach for estimating TEC stocks in the Bangladesh Sundarbans and also to monitor TEC stocks in mangroves and other tropical forests. The study also emphasised the importance of spatial conservation planning to safeguard the carbon-rich zones in the Bangladesh Sundarbans from anthropogenic tourism and development activities to support climate change adaptation and mitigation strategies.

Declaration of Authorship

I confirm that the material presented in this thesis has not previously been submitted by me or any other person for a degree in this or any other university. In all cases, where is relevant, material from the work of others has been duly acknowledged.

Md. Saidur Rahman

Commonwealth Scholar, funded by the UK government
Department of Geography
Durham University
April 2022

Publications and conference presentations

Journal articles

1. **Rahman, M.S**., Donoghue, D.N.M., Bracken, L.J., 2021. Is soil organic carbon underestimated in the largest mangrove forest ecosystems? Evidence from the Bangladesh Sundarbans. CATENA. 200, 105159. https://doi.org/10.1016/j.catena.2021.105159.

Authorship contribution: **Md. Saidur Rahman**: Conceptualisation, Data curation, Formal analysis, Investigation, Methodology, Visualisation, Writing – original draft, Writing – review & editing. **Daniel N.M. Donoghue, Louise J. Bracken**: Conceptualisation, Supervision, Funding Acquisition, Writing – review & editing.

2. **Rahman, M.S**., Donoghue, D.N.M., Bracken, L.J., Mahmood, H., 2021. Biomass estimation in mangrove forests: a comparison of allometric models incorporating species and structural information. Environmental Research Letters. 16(11), http://iopscience.iop.org/article/10.1088/1748-9326/ac31ee.

Authorship contribution: **Md. Saidur Rahman**: Conceptualisation, Data curation, Formal analysis, Investigation, Methodology, Visualisation, Writing – original draft, Writing – review & editing. **Daniel N.M. Donoghue, Louise J. Bracken**: Conceptualisation, Supervision, Funding Acquisition, Writing – review & editing. **Hossain Mahmood**: Data curation, Writing – review & editing.

Conference presentations

1. Presented poster on "Uncertainties in estimation of Spatial carbon dynamics in the Sundarbans mangrove forest" in the 5th **International Mangrove Macrobenthos & Management meeting** (MMM5), Singapore (1-5 July' 2019).

2. Presented oral presentation on “Biomass estimation in mangrove forest: a comparison of allometric models incorporating species and structural information” in the 20th **Commonwealth Forestry Conferences** organised by the University of British Columbia, Canada on 16-18 August’ 2021.

3. Presented poster on “Biomass estimation in mangrove forest: a comparison of allometric models incorporating species and structural information” in the **XV World Forestry Congress,** South Korea (2 – 6 May’ 2022).

4. Presented oral presentation on “Mapping ecosystem carbon stocks in the Sundarbans mangrove forest, Bangladesh” in the UK National Earth Observation Conference’ 2022 at National Space Centre, Leicester, UK on 05 – 08 September’ 2022.

Dedication

This thesis is proudly dedicated to…

All my beloved family

(my mother, my father, my wife, my sons, my brothers and all my friends)

Thanks for your endless love, sacrifices, prayers, supports and advice.

Acknowledgements

First of all, I am extremely grateful to my supervisors — Daniel N. M. Donoghue and Louise J. Bracken — for their continuous guidance and support over the last four years. You, both have been a great help from the start of my PhD journey from refining research ideas into the final product and help overcoming many challenges on the journey. I feel privileged to have Danny as my supervisor for your continuous encouragement to aim high and become passionate in mangrove research. I am grateful to Louise for your kind words and support over the last four years that didn't keep me down. Without both of your moral support, it was quite difficult to come into the end of the PhD journey. This PhD thesis is also enriched with valuable comments from two reviewers — Dr. Pete Bunting, Reader, Department of geography and earth sciences, Aberystwyth University and Professor Dr. Nick Rosser, Department of Geography, Durham University.

The phD research is funded by the Commonwealth Scholarship Commission (CSC) in the UK (Scholar no: BDCS-2017-55). I am grateful to the CSC for providing allowances to me and my family to stay with me in the UK. At the same time, I thank the University Grant Commission (UGC), Bangladesh and Ministry of Education, Bangladesh for nominating me as a preliminary candidate for the competition of commonwealth scholarship. I want to extend my gratitude to the Forestry and Wood Technology Discipline, Khulna University for permitting study leave to pursue PhD at Durham University. I am grateful to the Bangladesh Forest Department for giving permission for fieldwork in the Sundarbans. I am also grateful to Institute of Hazard, Risk and Resilience for research grants and Department of Geography, Durham University for small research grants, conference grants and to Ustinov College, Durham University for travel and research grants.

I would like to thank to the co-author of my second paper, Professor Dr. Mahmood Hossain for his contribution and encouragement to finish my PhD research. I am grateful to all field assistants worked with me during field work in the Sundarbans – Opu, Shamim, Shahadat, Shimul, Rashed, Naif, Mamun, Mitu, Zihad, Anamul and Rafiq. Without their help, it would be impossible for me to

complete this fieldwork. Thanks to all forest officials and boatmen who helped me exploring the Sundarbans. I am grateful to all my colleagues of Forestry and Wood Technology who inspired me always to pursue PhD in a world class university.

I am indebted to all colleagues from the Department of Geography, Durham University. In particular, I am grateful to Ms. Kathy Wood for her continuous administrative and financial support. My thanks also go to all laboratory staffs who provided all supports needed to complete my tasks. It has been a privilege to me to be as a colleague of numerous talented, diverse, and welcoming group of people. I can not forget the importance of coffee break at Manley room, which kept me alive and cheerful while working under pressure. Thanks to all my fellow researchers with whom my knowledge has been refined with diverse field of geography. Particularly I am grateful to a range of people at Durham- Gopi, Muyeol, Felipe, Ayushman, Chandika, Ramjee, Mildred, Iqbal, Ruusa, Naznin, Raihana, Ramesh, Samprada, Swastik, Sobhit, Ludo, Connie, Ritwika and many more, who kept me alive at Durham. Special thanks to all colleagues with whom I shared my office space in Skylab. I am grateful to all members of the Durham University staff cricket team who provided many joyous moments during summertime at Durham. I am also grateful to the Bangladeshi community – Topu, Bahar, Prity, Feisal, Asik, Nasir, Galib, Sodip who made small Bangladesh to me in the UK.

My special thanks go to my beloved wife, Shanu for your continuous support and keep me strong throughout the PhD journey. Special thanks for taking care of our three cutest son Rishan, Rihan and Rahin and provided me space to engage with PhD Studies. My sons are my inspirations for hard work and dedication for research. My final thanks to my families, father, mother, father-in-law, mother-in-laws, two brothers, sister-in-laws, my friends and all well-wishers. In particular, I am grateful to my late father-in-law whom I lost during my PhD journey.

Table of Contents

List of Figures

List of Tables

Abbreviation

AGC	Above-ground Carbon
AGB	Above-ground Biomass
BGB	Below-ground Biomass
BGC	Below-ground Carbon
DBH	Diameter at Breast Height at cm
H	Height in m
BFD	Bangladesh Forest Department
WD	Wood Density in gm cm^{-3}
TEC	Total Ecosystem Carbon
EBKRP	Enhanced Bayesian Regression Prediction
SOC	Soil Organic Carbon
GEE	Google Earth Engine
Mg ha^{-1}	Megagram per hectare
Tg	Teragram
NDC	Nationally Determined Contributions
SDG	UN Sustainable Development Goals
IPCC	Intergovernmental Panel on Climate Change
NDVI	Normalised Difference Vegetation Index
LAI	Leaf Area Index

Chapter 1

Introduction

1.1. Background

Mangrove vegetation can be found in 105 countries primarily in the tropics and subtropics (Hamilton and Friess, 2018; Tang et al., 2018) (Figure 1.1). Despite accounting for just 0.1% of the Earth's continental surface, mangrove forests are among the most carbon-rich forest biomes due to their high proportion of below-ground to above-ground biomass and their high capacity for carbon sequestration (Donato et al., 2011; Atwood et al., 2017). The ability to accumulate substantial amounts of carbon in the soil due to slow decomposition rate makes mangroves distinctive in comparison to other terrestrial ecosystems.

Mangrove forests across the tropics are threatened by factors related to climate change and anthropogenic impacts (Duke et al., 2007; UNEP, 2014). Data assimilated from a variety of published sources suggests that about 50% of the mangrove biome has been lost since the 1950s (Feller et al., 2010). The quality and quantity of this highly productive ecosystem is vulnerable to threats such as: large-scale commercial aquaculture and agriculture (Primavera, 2006; Richards and Friess, 2016); land reclamation (Peng et al., 2016); pollution and local and regional (few to hundreds of km^2) climate change induced stressors, such as sea-level rise (Lovelock et al., 2015a); drought (Duke et al., 2017; Lovelock et al., 2017); increased storminess and salinity (Alongi, 2015; Sarker et al., 2016); changed precipitation regimes, and increasing temperature and atmospheric CO_2 (Ward et al., 2016). Recent estimates report global mangrove decline is 2% from 2000 to 2012, which represent a contribution of 320 million tonnes of CO_2 to the atmosphere (Hamilton and Friess, 2018).

Despite the observed loss of mangrove forest area, the potential future impact of climate change suggests that mangrove ecosystems are resilient and have the potential to expand poleward (Alongi, 2015; Feller et al., 2017) and to continue to deliver resources for local livelihoods, carbon sequestration, biodiversity conservation and to provide other ecosystem services (Thomas et al., 2017). However, degradation and disturbance of the vegetation promotes the remineralization of soil carbon to CO_2. Thus, conservation and restoration of mangrove forest is vital to preserve carbon storage in soil. Nonetheless, restoration alone would not be enough to regain lost carbon in mangrove

soils over human lifespans since the carbon deposition takes thousands of years (Atwood et al., 2017). Therefore, reducing deforestation rates and maintaining existing areas would be the optimal conservation strategy.

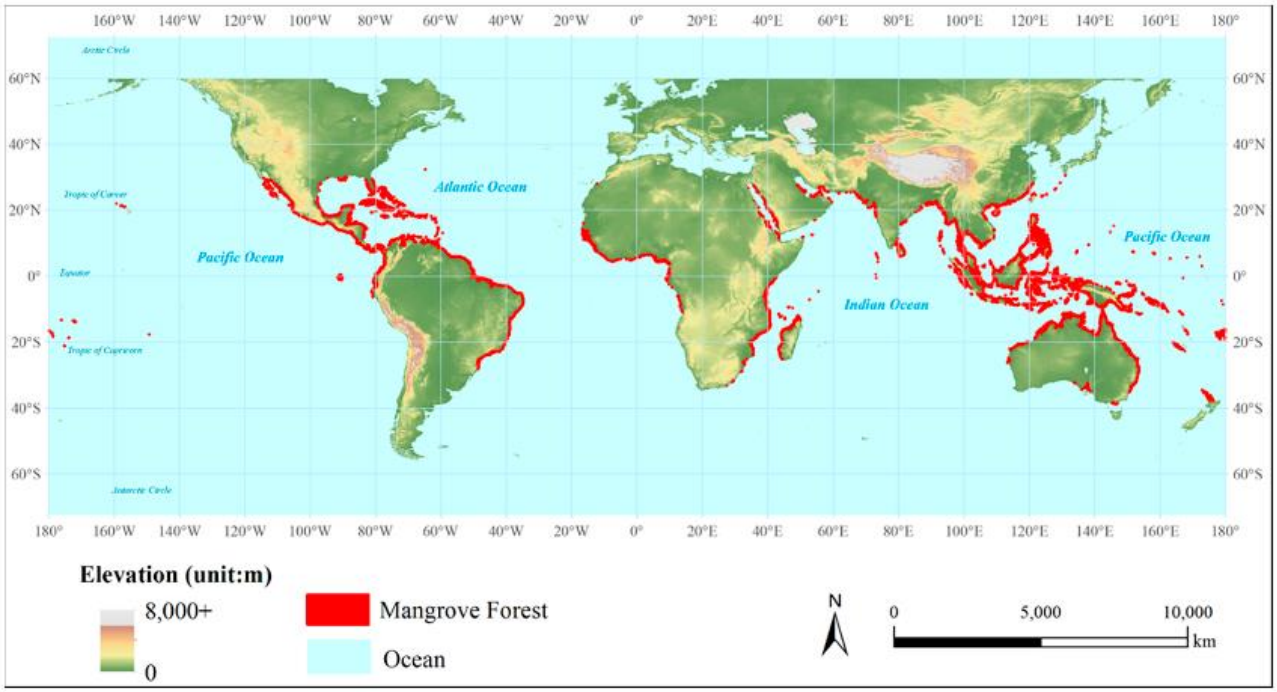

Figure 1.1: Global distribution of mangroves. Reproduced from Tang et al. (2018) CC BY 4.0.

Mangrove research has recently been gained substantial traction and momentum in international initiatives and policies including the International Blue Carbon Initiative, the Global Mangrove Alliance and the establishment of countries Nationally Determined Contribution (NDCs) for the Paris Agreement of the United Nations Framework Convention on Climate Change (UNFCCC) (Taillardat et al., 2018; Friess et al., 2020a). Because of a wider range of ecosystem goods and services provided to society, mangroves are an integral part of the UN Sustainable Development Goals (SDGs) (Ramsar Convention on Wetlands, 2018; Friess et al., 2020b; Worthington et al., 2020). Higher carbon sequestration rates in mangroves compared to other tropical forests has established mangroves a crucial factor in international incentive schemes such as United Nations Reducing Emissions from Deforestation and forest Degradation in Developing Countries (UN REDD^{+}) (Donato et al., 2011; Alongi, 2012; Kauffman et al., 2020). These initiatives have led countries to conserve existing mangroves and at the same time ensure a future reduction of greenhouse gas emissions whilst

fostering CO_2 sequestration (Adame et al., 2021). However, halting degradation and deforestation in mangroves and the accurate estimation of these changes in this important ecosystem is key to such financing mechanisms (IPCC, 2006; Alongi, 2011; Howard et al., 2014; IPCC, 2019).

The ability to sink CO_2, coupled with their capacity for coastal protection and encouraging sediment accretion, makes mangrove habitats an essential element for climate change adaptation and mitigation strategies including carbon trading initiatives, such as REDD+ (Reducing Emissions from Deforestation and Degradation) (Duarte et al., 2013; Lucas et al., 2014). Recent international climate policy discussions also prioritize mangrove conservation through 'avoided deforestation' under PES (Payments for Ecosystem Services) and such debates have highlighted novel funding paths for forest protection (Hamilton and Friess, 2018). However, there are considerable challenges for the implementation of conservation strategies, which include developing systems to quantify and monitor the carbon stocks through 'MRV' (Measuring, Reporting and Verifying) activities (Locatelli et al., 2014). Moreover, IPCC (the Intergovernmental Panel on Climate Change) sets targets with progressively more complex methods to provide greater levels of accuracy for carbon reporting from Tier 1 to Tier 3. The Tier 1 derives data from published global datasets, while Tier 3 uses data from detailed and repeatable locally-derived forest inventories (Penman et al., 2003). On the other hand, the Tier 2 is considered as intermediate which requires country-specific data to suit local conditions (IPCC, 2019). A Tier 3 approach requires more rigorous methods, including inventory data and models adapted to national conditions, which are repeatable, and driven by high-resolution activity data (Harris, 2016).

1.2. Rationale

1.2.1. Difficulty to relate forest loss to carbon and CO_2 emissions

The first step in the assessment of carbon stocks in any forest is to map the extent and loss/gain over time. One of the major challenges is to translate these changes in forest area to carbon stocks for the whole ecosystem. In mangrove forests, the carbon pool comprises above- and below-ground carbon (AGC and BGC); above-ground contains live and dead plants including stem, stump, branches, bark,

seeds and foliage, and the below-ground carbon consists of roots and soil carbon. Among these, the soil may account for more than 50% of the total carbon stocks in a forest followed by tree carbon including above-ground biomass (AGB) and live roots (Kauffman and Donato, 2012). The most accurate method to quantify forest carbon is to destructively sample trees with or without roots, dry and weigh the biomass (Brown et al., 1989). The whole-tree biomass is then converted to a mass of carbon by multiplying by a range between 0.45 to 0.50, assuming that the carbon content in plant biomass is constant (Twilley et al., 1992; Donato et al., 2011; Kauffman et al., 2011; Kauffman and Donato, 2012). Therefore, measuring or estimating biomass is the key step for quantifying carbon storage in any ecosystem. However, the destructive sampling method is very labour intensive and time consuming and cannot be applied across a landscape or a large spatial extent. Therefore, scientists have used variety of indirect techniques to scale up from field to global levels, including biome-average methods, the biomass expansion factor (BEF), root-shoot ratio, allometric methods, and remote sensing techniques (IPCC, 2006; IPCC, 2019).

Biome averaging is the simplest method which adheres to the IPCC's Tier 1, in which the average biomass value is obtained to approximate the carbon stocks of a region or nation. The average biome values are compiled from inventories of the Food and Agricultural Organization (FAO) (Houghton et al., 2001; Gibbs et al., 2007). Although this method is quick and easy, the estimation typically underestimates the contribution of young stands as biome averages are based on mature stands. Since the forest carbon stocks vary significantly with different geo-physical parameters, an average value cannot represent as entire forest or country. Moreover, this method yields low accuracy because the data are obtained only from few plots that may not represent the wider biome or region (FAO, 2010). Many national and regional above-ground biomass calculations are based on the 'Biomass Expansion Factor' (BEF). It is the average ratio between dry weight and stem weight measured from some representative harvested trees (Brown, 1997). Default root: shoot ratios are also used to estimate carbon stocks for national greenhouse gas (GHG) inventories. In the case of mangroves, the global mean root: shoot ratio is 0.39 (Hamilton and Friess, 2018). However, like biome averages, these BEF

and root: shoot values can vary with vegetation type, climatic and biophysical factors of an ecosystem (Magalhães and Seifert, 2015).

The above-ground biomass stocks can be directly inferred from tree biometric measurements by using an empirical allometric model (Brown, 1997). This model represents the relationship of tree biomass with the diameter at breast height (DBH), and occasionally with tree height, and/or the wood density of trees, derived from destructive sampling of trees. In the past, many allometric equations have been developed for mangroves (Saenger and Snedaker, 1993; Clough et al., 1997; Saenger, 2002; Ong et al., 2004; Comley and McGuinness, 2005; Soares and Schaeffer-Novelli, 2005; Hossain et al., 2012; Kangkuso et al., 2016). However, one of the major limitations is the quality of the data underpinning allometric models, which is often limited by time, cost and logistics (Chave et al., 2014). Therefore, uncertainties arise from destructive sampling due to the difficulty to extract root and branch biomass and also using allometric models.

Both Komiyama et al. (2005) and Chave et al. (2005) developed general allometric models for mangrove species, however, there remains a lack of empirical data to calibrate the models especially from mangroves in the Indian Ocean region. Therefore, the use of these equations in the ecologically diverse Sundarbans mangroves is still contentious. The Chave et al. (2005) allometric model has been widely used in all pan-tropical forests although it was originally developed for moist and wet forest types. Due to the level of uncertainty in the previous allometric equation, Chave et al. (2014) developed a new allometric model that includes tree height as a variable. Since mangroves significantly vary in growth and form across latitudinal gradients, off-site allometric equations could over-/underestimate the carbon storage of any particular ecosystem. Therefore, improved calibrated allometric models are needed from plot inventories or plot-inventory-calibrated remote sensing. This thesis aims to develop species-specific allometric models in the Sundarbans mangrove forest.

1.2.2. Spatial distribution of carbon storage in mangrove forest and identification of key drivers

The systematic study of mangrove ecosystems has increased in the last decade because of the mounting recognition of the importance of mangroves to climate change mitigation strategies and the

need for accurate carbon accounting at a national level. With the progressive development of the remote sensing, scientists are using this technology extensively, and contributing significantly to a number of high quality wall-to-wall biomass or carbon maps with high spatial resolution and accuracy (Ni-Meister, 2015). However, the calibration is still dependent on the ground-based estimation of carbon to allow for scaling up from plot measurements to national and global level carbon stocks through allometric equations (Saenger and Snedaker, 1993; Fatoyinbo and Simard, 2013).

Despite the extensive use of regional and global carbon mapping, the allometric equation itself has limitations due to the shortage of destructively sampled trees from which it is developed, and often, the reference collection points are unrepresentative of the wider study area (Hickey et al., 2018). Moreover, rather than being site- and species-specific, these equations include many uncertainties when applied at larger scales (Mitchard et al., 2013). Therefore, using the same allometric equations for all species or grouping wood density in the allometric equation would further average out species-level variations in carbon estimates, and so major uncertainties originate from poor data on the local distribution of carbon, which impacts to total nationally or globally summed carbon density (Mitchard et al., 2013; Ni-Meister, 2015). Recently published global and continental AGB estimates can be widely biased, due to an under representative sample size containing forest structural variables and the exclusion of the climatic regime or geophysical and geomorphological variables which are the key to understanding the spatial distribution of carbon at regional scales (Rovai et al., 2016). Therefore, it is important to identify key drivers for the variation of carbon across the landscape. In the case of below-ground biomass, major uncertainties arise. For example, Adame et al. (2017) found a 40% overestimate in biomass compared with destructive field measurement. This has serious implications on the accuracy of carbon estimation to fulfil country-specific reference levels in the UN REDD+ assessments. Therefore, country-specific or species-specific allometric models are needed to satisfy the global financing mechanisms for mangrove forests. Identifying key drivers for the spatial variation carbon stocks in mangrove forests should also be included in biomass or carbon assessment of mangrove forests.

1.2.3. Lack of accurate long-term gain-loss data

Whilst mangrove forests are carbon-rich, their contribution to the global carbon balance is still poorly understood due to a lack of historical long-term gain and loss data. One of the main requirements for historical data is to set up a benchmark for deforestation and degradation against which carbon emission reduction can be quantified. Due to constraints in data quality and availability, many countries rely on remote sensing in combination with field assessments to set up an appropriate reference level (Herold et al., 2011). Many attempts have been taken to map carbon stocks and fluxes at a global scale (for example, Baccini et al., 2012; Avitabile et al., 2016; Baccini et al., 2017). However, mangrove forests have largely been excluded from these global assessments because of their small spatial extent and the difficulties of mapping these forest types (Hutchison et al., 2014) (Table 1.1). Some global datasets included mangrove forest as a part of global tropical forests (9-14 in Table 1.1). However, there are some recent studies which specifically focused on mangrove forest in the world such as Bunting et al. (2018) and Bunting et al. (2022a; 2022b). A range of remote sensing sensors and algorithms were used to map global mangrove forests. Landsat (30 m) was mostly used for their global coverage and availability for longer time. This Landsat satellite was widely used to make reference level in most tropical forests including mangrove forests. However, the recent high-resolution satellites (Sentinel (10 m)) provide high potential to improve global mangrove forest covers in the world.

Table 1.1: List of earth observation-based global/ mangrove forest cover maps.

Mangrove/ Global dataset	ID	Products	Year	Sensor/others	Algorithm	Validation	Type of estimate	References
Mangrove forest	1	WCMC-012	1960-96	A wide range of sources	A global composite	-	Synthesis	Spalding et al. (1997)
	2	WCMC-011	1999-01	30 m Landsat	Unsupervised	-	Independent	Spalding et al. (2010)
	3	WCMC-010-Version 1.3	1997-2000	30 m Landsat (Global Land Survey)	Hybrid supervised and unsupervised	Secondary data sources	Independent	Giri et al. (2011)
	4	CGMFC-21	2000-2014	30 m UMD and Other Maps-based maps	UMD, WCMC-010, & Terrestrial Map (Olson *et al.*, 2001)	2011- the USGS National Land Cover Dataset	Synthesis	Hamilton and Casey (2016)
	5	Global carbon stocks	2000-2012	CGMFC-21 WCMC-10	Regression	Selected field data	Synthesis	Hamilton and Friess (2018)
	6	Global Mangrove Watch (GMW)	2010	ALOS PALSAR, Landsat and SRTM (30 m)	Classification (Extremely Randomized Trees	20 M points from 128 projects	Independent	Bunting et al. (2018)

				DEM	classifier)			
	7	GMW: Mangrove Forest Extent (v2.5)	2010	GMW (version 2.0), Sentinel-2	Classification (XGBoost binary classifier)	1000 random points in each of 60 sites	Synthesis	Bunting et al. (2022a)
	8	GMW: Mangrove Forest Extent change (v3)	1996-2020	L-band SAR from JAXA	map-to-image change detection	1000 random points in each of 60 sites	Synthesis	Bunting et al. (2022b)
Global forest	9	TREES-2	1998-2000	1 km SPOT4 VEGETATION	Unsupervised	Landsat TM	Independent	Stibig et al. (2003)
	10	GLC 2000	2000	1 km SPOT4 VEGETATION	Unsupervised	TREES-1	Independent	Bartholomé and Belward (2005)
	11	University of Maryland (UMD)	2000-2014	30 m Landsat	Decision tree	Google Earth	Independent	Hansen et al. (2013)
	12	Global Tree Canopy Cover	2000-2012	30 m Landsat	Regression tree Hansen et al. (2013)	-	Synthesis	Hansen et al. (2013)
	13	Global Forest/Non-Forest Map	2007-2010	25 m PALSAR/ PALSAR-2	Region specific rule-based backscatter threshold	Degree Confluence Project	Independent	Shimada et al. (2014)
	14	Global Forest/Non-Forest Map	2011-2016	TanDEM-X	Multi-clustering classification	Hansen et al (2013) and others	Independent	Martone et al. (2018)
	Note: WCMC-012: United Nations Environmental Programme (UNEP) World Conservation Monitoring Centre (WCMC),							

Moreover, surveying in remote mangroves is often hindered by high tides, mud, pneumatophores and wildlife, especially in the Sundarbans (Otero et al., 2018). Therefore, remote sensing techniques, such as optical, radar, and spaceborne or airborne LiDAR (Light detection and imaging) provide important opportunities to quantify above-ground carbon (AGC) coupled with ground data at various scales from individual trees to global coverage (Lucas et al., 2015). These techniques can help overcome the need for extensive fieldwork and provide data for global scale estimation of biomass and carbon in mangrove forests.

1.3. Aims and Objectives

This research project recognises the strengths and weaknesses of previous studies that have attempted to quantify carbon storage in mangrove forests. The work seeks to develop local species-specific models to estimate biomass and carbon in a very large mangrove forest by combining remote sensing data with field data and will address the following research and methodological questions:

1. Can the existing allometric models for biomass estimation be tailored to the dominant species of complex mangrove forests?
2. How do above- and below-ground carbon stocks vary spatially in a mangrove forest?
3. How accurately can carbon stocks be estimated by combining satellite imagery with field inventories data?
4. Which environmental drivers determine the spatial variation of above- and below-ground carbon stocks in a mangrove forest?

The specific aim of the research is to assess how much carbon is stored in both above- and below-ground in the Sundarbans mangrove forest. The specific objectives of the research project are as follows:

1. To review literature related to quantification of carbon storage in mangroves using remote sensing. This review aims to establish commonalities and differences among the methods and approaches used and to identify the factors affecting the quantification of carbon stocks (Chapter 2).
2. To measure soil organic carbon (SOC) in the Bangladesh Sundarbans mangrove forest and to better understand the relationship of SOC within three salinity zones (oligohaline, mesohaline and polyhaline) and between major forest types. The study also investigated the relationship between physical and chemical properties and vegetation characteristics with SOC to develop dependable predictive models of organic carbon (Chapter 4).
3. To develop species-specific allometric models and compare estimated biomass with global models in order to understand modelled uncertainties in biomass estimation. The study also investigated the variability of AGB in the Sundarbans by comparing measured and published wood density values at multiple spatial scales and with different sets of tree height measurement (Chapter 5).
4. To estimate above- and below-ground carbon stocks and uncertainties at plot scale and upscale these to carbon stocks and their uncertainties to the Sundarbans ecosystem level to produce ecosystem carbon map and error map based upon on a forest-type map. The study also aims to

compare the variability of ecosystem carbon stocks with vegetation types and salinity zonation (Chapter 6).

1.4. Thesis structure

The structure of this thesis contains seven chapters outlined below.

Chapter 2 provides an overview of carbon stocks in mangrove forests, their measurement methodologies using remote sensing and the uncertainties involved. Given the use of a variety of remote sensing sensors, resolutions, extrapolation algorithms, and validation methods in estimating carbon stocks of mangroves, this review aims to establish commonalities and differences and to identify the key factors affecting the quantification of carbon.

Chapter 3 describes an overview of the Bangladesh Sundarbans mangrove forest. It also includes the detailed research methodologies for estimating above- and below-ground carbon estimation in the forest.

Chapter 4 presents the quantification of SOC in the Sundarbans from sediment cores using laboratory analysis. The chapter introduces key debates of spatial variability of SOC in different mangroves worldwide and identified the causes of low SOC estimates in the Bangladesh Sundarbans. The chapter is published in the journal CATENA:

Rahman, M.S., Donoghue, D.N.M., Bracken, L.J., 2021. Is soil organic carbon underestimated in the largest mangrove forest ecosystems? Evidence from the Bangladesh Sundarbans. CATENA. 200, 105159. https://doi.org/10.1016/j.catena.2021.105159.

In this paper, all authors conceptualised the study together along with planning and research design. M. S. Rahman collected sediment cores from the Sundarbans and did the laboratory analysis. He prepared all graphs and wrote the manuscript. Donoghue, D. N. M. and Bracken, L. J. supervised the study and provided comments on the draft and paper submission.

Chapter 5 describes the development of species-specific allometric models to estimate AGB in the Sundarbans and investigates biomass variability using different sets of allometric models and

parameters from different sources (wood density and tree height). The study also estimates uncertainty in allometric models while estimating biomass in the Sundarbans. This chapter is published in Environmental Research Letters:

Rahman, M.S., Donoghue, D.N.M., Bracken, L.J., Mahmood, H., 2021. Biomass estimation in mangrove forests: a comparison of allometric models incorporating species and structural information. Environmental Research Letters. 16(11), http://iopscience.iop.org/article/10.1088/1748-9326/ac31ee

The contribution of authors in this article was as follows: Md. Saidur Rahman: Conceptualisation, Data curation, Formal analysis, Investigation, Methodology, Visualisation, Writing – original draft, Writing – review & editing. Daniel N.M. Donoghue, Louise J. Bracken: Conceptualisation, Supervision, Funding Acquisition, Writing – review & editing. Hossain Mahmood: Data curation, Writing – review & editing.

Chapter 6 describes the estimation of the above- and below-ground carbon stocks in the Sundarbans. It also provides the description of the development of the forest-type map from the satellite imagery and the prediction of carbon stocks at ecosystem level. Finally, the chapter describes methodologies to estimate uncertainties in carbon stocks in the Sundarbans. This chapter has been prepared to submit to the journal Global Change Biology:

Rahman, M. S., Donoghue, D. N. M. and Bracken, L. J. contributed to this chapter equally for conceptualisation and research design. M. S. Rahman conducted the forest inventory in the Sundarbans and prepared the chapter including data analysis, preparation of all graphs and writing. Both Donoghue, D. N. M. and Bracken, L. J. supervised the study and review-edited the chapter.

Chapter 7 summarises the overall results to meet the research aims and discusses the implications for the management and conservation of the Sundarbans mangrove forest. This chapter includes the main conclusions, recommendations, and proposed future work based on findings of the research.

Chapter 2

Dynamics of carbon stocks in mangrove forests and estimation methods

2.1. Introduction

Mangrove forests contain higher levels of carbon in the below-ground sediment than any other ecosystem. The above-ground carbon also contributes high levels of carbon in any mangrove forests. The diversity of components in mangrove forests require different quantification methods. Researchers have developed protocols to quantify both above- and below-ground carbon stocks from mangrove forests. A range of methodologies have also been developed to upscale field estimations to the ecosystem level using remote sensing and GIS technologies. However, each methodology has its own limitations and uncertainties in estimating carbon stocks. This chapter describes the methods used to estimate carbon stocks in mangrove forests and to upscale carbon stocks to the ecosystem level through remote sensing.

2.2. Carbon stocks in mangrove forests

Carbon stocks in a forest is the total carbon from vegetation, animals, sediments and water that absorb carbon (Howard et al., 2014). Like terrestrial forest ecosystems, carbon stocks in mangrove forests can be divided in to soil and biomass. However, while upland forests hold greater carbon in the above-ground, mangrove forests largely store most carbon into organic soil and below-ground roots, which altogether makes up to 85% carbon in the below-ground (Brown, 1997; Donato et al., 2011; Kauffman et al., 2020). Using data from five continents, Kauffman et al. (2020) found the mean total ecosystem carbon stocks is 856 ± 32 Mg ha^{-1}, while the below-ground soil and root comprises 741 ± 30 Mg ha^{-1}. This high carbon storage in the below-ground is mainly due to accumulation of sediment and organic matter over millions of years from both autochthonous (carbon from mangroves) and allochthonous (carbon from outside mangroves). Due to their spreading cable root networks in the below-ground, mangroves are often called as ‘bottom heavy plants’ (Komiyama et al., 2008). Therefore, they invest more carbon in the below-ground roots which generates a higher root-shoot ratio compared to terrestrial forests (Adame et al., 2017). The slow decomposition of organic matter as a result of water-logged and anaerobic conditions allows mangrove sediments to continuously accumulate carbon through time (Kauffman and Donato, 2012; Howard et al., 2014).

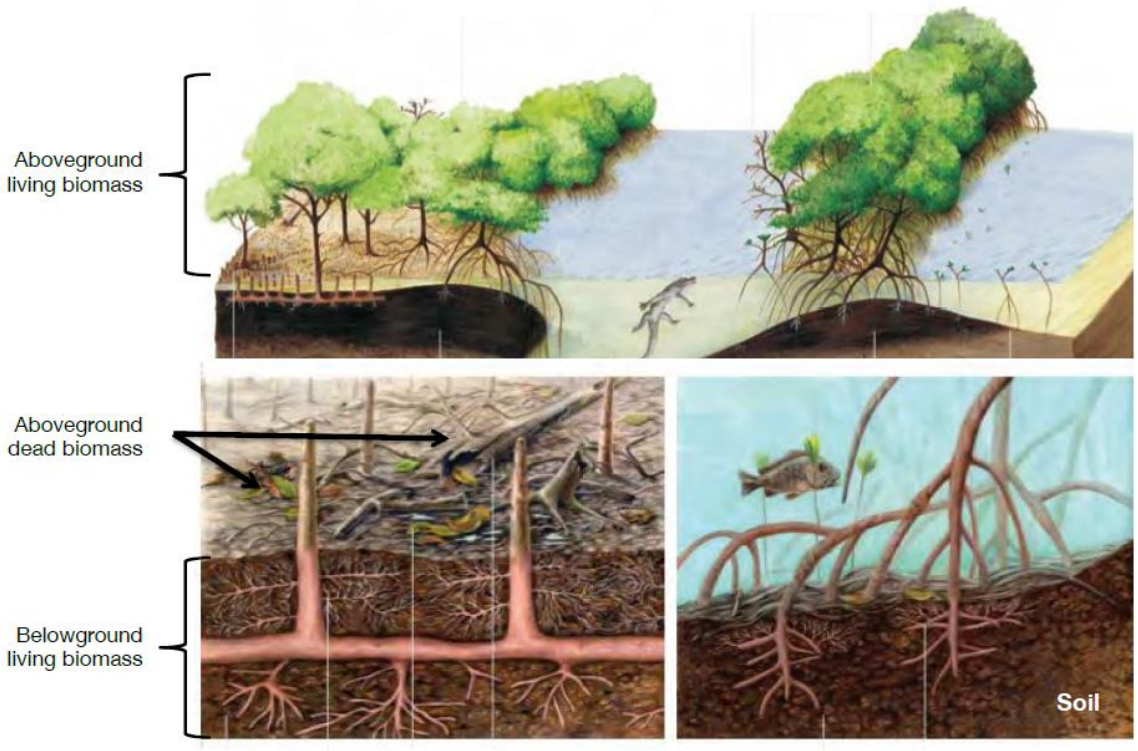

Figure 2.1 Different components of carbon stocks in mangrove forest. Reproduced with permission from Howard et al. (2014, p. 30).

The carbon stocks in mangroves can be divided into above-ground carbon (AGC) and below-ground carbon (BGC). The AGC stocks comprise carbon stored in live or dead standing trees, shrubs, herbs, dead and downed wood and pneumatophores (roots extended to above-ground) (Figure 2.1). On the other hand, BGC is composed of carbon in soils and roots (Howard et al., 2014). Negligible components in mangroves such as leaf litter and understorey vegetation such as seedlings, herbs, shrubs are usually not included in the carbon stocks assessments (Kauffman and Donato, 2012; Howard et al., 2014). The major portion of AGC comprises all living trees which are easy to quantify through measuring diameter at breast height (1.3 m) and the height of trees. These AGC components are heavily affected by landuse changes and constitutes a major portion of total carbon stocks (Howard et al., 2014). The lying dead wood can comprise 2.5–5.0% of the carbon stocks, but regular tides can export this mass to the rivers, however this may be important after cyclones as this disturbance can yield a large amount of dead wood in the forest floor (Simard et al., 2019). Mangroves form a range of specialised root systems namely pneumatophores, prop roots, knee roots

in the above-ground and comprise a significant amount of carbon to the AGC (Kauffman and Donato, 2012).

Sediment carbon constitutes the majority portion of the below-ground carbon (BGC) stocks. The dead litter and decomposed organic matter are the main components of soil carbon stocks (Howard et al., 2014). Living and dead roots are also an important pool of BGC, which is very difficult to measure as mangroves produce cable networks extending across large areas (Kauffman et al., 2020).

2.3. Carbon estimation in mangrove forests

The assessment of carbon stocks has gained interest since 2011 after the paper published by Donato et al. (2011) stating that mangroves are the most carbon-rich forests in the tropics. Standard protocols have been developed for assessing above- and below-ground carbon stocks in mangroves including sampling design, sample collection procedures, data interpretation and reporting (Kauffman and Donato, 2012; Howard et al., 2014). The IPCC developed three tiers of good practice and guidelines on assessing anthropogenic greenhouse gas (GHG) emissions and carbon removal from different ecosystems including mangroves (IPCC, 2006). The Tier 3 approach captures variability of carbon with greater accuracy and confidence incorporating site factors such as ecological zones, vegetation types and environmental gradients and thus is recommended to all countries if resources are available (IPCC, 2006; Kauffman and Donato, 2012; Howard et al., 2014). The Verified Carbon Standard (VCS), a voluntary certification programme for GHG emission reduction projects, developed carbon estimation methodologies specifically for the REDD^{+} initiative which also requires Tier 3 assessments (VCS, 2020).

While carbon in sediments is directly measured from the sediment samples, tree carbon is estimated from allometric models of biomass from tree structural parameters such as diameter, height and wood density (Kauffman and Donato, 2012; Kauffman et al., 2020). Therefore, a range of regional, pan-tropical and site-specific allometric models are available for mangroves (Komiyama et al., 2008; Chave et al., 2014; Mahmood et al., 2019). However, the use of non-mangrove models for mangrove species, and non-site-specific wood density does not provide the corresponding level of accuracy

especially when estimating biomass variability with vegetation types and environmental drivers (Owers et al., 2018; Rahman et al., 2021c). A standard conversion factor (usually 45-50%) is used to convert biomass into carbon (Kauffman and Donato, 2012; Howard et al., 2014). Application of a standard conversion factor may not reflect an accurate carbon proportion since the conversion rate is species-specific and varies with the component of trees such as stems, branches and roots (Owers et al., 2018). Overall, the carbon stocks of a mangrove forest is not spatially homogeneous, rather it varies due to species type, composition, structure, age, intertidal condition, salinity and other environmental variables (Owers et al., 2018; Kauffman et al., 2020; Rahman et al., 2021b). Therefore, site- and species-specific allometric models and site-specific variables are desirable to better reflect carbon stocks variability(Mahmood et al., 2019; Martínez-Sánchez et al., 2020; Rahman et al., 2021c).

2.4. Remote sensing methods for carbon measurement and upscaling

Since remote sensing imagery is widely used to upscale field inventory data to larger scales, several guidelines have been developed to reduce and report the uncertainty of biomass or carbon transparently (Global Observation of Forest Cover and Land Dynamics (GOFC-GOLD) sourcebook (GOFC-GOLD, 2016), Global Forest Observations Initiative (GFOI) guideline (GFOI, 2016) and Food and Agricultural Organisation (FAO) guideline (FAO, 2016)). While a range of available protocols provide standard guidelines to measure and monitor carbon stocks in any forest, it is always challenging to choose as appropriate methodology. However, the key to all these protocols is that they all meet the requirements of the Tier 3 approach of the IPCC guidelines.

Remote sensing (RS) imageries are frequently used to upscale plot level carbon stocks estimate to larger scales where additional environmental variables can be used to produce carbon maps at ecosystem, national, regional or global levels. Upscaling via remote sensing can be achieved in four ways — a) Stratify and Multiply (SM) Approach, b) Combine and Assign (CA) Approach, c) Ecological Models (EM) Approach, and d) Direct Remote Sensing (DR) Approach (Goetz et al., 2009). While the SM approach assigns an average carbon value to land cover/vegetation type map

(for example, Asner et al. (2010)), the CA approach is the extension of SM which uses kriging or co-kriging geostatistics techniques with multi-layered information in GIS (geographic information system) (for example, Gibbs et al. (2007) and Tyukavina et al. (2015)). The EM approach uses remote sensing (RS) information to parameterise the model (for example, Hurtt et al. (2004)) and the DR approaches are empirical models where RS data is calibrated to field estimates using a number of statistical and machine learning approaches such as neural network and regression tress (for example, Baccini et al., 2008; Saatchi et al., 2011; Baccini et al., 2012). Each of these methods has limitations in terms of data requirements and applicability. Since the SM approach uses average values for each class, it is unable to capture the wider variability within each class (Gibbs et al., 2007; Goetz et al., 2009). The CA approach has the advantage to use additional variables such as elevation, canopy heights and to add weights to prioritise one variable against another. However, it suffers from a lack of consistent spatial data (Goetz et al., 2009; Tyukavina et al., 2015; Ameray, 2018). The DM approach is best suited for monitoring carbon sequestration at larger scales and to prepare wall-to-wall carbon map (Goetz et al., 2015). However, for greater accuracy, the DM approach requires active RS data such as RADAR or LiDAR for training models and validation as these sensors measure forest biomass directly (Goetz et al., 2015).

With recent improvements in spatial and temporal resolution of RS data, scientists are able to use a variety of remote sensing techniques to help quantify carbon in mangrove forests (Table 2.1). The data from remote sensing sensors can be used to fill the spatial, attributional, and temporal gaps produced from forest inventories leading to estimates closer to actual values. However, the sensor does not provide a measurement of carbon content directly, and it is mostly related to the vegetation parameters (for example, crown size, tree height, texture and crown shadow), which are very much interlinked with tree biomass and carbon content (Ni-Meister, 2015). Therefore, remote sensing studies have focused on AGC, and this can act as predictor of other carbon pools such as BGC.

With the advancement of technology, researchers are now increasingly using sensors like RADAR (Radio Detection And Ranging), SAR (Synthetic Aperture Radar), InSAR (Interferometric Synthetic Aperture Radar) and LiDAR (Light Detection And Ranging) because of their increased accuracy for

measuring biomass from forests directly including mangrove forests (Table 2.1). The homogeneity of mangrove forest and the flat underlying topography have led scientists to use canopy height models (CHM) to measure AGB, generated from airborne and spaceborne stereo imaging, LiDAR and SAR interferometry. By using SRTM (Shuttle Radar Topographic Mission) and ICESat GLAS (Geoscience laser altimeter system) elevation data, Simard et al. (2010) estimated above-ground biomass in combination with field data. Application of a digital elevation model (DEM) from SRTM was found in Simard et al. (2006)'s study, where they measured the height of Florida mangroves, which was then combined with field biomass data to estimate biomass for the whole forest. Allometric models were used with the mangrove heights derived from the relationship between the ICESat GLAS canopy waveform contribution (CWC) and SRTM elevation (Simard et al., 2008). By using a Landsat-derived forest cover map and SRTM, Fatoyinbo et al. (2008) successfully estimated the above-ground biomass of Mozambique mangrove with allometric models.

Table 2.1: Application of remote sensing for studying mangrove carbon measurement.

Sensor	Country (Area)	Biomass parameters	Accuracy RMSE	Method	Study
Landsat, LiDAR RIEGL Q680i-S	Northern Western Australia	Canopy height	SD = ± 7.8 Mg AGB ha^{-1}	Regression	Hickey et al. (2018)
SRTM	Global mangrove 130,420 km^2	Canopy height	-	Regression	Tang et al. (2018)
Push-broom hyperspectral sensor	Malaysia	Individual crown area	-	Regression	Suhaili and Lawen (2017)
ALOS-2 PALSAR	Hai Pong City, Vietnam	DN to normalized radar sigma zero (backscatter coefficient)	RMSE = 0.299 R^2 = 0.78	Machine learning	Pham et al. (2017)
Worldview-2, ALOS ABNIR-2, ASTER VNIR, Landsat OLI 8, Hyperion hyperspectral	Indonesia	Vegetation index		Empirical modelling, PCA, Regression	Wicaksono (2017)
UAV RGB	Matang Mangrove Forest, Malaysia	Tree height	Biomass-height R^2= 0.75	Regression	Otero et al. (2018)
ALOS PRISM, ALOS World 3D-30m DSM	Mimika, Indonesia Sundarbans, Bangladesh Mahakam Delta, Indonesia	Canopy height	4.1, 3.6, 3.25	Regression	Aslan et al. (2018)
Interferometric Synthetic Aperture Radar (InSAR)	Mimika, Indonesia 193,226 km^2	Mangrove composition, canopy height	Classification 94.38%, kappa: 0.94, MAE 3 m. RMSE 7.28 m	Quantile regression methods	Aslan et al. (2016)
TanDEM-X, InSAR	Sundarbans, Bangladesh andIndia	Canopy height	RMSE 0.774 m, correlation 0.852	Regression	Lee et al. (2015)
TanDEM-X, InSAR	Mexico and Mozambique	Canopy height	RMSE 01.069-1.727 m, correlation 0.851-0.919	Regression	Lee and Fatoyinbo (2015)
ALOS-2 PALSAR	Hai Pong City, Vietnam	Backscatter coefficient	35.5 mg ha^{-1}, 41.3 mg ha^{-1}	Regression	Pham and Yoshino (2017)

The historical archive of optical imagery over the past few decades has brought a low-cost or error free solution for developing countries to conduct carbon monitoring in forests. In the case of mangroves, the most widely used optical imagery is Landsat TM (Fatoyinbo et al., 2008; Aslan et al., 2016; Omar et al., 2016), followed by SPOT-5 (Hamdan et al., 2013), IKONOS (Proisy et al., 2007), ALOS AVNIR-2 (Wicaksono et al., 2016), WorldView-2 (Candra et al., 2016), and GeoEye-1 (Jachowski et al., 2013). However, the accuracy of the carbon estimates is always hindered by cloud cover, image resolution, quality, revisit time, stand complexities and shadows from canopy and topography (Ni-Meister, 2015). These limitations can be overcome by object-based image analysis, textural image analysis, and species-specific allometric equations. For example, Couteron (2002) proposed a Fourier-based textural ordination method to capture structural diversity of the tree crown in relation to the growth stage and species in VHR (Very High Resolution) images.

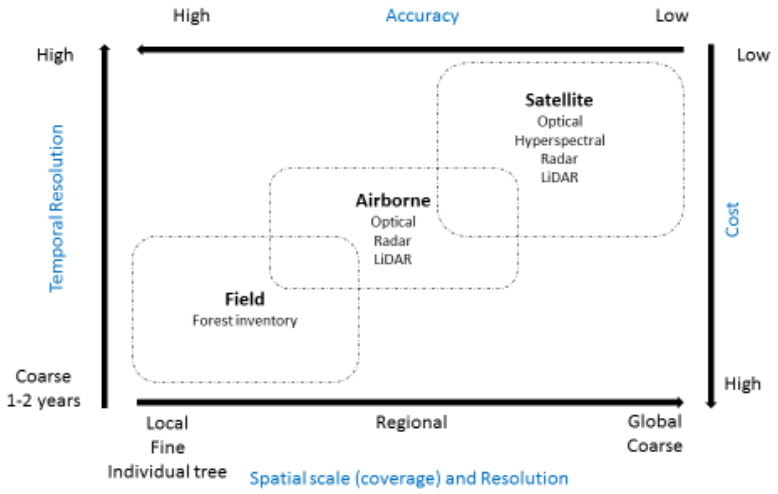

Figure 2.2: Spatial scale, temporal resolution, accuracy, and cost for different methods for monitoring and measuring carbon stocks. Modified from Bustamante et al. (2016, p. 96), License Number: 5411440943342, License date: Oct 17, 2022.

Due to the absence of spaceborne laser scanning sensors tailored to forestry, airborne LiDAR is considered the most accurate method to estimate biomass or to calibrate other satellite imagery (Ni-Meister, 2015). Otero et al. (2018) demonstrated the use of an unmanned aerial vehicle (UAV) with attached RGB camera to retrieve structural information in the Matang mangrove forest, Malaysia. However, large scale estimates of biomass through active sensors are hampered by the associated costs and operational limitations (Bustamante et al., 2016) (Figure 2.2). Despite these limitations,

LiDAR data have been increasingly used in mangrove studies in the recent years (Feliciano et al., 2017; Laurin et al., 2017; Fatoyinbo et al., 2018) and they have shown the measurement of AGC from airborne LiDAR for mangrove forests.

The use of optical sensors is restricted to detect land cover changes and the different biophysical properties (for example, NDVI (Normalised Difference Vegetation Index), LAI (Leaf Area Index)) and are linked statistically to the ground plot to map biomass (Lucas et al., 2015; Bustamante et al., 2016). On the other hand, estimating biomass needs information on wood volume or tree height. Therefore, three-dimensional (3D) remote sensing techniques have been extensively used because of the strong relationship between forest height and biomass (Fatoyinbo and Simard, 2013; Fatoyinbo et al., 2018). One of the main problems of using an optical and SAR (Synthetic Aperture RADAR) is the saturation effect, especially in any heterogeneous forest with high biomass. For instance, Asbridge et al. (2016) found SAR saturation of L-band above 100 Mg ha^{-1}. However, the saturation limit is not confined to a specific biomass level and is largely dependent on stand characteristics and macroecological structural properties (Joshi et al., 2017). For example, Lucas et al. (2007) retrieved low backscatter signal in the case of mangroves with large prop root system and high tides. Therefore, the threshold level varies as a function of the structure and composition of the forest.

2.5. Errors and uncertainties in carbon measurement

Errors and uncertainties in carbon estimation are involved in every phase of carbon estimation including the field inventory to the remote sensing measurement of area and carbon estimation. While error is defined as the difference between the true value and actual value of measurement and uncertainty is the lack of confidence of the parameter values (Harmon et al., 2007). Upscaling field carbon stocks estimation using remote sensing produces uncertainty due to geolocation mismatches with field plots, variable acquisition angles of satellite imagery, mismatches in tree representation, scale mismatches and temporal mismatches in time series analysis (Réjou-Méchain et al., 2019). The biomass measurement, conversion to carbon and upscaling to the ecosystem or larger scales (such as countries, regions) involves series of statistical models which accumulates uncertainties in each step

(Réjou-Méchain et al., 2019; Rahman et al., 2021c). The errors and uncertainties from field plots are therefore carried into the remote sensing and to the final carbon map, which altogether make it a challenging task to keep errors and uncertainties at low.

2.6. Conclusions

The literature review on carbon stocks dynamics in mangrove forests highlighted that the ecosystem carbon stocks is composed of both above- and below-ground carbon — either dead or alive, and sediment carbon. Given that the diverse nature of the different components of mangroves, each component needs different strategies to quantify stored carbon. Allometric models are largely used to infer biomass from tree attributes. However, for greater accuracy the carbon estimation needs species- and site-specific allometric models and vegetation attributes such as wood density and height. Therefore, standard protocols have been developed by different organisations and researchers.

Remote sensing is widely used to upscale field carbon estimates to the ecosystem level. Optical sensors are mainly used to measure forest area to combine field data to estimate carbon density in mangrove forests. Historical archives of remote sensing data allow us to monitor area or carbon stock changes in any mangrove forest area. On the other hand, RADAR and LiDAR, either airborne or satellite, are used to measure biomass directly however signal saturation can underestimate biomass as a result of the canopy density, tides and the type of root system.

Chapter 3

Study site and field work

3.1. The Sundarbans mangrove forest

The Sundarbans is the world's largest contiguous mangrove forest situated across Bangladesh (6,017 km^2, including water areas) and India (4,000 km^2) (Figure 3.1 and 3.2). Like all other mangroves, it also provides plethora of ecosystem services and products to the people of Bangladesh including protection from tsunamis and cyclones (Giri et al., 2008). Because of its outstanding ecological value, UNESCO declared a portion of the Sundarbans (1,395 km^2) as a World Heritage Site in 1997 (Siddiqi, 2001). Despite its recognized national and international importance, historically this forest has been threatened by illegal felling, land conversion, encroachment, shrimp farming, and increasing salinity (Ellison et al., 2000) and it is threatened by climate change and sea level rise over the next few decades (McLeod and Salm, 2006; Gilman et al., 2008; Alongi, 2015). According to the recent IPCC forecasts, this forest would be impacted by increasing sea surface temperatures from 1 to 3 ^{o}C and 18-20 cm sea level rise, and thereby, increasing salinity 0.5 PSU (Practical Salinity Unit) by 2100 (Church et al., 2013; Collins et al., 2013). Apart from impacts from other climatic and edaphic factors, salinity is the major determinant to vegetation change in the Bangladeshi part of the Sundarbans. During the monsoon, this forest usually experiences a large drop in salinity due to the huge network of upstream rivers criss-crossing through Bangladesh from the Himalayas (Hoque et al., 2006; Wahid et al., 2007), while in the winter the opposite effect is seen due to the lack of freshwater flow (Anwar and Takewaka, 2014). More than 90% of freshwater flow has been lost since 1974 due to the construction of the Farakka dam in the Indian border leading to higher salinity in the Sundarbans, especially in the western part.

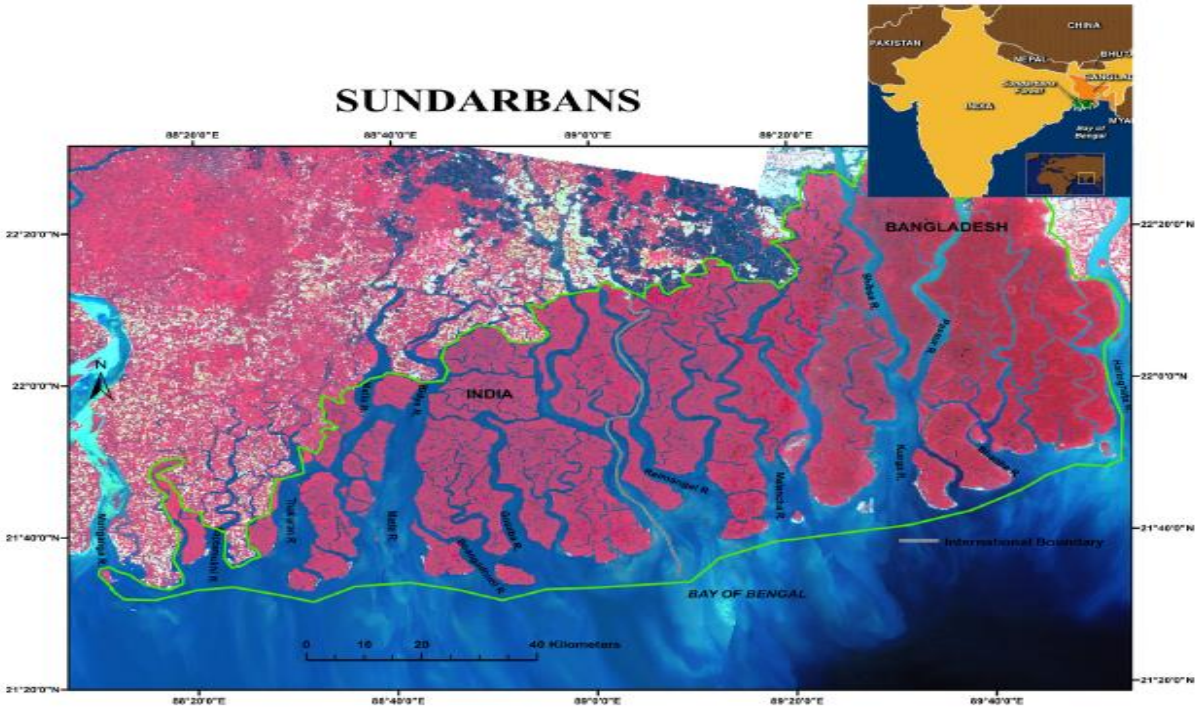

Figure 3.1: Location of Sundarbans between Bangladesh and India. Reproduced from Ghosh et al. (2016) CC BY 4.0.

3.1.1. Climate

The climate of the Sundarbans is warm, humid, and tropical, where annual precipitation varies from 1474 to 2265 mm and mean annual minimum and maximum temperature are between 29 ^{o}C to 31 ^{o}C between 1948 and 2011 (Chowdhury et al., 2016; Sarker et al., 2016).

3.1.2. Geology and soils of the Sundarbans

The Sundarbans mangrove forest lies in the south-western part of the Bengal Basin, one of the most extensive sediment reservoirs in the world composed of unconsolidated Quaternary deposits (Rudra, 2014). The rapid sedimentation followed by the tectonic collision of the Indian plate with the Tibetan plate and the Burmese plate in the Miocene triggered the formation of the Bengal Basin (Alam, 1989). Since the Holocene, the dynamic Ganges-Brahmaputra river system has been discharging sediments from the Sub-Himalaya and is still delivering >1 Gt/yr of sediment to the delta plain of India and Bangladesh (Islam et al., 1999; Syvitski and Milliman, 2007). The Sundarbans is of relatively recent origin (3,000-year B.P.) and this mangrove has developed as a result of both fluvial and tidal forces

depositing sediments to the GBM river mouth (Goodbred and Kuehl, 2000; Allison and Kepple, 2001; Rogers et al., 2013). Previously, the Ganges was the main source of sediments in the Sundarbans, however, recent changes have resulted from the merging of the Ganges and Brahmaputra which have now migrated to the eastward, far away from the Sundarbans (Rudra, 2014; Islam, 2016b). Together with the eastward migration of the primary GBM delta, the construction of the Farakka Barrage in the main Ganges River and earthen embankments surrounding the Sundarbans have reduced freshwater flow, resulting in reduced fluvial sedimentation in the Bangladesh Sundarbans. This geomorphological change, in turn, has led to increased remobilisation of sediments by tidal forces (Rogers et al., 2013; Hale et al., 2019; Bomer et al., 2020b). The changed pattern of freshwater flow has resulted in a salinity gradient increasing from the east to the west of the Sundarbans. Based on the soil salinity variation, the Sundarbans naturally divides into three distinct zones based; i) Oligohaline (LSZ) (<2 dS/m, decisiemens per metre), ii) Mesohaline (2-4 dS/m) and iii) Polyhaline (>4 dS/m) (Siddiqi, 2001; Chanda et al., 2016b).

The soil is mainly fine-grained, grey coloured, slightly calcareous, and mostly composed of silts to clayey silts (Allison et al., 2003; Bomer et al., 2020a). The subsurface sediment extends up to 6 m in depth in the landward direction and up to 4 m in depth in the seaward direction (Allison et al., 2003). The median grain size ranges between 16-32 μm reflecting the medium silt range. The average dry bulk density (0.81 g cm-3) is higher in the Sundarbans in comparison to other mangroves in the world (Bomer et al., 2020a). The soil physical and chemical properties are varied from the eastern to the western part of Bangladesh Sundarbans, the eastern part is softer, more fertile and receives more fresh sediments than the western part (Siddiqi, 2001). Soils are mostly neutral to alkaline (pH 6.5-8.0), whereas the polyhaline zone is more alkaline than the oligohaline zone. Soils of the western and southern polyhaline zone are comparatively richer in P, K, Na, Mg, Cl- and Fe, but lower in soil NH4- and Na than the eastern oligohaline zone (Siddiqi, 2001; Sarker et al., 2016). This pronounced differences in soil nutrients and salinity trigger the diversity and variability of vegetation composition in different parts of the Sundarbans.

3.1.3. Vegetation dynamics

A range of studies concluded that the extent of the Bangladesh Sundarbans was almost constant over the last 50 years (Emach and Peterson, 2006; Giri et al., 2007; Awty-Carroll et al., 2019). Based on per-pixel supervised classification methods, Giri et al. (2007) analysed multi-temporal satellite data from 1970s, 1990s, and 2000s using supervised classification approach and found that the areal extent of the Sundarbans has not changed significantly (approximately 1.2%) between 1970s to 2000s. The forest is however constantly changing due to erosion, aggradation, deforestation and mangrove rehabilitation programmes. The net forest area increased by 1.4% from the 1970s to 1990 and decreased by 2.5% from 1990 to 2000. The recent updated Global Mangrove Watch (GMW) estimates the area of the Sundarbans in 2010 as 4441.59 km^2 from their previous estimates of 4168.3 km^2, an increase of 273.29 km^2 (Bunting et al., 2018; Bunting et al., 2022a). However, these studies included coastal planted mangroves which are not inside the geographical boundary of the Sundarbans.

After analysing four forest inventories from 1926 to 1997, Iftekhar and Saenger (2008) reported a 0.03% annual decline of vegetation cover during the period 1981–1997 attributing to this temporal and spatial variation of salinity. Based on topographic maps and Landsat images, Reddy et al. (2016) estimated only 6.5% forest loss from 1930 to 2014. On the other hand, Potapov et al. (2017) found no net forest cover change as the forest gain compensated forest loss between 2000 and 2014. This raises questions whether there is any change in distribution of tree species, which is essential to understand the impacts of climate change and other drivers on any ecosystem. Ghosh et al. (2016) studied the species composition change over 38 years from 1977 to 2015 across the entire Sundarbans and found a 9.9% decline of both *Heritiera fomes* and *Excoecaria agallocha* and 12.9%, 380.4% and 57.3% rise in *Ceriops decandra*, *Sonneratia apetala* and *Xylocarpus mekongensis*, respectively. The study classified the whole Sundarbans from the field data obtained from only the Bangladesh area. Therefore, this study lacks representative training data and the classification accuracy is low, especially in the Indian Sundarbans. The most recent estimation by Mahmood (2015a) showed about 53% of the dominant *Heritiera fomes* population has declined over 108 years from 1906, and 37% of

the existing trees are seriously affected by 'Top dying disease' as a result of increased salinity. This result urges continuous monitoring of the forest in the species level to unravel our understating of biomass change, which would in turn help decision making regarding sustainable management of this forest.

Figure 3.2: Sundarbans mangrove forest. Left: view from ground in low tide (Photo: Sajjad Hossain Tuhin), Right: aerial view of species composition (Photo: Zaheer Iqbal Ezaz) (February 2019).

3.1.4. Permanent sample plots

In the Sundarbans, there were 120 permanent sampling plots (PSP) which were established in the beginning of the twentieth century to study and monitor the tree growth in 1987 (Figure 3.3). The area of the rectangular PSP is 20 m × 100 m which comprises 2,000 m^2. These locations were selected based on salinity, forest types, accessibility and for the representation of the nature of the ecosystem. The area is also divided into 55 compartments of variable sizes for the management as single unit. These compartments were used to operate felling operations in different management plans in the past.

Since the area of each PSP is very large, the present study took random small sized plots in each PSP. The location of all PSP is close to the riverside which is always subject to erosion. On the other hand, all PSPs did not cover the whole Sundarbans, therefore, additional 20 sample plots were taken outside the PSP to cover the whole Bangladesh Sundarbans.

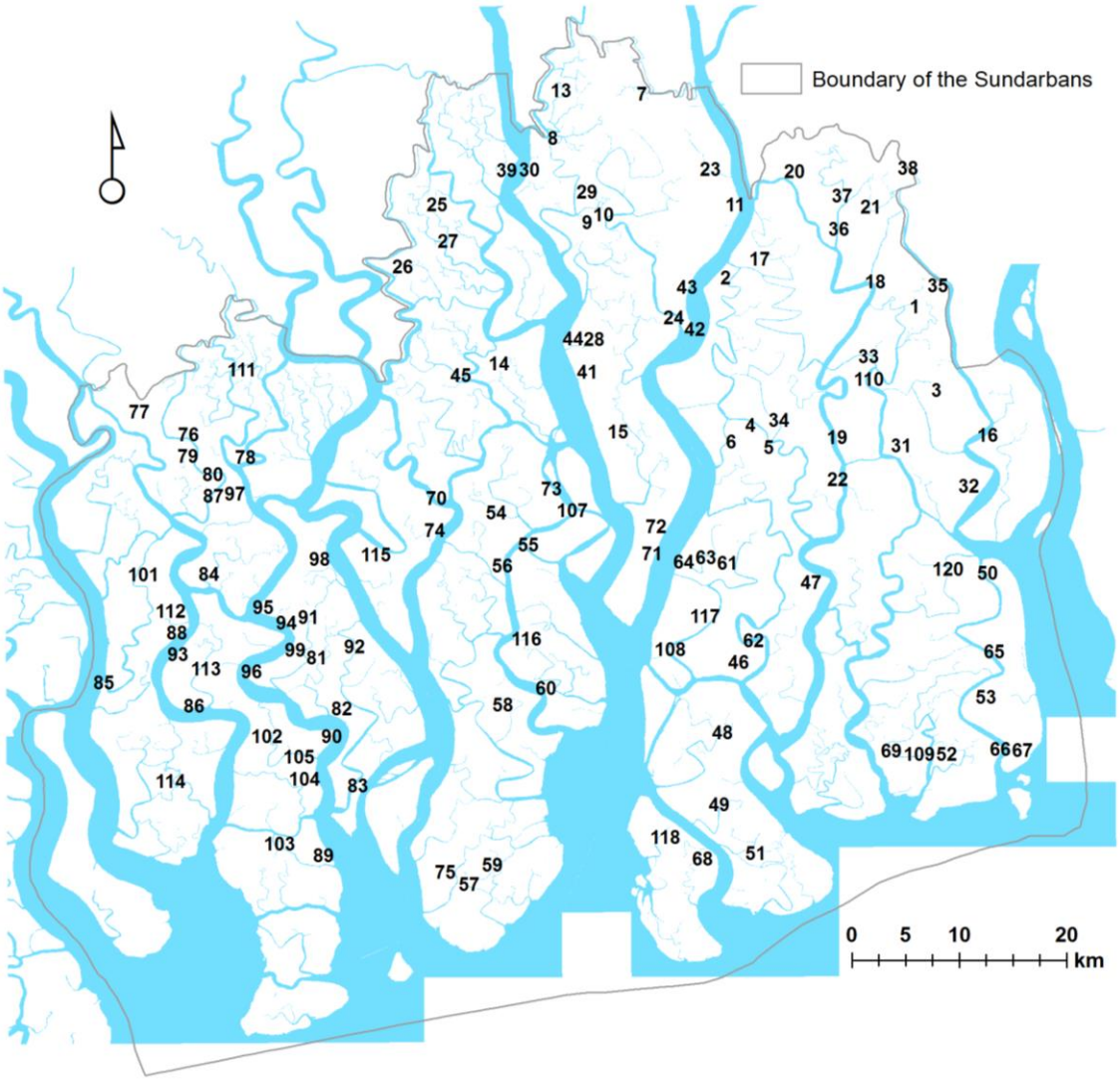

Figure 3.3: Location of the permanent sample plots in the Sundarbans. Reproduced from Mahmood (2015a) with permission.

3.1.5. Measurement of carbon stocks and allometric models

Until recently, the measurement of biomass and carbon stocks in the Sundarbans was mostly based on field measurements from a relatively small number of sample plots, sometimes unevenly distributed and based on an allometric model derived from other mangroves or tropical forest. According to Kauffman and Donato (2012), species specific regional equations are desired to produce greater accuracy in carbon measurement rather than general equations. Hence, most of the earlier studies may not be relevant for the measurement of carbon in the Sundarbans. Several complete inventories were conducted in the 1930s, 1960s, 1980s and 1990s for monitoring vegetation dynamics (Iftekhar and Saenger, 2008). The first comprehensive attempt to measure carbon stocks in the Sundarbans was

undertaken in 2009-10 under the Integrated Protected Area Co-Management (IPAC) project supported by U.S. Forest Service (USFS) and U.S. Agency for International Development (USAID). In order to measure changes in carbon stocks, the carbon stock was estimated using 1997 inventory data and compared with similar parameters of 2009-10 inventory (BFD, 2010). In both measurements, they used a locally derived volume equation and conversion factors to convert volume into biomass. By using an allometric equation, Rahman et al. (2015a) calculated carbon stocks at the whole ecosystem level by combining both above and below-ground from the data obtained in 2009-10 inventory by the Forest Department, Bangladesh. They investigated the variation of carbon stocks in different species/species groups and salinity ranges. However, the allometric equation, which was developed from other mangroves, may not represent the mangroves of the Indian subcontinent and thereby fails to achieve accuracy. Based on their study, Chanda et al. (2016b) simulated the carbon stocks in the Sundarbans by using Markov Chain and cellular automata in order to predict future carbon storage. Most recently, Kamruzzaman et al. (2017) measured above-ground carbon in the medium salinity zone. However, this study also did not use a locally derived allometric equation despite of having some species-specific allometric equations from both Bangladesh and India. Very recently GOB (2019) estimated total ecosystem carbon stocks in the Sundarbans using a field inventory and developed site-specific common allometric models by Mahmood et al. (2019).

3.2. Forest survey

Forest survey in the mangrove forest is always challenging for its proximity to the sea which enables people to move from one place to another using only river way. Again, the adaptation features of mangroves such as dense network of upright roots (pneumatophores) reduces the accessibility inside forests and thereby roaming in the forest needs extra effort and time compared to terrestrial forest (Figure 3.4). Moreover, the Sundarbans mangrove forest contains the Royal Bengal Tiger (*Panthera tigris*) which possesses a major life risk while surveying inside the forests. There are also some other furious animals such as snakes and crocodiles all over the Sundarbans (Figure 3.4). Therefore, safety issues are of major concern before doing forest survey inside the Sundarbans.

Figure 3.4: Challenges for fieldwork in the Sundarbans mangrove forest. Left: venomous snake inside the forest plot, Right: Pneumatophores of *Heritiera fomes* reduce the mobility inside forest.

3.2.1. Sampling design and data collection

The field work for this study was conducted in two phases (August 2018 and between February and April 2019). Temporary circular plots were established in each PSP with the radius of 11.3 m that accounts in total 400 m^2, one-fifth of the PSP. Due to the fact that most of the PSP is located near the riverbank and these 120 PSPs don't cover the whole Sundarbans, additional 20 plots were taken, which makes altogether 140 sample plots (Figure 3.5).

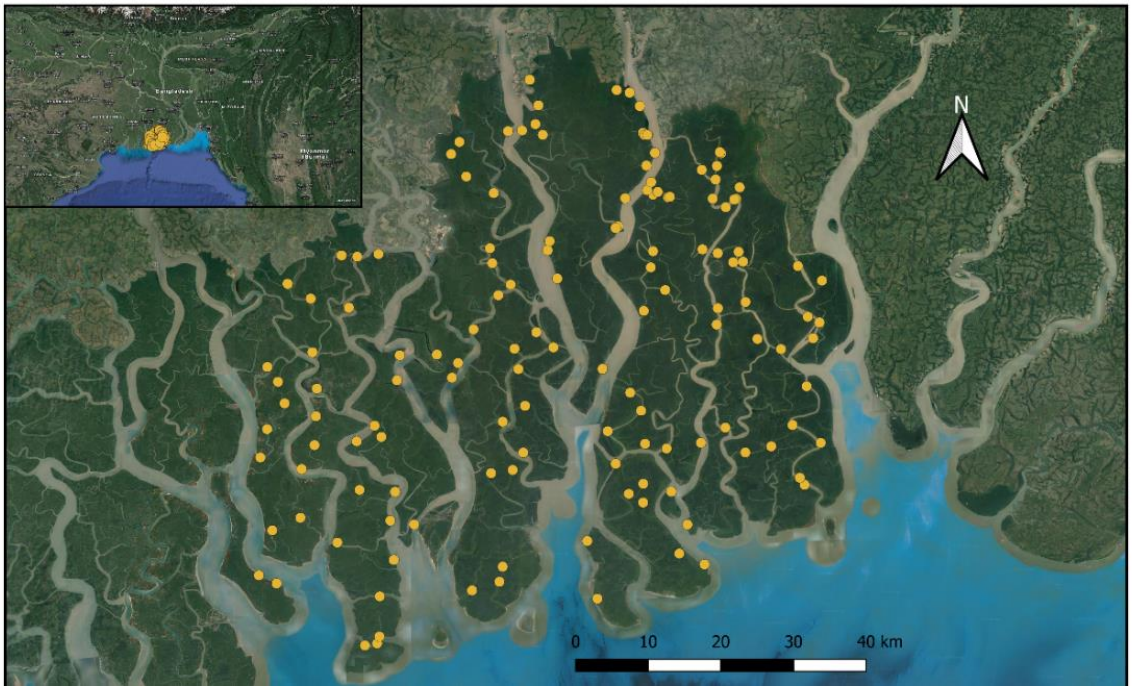

Figure 3.5: Plot location in the Sundarbans mangrove forest, Bangladesh. ESRI Basemap Sources: Esri, HERE, Garmin, FAO, NOAA, USGS, © OpenStreetMap contributors, and the GIS User Community.

The study collected biophysical information from the above-ground trees, poles, dead and down wood and pneumatophores. On the other hand, below-ground carbon was estimated and measured from roots and sediments, respectively. The study followed circular nested plot to retrieve data from all structural categories of above ground component. While the circular plot is designed to get data from the trees, it was also divided into three sub-plots with radius of 1m, 2m and 5m to take measurement of seedlings, saplings and poles (Figure 3.6). In case of trees and poles, Diameter at Breast Height (DBH) and total height was measured by a diameter tape and a Vertex III hypsometer (Haglöf, Sweden), respectively (Figure 3.7). In case of the presence of any buttresses, the DBH was measured above the buttresses (Figure 3.7). While there was any forking below the breast height (1.3 m), it was considered as two trees.

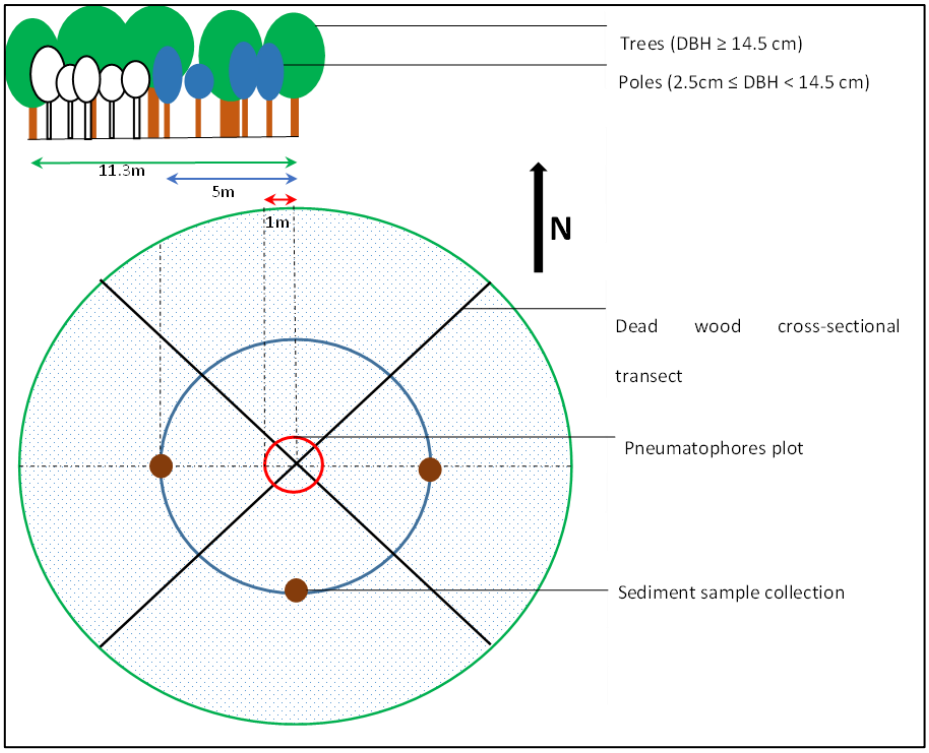

Figure 3.6: The nested circular plot and different measured components of vegetation and sediment in each segment.

Decay status of each tree was also recorded (if any) in three statuses: Decay 1, decay 2, Decay 3 with increasing number indicates more decay. In order measure the wood density, wood cores were collected at breast height (1.3 m) with increment borer for each tree species found in the plot (Figure 3.7). For pneumatophores, a 1 m × 1 m plot was used to count the number of pneumatophores for all species. For dead and down wood, two cross-sectional transect was taken to count the number of pieces in three categories based on diameter in the middle: Fine (> 0.6 cm), Small ((0.6-2.5 cm) and Medium (2.5-7.6 cm). In case of non-tree vegetation like *Nypa fruticans*, the number of leaves and for *Phoenix sylvestris*, the number of stems were counted. In order to measure carbon in pneumatophores and other non-tree such as, some specimens with variable sizes were weighed and subsequently brought to the laboratory for oven drying.

In this study, sediment samples were collected from 55 plots, of which 50 plots are from PSPs selected at random, and the remaining five plots are from outside PSPs to represent areas outside PSP. Sampling was undertaken in two phases: In the first phase, three sediment cores of 50 cm depth were

taken from 18 PSPs. After laboratory analysis of the samples from the first 18 PSPs, it was decided to extend the sediment sampling depth to 1 m and take two core samples from each plot because of little within-plot variation among the initial 54 core samples. In the second phase, an additional 37 PSPs were sampled with two cores sampled at each plot. Altogether, 126 sediment cores from 55 plots were sampled across the whole of the Bangladesh Sundarbans (Figure 3.8).

Figure 3.7: DBH and height measurement and collection of wood core. Top-left: DBH measurement by diameter tape above buttress, top-right: DBH measurement above forking, bottom-left: height measurement with a Vertex-III hypsometer, bottom-right: wood core collection through increment borer.

3.2.2. Laboratory analysis

For each core, samples were freeze-dried and re-weighted to determine the bulk density. Bulk density was calculated by dividing the dry mass of the soil by the volume of the soil. Soil pH and soil salinity (as soil conductivity) were measured from a portion of the homogenised dry soil for each core. Dried soils were diluted with distilled water (1:5 ratio), and subsequently, soil pH was measured using a Jenway 3510 Standard Digital pH Meter and soil salinity by a handheld Jenway 470 Conductivity Meter (Hardie and Doyle, 2012).

Figure 3.8: Sediment collection and the determination of SOC in the laboratory. Top-left: sediment core collection, top-right: sediment core, bottom-left: weighing sediment sample for measuring organic carbon, bottom-right: loading sediment sample in the CHN analyser.

To determine the soil organic carbon (SOC) and nitrogen content of the soil, any large stones or twigs were removed from the sample and subsequently homogenised and ground with a ball mill. 40 mg of the sediment were then passed through an elemental analyser (Thermo Scientific Flash 2000-NC Soil Analyzer) to derive the total carbon and nitrogen as a percentage (Figure 3.8). Inorganic carbon content was deducted from the total carbon to obtain the organic carbon percentage, according to Howard et al. (2014). The inorganic carbon content was measured from random samples across all salinity zones using an Analytik Jena Multi EA (Elemental Analyser) 4000. Soil organic carbon density (gm cm^{-3}) for each sample and total organic carbon content (Mg ha^{-1}) of each depth and core were measured according to Howard et al. (2014).

3.3. Conclusions

The Sundarbans is a unique ecosystem with high biodiversity compared to other mangrove forest. Despite some initiatives for the estimation of carbon stocks in the Sundarbans, there is no comprehensive study combining field inventory data with remote sensing to estimate ecosystem carbon stocks in the Bangladesh Sundarbans. Most studies used pan-tropical models which potentially do not represent species diversity and used wood density which may increase the uncertainty. In this regard, species-specific allometric models and carbon conversion factors may help to better capture the variability due to species composition.

Chapter 4

Is soil organic carbon underestimated in the largest mangrove forest ecosystems? Evidence from the Bangladesh Sundarbans

Rahman, M.S., Donoghue, D.N.M., Bracken, L.J., 2021. Is soil organic carbon underestimated in the largest mangrove forest ecosystems? Evidence from the Bangladesh Sundarbans. CATENA. 200, 105159. https://doi.org/10.1016/j.catena.2021.105159.

Abstract

Globally, mangroves sequester a large amount of carbon into the sediments, although spatial heterogeneity exists owing to a wide variety of local, regional, and global controls. Rapid environmental and climate change, including increasing sea-level rise, global warming, reduced upstream discharge and anthropogenic activities, are predicted to increase salinity in mangroves, especially in the Bangladesh Sundarbans, thereby disrupting this blue carbon reservoir. Nevertheless, it remains unclear how salinity affects the below-ground soil carbon despite the recognised effect on above-ground productivity. To address this gap, research was undertaken in the Bangladesh Sundarbans to compare total soil organic carbon (SOC) across three salinity zones and to explore any potential predictive relationships with other physical and chemical properties, and vegetation characteristics. Total SOC was significantly higher in the oligohaline zone (74.8 ± 14.9 Mg ha^{-1}), followed by the mesohaline (59.3 ± 15.8 Mg ha^{-1}), and polyhaline zone (48.3 ± 10.3 Mg ha^{-1}) (ANOVA, $F_{2, 500} = 118.9$, $p < 0.001$). At all sites (55 plots), the topmost 10 cm of soil contained a higher SOC density than the bottom depths (ANOVA, $F_{3, 500} = 30.1$, $p < 0.001$). On average, *Bruguiera* spp. stand holds the maximum SOC measured, followed by two pioneer species *Sonneratia apetala* and *Avicennia* spp. Multiple regression results indicated that soil salinity, organic C: N and tree diameter were the best predictor for the variability of the SOC in the Sundarbans ($R^2 = 0.62$). Despite lower carbon in the soil, the study highlights that the conservation priorities and low deforestation have led to less CO_2 emissions than most sediment carbon-rich mangroves in the world. The study also emphasised the importance of spatial conservation planning to safeguard the soil carbon-rich zones in the Bangladesh Sundarbans from anthropogenic tourism and development activities to support climate change adaptation and mitigation strategies.

4.1. Introduction

Mangroves are recognised as one of the most carbon-dense forest types in the world due to their efficient carbon sequestration capacity into both above and below-ground carbon pools (Donato et al., 2011; Alongi, 2012; Sanderman et al., 2018). Recent assessments of soil carbon suggest that

mangrove ecosystems contain, on an average, between 856 and 1,023 Mg of carbon per hectare, with the majority (~85%) of this carbon stored in the soil (Donato et al., 2011; Pendleton et al., 2012; Sanderman et al., 2018; Kauffman et al., 2020). This large amount of soil carbon is of global importance due to its potential to store sequestered CO_2 emissions for the long term and help to mitigate adverse effects of climate change (McLeod et al., 2011; Duarte et al., 2013; Abdullah et al., 2016). To recognise the importance of mangrove forests for carbon sequestration, the United Nations Environmental Programme (UNEP) designated this ecosystem as "Blue Carbon" along with other coastal vegetated ecosystems such as seagrass meadows and saltmarshes (Nellemann et al., 2009; Lovelock and Duarte, 2019; Macreadie et al., 2019). This growing worldwide importance of mangroves has led to a substantial reduction of mangrove loss leading to reductions in CO_2 emissions in the last three decades (Friess et al., 2019). At the same time, mangroves have gained substantial traction in being managed, protected and restored as part of national and global climate change mitigation policies and actions including Nationally Determined Contributions (NDC) towards the Paris Agreement and the climate action goal (goal 13) under United Nations Sustainable Development Goals (SDG) (Taillardat et al., 2018; Friess et al., 2020a). However, variability and uncertainty in SOC estimation is a key barrier to the inclusion of mangroves (and other blue carbon) in national and international policy tools and frameworks.

Despite covering only 0.1% of the world's total landmass, mangroves sequester more carbon per unit area than any other natural ecosystem (Atwood et al., 2017; Lovelock and Duarte, 2019). With autochthonous inputs from the productive above-ground, mangrove soils store large quantities of carbon as a result of the low decomposition rate resulting from anoxic conditions (Alongi, 2002; Donato et al., 2011). Mangroves are also highly efficient traps for allochthonous (from outside of the ecosystem) inputs through their dense network of above-ground roots. The rising elevation of mangroves in response to sea-level rise allows large accommodation spaces to sequester more carbon in the soil, which barely reaches saturation (Krauss et al., 2014; Rogers et al., 2019). Therefore, mangroves act as an efficient carbon store despite continuous threats from deforestation, land-use change, sea-level rise, and climate change.

Blue carbon research across the globe has highlighted considerable spatial heterogeneity in soil organic carbon (SOC) at multiple scales (Atwood et al., 2017; Sanderman et al., 2018). At a regional and global scale, SOC variability has been linked to net primary productivity (Alongi, 2012; Twilley et al., 2017), latitude/climate (Rovai et al., 2018; Twilley et al., 2018; Kauffman et al., 2020), coastal geomorphology (Rovai et al., 2018; Twilley et al., 2018) and Holocene sea-level trends (Rogers et al., 2019). These physical and biological factors and geomorphic processes promote and develop unique coastal environmental settings, which ultimately drive macroscale variation in SOC (Rovai et al., 2018). The site-specific variability in SOC is largely attributed to differences in species composition (Ren et al., 2008), stand age (Lovelock et al., 2010; Donato et al., 2011), sources of allochthonous particles (Bouillon and Boschker, 2006; Yang et al., 2014), soil physicochemical properties (Freeman et al., 2004; Kristensen et al., 2008; Banerjee et al., 2018), elevation and tidal regimes (Liu and Lee, 2006; Spivak et al., 2019), plant-litter biochemistry (Kristensen et al., 2008; Brodersen et al., 2019) and plant-microbe interactions (Fontaine et al., 2007; Alongi, 2014). Several soils and environmental characteristics such as pH, salinity, organic matter, precipitation and tidal inundation influence mangrove productivity and can also directly or indirectly influence SOC (Yando et al., 2016). Therefore, careful consideration of relevant factors is vital for reliable estimation of SOC at any particular spatial scale.

Table 4.1: Comparison of Soil Organic Carbon (SOC) density and stocks among studies in the Sundarbans and globally.

Study area		**Study**	**Sample size**	**Depth (cm)**	**Methods**	**Mean Soil organic carbon percentage (%) (range)**	**Mean Soil organic carbon density (gm/cm^3) (range)**	**Mean top m Soil Organic Carbon Storage (Mg/ha) (range)**
Sundarbans	Bangladesh	Bomer et al. (2020a)	56	100 cm	Coring, CHN analyser	0.9 (0.6-1.5)	0.010 (0.008-0.011)	-
		Khan and Amin (2019)	35	15 cm (0-15)	Coring, wet oxidation	0.6 (0.4 – 1.0)	-	-
		Sanderman et al. (2018)	-	100 cm	Literature and model based	-	-	127 (74- 463)
		Atwood et al. (2017)	-	100 cm	Literature and model based	-	-	118
		Prasad et al. (2017)	400	100 cm (1 cm interval)	Coring, CN analyser	1.25 (0.8 – 2.4)	-	-

		Hossain and Bhuiyan (2016)	96	5 cm (0-5)	Coring, wet oxidation	1.2 (0.6 – 2.0)	-	-
		Rahman et al. (2015a)	150	100 cm (0-30, 30-100)	Coring, wet oxidation	-	0.011 (0.007 – 0.014)	112 (90 – 134)
		Donato et al., (2011)	4	100 cm (0-30, 30-100)	Coring, wet oxidation	1.7 (1.6-1.7)	0.016 (0.015–0.016)	-
		Allison et al. (2003)	4	600 cm (0-600)	Coring, CHN analyser	0.5 -1.1	-	-
	India	Dutta et al. (2019)	48	40 cm (0-10, 10-20, 20-30, 30-40)	Coring, wet oxidation	1.25 (0.8-1.6)	-	-
		Prasad et al. (2017)	300	100 cm (1 cm interval)	Coring, CN analyser	0.8-5.2	-	-
		Dutta et al. (2013)	15	25 cm (0-5, 5-10, 10-15,15-20, 20-25)	Coring, TOC analyser	1.8 (1.2 – 2.1)	0.017 (0.013 – 0.019)	-
		Banerjee et al. (2012)	140	40 cm (0-10, 10-20, 20-30, 30-40)	Coring, wet oxidation	1.0 (0.5 – 1.4)	0.011 (0.007 – 0.015)	-
		Mitra et al. (2012)	120	40 cm (0-10, 10-20, 20-30, 30-40) cm	Coring, wet oxidation	0.7 (0.4 – 1.1)	0.009 (0.006 – 0.012)	-
		Ray et al. (2011)	16	30 cm (0-30)	Coring, wet oxidation	0.6 (0.5-0.7)	-	-
Global studies		Kauffman et al. (2020)	190 sample plot data from 5 continents in different soil depth			-	-	334 (33 – 789)
		Sanderman et al. (2018)	Model based estimation of carbon from literature values of 1812 samples			-	-	361 (94-628)
		Rovai et al. (2018)	Model based estimation of carbon from literature values of 932 samples			-	0.033 (0.001 – 0.153)	-
		Atwood et al. (2017)	Literature based estimation from 1230 sampling locations			-	-	283 (15 – 1527)
		IPCC (2014)	Literature based estimation			-	-	428
		Jardine and Siikamäki (2014)	Model based estimation of carbon from literature values of 932 samples			5.7 (0.1 – 43.3)	0.032 (0.014 – 0.115)	369 (272 – 703)
		Donato et al. (2011)	Field based data from Indo-pacific area of 25 samples			11.9 (1.7 -21.5)	0.043 (0.016 – 0.076)	-

The Sundarbans is the largest contiguous mangrove forest in the world and is situated in the lower delta plain of the Ganges-Brahmaputra-Meghna (GBM) delta and stretches across political boundaries between Bangladesh and India (Giri et al., 2011; Sarker et al., 2016). It is either mostly excluded from the global estimates of mangrove SOC (Table 3.1) or is underrepresented due to a limited number of samples or perceived poor data quality (Donato et al., 2011; Jardine and Siikamäki, 2014; Atwood et al., 2017; Sanderman et al., 2018; Twilley et al., 2018; Kauffman et al., 2020). A range of studies into SOC content in mangrove soils of the Sundarbans have been carried out (Table 3.1), but these all have

limitations. The first comprehensive carbon inventory throughout the Sundarbans was completed by the Bangladesh Forest Department (BFD) in 2009-10; however, the wider vertical sample depth might have an effect on the SOC estimation within the top meter (Rahman et al., 2015a). Allison et al. (2003) and Donato et al. (2011) investigated soil organic carbon at greater depths (>1 m) in the Bangladesh Sundarbans, however, the number of samples (2 and 6 respectively) was not sufficient to address the variability within the forests. Studies by Khan and Amin (2019) and Hossain and Bhuiyan (2016) measured SOC from different parts of the Sundarbans, however, the sampling was only performed within the top 15 cm. All previous studies of SOC in the Sundarbans have limitations resulting from low spatial sampling intensity and limited analysis of soil depth range. Moreover, some global studies like Rovai et al. (2018) argued that past climate-based estimation overestimated SOC by up to 86% for deltaic settings like the Sundarbans. Therefore, accurate investigation on the spatial variation of soil organic carbon and the identification of major controls for such variation in the Bangladesh Sundarbans is urgently needed.

Increasing salinity in the inundated mangroves stimulate a wide range of biogeochemical reactions-including enhancing sulphate concentrations, cation exchange, ionic and osmotic stress, acidity, and turbidity and at the same time reducing soil redox potential and oxygen levels (Setia et al., 2013; Luo et al., 2019). These soil biogeochemical changes in turn alter sediment characteristics and modify plant and microbe communities, which ultimately affect both the soil organic carbon pool and quality. Increased soil salinity affects organic matter solubility by altering flocculation of different soil particles (Wong et al., 2009; Wong et al., 2010; Rath and Rousk, 2015). Investigations of tidal wetlands across the world reveals a significant negative relationship between the soil organic carbon pool and salinity (Nyman et al., 1990; Craft, 2007; Więski et al., 2010; Morrissey et al., 2014; Hu et al., 2016). High soil salinity decreases decomposition rates by lowering microbial activity in the soil and lowers autochthonous carbon input by reducing plant productivity leading to lower organic carbon in the soil (Baldwin et al., 2006; Marton et al., 2012; Setia et al., 2013; Liu et al., 2017; Zhao et al., 2017). High salinity in general acts as an inhibitor of carbon mineralisation, however the opposite is also evident in some studies suggesting that a small increase in salinity promotes

mineralisation process in the oligohaline zone, while in the mesohaline and polyhaline zones, elevated salinity reduces the mineralisation rate (Luo et al., 2019). Therefore, the impact of salinity on the soil organic carbon pool and quality is not uniform in all wetland settings, rather it depends on the local geomorphology and hydrological characteristics.

The aim of the present study is to estimate soil organic carbon (SOC) in the Bangladesh part of the Sundarbans mangrove forest and to better understand the relationship of SOC within three salinity zones (oligohaline, mesohaline and polyhaline) and major forest types. The study hypothesises that higher salinity zones (polyhaline) would yield a lower organic soil carbon stocks as a reflection of lower productive vegetation and altered soil physical and biological processes compared with the lower salinity zone (oligohaline). The relationships between physical and chemical properties and vegetation characteristics with SOC are also investigated to develop dependable predictive models for this forest. The novelty of this study lies in the extensive stratified random sampling from across the Bangladesh Sundarbans combined with vertical investigation of soil depth up to 1 m.

4.2. Material and methods

4.2.1. Study area

The Sundarbans is the largest single block of mangrove forest in the world and a Ramsar and UNESCO World Heritage site (Figure 3.1) (Giri et al., 2011; Sarker et al., 2016). The Bangladesh Sundarbans is situated between 21º30’ N and 22º30’ N and 89º00’ E and 89º55’ E. The climate of the Sundarbans is warm, humid, and tropical, where annual precipitation varies from 1474 to 2265 mm and mean annual minimum and maximum temperature are between 29º C to 31º C (Chowdhury et al., 2016; Sarker et al., 2016). Based on the soil salinity variation, the Sundarbans naturally divides into three distinct zones based; i) Oligohaline (LSZ) (<2 dS/m, decisiemens per metre), ii) Mesohaline (2-4 dS/m) and iii) Polyhaline (>4 dS/m) (Siddiqi, 2001; Chanda et al., 2016b).

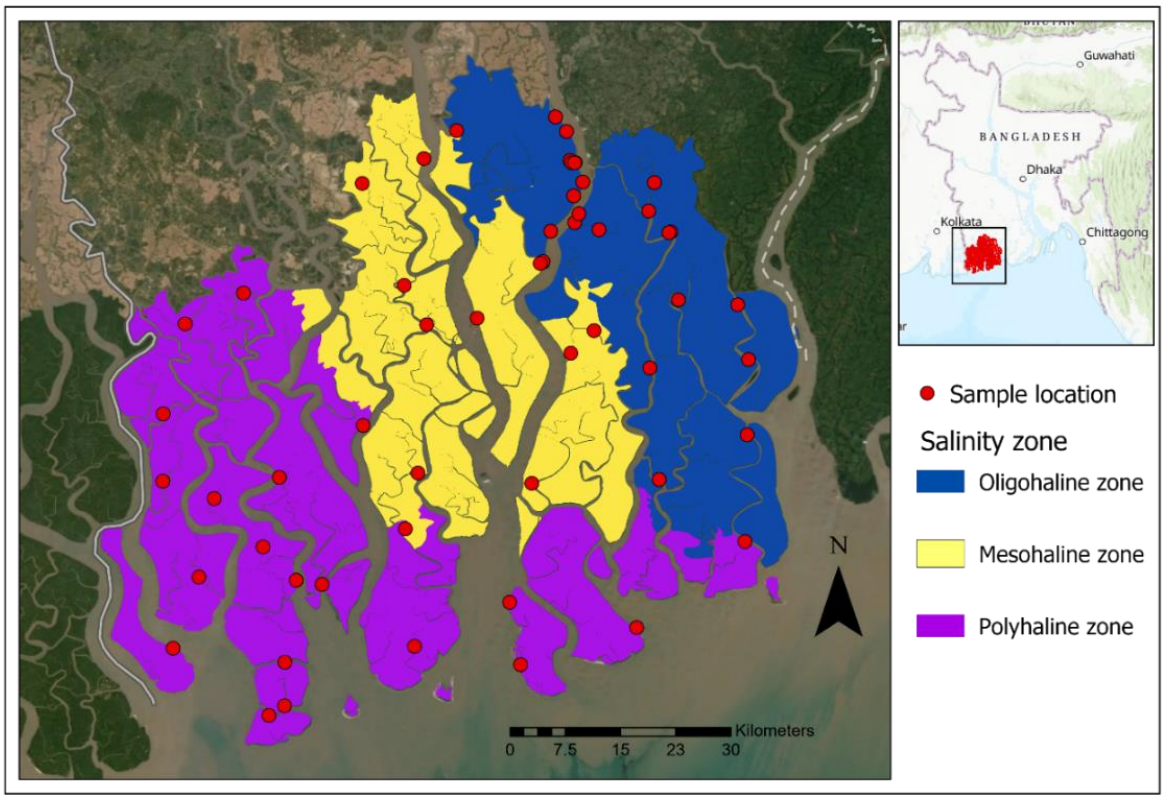

Figure 4.1: Sundarbans mangrove forest, Bangladesh. Legend colour represents three major salinity zones (Chanda et al., 2016b). ESRI Basemap Sources: Esri, HERE, Garmin, FAO, NOAA, USGS, © OpenStreetMap contributors, and the GIS User Community.

Several studies have identified a relationship between tree species abundance along the east-west salinity gradient (Iftekhar and Saenger, 2008; Aziz and Paul, 2015; Sarker et al., 2016; Sarker et al., 2019a). Although *Excoecaria agallocha* is abundant in all three salinity zones, *Heritiera fomes* (the characteristic species in the Bangladesh Sundarbans) is dominant in both the oligohaline and mesohaline zones, whereas *Ceriops decandra* is abundant in the polyhaline zone (Sarker et al., 2019a). Some pioneer species, such as *Avicenna* spp. and *Sonneratia apetala* are also present in the mudflats all over the Sundarbans. A short description of all 23 tree species from 10 families found in this study is presented in Table A.1.

4.2.2. Geology and soils of the Sundarbans

The Sundarbans mangrove forest lies in the south-western part of the Bengal Basin, one of the most extensive sediment reservoirs in the world composed of unconsolidated Quaternary deposits (Rudra, 2014). The rapid sedimentation followed by the tectonic collision of the Indian plate with the Tibetan plate and the Burmese plate in the Miocene triggered the formation of the Bengal Basin (Alam, 1989).

Since the Holocene, the dynamic Ganges-Brahmaputra river system has been discharging sediments from the Sub-Himalaya and is still delivering >1 Gt/yr of sediment to the delta plain of India and Bangladesh (Islam et al., 1999; Syvitski and Milliman, 2007). The Sundarbans is of relatively recent origin (3,000-year B.P.) and this mangrove has developed as a result of both fluvial and tidal forces depositing sediments to the GBM river mouth (Goodbred and Kuehl, 2000; Allison and Kepple, 2001; Rogers et al., 2013). Previously, the Ganges was the main source of sediments in the Sundarbans, however, recent changes have resulted from the merging of the Ganges and Brahmaputra which have now migrated eastward, far away from the Sundarbans (Rudra, 2014; Islam, 2016b). Together with the eastward migration of the primary GBM delta, the construction of the Farakka Barrage in the main Ganges River and earthen embankments surrounding the Sundarbans have reduced freshwater flow, resulting in reduced fluvial sedimentation in the Bangladesh Sundarbans. This geomorphological change, in turn, has led to increased remobilisation of sediments by tidal forces (Rogers et al., 2013; Hale et al., 2019; Bomer et al., 2020b). The changed pattern of freshwater flow has resulted in a salinity gradient from the east to the west of the Sundarbans.

The soil is mainly fine-grained, grey coloured, slightly calcareous, and mostly composed of silts to clayey silts (Allison et al., 2003; Bomer et al., 2020a). The subsurface sediment extends up to 6 m in depth in the landward direction and up to 4 m in depth in the seaward direction (Allison et al., 2003). The median grain size ranges between 16-32 μm reflecting the medium silt range. The average dry bulk density (0.81 g cm^{-3}) is higher in the Sundarbans in comparison to other mangroves in the world (Bomer et al., 2020a). The soil physical and chemical properties are varied from the eastern to the western part of Bangladesh Sundarbans, the eastern part is softer, more fertile and receives more fresh sediments than the western part (Siddiqi, 2001). Soils are mostly neutral to alkaline (pH 6.5-8.0), whereas the polyhaline zone is more alkaline than the oligohaline zone. Soils of the western and southern polyhaline zone are comparatively richer in P, K, Na, Mg, Cl^- and Fe, but lower in soil NH^{4-} and Na than the eastern oligohaline zone (Siddiqi, 2001; Sarker et al., 2016). This pronounced differences in soil nutrients and salinity trigger the diversity and variability of vegetation composition in different parts of the Sundarbans.

4.2.3. Sediment and tree data collection

In the Bangladesh Sundarbans, permanent sample plots (PSP) were established in 1986 by the ODA (Overseas Development Administration) for monitoring growth, regeneration, and long-term ecological changes (Chaffey et al., 1985). A total of 120 PSPs (20 m × 100 m) were established to measure growth rate, regeneration, stocking, and crop composition based on salinity, forest type and accessibility (Iftekhar and Saenger, 2008; Sarker et al., 2019b) (Figure 3.1). In this study, sediment samples were collected from 55 plots, of which 50 plots are from PSPs selected at random, and the remaining five plots are from outside PSPs to represent areas outside PSP. Sampling was undertaken in two phases: In the first phase, three sediment cores of 50 cm depth were taken from 18 PSPs. After laboratory analysis of the samples from the first 18 PSPs, it was decided to extend the sediment sampling depth to 1 m and take two core samples from each plot because of little within-plot variation among the initial 54 core samples. In the second phase, an additional 37 PSPs were sampled with two cores sampled at each plot. Altogether, 126 sediment cores from 55 plots were sampled across the whole of the Bangladesh Sundarbans (Figure 3.1).

The location of the cores within a PSP was decided by establishing a random circular plot with a radius of 11.3 m (an area of 400 m^2). Within each plot, a small circular plot was laid with a 5 m radius and sediment cores were taken from east, west and south side (east and west for two cores) from the centre, perpendicular to each other. The cores were taken using an open-faced auger (6 cm diameter), which was further subdivided into four depths (0-10, 10-30, 30-50 and 50-100 cm), following the method of Kauffman and Donato (2012). Sediment sub-samples were taken from the middle of each core section with fixed 2.5 cm length, sealed in plastic bags and subsequently placed in an icebox to reduce oxidation. The sub-samples were kept below 4 ^{O}C in zip-sealed plastic bags until laboratory processing.

For vegetation data, the Diameter at Breast Height (DBH) and height were measured for all trees within the 11.3 m radius plot. DBH was measured at 1.3 m and height was measured with a Vertex-III hypsometer. For small trees with a DBH <14.5 cm, a smaller circular plot (radius 5 m) was nested within the 11.3 m plot. The elevation of each plot was calculated by subtracting the mean tree height

of the plot from the Digital Surface Model (DSM) taken from the TanDEM-X 90 m satellite data (Hawker et al., 2019). For major forest types, single-species dominance was determined when the relative composition is >75%, and the remaining forest types are termed as a Mixed type.

4.2.4. Laboratory analysis

4.2.4.1. Soil physical and chemical properties

For each core, samples were freeze-dried and re-weighted to determine the bulk density. Bulk density was calculated by dividing the dry mass of the soil by the volume of the soil. Soil pH and soil salinity (as soil conductivity) were measured from a portion of the homogenised dry soil for each core. Dried soils were diluted with distilled water (1:5 ratio), and subsequently, soil pH was measured using a Jenway 3510 Standard Digital pH Meter and soil salinity by a handheld Jenway 470 Conductivity Meter (Hardie and Doyle, 2012).

4.2.4.2. Total soil organic carbon (SOC)

To determine the soil organic carbon (SOC) and nitrogen content of the soil, any large stones or twigs were removed from the sample and subsequently homogenised and ground with a ball mill. 40 mg of the sediment were then passed through an elemental analyser (Thermo Scientific Flash 2000-NC Soil Analyzer) to derive the total carbon and nitrogen as a percentage. Inorganic carbon content was deducted from the total carbon to obtain the organic carbon percentage, according to Howard et al. (2014). The inorganic carbon content was measured from random samples across all salinity zones using an Analytik Jena Multi EA (Elemental Analyser) 4000. Soil organic carbon density (gm cm^{-3}) for each sample and total organic carbon content (Mg ha^{-1}) of each depth and core were measured according to Howard et al. (2014).

4.2.5. Statistical Analysis

All statistical analysis and graphics used R 3.6.1 for Windows (R Core Team, 2019). Total organic carbon (Mg ha^{-1}), organic carbon density (gm cm^{-3}) and bulk density (gm cm^{-3}) among three salinity zones and four depths were compared with two-way analysis of variance (ANOVA) test using the

'car' package (Fox and Weisberg, 2019). In order to compare soil organic carbon among vegetation types, total organic carbon (Mg ha^{-1}) was compared with one-way analysis of variance (ANOVA). The results of ANOVA are summarized in Supplementary Information. To derive the relationship among organic carbon density (g cm^{-3}), bulk density and total nitrogen content, data from all the core subsections (n = 512) were used. To examine the relationship among SOC and soil physical and chemical parameters (soil salinity, pH, bulk density, Total N, organic C: N, elevation, latitude and longitude) and vegetation characteristics (species richness, tree density, mean DBH and mean height), stepwise multiple linear regression analysis was undertaken. SOC was considered as the dependant variable, whereas all the selected parameters were independent variables. Correlation analysis and principal component analysis (PCA) were carried out to decrease the number of explanatory variables and to reduce collinearity in the regression model. All the variables were standardised before PCA according to Legendre and Legendre (2012). Eigenvalues greater than one were retained and variables with factor loadings >0.35 were treated as potential explanatory variables for the regression model (Jackson, 1993). In all cases, the data were logarithmic (natural) transformed (if needed) to meet the assumptions of normality and equal variances by using Shapiro Wilk and Levene's tests, respectively and subsequently back-transformed to present graphically. The graphical output of the linear model was generated using the 'ggplot2' package (Wickham, 2016).

4.3. Results

4.3.1. Soil organic carbon, salinity zones and soil depth

The average SOC density varied from 0.003 gm cm^{-3} to 0.009 gm cm^{-3} in different salinity zones and soil depths (two-way ANOVA for Ln (SOC density), salinity zones, $F_{2, 500} = 112.3$, $p < 0.001$ and soil depths, $F_{3, 500} = 30.1$, $p < 0.001$) (Figure 3.2, Table A.2). Both salinity zone and soil depth had a significant interaction effect on the variability of SOC density in the Sundarbans ($F_{6, 500} = 3.5$, $p < 0.01$) (Table A.2). Significantly higher SOC density was found in the topmost depth followed by the subsequent three depths; however, SOC density in the intermediate depths (between 10-30 cm and 30-50 cm) are not significantly different (Figure 3.2B), which indicates the unequal variability of SOC

with soil depth. The oligohaline zone comprises higher SOC density (gm cm^{-3}) followed by mesohaline and polyhaline zone indicating higher soil organic carbon in the low salinity areas.

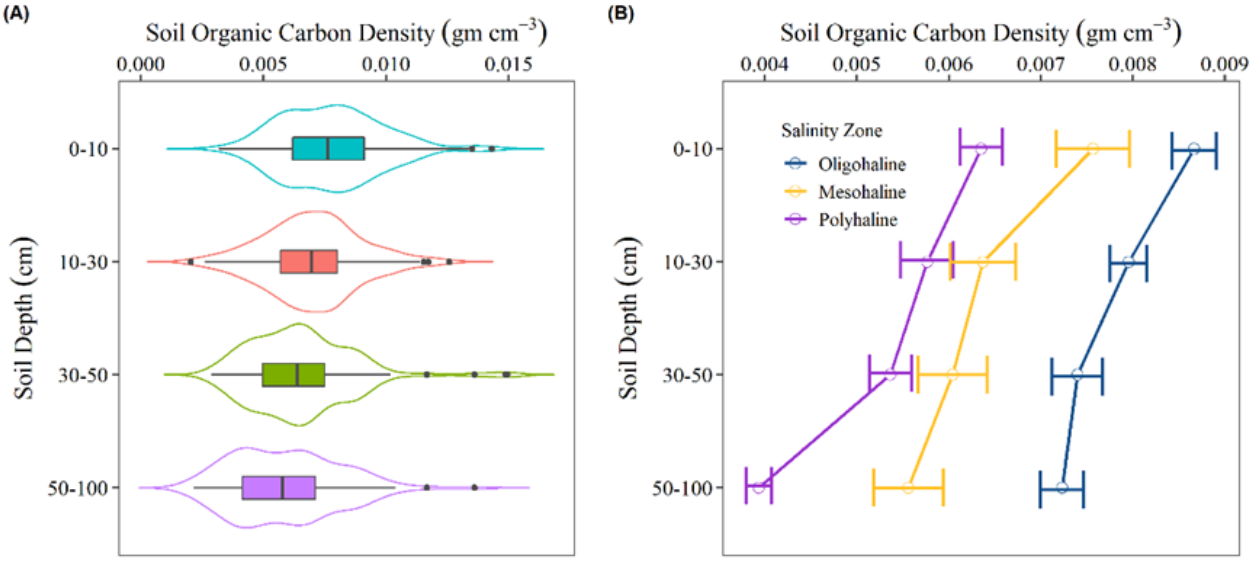

Figure 4.2: (A) The distribution of soil organic carbon (SOC) density (gm cm^{-3}) in four soil depths presented as violin-box plot, where the black vertical line represents the median and black dots are outliers. Here, the width of violin plot represents the proportion of the data located there as a measure of kernel probability density. (B) Average SOC density (gm cm^{-3}) in three salinity zones and four soil depths.

The bulk density (BD) of the soil revealed an opposite trend as significantly higher bulk density was observed in the higher salinity zones and in the 50-100 cm soil depth (two-way ANOVA for Ln (bulk density (gm cm^{-3})), salinity zones, $F_{2,\ 500} = 22.2$, $p < 0.001$ and soil depth, $F_{3,\ 500} = 46.2$, $p < 0.001$) (Figure A.1, Table A.3). Likewise, SOC density, the soil organic carbon storage (SOC) for different depths was significantly different among the three salinity zones and the four soil depths (two-way ANOVA for Ln (SOC), salinity zones, $F_{2,\ 500} = 118.9$, $p < 0.001$ and soil depth, $F_{3,\ 500} = 526.2$, $p < 0.001$) (Figure 3.3 & Figure 3.4, Table A.4). However, higher amounts of SOC were found in the 50-100 cm depth in comparison to above (Figure 3.4). The top meter SOC ranges from 26.2 Mg ha^{-1} to 107.9 Mg ha^{-1} where the oligohaline zone comprises the highest SOC (74.8 Mg ha^{-1}), followed by the mesohaline (59.3 Mg ha^{-1}), and the polyhaline zone (48.3 Mg ha^{-1}) (Table 3.2).

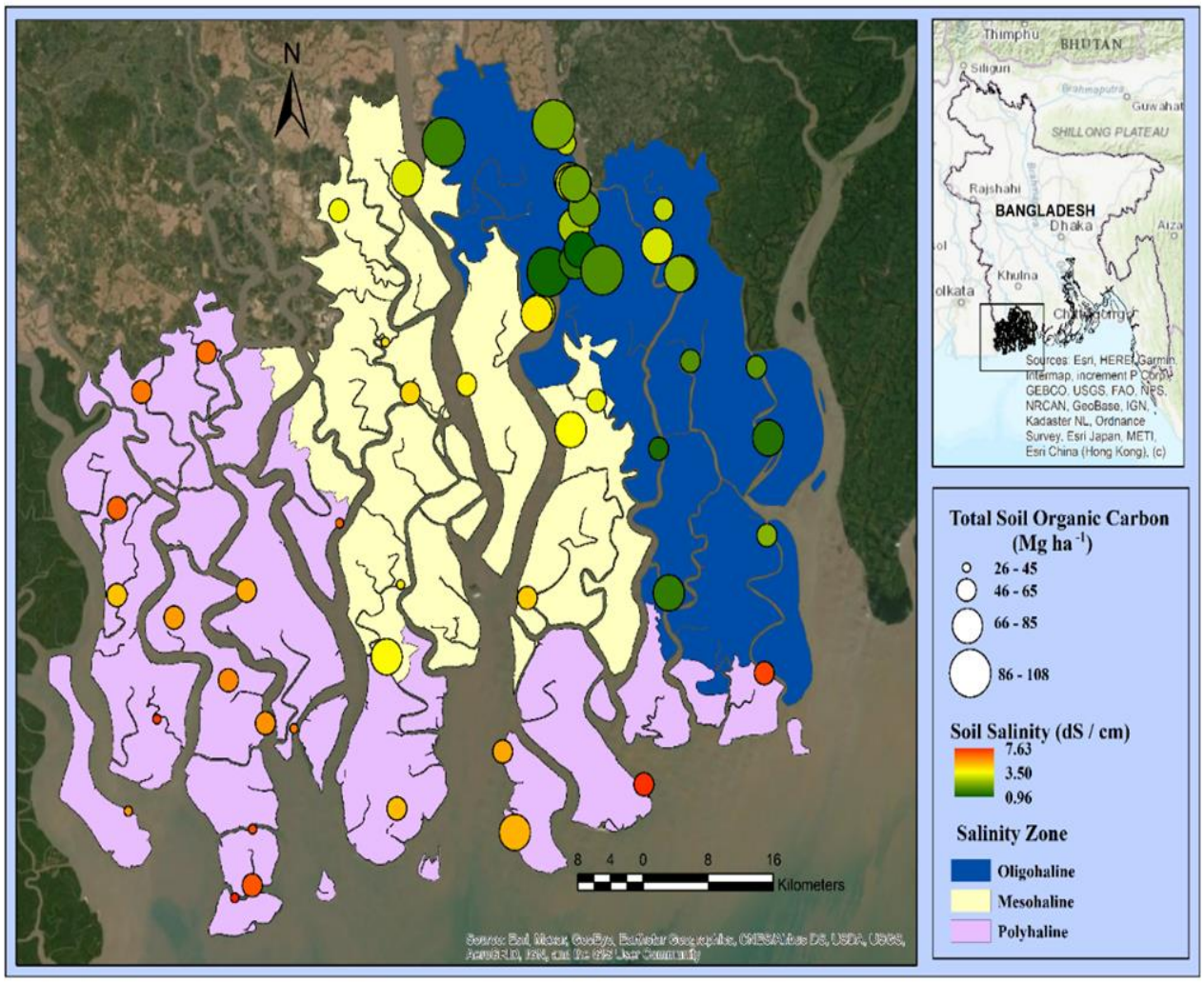

Figure 4.3: Spatial distribution of total soil organic carbon (SOC) (Mg ha^{-1}) and soil salinity (dS/cm) in the Sundarbans. Note that circle represents the amount of SOC and gradual colour ramp reveals soil salinity indicating green to red as from low to high salinity. Three major salinity zones are represented according to (Chanda et al., 2016b).

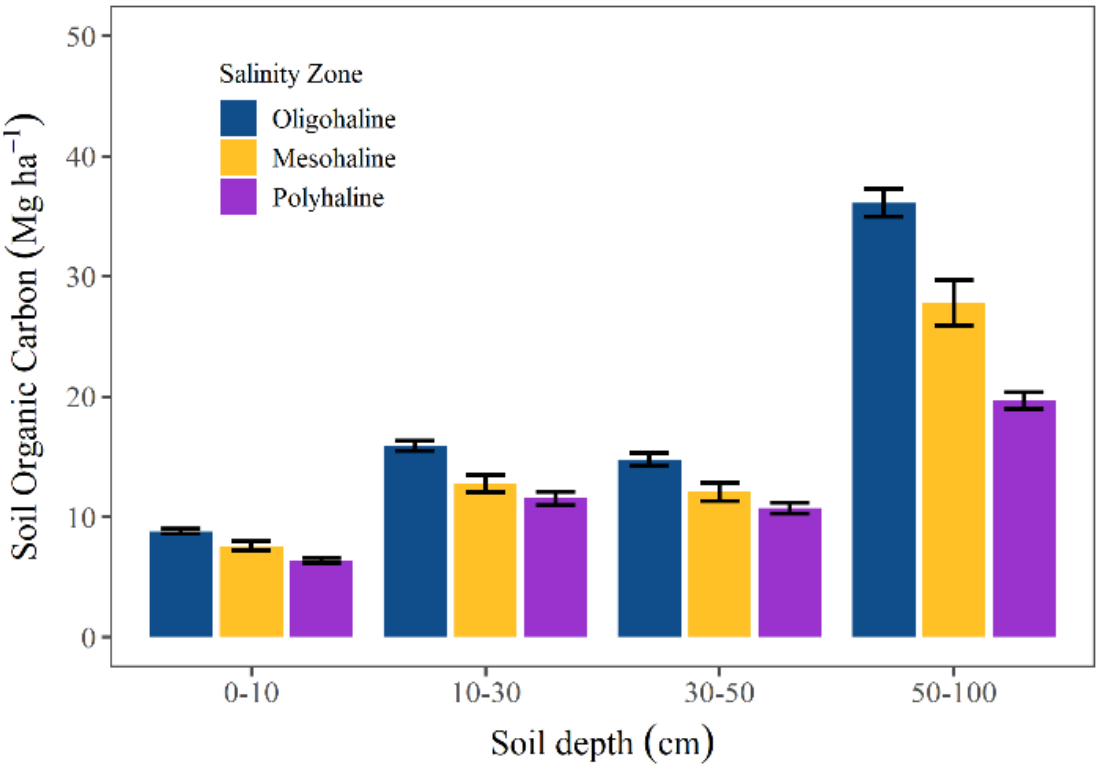

Figure 4.4: Average total soil organic carbon (Mg ha^{-1}) in different soil depth windows in three salinity zones.

Table 4.2: Overview of measured soil parameters and vegetation characteristics. Values are presented as mean (± SD), where n ≥ 3. Lowercase letters indicate significant variability among salinity zones, according to least-significant difference (LSD) test at α = 0.05.

Salinity zone	**Bulk density (gm cm^{-3})**	**Soil pH**	**Soil salinity (EC dS/cm)**	**Total Soil Organic Carbon (Mg ha^{-1})**	**Total Nitrogen (Mg ha^{-1})**	**Organic C: N**	**Elevation (m)**	**Stem Density (ha^{-1})**	**Height (m)**	**DBH (Diameter at Breast Height) (cm)**
Oligohaline	0.58 (0.07) ^{b}	7.06 (0.26) ^{c}	1.49 (0.32) ^{c}	74.77 (14.93) ^{a}	2.66 (1.19) ^{b}	21.30 (7.23) ^{a}	3.39 (1.78) ^{b}	5,009 (2,485) ^{b}	7.98 (2.03) ^{a}	8.12 (2.41) ^{a}
Mesohaline	0.62 (0.04) ^{ab}	7.43 (0.19) ^{b}	3.07 (0.56) ^{b}	59.30 (15.80) ^{b}	3.52 (1.08) ^{a}	17.30 (6.87) ^{a}	3.67 (1.01) ^{ab}	6,876 (3,290) ^{ab}	7.88 (2.63) ^{a}	8.60 (5.36) ^{ab}
Polyhaline	0.63 (0.05) ^{a}	7.80 (0.26) ^{a}	5.56 (0.85) ^{a}	48.25 (10.32) ^{c}	3.81 (0.98) ^{a}	13.08 (3.00) ^{b}	4.79 (1.52) ^{a}	8,750 (4,798) ^{a}	5.98 (1.66) ^{b}	6.72 (4.12) ^{b}

4.3.2. Soil organic carbon and forest types

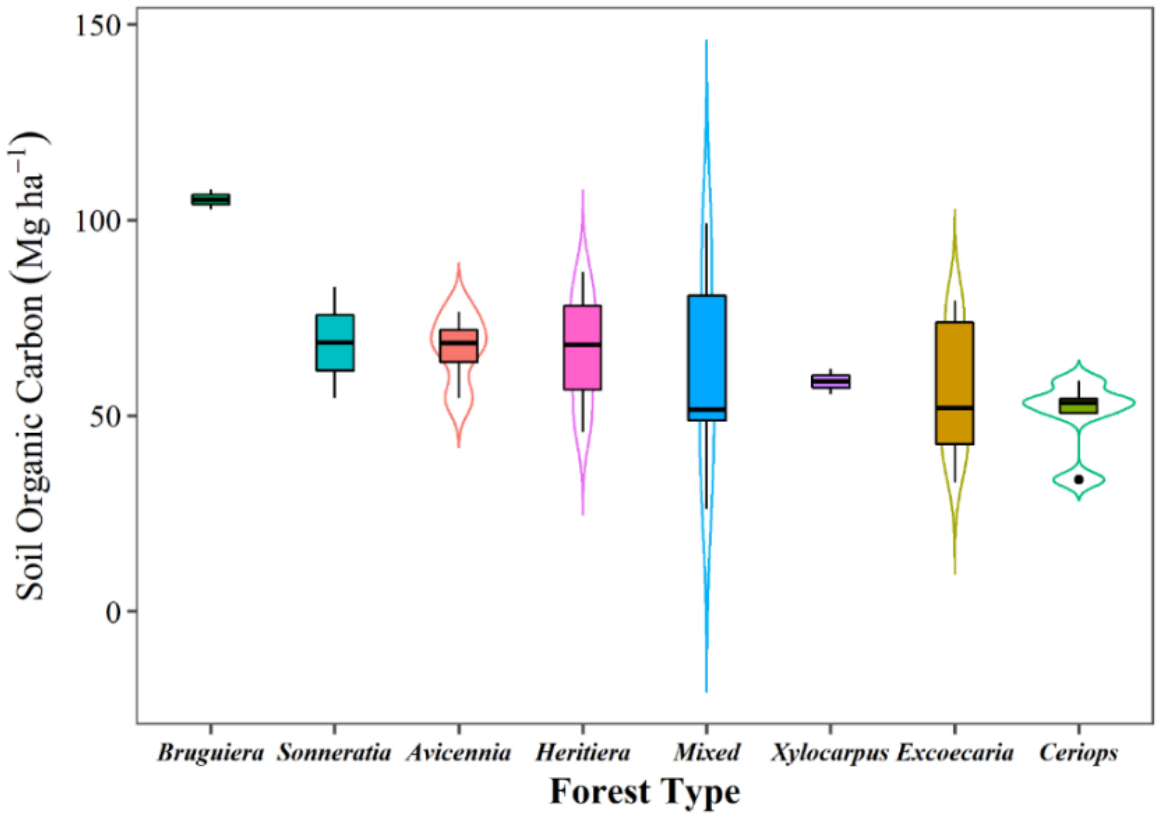

Figure 4.5: Integrated violin-box plot shows average soil organic carbon (SOC) in major forest types in the Sundarbans. The black vertical line of box plot represents the median and the width of violin plot represents the proportion of the data located there as a measure of kernel probability density.

One-way ANOVA revealed that SOC varied with major forest types in the Sundarbans ($F_{7, 47} = 3.3$, $p < 0.01$) (Table A.5). As shown in Figure 3.5, the average SOC content in the *Bruguiera* spp. stand was the highest, with an average of 105.3 Mg ha^{-1}, followed by *Sonneratia* spp. and *Avicennia* spp., with an average of 68.7 Mg ha^{-1} and 67.1 Mg ha^{-1}, respectively. The Tukey HSD test showed that the other forest types had no significant effect on SOC content, which ranges from 50.2 Mg ha^{-1} to 67.0 Mg ha^{-1} for *Ceriops* and *Heritiera* forest types, respectively (Table A.6).

4.3.3. Soil physical and chemical properties and vegetation characteristics

The soil physical and chemical properties and vegetation characteristics vary considerably among the three salinity zones (Table 3.2). As expected, oligohaline zones had relatively low average soil bulk density, pH, and soil salinity, in comparison to higher salinity zones. Additionally, significantly higher SOC and lower total N contributes higher organic C: N in the oligohaline zone, although it is similar to the mesohaline zone (p <0.05). BD and SOC density showed a statistically significant negative relationship (r = -0.47, p <0.001) (Figure 3.6A). However, the soil organic carbon (SOC) density and soil nitrogen density is significantly positively correlated with soil nitrogen density across the Sundarbans (r = 0.66, p <0.001) (Figure 3.6B). Analysis from the satellite and tree height data reveals that the average elevation of the topography is higher in the polyhaline zone. The average DBH and height of the trees were statistically significantly higher in both the oligohaline and mesohaline zone, whereas the average stem density was higher in both the mesohaline and polyhaline zone (p <0.05). The bivariate relationships between SOC and other soil physical and chemical properties and vegetation characteristics are presented in the supplementary Figure A.2.

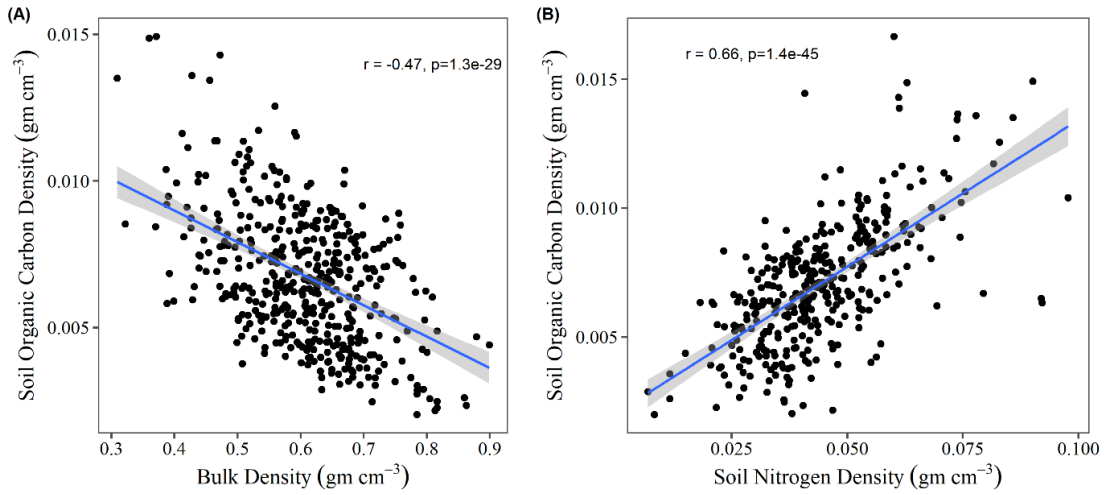

Figure 4.6: (A) Relationship between bulk density and soil organic carbon density. (B) Relationship between soil nitrogen density and soil organic carbon density.

4.3.4. Relationship of SOC with soil and vegetation properties

SOC content was positively correlated with tree DBH, tree height, organic C: N, latitude and longitude, but negatively correlated with soil salinity, bulk density, soil pH, tree density and elevation ($p < 0.05$) (Figure 3.7). As total nitrogen and species richness did not show any significant correlation with SOC content, these two parameters were discarded from the subsequent PCA analysis. The measured properties also showed a significant positive and negative correlation amongst themselves, which indicates a source of multicollinearity, a phenomenon which makes multiple regression unreliable. Therefore, principal component analysis was used to identify and group those properties that influence SOC the most to overcome the influence of multicollinearity.

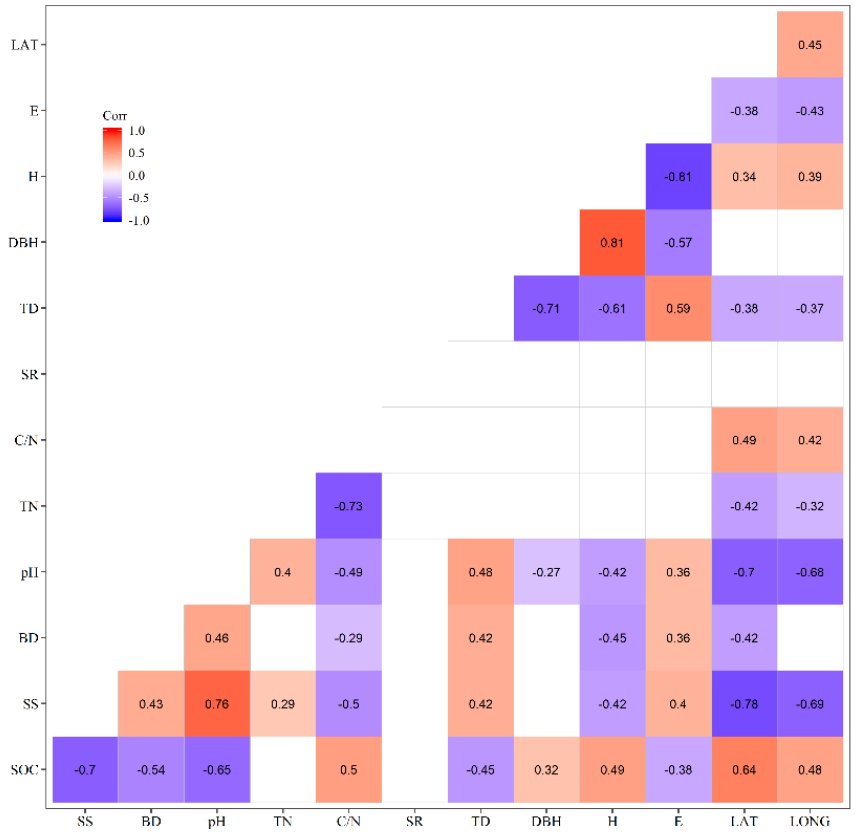

Figure 4.7: Correlation matrix among SOC and other physicochemical, geophysical and vegetation properties. The number of each block shows the Spearman's rank correlation coefficients at $p < 0.05$, where red and violet colour represents respective positive and negative correlations. The white block indicates the correlation coefficient is statistically insignificant. The soil properties: SOC = Soil organic carbon, SS= soil salinity, BD = Bulk density, pH= soil pH, TN = Total Nitrogen, C: N = organic C- total Nitrogen ratio, the vegetation characteristics: SR = Species richness, TD = Tree density, DBH = mean Diameter at Breast Height, H= Mean height and geophysical properties: E= Elevation, LAT = Latitude and LONG= Longitude.

Principal component analysis (PCA) was performed with ten variables to assemble and isolate the smallest possible variable subsets to explain the variation of the dataset (Figure 3.8). The PCA result indicates that the first two principal components explained more than two-thirds of the total variation with an eigenvalue greater than 1. The most important component (PC1) explained 49.5% with the highest loadings (>0.35) for soil SS (soil salinity) and pH. On the other hand, the second component showed higher loadings for tree H, DBH and soil C: N with 20% explained variation (Table A.7). As soil SS and pH are highly correlated with each other (r = 0.76, $p < 0.05$) (Figure 3.7), the variable with the highest loading, soil SS, was selected from the first component for the regression model. Similarly, tree H was discarded due to collinearity with tree DBH and therefore, tree DBH and soil C: N was selected from the second component.

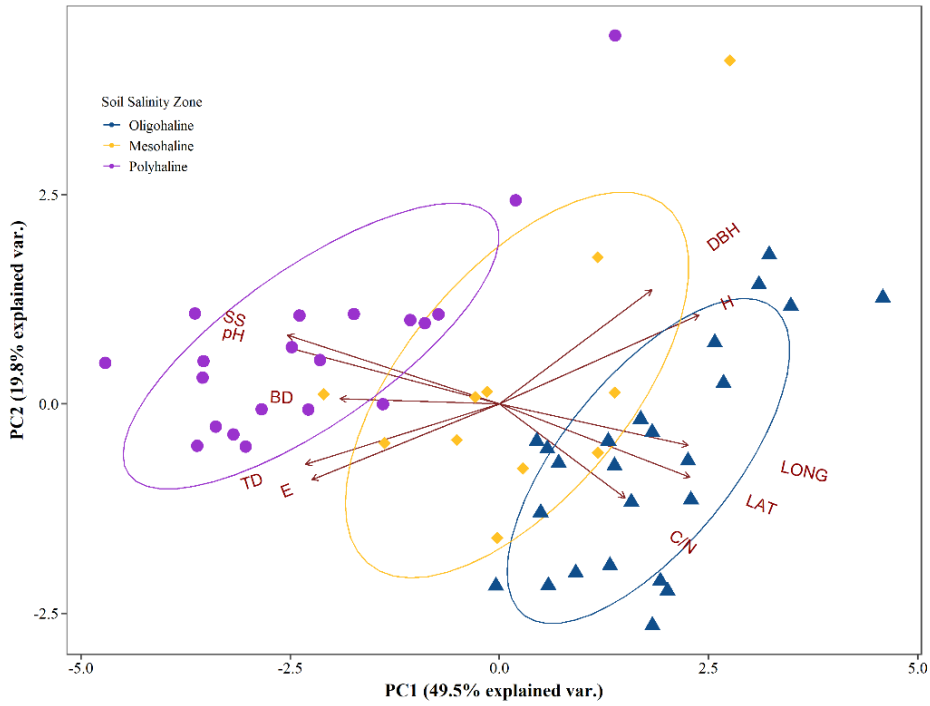

Figure 4.8: Principal component analysis (PCA) biplot of soil physicochemical, geophysical and vegetation characteristics as vectors (n = 10) and mangroves areas are coloured coded as three salinity zones (n = 55). The soil physicochemical properties included SS= soil salinity, pH= soil pH, BD = Bulk density, C: N = organic C-total Nitrogen ratio, geophysical properties comprised LAT = Latitude, LONG= Longitude, E= Elevation, and the vegetation characteristics included TD = Tree density, DBH = mean Diameter at Breast Height, H= Mean height. Here, perpendicular direction signifies uncorrelated relationship, while negative and positive correlated vectors are presented in the opposite vectors and small angle vectors, respectively.

Table 4.3: Summary statistics of regression model. Here, SS = Soil salinity, C: N = Soil organic carbon: Nitrogen and DBH= tree Diameter at breast height.

Model	R^2	Adjusted R^2	C(p)	AIC	RMSE
1. SS	0.508	0.498	18.217	-10.457	0.212
2. SS and C: N	0.590	0.574	8.650	-18.513	0.196
3. SS, C: N and DBH	0.637	0.616	4.00	-23.255	0.186

By using the PCA-derived subset of variables, the relationship between SOC and soil and vegetation properties was obtained by using stepwise multiple linear regression (MLR). The regression results showed that soil salinity alone could explain 50% SOC variability in the Sundarbans, however, the skill of the model increases to 57% and 62% when soil C: N or soil C: N and tree DBH are added to the model (Table 3.3). Although all three regression models are highly significant (Table A.8), the best subset of MLR model was selected based on the largest adjusted R^2 value and the smallest Mallow's Cp, AIC (Akaike Information Criteria) and RMSE (Root Mean Squared Error) and presented in Eq.1.

$$\text{Ln}\,(\text{SOC}) = 3.439 - 0.077\,\text{SS} + 0.274\,\text{Ln}\,(\text{C: N}) + 0.017\,\text{DBH} \quad \text{Eq. 1}$$

4.4. Discussions

The reported average soil organic carbon (SOC) density in this study is lower than previous estimates for the Sundarbans and far lower than average estimates of SOC density from global mangroves (Table 3.1). SOC density, the standardized carbon stocks measurement with depth, is the most useful parameter to compare SOC between different forests (Donato et al., 2011; Weiss et al., 2016). However, due to unreported bulk density, it was not possible to convert from the reported organic carbon (%) to SOC density for most studies. Despite a greater range of soil organic carbon (SOC) percentage in this study (0.3 – 4.4%), the average value (1.2%) is in line with most previous studies, although higher than estimates published by Ray et al. (2011), Banerjee et al. (2012), and Allison et al. (2003). These differences are likely to be attributed to variable sampling strategies along with variable soil depth or different methods used for carbon estimation. Likewise SOC density, the

average top 1 m SOC storage in the Bangladesh Sundarbans (50.9 ± 15.2 Mg ha^{-1}) is almost half of the previous estimate by Rahman et al. (2015a), Sanderman et al. (2018) and Atwood et al. (2017). Estimates of soil organic carbon could fluctuate based on the differences in sampling design, choice of analytical method and soil depth (Howard et al., 2014; Nayak et al., 2019). In the case of mangroves, Passos et al. (2016) found overestimation of organic carbon measured with the oxidation method in comparison to the elemental analyser. Anaerobic microbial decomposition yields reduced soil compounds (i.e., Fe^{2+}, S^{2-}, Mn^{2+}, and Cl^{-}) in mangroves, which might interfere with organic carbon determination with chemical oxidation method (Nelson and Sommers, 1996; Bisutti et al., 2004; De Vos et al., 2007; Nóbrega et al., 2015). Apart from using different methods, the SOC variation may originate from the consideration of soil depth in the sample design as the SOC concentration is a function of soil depth and shows considerable variability (Wuest, 2009; Kauffman and Donato, 2012; Jandl et al., 2014). Moreover, using coring for sampling might have an influence on soil bulk density estimation leading to lower SOC stocks estimation in deeper soils (Rau et al., 2011; Gross and Harrison, 2018).

In comparison to global studies, the estimated top 1 m SOC stocks are lower in the Sundarbans than the reported average from sites distributed all over the world (Table 3.1). Based on model-based georeferenced database of mangrove SOC, the global SOC map showed that the Sundarbans contains the lowest SOC stocks per ha in the world (Sanderman et al., 2018). Compared to direct estimates from 190 global sites by Kauffman et al. (2020), the Sundarbans contains higher SOC than only two other mangrove forests, the Porto Céu mangrove in Brazil (48 Mg ha^{-1}) and the Bu Tinah Janoub in the United Arab Emirates (33 Mg ha^{-1}), located in lower and higher latitudes respectively than the Sundarbans. However, global comparison in soil carbon among tropical, subtropical and temperate mangroves showed a contrasting relationship with latitude (Atwood et al., 2017; Twilley et al., 2018; Kauffman et al., 2020; Ouyang and Lee, 2020). Both Kauffman et al. (2020) and Ouyang and Lee (2020) found significantly lower soil carbon in mangroves >20 °N, although the former study had fewer samples largely limited to the middle east hyper arid mangroves. On the other hand, Atwood et al. (2017) and Twilley et al. (2018) documented the poor relationship between latitude and SOC

stocks. This poor relationship might be attributed due to the poor representation of samples in the studies from the subtropical mangroves like the Sundarbans.

The low soil carbon in the Sundarbans is largely due to high mineral sediment deposition (Sanderman et al., 2018; Twilley et al., 2018), low burial rate (Ray et al., 2011), rapid turnover rate (Ray et al., 2018), historical logging, stand age (Marchand, 2017), plant litter quality (Rovai et al., 2018) and biological processes. Being both a tide and river-dominated ecosystem, the carbon allocation in the above and below-ground is very complex, largely dependent on the local and regional geomorphic and geophysical drivers (Twilley et al., 2018). In riverine deltas, trees invest much of the carbon to the above-ground to keep pace with sedimentation and sea-level rise, which is evident in the oligohaline zone with greater forest productivity (Twilley et al., 2018; Sarker et al., 2019a; Sarker et al., 2019b). Moreover, research has highlighted that mangroves subjected to frequent cyclones leading to temporary losses of above-ground carbon are usually followed by rapid below-ground carbon gains during recovery process according to the 'Ecosystem Development' theory (Odum, 1969; Danielson et al., 2017; Kominoski et al., 2018). These rapid carbon gains in the above-ground and the disturbance from the catastrophic cyclones could be the source of higher autochthonous input to the below-ground. Nonetheless, higher tidal amplitude in the Sundarbans leads to higher carbon export totalling 7.3 Tg C yr^{-1} to the adjacent Bay of Bengal, which is higher than any other mangroves in the world (Ray et al., 2018). This rapid carbon turnover results in reduced burial of organic matter (0.18%) in the soil (Ray et al., 2011). Moreover, the pronounced tidal cycle in the Sundarbans affects carbon burial process by altering soil water chemistry (Chatterjee et al., 2013; Spivak et al., 2019). Besides the high carbon turnover rate, the Sundarbans is believed to have become tidally active in the recent past due to reduced freshwater flow from the Ganges-Brahmaputra-Meghna river (Rogers et al., 2013; Hale et al., 2019). However, despite the historical reduction of sedimentation, the Sundarbans is itself still keeping pace with sea-level rise with the highest average surface elevation and vertical accretion rate (0.74 and 2.71 cm yr^{-1}) compared to the worldwide average (Bomer et al., 2020a; Bomer et al., 2020b). This high sedimentation rate is the outcome of the massive flux of clastic sediments which attenuates the amount of organic carbon per unit area.

The century-long historical exploitation in the Sundarbans before the felling moratorium in 1989 has largely decreased the population of threatened tree species (Siddiqi, 2001; Sarker et al., 2011). This in turn is likely to have lessened the continuous autochthonous input of organic matter in the forest and reduced the overall stand age. Studies also showed that historical harvesting had altered the species composition in the Sundarbans, with decreasing abundances of *Heritiera fomes*, *Ceriops decandra* and *Xylocarpus mekongensis* and increasing for *Excoecaria agallocha* (Sarker et al., 2016). The SOC stocks also depends on the age of the stands as evident in the chrono sequence study on SOC stocks in French Guiana which revealed that the SOC varied from 4 to 107 Mg ha^{-1} from young stand to senescent stage (Marchand, 2017). In addition, studies have suggested that lower organic carbon in the soil is mostly associated with higher C: N of the plant litter which has resulted from lowering decomposition speed and decreasing carbon-use efficiency of the decomposer (Bouillon et al., 2003; Zhou et al., 2019). Compared to mangrove associates, the senescent leaves of true mangroves contain considerably higher C: N (~33) in the Indian part of Sundarbans (Chanda et al., 2016a). Kamruzzaman et al. (2019) observed a decreasing trend of C: N of the leaf litter in both forest floor and buried condition starting from 40, but barely reached below 30 after 196 days of decomposition study, suggesting N limitation in the oligohaline zone of the Bangladesh Sundarbans. The low organic carbon can also be attributed to the abundance of leaf-consuming organisms ingesting organic litter detritus both at surface and subsurface in burrows. The Sundarbans encompasses a wide range of gastropod species (for example, *Cerithedia cingulata*, *Cymia lacera*) that predominantly consume mangrove detritus (Nayak et al., 2014).

Variation in SOC stocks among different forest types is often mediated by the primary productivity, resources allocation in different parts (for example, above and below-ground) and microorganism activity which is driven by a number of biological (example, bioturbation and species composition) and physical (for example, soil texture, salinity, inundation and nutrients) factors (McLeod et al., 2011). Therefore, differing stand structure and composition of mangrove forests in different tidal regimes yield variable SOC stocks (Lacerda et al., 1995; Gleason and Ewel, 2002). Moreover, the long and short-term resilience and resistance of microbial communities is largely dependent on the

structure and zonation of mangrove communities reflecting environmental gradients (Capdeville et al., 2019). In this study, the species with higher SOC stocks such as *Bruguiera* spp., *Sonneratia* spp. and *Avicennia* spp. are frequently inundated due to proximity to the river and low lands as compared to other species in the Sundarbans (Siddiqi, 2001; Sarker et al., 2016). These high inundation regimes, in turn, lead to increased microbial activity and a higher level of dissolved organic carbon in the (Wang et al., 2013; Chambers et al., 2014; Chambers et al., 2016). Regular tides also bring sediments along with high allochthonous input whereas the raised less-inundated areas foster autochthonous SOC and less microbial activity (Lovelock et al., 2015b; Woodroffe et al., 2016). Rao et al. (1994) found almost double C: N ratio in fresh leaves of *Bruguiera* spp. compared with other mangrove species, suggesting a higher input of autochthonous carbon. Being the pioneer species in the succession of the Sundarbans, both *Sonneratia* spp. and *Avicennia* spp. are resilient to disturbances leading to higher SOC than climax and seral species (Table A.1) and accumulate a large quantity of organic litter in the tidal channel close to the river or seafront (Sarker et al., 2016; Bomer et al., 2020a). The variability of SOC stocks found here among forest types followed a similar pattern to the global studies by Atwood et al. (2017), except for *Sonneratia* spp. which was found to hold less SOC stocks than *Heritiera* and *Ceriops*. On the other hand, Kauffman et al. (2020) found significantly lower below-ground carbon stocks in *Avicennia* spp., especially in the arid mangroves of Middle-East Asia, which is solely occupied by this species. Therefore, the impact of above-ground vegetation on below-ground is largely site-specific, and depends on a wide range of factors.

The unexplained variation of the best multiple regression models (R^2 = 0.64) highlights the necessity of including other soil and environmental parameters such as soil cations and anions, clay characteristics and texture, precipitation, temperature, and river discharge. This study did not address these properties but suggests future studies incorporate a wider range of parameters to gain a better understating of organic carbon dynamics in the Sundarbans. In particular, for better ecosystem management, future research should include information relating to contextualising soil (for example, soil texture, grain size and minerology), biogeochemical (for example, important properties of soil and pore-water chemistry such as sulphate, oxygen, nitrate, ferric oxides in case of mangroves) and

ecological (for example, vegetation and plat-microbe interaction) properties (Luo et al., 2019; Spivak et al., 2019). However, soil salinity is considered as the outcome or proxy for the combined impact of these climatic and environmental variables in the Sundarbans resulting pronounced differences of SOC stocks among the three salinity zones (Sarker et al., 2016; Sarker et al., 2019b; Rahman et al., 2020). Several previous studies have confirmed that salinity determines the strong zonation of tree species and diversity in the Sundarbans, which in turn leads to comparatively higher diversity and taller tree species in the oligohaline followed by mesohaline and polyhaline zone (Aziz and Paul, 2015; Sarker et al., 2016; Sarker et al., 2019a; Sarker et al., 2019b; Rahman et al., 2020). Comparatively higher productive trees (for example, higher DBH and higher height) promotes organic matter accumulation through producing higher litter mass and increases SOC stocks by forming stable aggregates from roots and pneumatophores (Lange et al., 2015). The three salinity zones also comprise differential soil physical and chemical properties and vegetation characteristics that usually affects SOC storage by influencing microbial decomposition, soil water chemistry, plant-microbe interaction, and plant litter quality. While comparing nutrient concentration in the leaf litter of *Sonneratia apetala*, one of the major pioneer species in the Sundarbans, Nasrin et al. (2019) found lowest concentrations of N, P and K and the highest concentrations of Na in the polyhaline zone, reflecting higher C: N in the leaf litter. However, the low SOC in the polyhaline zone is also coincided with the low C: N indicting inwelling of marine and terrestrial suspended particulate materials (Bouillon et al., 2003). The strong positive correlation ($r = 0.66$, $p < 0.001$) between carbon and nitrogen density indicates that the source of carbon and nitrogen is likely to be same and can vary spatially (Matsui et al., 2015).

Although the Sundarbans is considered to be of recent origin, the large accommodation space exists due to accretion and erosion with historical relative sea-level variability (Goodbred and Kuehl, 2000; Tyagi and Sen, 2019). Therefore, the Sundarbans might have a 3 m organic layer in the seaward direction and much more in the landward (Allison et al., 2003). By considering this vertical depth and the area covered by mangrove forest, the Sundarbans are likely to contain considerable volumes of soil organic carbon. Previous research has demonstrated that mangroves holding higher carbon

storage also have a higher rate of deforestation with 50% mangrove loss attributed to Indonesia, which holds about 25% of soil carbon in the world's mangroves; the figure increases to 75% when Malaysia and Myanmar are considered (Atwood et al., 2017). Therefore, mangroves from these countries are considered as a significant source of emissions due to high deforestation and forest conversion (Hamilton and Friess, 2018). On the other hand, in Bangladesh, despite the lower SOC stocks in the Sundarbans mangrove forest demonstrated by this paper, recent positive trends in forest cover demonstrate the value of blue carbon conservation and an improved understanding of carbon storage will be of benefit to the inclusion of mangroves in national and international climate strategies and policies.

4.5. Conclusions

The top meter of soil organic carbon (SOC) per area in the Bangladesh Sundarbans is lower than has previously been reported. However, the total SOC will likely to be greater if total vertical depth is considered. The soil organic carbon stocks (SOC) in the Sundarbans is largely influenced by soil salinity, probably by amending the forest productivity and microbial activity. The results highlighted that increasing salinity as result of predicted sea-level rise will likely have pronounced effects on future soil carbon accumulation rates by altering the soil environment and vegetation characteristics. The study underlines the importance of spatial conservation planning measures and initiatives to conserve and maximize carbon accumulation and to contribute to global climate change adaptation and mitigation strategies. Results suggest that high sediment carbon zone in the eastern part of the Sundarbans is highly vulnerable to tourism and economic development activities. In terms of climate change mitigation and adaptation, the conservation of the existing carbon stocks should receive much higher priority rather than the debates of high-low carbon stocks. The Bangladesh Sundarbans can act as an important blue carbon hotspot due to the high sedimentation and carbon sequestration rate and conservation priority by the government. However, disturbances such as sea-level rise, global warming, eutrophication, and landscape development might hinder this conservation activities in the future.

Chapter 5

Biomass estimation in mangrove forests: a comparison of allometric models incorporating species and structural information

Rahman, M.S., Donoghue, D.N.M., Bracken, L.J., Mahmood, H., 2021. Biomass estimation in mangrove forests: a comparison of allometric models incorporating species and structural information. **Environmental Research Letters**. 16(11), http://iopscience.iop.org/article/10.1088/1748-9326/ac31ee

Abstract

Improved estimates of above-ground biomass are required to improve our understanding of the productivity of mangrove forests to support the long-term conservation of these fragile ecosystems which are under threat from many natural and anthropogenic pressures. To understand how individual species affects biomass estimates in mangrove forests, five species-specific and four genus-specific allometric models were developed. Independent tree inventory data were collected from 140 sample plots to compare the above-ground biomass (AGB) among both the species-specific models and seven existing frequently used pan-tropical and Sundarbans-specific generic models. The effect of individual tree species was also evaluated using model parameters for wood densities (from individual trees to the whole Sundarbans) and tree heights (individual, plot average and plot top height). All nine species-specific models explained a high percentage of the variance in tree AGB (R^2 = 0.97 to 0.99) with the diameter at breast height (DBH) and total height (H). At the individual tree level, the generic allometric models overestimated AGB from 22% to 167% compared to the species-specific models. At the plot level, mean AGB varied from 111.36 Mg ha^{-1} to 299.48 Mg ha^{-1}, where AGB significantly differed in all generic models compared to the species-specific models ($p < 0.05$). Using measured species wood density (WD) in the allometric model showed 4.5% to 9.7% less biomass than WD from a published database and other sources. When using plot top height and plot average height rather than measured individual tree height, the AGB was overestimated by 19.5% and underestimated by 8.3% ($p < 0.05$). The study demonstrates that species-specific allometric models and individual tree measurements benefit biomass estimation in mangrove forests. Tree level measurement from the inventory plots, if available, should be included in allometric models to improve the accuracy of forest biomass estimates, particularly when upscaling individual trees up to the ecosystem level.

5.1. Introduction

There has been a global effort to develop accurate and efficient methods to quantify above-ground carbon (measured as biomass) in mangrove forests (Hutchison et al., 2014; Ni-Meister, 2015; Baccini

et al., 2017; Lagomasino et al., 2019). A range of remote sensing technologies can indirectly infer forest biomass but field data are needed to calibrate and validate products (Gibbs et al., 2007; Chave et al., 2019; Réjou-Méchain et al., 2019). Destructive harvesting of trees provides the most precise estimates of above-ground biomass (AGB), yet is impractical, laborious, costly and often illegal (Komiyama et al., 2008; Edwards et al., 2019) and so mathematical models have been developed to estimate tree biomass from easily measured biophysical parameters (tree diameter at breast height (DBH), height (H), or wood density (WD)) (Brown, 1997; Komiyama et al., 2005; Picard et al., 2012; Chave et al., 2014). These models are known as allometric models. However, this method of estimation can yield a large degree of uncertainty scaling up from individual tree biomass to plot- and forest-level as uncertainties associated with individual trees are propagated (van Breugel et al., 2011; Petrokofsky et al., 2012; Réjou-Méchain et al., 2019). The choice of appropriate allometric model is therefore critical to reduce uncertainties in the estimation of forest biomass.

All allometric models have limitations since they are based on a limited number of destructively sampled trees and often the sample locations are unrepresentative of forest heterogeneity (Weiskittel et al., 2015; Hickey et al., 2018). These models also introduce an uncertainty when applied to species without destructive sampling (Mitchard et al., 2013; Ngomanda et al., 2014; Mahmood et al., 2019). For example, De Souza Pereira et al. (2018) found AGB estimation errors between minus 18% and plus 14% when using biome-specific allometries rather than species-specific ones in Brazilian mangrove forests. On the other hand, a few studies have shown that generic models can outcompete locally developed models (Rutishauser et al., 2013; Stas et al., 2017). Uncertainties also arise from inappropriate use of regression models without considering collinearity of parameters, uncritical use of model dredging and inappropriate criteria for model selection (Sileshi, 2014; Vorster et al., 2020). Recently published global and continental AGB estimates contain errors due to an under representative sample size and the exclusion of the climatic regime, geophysical and geomorphological variables, which are key to understanding the spatial distribution of biomass (Rovai et al., 2016). Inclusion of biophysical parameters such as wood density and tree height can help to capture geographical heterogeneity and also act as a suitable proxy of environmental drivers such as

variations in salinity which affects the growth rate, wood density, species composition and tree height (Mahmood et al., 2019; Rahman et al., 2020; Virgulino-Júnior et al., 2020; Rahman et al., 2021b).

Although wood density is an important variable for assessing carbon content, it is rarely measured during field inventories. Most studies identify species and then use published wood density values from a database of generic values (Njana et al., 2016; Réjou-Méchain et al., 2019). Using the same or grouped wood density in the allometric model tends to smooth species-level variations in AGB (Mitchard et al., 2013; Ni-Meister, 2015). The inclusion of tree height has a large effect on individual tree and forest AGB (Feldpausch et al., 2012). Any errors introduced during individual tree height measurements can originate from the choice of methods and/or instruments and can be propagated as estimates are scaled up (Larjavaara and Muller-Landau, 2013). For example, the use of Height-Diameter (H-D) models, developed from the height and stem diameter of individual trees, often exhibit uncertainty due to wider height-variation at different spatial scales (Feldpausch et al., 2011; Vieilledent et al., 2012). Space-borne and air-borne LiDAR and RADAR technologies can improve the accuracy of the height measurement and have been used to develop canopy height models (CHM) (Fatoyinbo et al., 2021).

The Sundarbans mangrove forest is one of the largest and most bio-diverse mangroves in the world, located across Bangladesh and India. It contains the highest carbon densities (345 Mg ha^{-1}) in both above- and below-ground among all forests in Bangladesh (GOB, 2019; Henry et al., 2021). The Bangladesh Forest Department estimated carbon stocks in the Sundarbans in 2009 and 2015 using pan-tropical allometric models and Sundarbans-specific generic models (BFD, 2010; Rahman et al., 2015a; Mahmood et al., 2019; Henry et al., 2021). Other studies such as Kamruzzaman et al. (2017) and Azad et al. (2020) used pan-tropical generic models to estimate AGB in selected areas. However, species-specific allometric models are not yet available to estimate above-ground biomass in the Sundarbans. Therefore, it is timely to examine whether species-specific allometric models using measured wood densities and tree heights can yield more accurate estimates of AGB in the Sundarbans and in mangrove forests more generally. The aim of this paper is to report research that compares a range of sources of uncertainty in allometric models, wood density, and height

measurement for AGB in the Sundarbans mangrove forest, Bangladesh. First, the study compares site- and species-specific AGB between the Sundarbans and pan-tropical generic allometric models for variability of above-ground tree biomass. Secondly, the study determines variability of AGB in the Sundarbans by comparing measured and published wood density values at multiple spatial scales. Thirdly, the study quantifies the impact of different methods of tree height determination on estimates of AGB in mangrove forests.

5.2. Material and methods

5.2.1. Study area

The Bangladesh Sundarbans is situated between 21º30' N and 22º30' N and 89º00' E and 89º55' E in the lower plain of the Ganges-Brahmaputra-Meghna (GBM) delta covering an area of 6,017 km^2 (Figure 4.1) (Giri et al., 2011; Aziz and Paul, 2015; Sarker et al., 2016). The forest is of international significance as a Ramsar and UNESCO World Heritage site. It provides a number of valuable ecosystem services such as protecting inland areas from storms and tidal surges (Barua et al., 2020). The near-constant mean annual minimum and maximum temperature (29 ºC – 31 ºC) and high annual rainfall (1474 mm to 2265 mm) made the climate of the Sundarbans warm and humid between 1948 and 2011 (Chowdhury et al., 2016; Sarker et al., 2016). The soil is fine-gained silt and clay and slightly calcareous (Siddiqi, 2001). The Sundarbans has a distinct salinity zonation with the high salinity zone in the west (polyhaline) to low salinity zone (oligohaline) in the east along with medium salinity zone (mesohaline) between (Siddiqi, 2001; Chanda et al., 2016b). Salinity regulates the geomorphology and hydrological characteristics and also the morphology, growth and distribution of plant species (Sarker et al., 2016; Sarker et al., 2019a; Rahman et al., 2020; Rahman et al., 2021b).

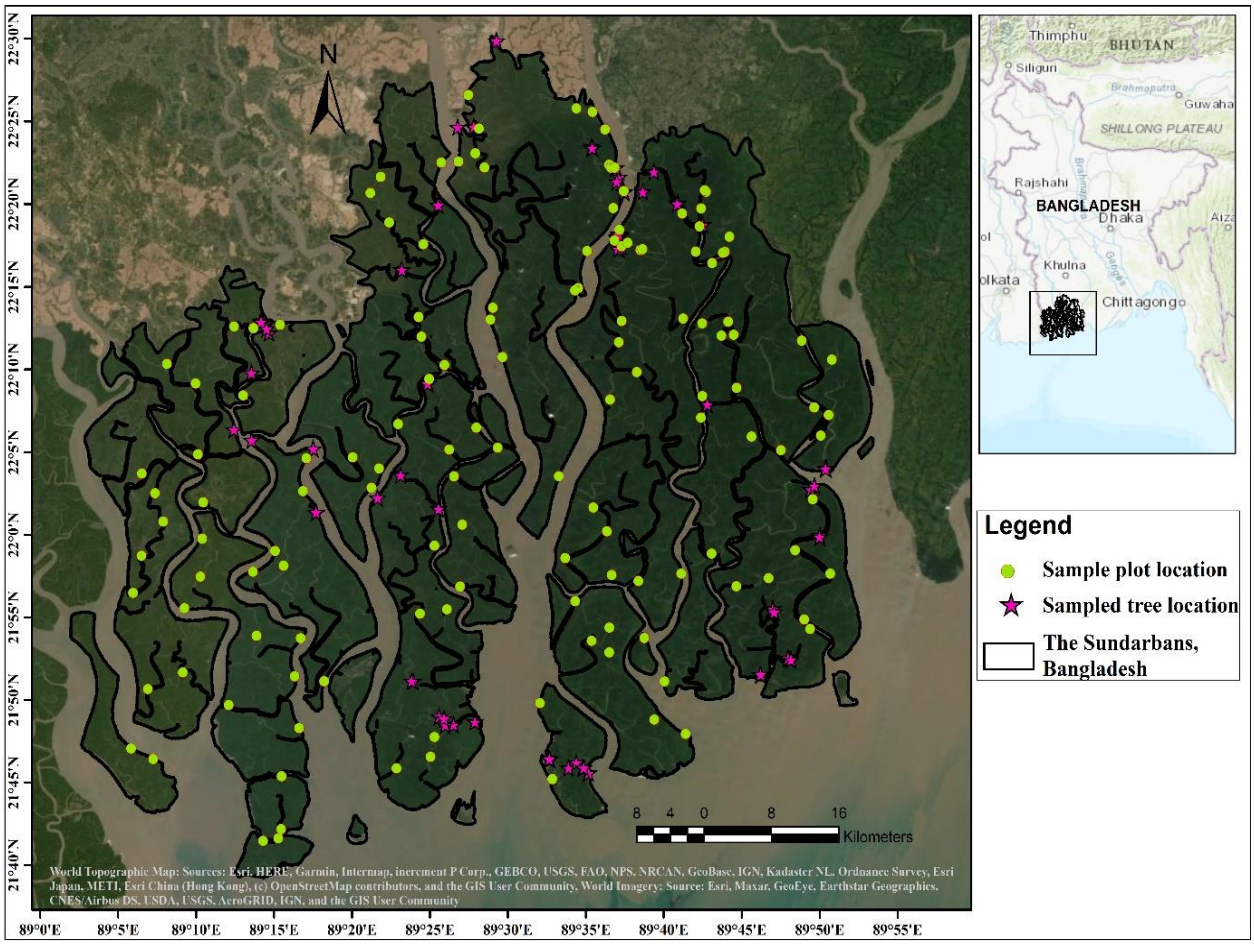

Figure 5.1: Sample plot location in the Sundarbans mangrove forest, Bangladesh. The pink star indicates tree location by Mahmood et al. (2019).

5.2.2. Allometric models in the Sundarbans

Species-specific allometric models are not available for all species in the Sundarbans as destructive sampling was not permitted due to an imposed felling moratorium since 1989 (Mahmood et al., 2019). However, four species-specific models were developed through destructive sampling in the Bangladesh Sundarbans (Table 4.1). Three generic allometric models were recently developed for 14 species by using semi-destructive sampling methods where biomass of stems and larger branches were measured through volume and wood density, and small branches and foliage through weighing after pruning (Mahmood et al., 2019). Published pan-tropical models have also been used to estimate biomass in the Sundarbans (Rahman et al., 2015a; Kamruzzaman et al., 2017; Kamruzzaman et al., 2018).

Table 5.1: Allometric models used for measuring above-ground biomass in the Sundarbans

Model no.	Site, Species	Allometric model	N	Identity in this paper and source
Bangladesh Sundarbans and Species-specific				
1	*Aegialitis rotundifolia*	$AGB=5.49GCH^2- 251.36\ H – 0.07\ HCH +0.75\ (GCH\times H \times HCH)$	29	Siddique et al. (2012)
2	*Aegiceras corniculatum*	$\sqrt{AGB}= 0.48\ DBH-0.13$	50	Mahmood et al. (2016b)
3	*Ceriops decandra*	$AGB= 4.70\ GCH^{2.41}$	48	Mahmood et al. (2012)
4	*Kandelia candel*	$AGB= 0.21\ DBH^2+0.12$	25	Mahmood et al. (2016a)
Bangladesh Sundarbans and generic model				
5	For 14 species *Aglaia piculate*, *Avicennia officinalis*, *Avicennia marina*, *Bruguiera gymnorrhiza*, *Bruguiera piculate* , *Excoecaria agallocha*, *Heritiera fomes*, *Lumnitzera piculat*, *Rhizophora piculate*, *Rhizophora mucronata*, *Sonneratia apetala*, *Sonneratia caseolaris*, *Xylocarpus granatum*, *Xylocarpus moluccensis*	$\ln(AGB)= -1.9272+2.3517\ \ln(DBH)$	260	Mahmood_2019_D (Mahmood et al., 2019)
6		$\ln(AGB)= -2.4317+2.1341\ \ln(DBH) +0.4953\ \ln(H)$	260	Mahmood_2019_DH (Mahmood et al., 2019)
7		$\ln(AGB)= -6.7189+2.1634\ \ln(DBH) +0.3752\ \ln(H)+0.6895\ \ln(WD)$	260	Mahmood_2019_DHW (Mahmood et al., 2019)
World or Pantropical and generic model				
8	Pantropical, all species	$AGB= 0.0673\times(WD\times DBH^2\times H)^{0.976}$	4,004	Chave_2014_DHW (Chave et al., 2014)
9	Pan-tropical, mangrove species	$AGB= 0.0509\times(WD\times DBH^2 \times H)$	84	Chave_2005_DHW (Chave et al., 2005)
10	Pan-tropical, mangrove species	$AGB= WD \times \exp(-1.349+1.980\ \ln(DBH) +0.207\ (\ln(DBH))^2 -0.0281\ (\ln(DBH))^3)$	84	Chave_2005_DW (Chave et al., 2005)
11	South-East Asia, mangrove species	$AGB= 0.251\times WD\times DBH^{2.46}$	104	Komiyama_2005_DW(Komiyama et al., 2005)

Here AGB = Total above-ground biomass (Kg), N = Number of destructive/semi-destructive samples, DBH = Diameter at breast height (cm), H = Total height (m), WD = Wood density (gm cm^{-3}, model-7: kg m^{-3}), GCH= Girth at collar height (cm), HCH = Height of collar girth point (m).

5.2.3. Development of species-specific allometric model

A conceptual diagram of the research methodology is presented in the Figure 4.2. The species-specific allometric models were developed from the semi-destructive sampling (324 individuals, 13 species, except *Sonneratia caseolaris*) from Mahmood et al. (2019), where above-ground biomass (kg/tree) was presented along with diameter at breast height (DBH) and total height (H) (Figure 4.1). Species-specific models for *Sonneratia caseolaris* were not developed as the independent tree inventory data did not have any individuals of this species. Out of 13 species, eight species (*Avicennia officinalis, A. marina, Bruguiera gymnorrhiza, B. piculate , Rhizophora piculate, R. mucronata, Xylocarpus granatum* and *X. moluccensis*) were merged into genus level to yield sufficient data for model fitting.

Therefore, nine allometric models were developed for *Aglaia piculate*, *Avicennia* spp., *Bruguiera* spp., *Excoecaria agallocha*, *Heritiera fomes*, *Lumnitzera piculat*, *Rhizophora* spp., *Sonneratia apetala*, and *Xylocarpus* spp.

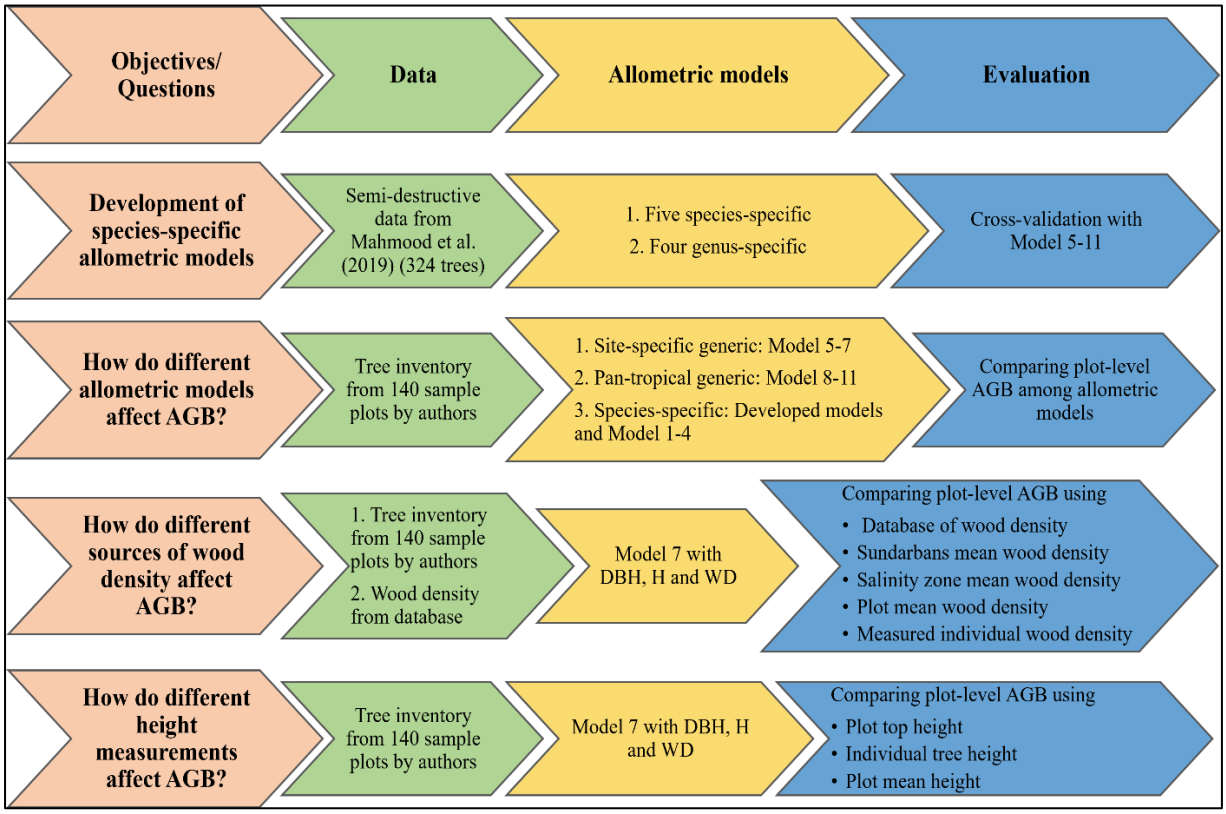

Figure 5.2: Conceptual diagram of the research methodology. The model numbers are labelled according to Table 4.1. Here, DBH: Diameter at Breast Height, H: Height and WD: Wood density.

Log-linear ordinary least square regression (OLS) was used to fit models to predict above-ground biomass for each species. The choice of log-linear regression over nonlinear regression was done by comparing the error distribution of biomass. According to Xiao et al. (2011), the linear regression of log-transformed data better characterizes multiplicative, heteroscedastic and lognormal error, whereas the nonlinear regression performs additive, homoscedastic, normal error. The goodness of fit of two models were compared and the lower value of Akaike's information criterion (AIC) provides significantly better fit when the magnitude of the difference of AIC is greater than 2 (Burnham and Anderson, 2002). These two models were compared for all species following Xiao *et al.* (2011). In all cases, the log-linear regression provided a significantly better fit (Table B.1). Therefore, the following

six log-linear regression models were used to fit AGB as the dependent variable, and diameter at breast height (DBH) and tree height (H) as independent variables.

$$E1: \ln(AGB) = \ln(a) + b \ln(DBH)$$

$$E2: \ln(AGB) = \ln(a) + b \ln(H)$$

$$E3: \ln(AGB) = \ln(a) + b \ln(DBH \times H)$$

$$E4: \ln(AGB) = \ln(a) + b \ln(DBH^2 \times H)$$

$$E5: \ln(AGB) = \ln(a) + b \ln(DBH \times H^2)$$

$$E6: \ln(AGB) = \ln(a) + b \ln(DBH) + c \ln(H)$$

The underlying assumptions for the regression analysis such as normality of residuals and heteroscedasticity were used to judge the suitability of each regression model. Percent relative standard errors (PRSE) of each regression coefficient were measured according to Sileshi (2014), where PRSE > 25 is considered an unreliable model. The multicollinearity of each model was measured with the variance inflation factor (VIF), where VIF > 5 indicates high collinearity among independent variables. Due to high multicollinearity, complex models with more independent variables were not considered in this study. After obtaining the eligible potential models for each species, the best models were selected by the lowest second-order Akaike Information Criterion (AICc) and Residual Standard Error (RSE), and the highest Akaike Information Criterion weight (AICw) and coefficient of determination (R^2) values (Picard et al., 2012; Sileshi, 2014; Mahmood et al., 2019; 2020). Models with non-significant parameter of estimates were not considered, regardless of meeting the criteria outlined. Since, the AICw provides the likelihood of each model to be the best, it was given highest priority compared with other parameters (Sileshi, 2014). For all models, the correction factor (CF) was calculated to minimise systematic bias while converting biomass from ln scale to a normal scale (Sprugel, 1983). The K-fold cross-validation technique was used to validate the best model. This technique randomly divides the original dataset into K subsets (10 in this case) of equal sizes, where each subset is validated with K-1 subsets (James et al., 2013). The K-fold

validation technique was also run for the Sundarbans-specific and the pantropical generic model (model no. 7 -11 in Table 4.1) to measure tree level variability in AGB in the Sundarbans.

5.2.4. Tree inventory

Above-ground tree data were collected from 140 random sample plots within the Bangladesh Sundarbans (Figure 4.1). Out of 140 sample plots, 120 plots were randomly placed within Permanent Sample Plots (PSP) (20 × 100 m) established by the Bangladesh Forest Department whilst the remaining 20 plots were outside of the PSP. These sample plots are distributed in all 55 compartments (administrative unit) in the Bangladesh Sundarbans covering all three salinity zones (oligohaline, mesohaline and polyhaline) and forest types (Iftekhar and Saenger, 2008; Sarker et al., 2019b). Each plot consists of a circular plot with the radius of 11.3 m (400 m^2) for measuring bigger trees (DBH > 14.5 cm) and a smaller circular plot within this of 5 m radius (79 m^2) for smaller trees (DBH > 2.5 to 14.5 cm) (Figure B.1). After establishing the plots, all individual trees (DBH > 2.5 cm) were marked, and DBH and total height (H) measured by using a diameter tape and a Vertex III hypsometer (Haglöf, Sweden), respectively. A Haglöf wood increment borer (5.15 mm diameter and 300 mm bit length) was used to collect woody specimen at DBH point to determine the wood density (WD) of studied species according to Wiemann and Williamson (2013). The WD (gm cm^{-3}) was then measured from the volume and dry mass of the specimen. The cylindrical volume was measured in the field from the diameter and length of the specimen and brought to the laboratory for oven-drying at 105 ^oC until constant weight was obtained.

5.2.5. Variability of Above-ground biomass in the Sundarbans

The magnitude and pattern of differences in AGB at plot level in the Sundarbans were compared by using different allometric models with an independently collected inventory from the Sundarbans. Plot level AGB variability was measured by actual AGB difference (Mg ha^{-1}), absolute difference (Mg ha^{-1}) and relative absolute difference (%) among different allometric models.

5.2.5.1. AGB variability between allometric models

Measured DBH, H and WD were used in the species-specific allometric models and other site-specific and pan-tropical generic models (Model 7-11 in Table 4.1) to assess AGB at the individual tree level. In order to compute plot-level AGB estimates per hectare (Mg ha^{-1}), a hectare expansion factor (HEF) for each stem was used according to the size of the sample plot (i.e., HEF = 25 for bigger plots, and HEF = 126.58 for smaller sub-plot) and subsequently summed up all tree biomass in each plot to get plot biomass. To estimate biomass from the species-specific models, the developed nine species-specific models were used alongside four published species-specific models (Model 1-4 in Table 4.1). If no species-specific allometric model was available, models for similar genus or family level were applied. Since measuring the girth at collar height (GCH) for *Ceriops decandra* and *Aegialitis rotundifolia* is laborious and time consuming, DBH was measured in the field and subsequently converted to GCH from a relationship between DBH and GCH of 50 individuals (Figure B.2).

5.2.5.2. AGB variability with wood density

Variation of tree AGB was compared with measured and database-sourced WD obtained from published wood density including the Global WD database (Chave et al., 2009; Zanne et al., 2009), World Agroforestry's tree functional attributes and ecological databases (ICRAF, 2016) and from Bangladesh Forest Research Institute (BFRI) (Sattar et al., 1995). The Sundarbans-specific generic allometric model (Model 7: Mahmood_2019_DHW) was used for comparison of AGB from multiple WD sources. If there was no measured wood density for any species, the WD from the same genus or family was used. Instead of applying species WD, plot-level mean WD, salinity zone WD and Sundarbans level WD were used to investigate how the spatial scale of WD variation on AGB estimates in the Sundarbans. To measure salinity zone mean WD, measured WD were averaged according to three salinity zones in the Sundarbans according to Rahman et al. (2021b).

5.2.5.3. AGB variability with tree height

To derive the variation of AGB from different height measurements, mean height and maximum height from each plot was used in Model 7 (Mahmood_2019_DHW). The Model 7 was used in this case as it originated from the Sundarbans and contains both H and WD parameters.

5.2.6. Statistical Analysis

All statistical analysis and graphics used R4.0.4 for Windows in Rstudio Version-1.4.1106 (R Core Team, 2020). The normality of residuals, heteroscedasticity and multicollinearity of each regression model were tested with a Shapiro-Wilk normality test by using 'R stats' base package, studentized Breusch-Pagan (BP) test by using 'lmtest' package and Variance Inflation Factor (VIF) test using 'car' package, respectively (Zeileis and Hothorn, 2002; Fox and Weisberg, 2019). Second-order Akaike Information Criterion (AICc) for the fitted regression model was assessed by 'MuMIn' package (Bartoń, 2020). K-fold cross validation was run using the 'caret' package and model accuracy was compared with Mean Absolute Error (MAE) and Root Mean Squared Error (RMSE) (Kuhn, 2008). Pairwise comparison of tree AGB between the species-specific and other models were tested either by paired t-test if the underlying assumptions such as normality and heteroscedasticity were met; otherwise, Wilcoxon signed-rank non-parametric test was used. The 'rstatix' package was used for Wilcoxon signed-rank test and 'R stats' base package was used for paired t-test (Kassambara, 2020). The graphical output was generated using the 'ggplot2' 'ggeffects' and 'cowplot' package (Wickham, 2016; Lüdecke, 2018; Wilke et al., 2019).

5.3. Results

5.3.1. Species-specific allometric model

Out of 54 log-linear regression models for nine species, 26 models passed all four criteria including normality of residuals, heteroscedasticity, PRSE and VIF (Table B.2). These 26 models were then fitted species-wise to the 324 semi-destructively harvested tree dataset with DBH and H: *Aglaia piculate* (19), *Avicennia* spp. (41), *Bruguiera* spp. (31), *Excoecaria agallocha* (35), *Heritiera fomes*

(97), *Lumnitzera piculat* (13), *Rhizophora* spp. (17), *Sonneratia apetala* (20), and *Xylocarpus* spp. (51).

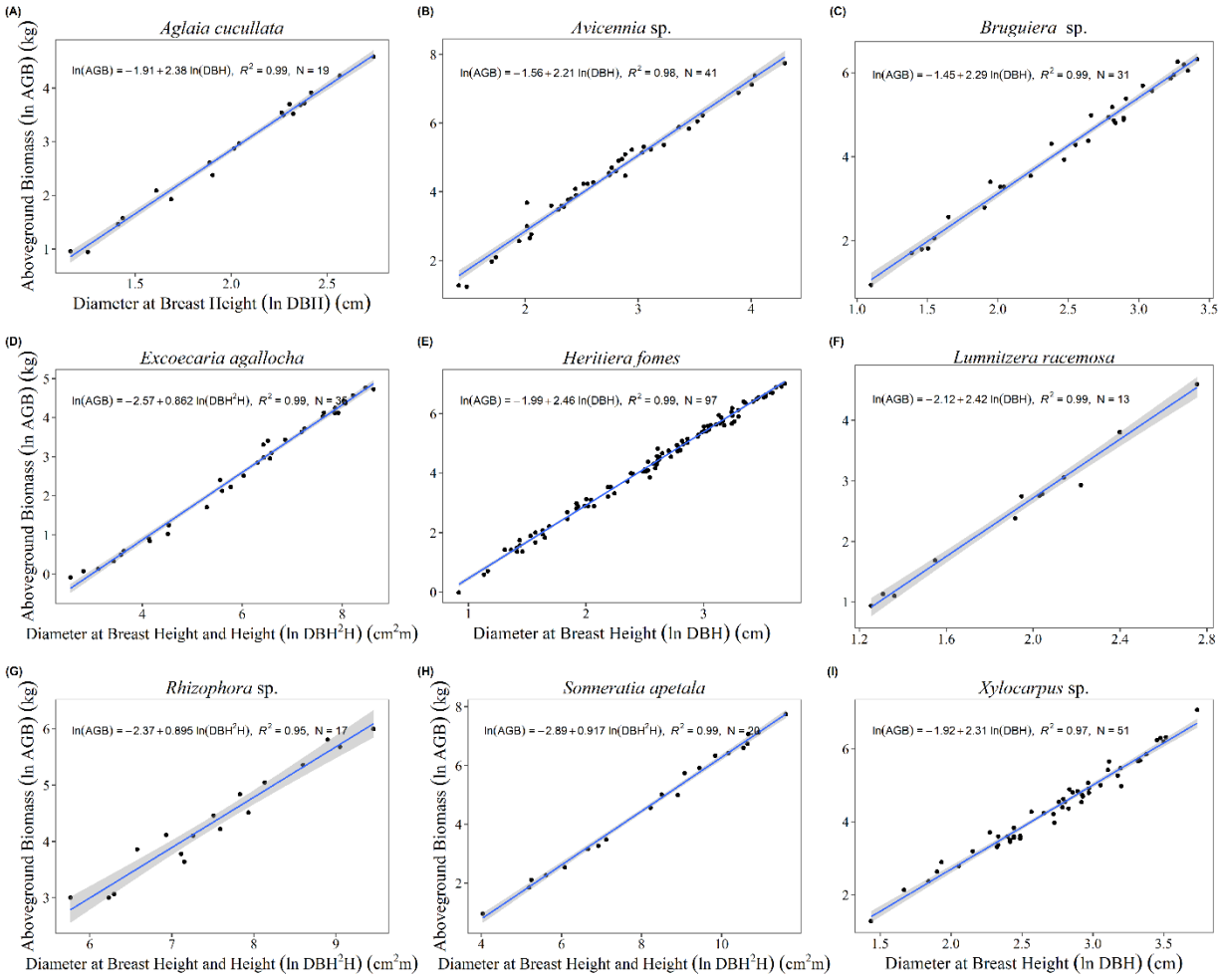

Figure 5.3: Best species-specific allometric model for above-ground biomass in the Sundarbans.

Out of 26 models, the best nine species-specific models are presented for each species group (Table 4.2; Figure 4.3). The AIC weight shows that the best-chosen models for *Aglaia piculate*, *Bruguiera* spp., *Excoecaria agallocha*, *Heritiera fomes*, and *Xylocarpus* spp. have 100% chance for being the best model, while *Avicennia* spp., *Lumnitzera piculat*, *Rhizophora* spp. and *Sonneratia apetala* have 81%, 94%, 82%, and 71%, respectively chance to be the best model (Table 4.3). In the case of *Sonneratia apetala*, while E6 models had the highest and lowest RSE and AIC value, the E4 model was chosen based on higher AICw for its greater chance for being the best model. The adjusted coefficient of determination (R^2) varied from 0.77 to 0.99 for all models. All species-specific models comprised a single predictor value with only DBH for six species: *Aglaia piculate*, *Avicennia* spp.,

Bruguiera spp., *Heritiera fomes*, *Lumnitzera piculat*, and *Xylocarpus* spp. and with combination of DBH and H ($DBH^2 \times H$) for *Excoecaria agallocha*, *Sonneratia apetala*, and *Rhizophora* spp.

Table 5.2: Regression results for all species-specific allometric models in the Sundarbans.

Species	Eq. no.	Model, ln (AGB) =	a*	b	c	Adj. R^2	RSE	AICc	AIC_W	CF
Aglaia cucullata	**E1**	**$\ln(a) + b \ln(DBH)$**	-1.9066	2.3784		0.9915	0.1047	-26.3501	1.00	1.0055
	E5	$\ln(a) + b \ln(DBH \times H^2)$	3.7114	1.0918		0.9585	0.2316	3.8164	0.00	1.0980
	E2	$\ln(a) + b \ln(H)$	4.5892	3.7109		0.8554	0.4324	27.5502	0.00	1.0272
***Avicennia* spp.**	**E1**	**$\ln(a) + b \ln(DBH)$**	-1.5554	2.2069		0.9781	0.2287	0.0103	0.81	1.0265
	E4	$\ln(a) + b \ln(DBH^2 \times H)$	-2.7625	0.9520		0.9765	0.237	2.8854	0.19	1.0285
***Bruguiera* spp.**	**E1**	**$\ln(a) + b \ln(DBH)$**	-1.4473	2.2870		0.9845	0.1926	-9.3234	1.00	1.0187
	E3	$\ln(a) + b \ln(DBH \times H)$	-2.7982	1.5246		0.9649	0.2901	16.0743	0.00	1.0430
	E5	$\ln(a) + b \ln(DBH \times H^2)$	-3.1823	1.1004		0.9178	0.4439	42.4386	0.00	1.1035
Excoecaria agallocha	**E4**	**$\ln(a) + b \ln(DBH^2 \times H)$**	-2.5721	0.8623		0.9903	0.1539	-26.9780	1.00	1.0119
	E3	$\ln(a) + b \ln(DBH \times H)$	-2.9335	1.4173		0.9801	0.2200	-1.9475	0.00	1.0245
	E5	$\ln(a) + b \ln(DBH \times H^2)$	-3.3198	1.0359		0.9591	0.3152	50.1953	0.00	1.0509
	E2	$\ln(a) + b \ln(H)$	-4.0227	3.6582		0.8558	0.5919	67.3342	0.00	1.1915
Heritiera fomes	**E1**	**$\ln(a) + b \ln(DBH)$**	-1.9944	2.4603		0.9931	0.1434	-97.2721	1.00	1.0103
Lumnitzera racemosa	**E1**	**$\ln(a) + b \ln(DBH)$**	-2.1151	2.4187		0.9858	0.1342	-8.8255	0.94	1.0090
	E4	$\ln(a) + b \ln(DBH^2 \times H)$	-3.2562	1.0631		0.9783	0.1663	-3.2570	0.06	1.0139
	E3	$\ln(a) + b \ln(DBH \times H)$	-4.0458	1.8671		0.9558	0.2373	5.9931	0.00	1.0286
	E5	$\ln(a) + b \ln(DBH \times H^2)$	-4.9734	1.4650		0.8994	0.3579	16.6722	0.00	1.0661
***Rhizophora* spp.**	**E4**	**$\ln(a) + b \ln(DBH^2 \times H)$**	-2.3744	0.8953		0.9467	0.2226	2.8788	0.82	1.0251
	E3	$\ln(a) + b \ln(DBH \times H)$	-2.8960	1.5009		0.9358	0.2443	6.0407	0.17	1.0303
	E5	$\ln(a) + b \ln(DBH \times H^2)$	-3.4321	1.1161		0.9065	0.2948	12.4334	0.01	1.0444
Sonneratia apetala	**E4**	**$\ln(a) + b \ln(DBH^2 \times H)$**	-2.8869	0.9170		0.9938	0.1633	-10.3304	0.71	1.0134
	E6	$\ln(a) + b \ln(DBH) + c \ln(H)$	-2.6715	1.9068	0.7430	0.9939	0.1625	-8.5123	0.29	1.0133
	E3	$\ln(a) + b \ln(DBH \times H)$	-3.6314	1.5533		0.9854	0.2518	6.9904	0.00	1.0322
	E5	$\ln(a) + b \ln(DBH \times H^2)$	-4.4509	1.1706		0.9582	0.4256	27.9819	0.00	1.0948
	E2	$\ln(a) + b \ln(H)$	-5.6705	4.2261		0.7723	0.9932	61.8759	0.00	1.6375
***Xylocarpus* spp.**	**E1**	**$\ln(a) + b \ln(DBH)$**	-1.9174	2.3100		0.9720	0.1989	-15.5152	1.00	1.0200

Here bold and light grey shaded models are the best model for each species, a* stands for ln (a), all parameters of estimates (a, b and c) are significant at $p < 0.05$. R^2: Coefficient of determination, RSE: Residual standard error, AICc: with small sample bias adjustment, AICw: weighted AIC, CF = Correction factor for converting log scale into normal scale.

The 10-fold cross validation showed that the species-specific model gives the lowest average Mean Absolute Error (MAE) of all species in comparison to three Sundarbans-specific and four pan-tropical generic allometric models (Figure 4.4, Table B.4). The lowest average MAE revealed that the species-specific models performed well to predict the AGB in the Sundarbans. AGB estimation at tree level had mean relative absolute difference in MAE between 21.85% with the Mahmood_2019_DHW model to the maximum 167.43% with the Komiyama_2005_DW model followed by the Chave_2005_DHW and the Chave_2014_DHW model (Table B.4). The paired t-test of MAE for species-specific models with generic models showed that there is no significant difference of MAE with three Sundarbans-specific models (p >0.05); however, all four pan-tropical models showed significantly higher MAE than the species specific-model (p <0.05). The largest error was obtained for *Excoecaria agallocha* with the Komiyama_2005_DW model.

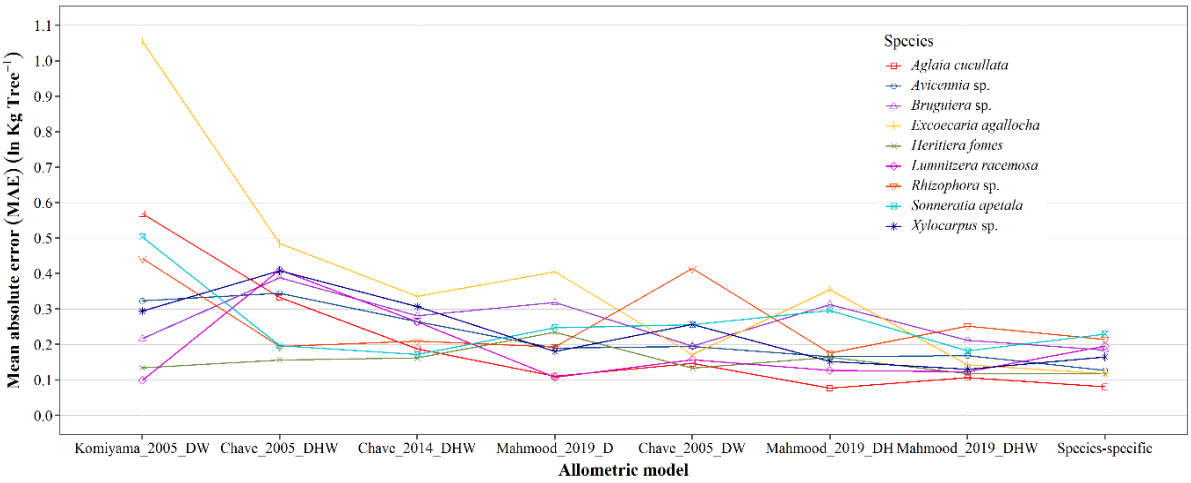

Figure 5.4: Species-wise mean absolute error (MAE) of tree AGB with all allometric models after 10-fold cross validation. The models are arranged from highest average MAE to minimum.

5.3.2. Above-ground tree biomass in the Sundarbans

The tree inventory in the Bangladesh Sundarbans indicates a total of 24 tree species. The mean DBH, height, measured and database-sourced wood density of all tree species are presented in the Table 4.3. The DBH and H distribution are presented in the supplementary Figures B.3 and B.4. The frequency distribution of the top ten species based on basal area (m^2 ha^{-1}) and tree density (trees ha^{-1}) showed

that *Excoecaria agallocha*, *Heritiera fomes* and *Ceriops decandra* comprise 90% of the stems in the Sundarbans, although they represent 60% in terms of basal area (Figure 4.5). *Excoecaria agallocha* and *Heritiera fomes* was within the top two species in both categories; *Ceriops decandra* was the third in terms of tree density, however, sixth in case of basal area for its lower DBH.

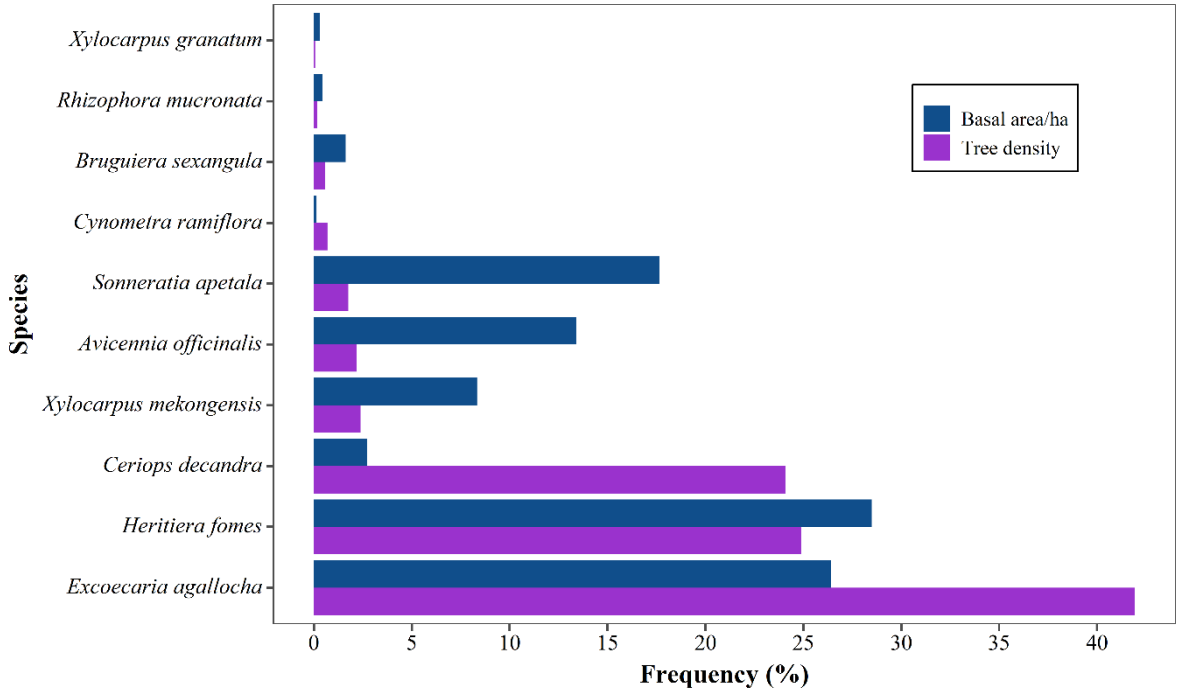

Figure 5.5: Frequency distribution of the 10 most frequently occurring species based on basal area (m^2 ha^{-1}) and tree density (tree ha^{-1}).

Table 5.3: List of tree species found in the Sundarbans with taxonomy and structural parameters.

Sl No.	Latin name	Local name	Family	Mean DBH (cm ± s.d.)	Mean Height (m ± s.d.)	Measured Mean Wood Density (gm cm^{-3} ± s.d.)	Mean Wood Density from database (gm cm^{-3} ± s.d.)**
1.	*Aegialitis rotundifolia Roxb.*	Nunia	*Plumbaginaceae*	6.86 (± 2.85)	3.94 (± 1.71)	-	0.50 ((± 0.05)
2.	*Aegiceras corniculatum* (L.) Blanco	Kholshi	*Primulaceae*	5.69 (± 2.67)	5.73 (± 2.18)	0.74	0.60 ((± 0.08)
3.	*Aglaia piculate* (Roxb.) Pellegr. *	Amur	*Meliaceae*	3.58 (± 1.16)	4.70 (± 1.62)	0.50	0.62 ((± 0.12)
4.	*Avicennia alba* Blume.	Sada Baen	*Avicenniaceae*	14.10 (± 0.85)	8.70 (± 2.40)	0.72 (± 0.08)	0.70 ((± 0.12)
5.	*Avicennia marina* (Forssk.) Vierh.	Moricha Baen	*Avicenniaceae*	10.40 (± 5.26)	10.87 (± 5.77)	0.55	0.64 ((± 0.09)
6.	Avicennia officinalis L.	Kala Baen	*Avicenniaceae*	21.20 (± 13.40)	11.56 (± 5.13)	0.61 (± 0.07)	0.65 ((± 0.08)
7.	*Bruguiera gymnorrhiza* (L.) Lam.	Lal Kakra	*Rhizophoraceae*	7.40	5.80	-	0.76 ((± 0.08)
8.	*Bruguiera piculate* (Lour.) Poir.	Holud Kakra	*Rhizophoraceae*	15.75 (± 3.95)	6.96 (± 3.02)	0.69 (± 0.03)	0.83 ((± 0.12)
9.	*Cerbera manghas* L. *	Dakur	*Apocynaceae*	8.92 (± 0.08)	0.72 (± 0.08)	0.35 (± 0.01)	0.47 ((± 0.05)
10.	*Ceriops decandra* (Griff.) Ding Hou	Goran	*Rhizophoraceae*	3.31 (± 0.80)	3.97 (± 0.95)	0.73 (± 0.07)	0.73 ((± 0.25)
11.	*Cynometra ramiflora* L. *	Singra	*Fabaceae*	4.25 (± 1.55)	5.05 (± 1.47)	0.66 (± 0.05)	0.84 ((± 0.10)
12.	*Excoecaria agallocha* L.	Gewa	*Euphorbiaceae*	6.93 (± 4.04)	6..71 (± 2.49)	0.42 (± 0.08)	0.43 ((± 0.06)
13.	*Excoecaria indica* (Willd.) Muell. Arg. *	Batul	*Euphorbiaceae*	6.60	6.80	0.41	0.50 ((± 0.02)
14.	*Heritiera fomes* Buch. -Ham.	Sundri	*Malvaceae*	8.57 (± 6.58)	8.03 (± 4.16)	0.75 (± 0.07)	0.88 ((± 0.11)
15.	*Hibiscus tiliaceus* L. *	Bola	*Malvaceae*	3.90	5.00	-	0.48 ((± 0.06)
16.	*Intsia bijuga* (Colebr.) Kuntze *	Bhaila/Bhola	*Fabaceae*	4.40 (± 0.79)	5.17 (± 0.81)	-	0.71 ((± 0.20)
17.	*Kandelia candel* (L.) Druce	Vatkathi	*Rhizophoraceae*	11.87 (± 5.09)	7.77 (± 1.15)	0.58 (± 0.05)	0.52 ((± 0.05)
18.	*Lumnitzera piculat* Willd.	Kirpa	*Combretaceae*	5.23 (± 1.84)	5.99 (± 1.13)	0.82 (± 0.13)	0.83 ((± 0.08)
19.	*Millettia pinnata* (L.) Panigrahi*	Karanj	*Fabaceae*	5.70	6.30	0.55	0.61 ((± 0.05)
20.	*Rhizophora piculate* Blume.	Bhora Jhana	*Rhizophoraceae*	13.54	0.72	-	0.88 ((± 0.21)
21.	*Rhizophora mucronata* Lamk.	Jhana Garjan	*Rhizophoraceae*	15.42 (± 3.72)	10.38 (± 2.65)	0.95 (± 0.05)	0.85 ((± 0.10)
22.	*Sonneratia apetala* Buch. -Ham.	Keora	*Lythraceae*	29.35 (± 12.84)	17.97 (± 5.90)	0.54 (± 0.07)	0.53 ((± 0.11)
23.	*Xylocarpus granatum* K.D. Koen.	Dhundul	*Meliaceae*	18.77 (± 12.03)	8.08 (± 2.66)	0.58 (± 0.05)	0.67 ((± 0.14)
24.	*Xylocarpus moluccensis* (Lam.) M. Roem	Passur	*Meliaceae*	15.51 (± 10.80)	9.39 (± 3.95)	0.65 (± 0.09)	0.65 ((± 0.09)

* Indicates mangrove associates according to Tomlinson (2016). Abbreviation: DBH = Diameter at Breast Height. Values without s.d. indicates single observation. ** Multiple wood density values from different sources.

The mean above-ground biomass varied from 111.36 Mg ha^{-1} with the Chave_2005_DHW model to the highest 299.48 Mg ha^{-1} for Chave_2005_DW model (Figure 4.6). Except for Chave_2005_DHW

and Chave_2014_DHW, all other models yielded higher AGB than the species-specific model (123 Mg ha^{-1}). The mean relative absolute difference in AGB ranged from 9% with Mahmood_2019_DHW to 142% with Chave_2005_DW. Pairwise comparison with the Wilcoxon Signed-Rank Test between species-specific and other models showed that all generic models measured significantly different AGB than the species-specific model in the Sundarbans (p <0.05). Both Chave_2005_DW and Komiyama_2005_DW overestimated AGB (supplementary Table B.5). The absolute difference between allometric models tended to increase with DBH in all species, suggesting that larger trees are crucial for estimating AGB with a variety of available allometric model leading to a greater error and uncertainty.

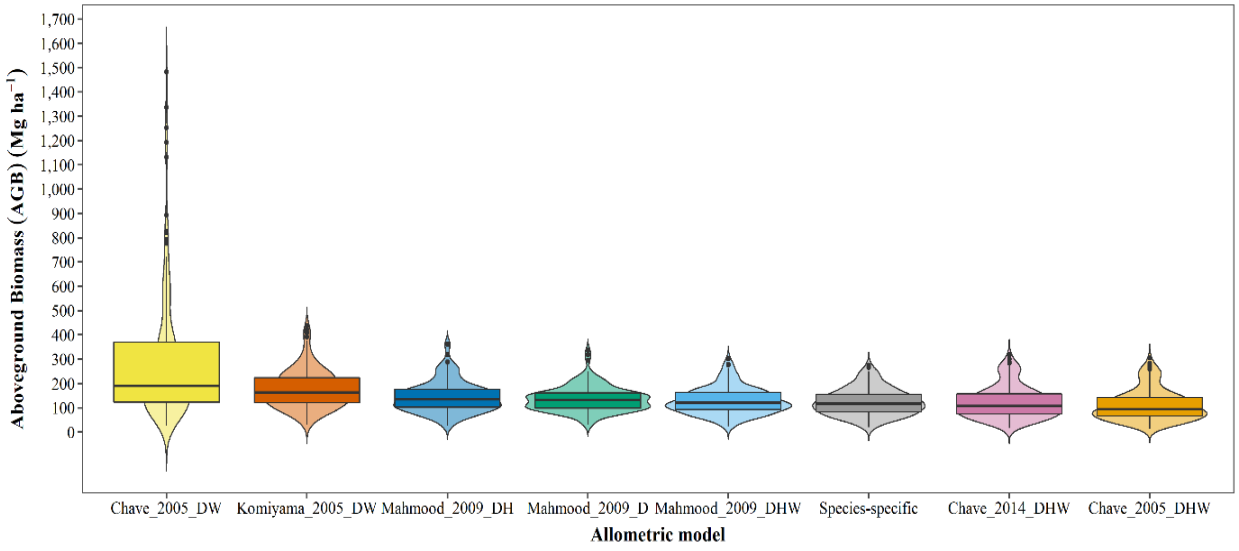

Figure 5.6: Comparison of above-ground biomass (Mg ha^{-1}) with different allometric models. The models are arranged from the highest median AGB to the lowest. The black horizontal line of box plot for each model represents the median and the width of violin plot represents the proportion of the data located there as a measure of kernel probability density. The black dots represent the outliers, which are 1.5 times of the interquartile range above the upper quartile and below the lower quartile (McGill et al., 1978)

Table 5.4: Pairwise comparison test of plot-level AGB from species-specific and other allometric models.

Model comparison	Mean difference biomass (Mg ha^{-1})	Mean absolute difference biomass (Mg ha^{-1})	Mean relative absolute difference (%)	Wilcoxon Signed-Rank Test (Z), *p*-value
Comparison of different allometric model				
Species-specific – Mahmood_2019_DHW	-5.18	11.38	9.21	Z = -5.13, p <0.05
Species-specific – Chave_2014_DHW	0.79	17.38	14.07	Z = -2.89, p <0.05
Species-specific – Mahmood_2019_D	-12.66	19.66	15.92	Z = -6.40, p <0.05
Species-specific – Chave_2005_DHW	12.59	21.07	17.06	Z = -6.51, p <0.05
Species-specific – Mahmood_2019_DH	-21.27	23.37	18.92	Z = -7.95, p <0.05
Species-specific – Komiyama_2005_DW	-52.47	52.57	42.57	Z = -10.26, p <0.05
Species-specific – Chave_2005_DW	-175.67	175.75	142.31	Z = -10.26, p <0.05
Comparison from different Wood Density (WD)				
Measured WD – Plot mean WD	-3.16	5.83	4.53	Z = -5.86, p <0.05
Measured WD – Database WD	-4.82	9.91	7.70	Z = -3.83, p <0.05
Measured WD- Salinity zone mean WD	-4.08	12.46	9.68	Z = -3.54, p <0.05
Measured WD – Sundarbans mean WD	-4.29	12.47	9.69	Z= -3.59, p < 0.05
Comparison from different Tree Height (m)				
Individual Height – Plot mean Height	10.70	10.70	8.31	Z = -13.68, p <0.05
Individual Height -Plot top Height	-25.04	25.04	19.46	Z = -13.68, p <0.05

AGB was significantly higher when models used published WD values compared to species-specific measured WD (Wilcoxon Signed-Rank Test, p <0.05) (Figure 4.7A, Table 4.4). The maximum mean relative difference biomass was for Sundarbans mean WD followed by salinity zone mean WD and database-derived WD. Looking at different sources of height data, using plot top height tended to overestimate AGB by 19.46%, while using average height underestimated AGB by 8.31% compared to the measurements from Individual species (Figure 4.7B, Table 4.4).

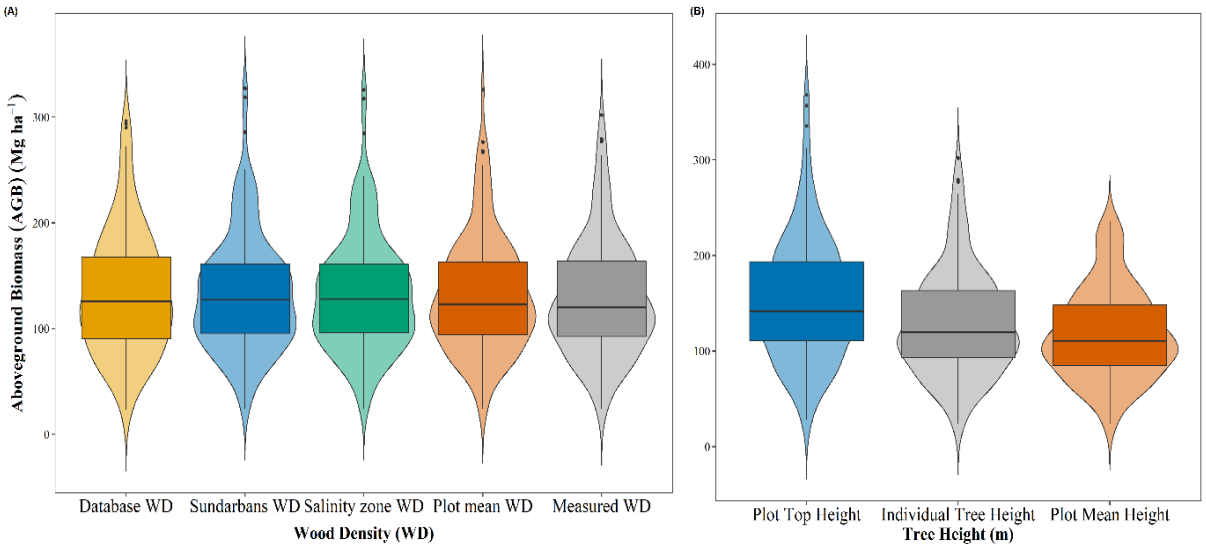

Figure 5.7: Comparison of above-ground biomass with A) different wood density and B) different height parameters. The parameters are arranged from the highest median AGB to the lowest. For details of the violin-box plot, see Figure 4.6.

5.4. Discussions

The results show that the species-specific allometric models provide the lowest average mean absolute error (MAE) for all species in the Sundarbans (Figure 4.4, Table B.4). However, the three Sundarbans-specific generic models showed no significant difference of mean MAE at tree-level compared with the species-specific models (Table B.4). At plot-level, all local and pan-tropical generic models either overestimated or underestimated AGB when compared to local species-specific models (Figure 4.6). Several studies have concluded that site-specific AGB models estimate biomass or carbon with less error than regional or pan-tropical models; as seen in studies in the Sundarbans mangrove forest (Mahmood et al., 2019), lowland Dipterocarp forest in Indonesia (Basuki et al., 2009), degraded landscape in Northern Ethiopia (Mokria et al., 2018), central African forest (Ngomanda et al., 2014) and Mexican tropical humid forests (Martínez-Sánchez et al., 2020). In contrast, only a few studies report better performance from regional or pan-tropical models and these appear to result from large uncertainties in the data used to build the local model; for example, West Africa (Aabeyir et al., 2020). The accuracy of these generic models for a particular forest depends on whether these models incorporate sufficient samples from that forest. Chave et al. (2014) point out that the discrepancy between local models and their own model (Chave_2014_DHW) in wet forests

(including mangroves) is largely due to failure to address the wider variation of tree form and other characteristics like buttresses, which are common in the Sundarbans. Their previous model (Chave_2005_DW) overestimated AGB in the Sundarbans because of its inability to estimate biomass from larger trees (DBH > 42 cm) (Chave et al., 2005). However, surprisingly, the worldwide generic models for mangroves also overestimate AGB, possibly because of the samples drawn from the mangroves of Asia-Pacific and Australia (Komiyama et al., 2008).

The structure and morphological characteristics of all mangroves vary according to their ability to adapt to environmental conditions such as salinity, which is less pronounced in other wet and dry tropical areas (Ball and Pidsley, 1995; Tomlinson, 2016). Environmental drivers such as salinity and water deficit are considered the main stressors for the growth and development of mangroves, including the Sundarbans. For example, the third most abundant species in the Sundarbans, *C. decandra*, is a multi-stemmed bushy species, on the other hand, the top two, *H. fomes* and *E. agallocha* are tree-like structures. The pantropical models yielded a large error in the dwarf, bushy species and other true mangrove species in the Sundarbans (Table B.5). Moreover, the extreme salinity has reduced the stature (Rahman et al., 2015a), trunk diameter (Rahman et al., 2020) and the leaf area (Khan et al., 2020b) of *H. fomes* and *S. apetala*, present in all three salinity zones in the Sundarbans. Due to this morphological variation, Banerjee et al. (2013) highlighted the importance of developing models based on salinity zonation.

This study demonstrates that when using measured wood densities and individual tree heights, generic equations yield accurate estimates of AGB in mangroves at the plot scale (Figure 4.7). Most species had a higher published WD than the measured value seen in Table 4.3 (Henry et al., 2010). The use of WD from different databases such as the Global WD database resulted in a 9% variation for species having multiple values, which could provide a significant variation in AGB if upscaled (Réjou-Méchain et al., 2019). Averaging WD at the plot scale, salinity zone scale or ecosystem scale also introduces errors. While WD is considered an important variable to capture a range of characteristics such as high density versus low density timber species, climax versus pioneer species or primary versus secondary species, the use of WD value from the secondary sources or averaging them in the

higher scales might not reflect the true biomass (Slik et al., 2008; Kenzo et al., 2009). Phillips et al. (2019) noted significant AGB error in the Amazon rainforest while scaling up from the plot level to forest and Amazon-wide level. Yuen et al. (2016) observed 31 Mg ha^{-1} higher AGB with the difference of measured and published WD of only 0.13 gm/cm^3.

Among nine developed models, six showed that DBH alone is a strong predictor of AGB across the Bangladesh Sundarbans. The remaining three models of *E. agallocha, S. apetala,* and *Rhizophora* spp. showed sensitivity to height. However, the inclusion of top height or average height instead of using individual tree height can increase the error at the plot level and above. Kearsley et al. (2013) observed a 24% overestimation of AGB in the central Congo Basin by using a regional Height-Diameter relationship developed by Feldpausch et al. (2012) compared to the local relationship. On the other hand, using mean height could reduce the difficulty of taking height measurements in dense forests, yet may lead to a significant underestimation of AGB (Hunter et al., 2013). The difficulty of measuring height under a dense forest canopy allows researchers to use a H-D relationship or to use bioclimatic variables in allometric models. However, these also lead to non-uniform bias in biomass estimation (Réjou-Méchain et al., 2019).

Although species-specific WD and individual height data can be used to accurately estimate AGB at the plot and ecosystem level, collecting species information is impractical in highly diverse mixed tropical forests such as in Amazonia, Southeast Asia and the Congo basin, which comprise of more than 53,000 tree species (Feldpausch et al., 2012; Slik et al., 2015). Mangroves, by comparison exhibit less diversity. Developing allometric models for dominant species could improve the biomass inventory. For example, in the Sundarbans only 28 species were recorded (24 in this survey) and just three species (*E. agallocha, H. fomes* and *C. decandra*) constitute about 90% of stand density (Figure 4.5), which implies that developing three allometric models is enough to produce acceptable AGB estimates in the Sundarbans (GOB, 2019). The model used for *C. decandra* was developed by destructive sampling from Mahmood et al. (2012) and so this study recommends developing models with destructive samples from all salinity zones for *H. fomes* and *E. agallocha*.

The errors and uncertainties in the individual tree and plot level AGB estimates will result in large errors when scaling up to the ecosystem, region or country level by remote sensing (RS) techniques. Réjou-Méchain et al. (2019) described the errors due to poor choice of allometric models and failure to capture variabilities of WD and H as uniform and non-uniform bias. Uniform bias systematically propagates over- or underestimation whereas non-uniform bias is related to an inability to capture the variabilities across landscapes, for example, WD and H variation among successional stages or environmental gradients such as the salinity in the Sundarbans (Rahman et al., 2020). These two types of bias, in addition to mapping errors resulting from the use of remote sensing, may result in serious anomalies in national and global carbon budgets and result in poor understanding of species contribution to ecosystem processes and function in mangroves.

5.5. Conclusions

This study developed and tested five species-specific and four genus-specific allometric models for the nine most important species in the Sundarbans. All developed models explained a high percentage of the variance in tree AGB (R^2 = 0.97 to 0.99) using measured diameter at breast height (DBH) and total height (H) data. At the individual tree level, the generic allometric models overestimated AGB between 22% to 167% compared to the species-specific models and at the plot level, they showed statistically significant AGB differences compared to the species-specific models ($p < 0.05$). Measured wood density (WD) showed 5-10% less biomass than WD from database and other sources, and AGB was overestimated by up to 20% when using plot top height and underestimated by 8% using plot average height data rather than individual tree heights. The study concludes that biomass estimation in mangroves forests always benefit from species-specific models and individual tree measurements when appropriate input data are available. Tree level measurements from inventory plots play an important role for the improved estimation of forest biomass while scaling from individual trees up to the ecosystem level. Improved estimates of AGB will improve support our understanding of the productivity of mangrove forests, information that is needed for the long-term conservation of these fragile ecosystems that face many natural and anthropogenic pressures.

Chapter 6

Mapping ecosystem carbon stocks in the Bangladesh Sundarbans

6.1. Introduction

Mangrove forests throughout the world provide a range of ecosystem services to local and global communities (Himes-Cornell et al., 2018; Friess et al., 2020b). Their role in sequestering atmospheric CO_2 as biomass in woody material and as organic matter in sediments plays an important role in mitigating climate change (Duarte, 2017; Kauffman et al., 2020; Macreadie et al., 2021). Despite these benefits, it is estimated that about half the area of the world's mangrove forests have been lost during the last century (Feller et al., 2010). Nevertheless, data from FAO and independent research suggests that the decline of mangrove has reduced to about 7% in the last three decades and mangroves continue to be lost or degraded due to a range of anthropogenic activities, pollution and climate change (FAO, 2020; Goldberg et al., 2020; Su et al., 2021). A single unit loss of mangrove forest emits more greenhouses gases than other tropical forests due to high carbon density in the forest sediments (Donato et al., 2011; Kauffman et al., 2020). Therefore, a global alliance to curb mangrove destruction and fostering conservation and restoration of degraded mangrove forest has recently been established via national and international policies and practices such as UN REDD$^+$, Payment for Ecosystem Services (PES), International Blue Carbon Initiative and the Global Mangrove Alliance Blue Carbon initiatives (Taillardat et al., 2018; Friess et al., 2020a).

The ecosystem carbon stocks is mainly composed of both above- and below-ground carbon from tree body parts (either dead or alive) and sediment carbon (IPCC, 2006; Donato et al., 2011). While sediment carbon is directly measured from sediment samples, tree carbon components are estimated from allometric models as biomass derived from tree structural parameters such as diameter, height and wood density of trees (Kauffman and Donato, 2012; Kauffman et al., 2020). Therefore, a range of regional, pan-tropical and site-specific allometric models are available for mangroves (Komiyama et al., 2008; Chave et al., 2014; Mahmood et al., 2019). However, the use of non-mangrove models for mangrove species, and non-site-specific wood density does not provide the corresponding level of accuracy, especially when estimating biomass variability with vegetation types and environmental drivers (Owers et al., 2018; Rahman et al., 2021c). A standard conversion factor (usually 45-50%) is used to convert biomass into carbon (Kauffman and Donato, 2012; Howard et al., 2014). Application

of a standard conversion factor does not reflect the accurate carbon proportion since the conversion rate is species-specific and varies with the component of trees such as stems, branches and roots (Owers et al., 2018). Overall, the carbon stocks of a mangrove forest is not spatially homogeneous, rather it depends on spatial variability resulting from species type, composition, structure, age, intertidal condition, salinity and other environmental variables (Owers et al., 2018; Kauffman et al., 2020; Rahman et al., 2021b). Therefore, site- and species-specific allometric models and site-specific variables such as wood density and conversion factors are desirable to better reflect the carbon stock (Mahmood et al., 2019; Martínez-Sánchez et al., 2020; Rahman et al., 2021c).

Remote sensing (RS) imagery is frequently used to upscale plot level carbon stocks to larger scales where additional environmental variables can be used to produce carbon maps at ecosystem, national, regional or global level. Upscaling through remote sensing can be done in four ways; a) Stratify & Multiply (SM) Approach, b) Combine & Assign (CA) Approach, c) Ecological Models (EM) Approach and d) Direct Remote Sensing (DR) Approach (Goetz et al., 2009). While the SM approach assigns an average carbon value to a land cover/vegetation type map (for example, Asner et al. (2010)), the CA approach is the extension of SM which uses kriging or co-kriging geostatistics techniques with multiple-layers of information in GIS (geographic information system) (for example, Gibbs et al. (2007) and Tyukavina et al. (2015)). The EM approach uses remote sensing (RS) to parameterise the model (Hurtt et al., 2004) and the DR approaches are basically empirical models where RS data is calibrated to field estimates using a number of statistical and machine learning approaches such as neural networks and regression tress (Baccini et al., 2008; Saatchi et al., 2011; Baccini et al., 2012). Each of these methods has limitations in terms of data requirements and applicability. Since the SM approach uses average value for each class, it is unable to capture the wider variability within that class (Gibbs et al., 2007; Goetz et al., 2009). The CA approach has the advantage that it uses additional variables such as elevation, canopy height and adds weights to prioritise one variable over another. However, it suffers from a lack of consistent spatial data (Goetz et al., 2009; Tyukavina et al., 2015; Ameray, 2018). The DM approach is best suited for monitoring carbon sequestration at larger scales and to prepare wall-to-wall carbon maps (Goetz et al., 2015).

However, for greater accuracy, this DM approach requires active RS data such as RADAR or LiDAR for training models and validation as these sensors measure forest biomass directly (Goetz et al., 2015). Upscaling field carbon stocks measurements through remote sensing introduces uncertainty from geolocation mismatch with field plots, variable acquisition angles of satellite images and mismatches in scale (Réjou-Méchain et al., 2019). The biomass measurement, conversion to carbon and upscaling to the ecosystem level or larger scales (such as countries, regions) involves using a series of statistical models that accumulate uncertainties in each step (Réjou-Méchain et al., 2019; Rahman et al., 2021c). The errors and uncertainties from field plots are incorporated into the remote sensing-based forest area estimates to generate the final carbon map. Altogether it is a challenging task to keep errors and uncertainties in carbon estimation as low as possible.

Until recently, the estimation of carbon stocks in the Bangladesh Sundarbans was mostly based on field measurements that used the same allometric models for all species, which originated from other mangroves or tropical forests (Rahman et al., 2021c). The first comprehensive attempt to quantify carbon stocks in the Sundarbans was undertaken by Rahman et al. (2015a) with the inventory data from the Bangladesh Forest Department (BFD, 2010). By using the same data, Chanda et al. (2016b) simulated the blue carbon by using Markov Chain and cellular automata in order to predict future carbon stocks in the Sundarbans. A range of studies have estimated carbon stocks and sequestration in some parts of the Sundarbans such as in the oligohaline zone (Kamruzzaman et al., 2017; Kamruzzaman et al., 2018; Ahmed and Kamruzzaman, 2021), mesohaline zone (Azad et al., 2020) and in all three salinity zones (Ahmed and Kamruzzaman, 2021). The use of pantropical allometric models in all these studies may not represent the mangroves of the Indian subcontinent well and so fail to achieve the desired level of accuracy. However, the Bangladesh Forest Inventory (BFI) estimated total ecosystem carbon in the Sundarbans and other forests by developing common allometric models for major species (Mahmood et al., 2019; Henry et al., 2021). At present, species-specific allometric models are available for 14 species in the Sundarbans, which can be used to estimate carbon stocks with a greater accuracy (Hossain et al., 2016; Rahman et al., 2021c). Both Chanda et al. (2016b) and GOB (2019) estimated the total

ecosystem carbon stocks in the Bangladesh Sundarbans through remote sensing with the SM approach by assigning average values of each vegetation class or total land area, thus overlooking the distribution of species. In this regard, species-specific allometric models and conversion factors may capture the variability due to species. On the other hand, the species distribution in the Sundarbans is controlled by a range of environmental drivers such as salinity intrusion, historical harvesting, increasing community size, siltation, diseases and soil alkalinity (Sarker et al., 2016; Sarker et al., 2019b; Rahman et al., 2020). Upscaling plot level estimations with a forest-type map should capture these environmental and biotic stressors affecting ecosystem carbon stocks in the forest.

The aim of this research is to estimate carbon stocks in the Bangladesh Sundarbans at different spatial scales and to quantify uncertainty in the estimation. The study hypothesises that the use of species-specific allometric models, wood density and carbon fraction will yield above- and below-ground carbon stocks at the individual, plot and ecosystem scales with reduced uncertainty. The specific objectives of this study are to: 1) Estimate above- and below-ground carbon stocks at plot scale; 2) Compare the variability of ecosystem carbon stocks with vegetation types and salinity zonation; 3) Produce a forest-type map by comparing pixel-based and object-based classification methods; 4) Upscale plot level carbon stocks to the Sundarbans ecosystem level to produce an ecosystem carbon map by using forest-type map.

6.2. Methods

6.2.1. Study site

The study was conducted in the Bangladesh Sundarbans, situated between 21° 14′ N and 22° 25′ N latitude and 89° 34′ E and 89° 43′ E longitude and which comprises about 60% of the world's largest mangrove forest, the Sundarbans. The forest is internationally recognised as a Ramsar and UNESCO World Heritage site and home of world famous Royal Bengal Tiger (*Panthera tigris tigris*) (Aziz and Paul, 2015). About 7.5 million people are directly and indirectly dependent on the Sundarbans and it

provides a number of valuable ecosystem services for their wellbeing, livelihood and protection from cyclones and tidal surges (Abdullah et al., 2016; Barua et al., 2020; Rahman et al., 2021a). The climate of this forest can be described as warm, humid, and tropical, with annual precipitation varying from 1,474 to 2,265 mm and mean annual minimum and maximum temperature varying from 29 ^{o}C to 31 ^{o}C between 1948 and 2011 (Sarker et al., 2016; Rahman et al., 2020). Silt and clay are the dominant soil texture in this forest (Siddiqi, 2001).

The Bangladesh Sundarbans shows a distinct salinity gradient from east to west and therefore, several studies have demarcated three distinct salinity zones based on soil salinity — i) Oligohaline (<2 dS/m, ii) Mesohaline (2-4 dS/m) and iii) Polyhaline (>4 dS/m) (Figure 3.1) (Siddiqi, 2001; Chanda et al., 2016b). Salinity influences the geomorphology and hydrological characteristics which ultimately regulates the morphology, growth and distribution of plant species (Sarker et al., 2016; Sarker et al., 2019a; Rahman et al., 2020; Rahman et al., 2021b). The composition and diversity of tree species is heavily controlled by the east-west salinity gradient (Sattar et al., 1995; Iftekhar and Saenger, 2008; Sarker et al., 2019a; Sarker et al., 2019b). Overall, *Excoecaria agallocha* is abundant in all three salinity zones, whereas the characteristic tree species, *Heritiera fomes* is present in both oligohaline and mesohaline zones and *Ceriops decandra* in the polyhaline zone (Sarker et al., 2019b; Rahman et al., 2021a). Besides these species, some pioneer species such as *Avicenna* spp. and *Sonneratia apetala* are also abundant in the mudflats all over the Sundarbans. The list of species from the vegetation survey is presented in the Table 4.3.

6.2.2. Sampling design and data collection

The Forest Department of Bangladesh (BFD) regularly monitors the tree growth and regeneration from 120 permanent sampling plots (PSP), established at the beginning of the twentieth century (Chaffey et al., 1985). The area of the rectangular PSP is 20 m × 100 m comprising a total of 2,000 m^2. In each PSP, a temporary circular plot was established from August 2018 to April 2019 with the radius of 11.3 m (400 m^2 in total), one-fifth of the PSP, to collect biophysical attributes from the forest. As most of the PSPs are located near the riverbank and these PSPs do not cover seaward side

(Southern part of the Bangladesh Sundarbans), an additional 20 plots were established, which comprises in total of 140 plots (Figure 5.1).

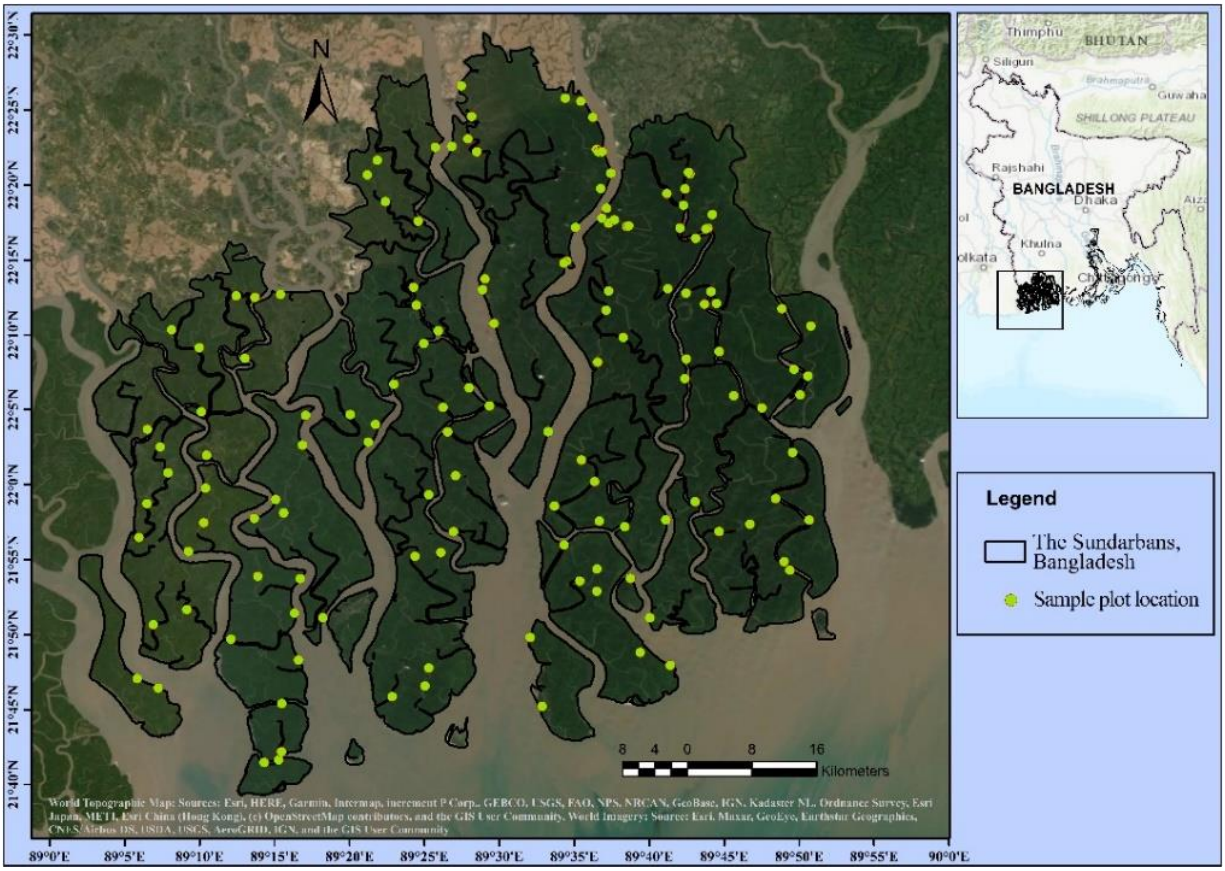

Figure 6.1: Plot location in the Sundarbans mangrove forest, Bangladesh.

The circular plot was designed to collect data from trees. Two additional circular plots were taken inside the main plot with a radius of 5 m and 1 m to collect information from poles (DBH < 14.5 cm) and pneumatophores (Figure 5.2). Additionally, 2-3 sediment cores were taken from each plot for soil carbon measurement and two-cross sectional transects were established to collect information on down wood lying on the forest floor.

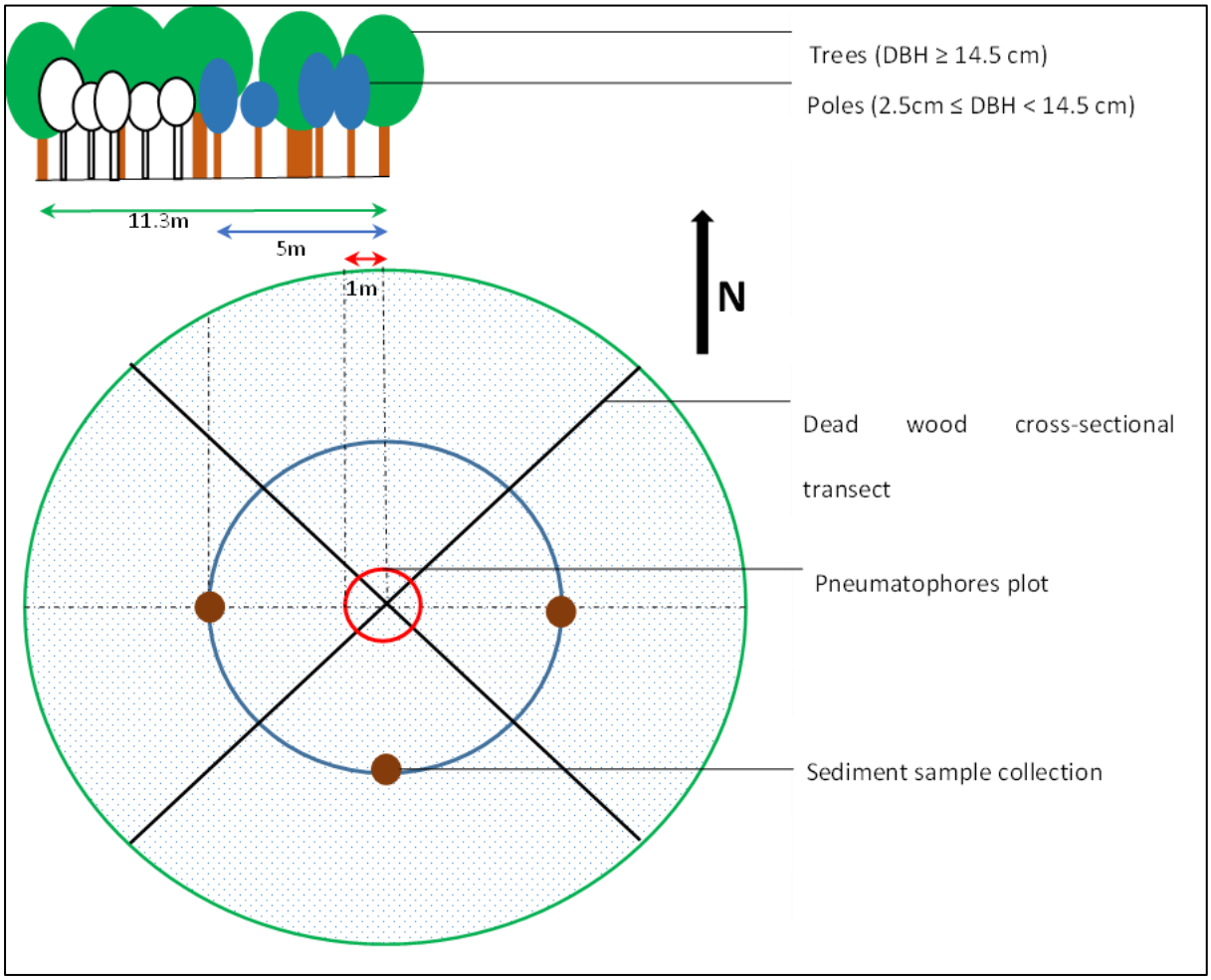

Figure 6.2: The nested circular plot and measured components inside the plot.

6.2.3. Estimation of above-ground carbon

The above-ground carbon of a forest consists of carbon from live and dead trees, non-woody species, poles, saplings, and seedlings, dead and downed wood, pneumatophores and litter. Since seedlings and saplings constituted a negligible amount of carbon, these two components were not measured in the field inventory (Kauffman and Donato, 2012). Above-ground biomass (AGB) for each component was estimated with the collected biophysical attributes from the forest plots separately for each component. Species-specific carbon fraction for stem and root biomass were developed for seven species in the Sundarbans by Chanda et al. (2016b). The average carbon fraction for stem and root is 51.8% and 48.9%, respectively. These species-specific values were used to convert biomass into carbon for stem and root biomass. In the case of unavailability for any species, the value of same

family or wood density was used. In the case of dead and down wood and pneumatophores, the average value of root biomass (48.9%) was used. After calculating the carbon stocks of each component, the above- and below-ground carbon was converted into a unit area scale (per hectare). Therefore, a hectare expansion factor (HEF) was used for the main and sub-plot (i.e., HEF = 25 for main plots, and HEF = 126.58 for smaller sub-plot) and expressed as Mg ha^{-1}. The detailed data collection method and measurement of biomass are described below.

6.2.3.1. Standing live trees

The standing live trees from sampling plots are divided in to two categories, i) Trees: DBH is greater than 14.5 cm and ii) Poles: DBH is between 2.5 -14.5 cm as the number of poles are more abundant than trees and getting information from all poles was time consuming, laborious and risky due to animal attack. In case of trees and poles, DBH was measured with a diameter tape and total height was measured using a Vertex-III hypsometer (Haglöf, Sweden). From each plot, the WD (gm cm^{-3}) was measured from one representative tree for each species with a wood specimen collected with a Haglöf wood increment borer (diameter 5.15 mm and bit length 300 mm) following Wiemann and Williamson (2013). The nine developed genus- and species-specific allometric models from Rahman et al. (2021c) (Chapter 4, Table 4.2) were used to estimate AGB of individual tree and pole in kg. Additionally, four locally derived species-specific models (Model 1-4 in Table 4.1) were also used for the respective tree species. In all cases, measured biophysical parameters such as DBH, H and WD were used in all models, as necessary. In cases where species-specific models were not available, models from the same genus or family were used. For *Ceriops decandra* and *Aegialitis rotundifolia*, DBH was converted to Girth at Collar Height (GCH) as described in the 4.2.5.1.

6.2.3.2. Standing dead trees and non-woody components

Standing dead trees were recorded as three categories of decay status depending on the amount of existing dead branches and twigs during the time of sampling: Decay I: dead trees with large branches along with small branches and twigs; Decay II: dead trees with only major large branches; and Decay III: dead stems with no or few small or large branches (Kauffman and Donato, 2012). The biomass of

each category of standing dead trees was calculated by using subtraction following Kauffman and Donato (2012). The biomass of Decay I trees was estimated by subtracting 2.5% from the calculation of live tree biomass since these trees are without foliage according to Kauffman and Donato (2012). The biomass of decay II categories is commonly 10-20% of live tree biomass as these trees are without foliage and fine branches (Kauffman and Donato, 2012) and mid value of 15% was used in this study. The best approach to measure biomass of the decay III dead trees is to calculate volume and subsequently multiplied by wood density according to Kauffman and Donato (2012). However, this estimation requires tree base diameter data in addition to DBH and height of trees to calculate the taper function. Since this study did not measure the base diameter of dead trees, it used an arbitrary value of 50% of live tree biomass for decay III dead trees as these trees are mostly without any foliage, and have fine and large branches (Kauffman and Bhomia, 2017).

In the case of non-woody species, the number of leaves of *Nypa fruticans* and the number of stems of *Phoenix paludosa* were also recorded from each sample plot. A few representatives of leaves and stems of variable sizes were brought to the laboratory for oven drying at 70 °C for leaves and 105 °C for stems to determine the dry biomass per specimen. The average dry biomass of these leaves and stems were used to calculate total biomass of non-woody vegetation for each plot.

6.2.3.3. Dead wood and pneumatophores

In each sample plot, two cross-sectional transects were laid inside the plot to calculate the mass of dead and downed wood. At each transect, the diameter of each downed wood was measured using digital slide calliper and divided in to four categories based on the diameter at the mid-point: fine (> 0.6 cm), small (0.6-2.5 cm), medium (2.5-7.6 cm) and large (< 7.6 cm). The carbon stocks of different sized down wood was calculated by using the volumetric equation described in Kauffman and Donato (2012). In order to convert biomass to carbon, the specific gravity (gm cm^{-3}) for each class was used following Kauffman and Donato (2012).

Mangroves exhibit numerous pneumatophores above-ground which contain a high biomass. The central 1 m sub-plot was used to count the number of pneumatophores. Some representative

pneumatophores of variable sizes were cut and subsequently brought to the laboratory for oven drying at 105°C to determine the dry biomass and the average conversion factor was then applied to get dry biomass of all measured pneumatophores.

6.2.4. Below-ground carbon measurement

The below-ground carbon is composed of mainly of carbon from roots and soil. The root carbon was measured using allometric models and incorporating soil carbon measurements from laboratory analysis. Species-specific conversion factors were used to convert root biomass into root carbon following Chanda et al. (2016b).

6.2.4.1. Below-ground root biomass

Mangroves form cable root systems underneath the surface; therefore, extraction and measurement of root biomass is labour intensive and difficult (Kauffman and Donato, 2012; Adame et al., 2017). Common or species-specific allometric models are largely used to infer root biomass in relation to above-ground parameters of trees such as DBH, height and/or wood density (Komiyama et al., 2005). However, after analysing available global datasets on below-ground root biomass, Adame et al. (2017) concluded that using common allometric models overestimates root biomass compared with using species-specific models. Therefore, the root biomass was estimated from species-specific allometric models from different mangrove forests (Table 5.1). Where allometric models were not available for any species, the common allometric model for root biomass, developed by Komiyama et al. (2005), was used to estimate root biomass of all trees and poles.

Table 6.1: List of species-specific allometric models for estimating root biomass in mangrove forest.

Target species	**Used models**	**Allometric models B (Kg) =**	**R^2; N**	**Source**	**Study area**
Sonneratia apetala	*Sonneratia* spp. (*S. alba* and *S. caseolaris*)	$0.230\ WD\ (DBH^2H)^{0.740}$	0.94; 30	Kusmana et al. (2018)	Central Java, Indonesia
Avicennia alba, A. marina, A. officinalis	*Avicennia marina*	$1.28\ DBH^{1.17}$	0.80; 14	Comley and McGuinness (2005)	Darwin harbour, Australia
Bruguiera piculate , B. gymnorrhiza	*Bruguiera* spp.	$0.0188\ (DBH^2H)^{0.909}$	unknown; 11	Tamai et al. (1986)	Southern Thailand

Ceriops decandra, Aegialitis rotundifolia	*Ceriops australis*	$0.159\ DBH^{1.95}$	0.87; 9	Comley and McGuinness (2005)	Darwin harbour, Australia
Rhizophora piculate, R. mucronata	*Rhizophora apiculata*	$0.00698\ DBH^{2.61}$	99;11	Ong et al. (2004)	Matang Mangrove Forest, Malaysia
Xylocarpus granatum, X. moluccensis	*Xylocarpus granatum*	$0.145\ DBH^{2.55}$	0.99; 6	Poungparn et al. (2002)	Southern Thailand
Kandelia candel	*Kandelia obovata*	$0.0483\ (DBH^2H)^{0.834}$	unknown; 5	Hoque et al. (2011)	Manko Wetland, Japan
Aegiceras corniculatum, Aglaia piculate, Cerbera manghas, Cynometra ramiflora, Excoecaria agallocha, Excoecaria indica, Heritiera fomes, Hibiscus tiliaceus, Intsia bijuga, Lumnitzera piculat, Millettia pinnata	Common allometric models	$0.199\ WD^{0.899}DBH^{2.22}$	0.95; 26	Komiyama et al. (2005)	Thailand
Here B = Dry biomass, N = Number of samples, GCH = Girth at collar height, HT = Total Height, HCH = Height at collar girth point, DBH = Diameter at breast height (1.3 m), R^2 = Coefficient of determination, WD = wood density (gm cm^{-3})					

6.2.4.2. Soil carbon

The 1 m soil carbon stocks data was collected for 55 plots from Rahman et al. (2021b) and the method for sample collection and analysis is described in sections 3.2.3 and 3.2.4.

6.2.5. Mapping forest types

Upscaling ecosystem carbon stocks require interpolation of field estimates to the extent of the forest and the development a mapped forest types to enable the regulation of the carbon stocks in any ecosystem. Since both above- and below-ground carbon stocks varies with forest type (Rahman et al., 2015a; Rahman et al., 2021b), a forest type map was produced from Sentinel-2 surface reflectance using Google Earth Engine (GEE). GEE is a cloud computing platform providing high-performance computing resources for processing, rapid prototyping and visualization of complex spatial analyses from a large geospatial dataset (Chen et al., 2017; Gorelick et al., 2017). GEE is useful to pick multi-

temporal cloud-free satellite images to produce temporal (for example, yearly) mosaics. A wide range of classifiers are also available in the platform such as Classification and Regression Trees (CART), Support Vector Machine (SVM), Continuous I Bayes classifier, Decision Tree (DT), Linear Regression, Maximum Entropy classifier and Random Forest (RF).

6.2.6. Dataset composition

Sentinel-2 MSI (Multispectral Instrument) surface reflectance (SR) imagery was selected to develop a cloud-free composite dataset during the fieldwork period from February 2019 to April 2019 (Figure 5.3). This period is the dry winter in the Sundarbans and therefore less likely to have cloudy pixels. Sentinel-2 MSI is a wide-swath multi-spectral imaging mission by European Space Agency (ESA) providing some image bands of 10 m resolution for monitoring of vegetation, soil and water (ESA, 2022). Cloud free images (0% cloudy pixels) were filtered from the Sentinel-2 SR level-2A image collection available in GEE platform as 'COPERNICUS/S2_SR' within the specified period. The study used six image bands B2, B3, B4, B6, B8 and B11 representing Blue, Green, Red, Red edge 2, Near Infra-red (NIR) and Short-wave infra-red 1 (SWIR) respectively. Since the resolution of B6 and B11 bands is 20 m, these were resampled (bilinear) to 10 m harmonising with other bands. A separate cloud cover filtering was used for the initial 16 images by using the quality pixel band of Sentinel 2, which allowed dense and cirrus clouds and shadows to be masked. Three spectral indices including NDVI (Normalised Difference Vegetation Index, Modified Normalised Difference Water Index (MNDWI) and Bare Soil Index (BSI) were used to discriminate pixels between forests, water and bare soil areas. NDVI is a widely used vegetation index to indicate measures of vegetation health, therefore it helps to discriminate among different tree species and with bare soil and water. On the other hand, MNDWI and BSI are widely used for land use mapping to discriminate water and bare soil than other land use types. The derivation of each index is given below-

$$NDVI = \frac{NIR - RED}{NIR + RED} \text{ … … … … … ….Eq. 1 (Rouse et al., 1974).}$$

$$MNDWI = \frac{GREEN - SWIR1}{GREEN + SWIR1} \text{ … … … … … ….Eq. 2 (Xu, 2006)}$$

$$BSI = \frac{(SWIR1 + RED) - (NIR + BLUE)}{(SWIR1 + RED) + (NIR + BLUE)} \text{ … … … … … ….Eq. 3 (Rikimaru et al., 2002)}$$

Here, NIR = Near Infra-Red band (B8), RED = Red band (B4), GREEN = Green band (B3), SWIR1 = Short wave Infra-Red band (B11) and BLUE = Blue band (B2). The band number in parentheses indicates the band name in Sentinel-2. The resolution of SWIR1 is 20 m, therefore it was downsampled to 10 m before calculating the index.

In addition to the above data, the study also included the global forest canopy height map, 2019, developed through integration of the Global Ecosystem Dynamics Investigation (GEDI) and Landsat time series data (Potapov et al., 2021). Since the Bangladesh Sundarbans have a height gradient from the east to the west part, the inclusion of canopy height data in the classification is expected to help classify different forest-types (Lee et al., 2015; Rahman et al., 2021b). The 30 m height map was then converted to 10 m through bilinear resampling in GEE.

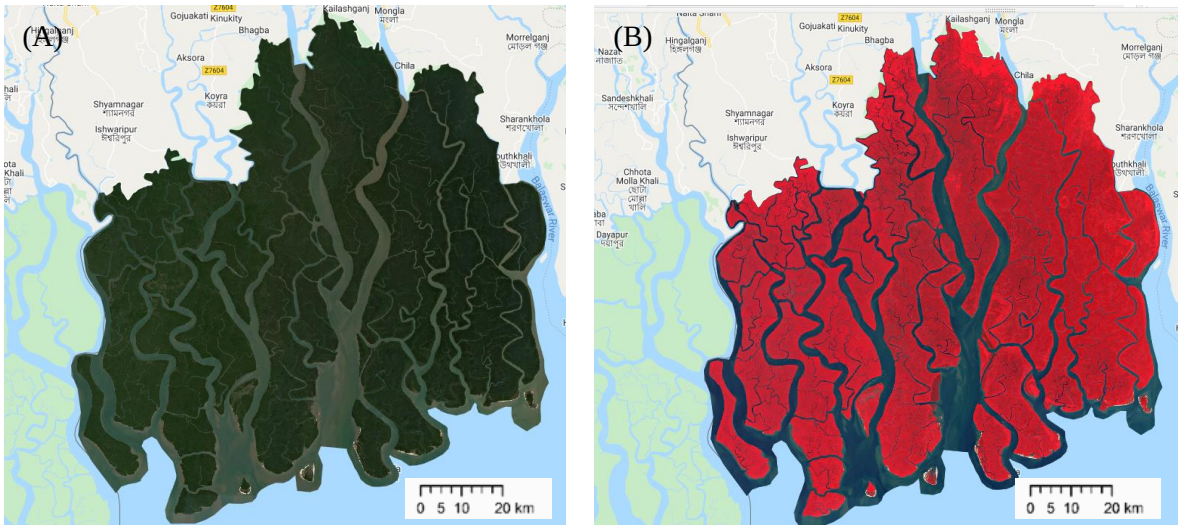

Figure 6.3: Median composite image of Sentinel-2 image collection of the Sundarbans, Bangladesh visualised in A) RGB colour and B) False colour.

The Bangladesh Sundarbans covers three tiles of Sentinel-2 MSI satellite images with mainly T45QYE, but also T45QXE and T45QYD. The initial image filtering provided 17 cloud free images with the selected 6 bands during the field work period between February to April' 2019. All these image collections were used to calculate the median to compose the 10 m base data cube (BDC). Thus, the final composite image is composed of 10 bands including Sentinel-2 (6), spectral indices (3) and a canopy height band.

6.2.7. Determination of forest type

Forest type was determined according to the composition of each species (the percentage of individuals of trees and poles) presented in each sample plot. Single species dominance (for example, *Heritiera* only) was considered when the composition of a species is ≥ 70%. If one species was ≥ 50% and another species ≥ 25%, then the plot was named by those two species such as *Heritiera_Excoecaria*. If one species was ≥ 50% and there was no other species ≥ 25%, then the forest-type was designated as single species followed by "Mixed" type (for example, *Xylocarpus*_Mixed). If there was no dominant single species (< 50%) then the sample plot was considered as "Mixed". The plot forest-type data was used to extract spectral signatures or pixel values of all bands of the final composite image. These extracted values were then used in a hierarchical clustering to merge similar forest-types and to identify unique forest-types discriminating spectral signatures and other values in the composite image. The hierarchical clustering was conducted with the "ggdendro" package by using Euclidean distance computation along with the "Ward.2" agglomeration method in R 4.0.4 for Windows (Murtagh and Legendre, 2014).

6.2.8. Forest type classification

A supervised classification method was used to classify forest types in the Sundarbans, where plot forest-type was used to train the classifier (Chen and Stow, 2002). To train the classifier, 70% of field plots were chosen randomly and the remaining 30% were used to validate the forest-type map. The randomisation was done in such a that each class must be included at least once as both training and validation. Since the Bangladesh Sundarbans consists of approximately 40% water and barren land, 15 points were marked each as water and barren land in the GEE interface through visual inspection from high-resolution satellite imagery using Google Maps data inside the GEE environment. The randomisation for both validation and training To match with the size of sample plots, a circular buffer of 11.3 m was established for each point.

Both pixel-based and object-based image classification methods were used in this study with two machine learning classifiers, Random Forest (RF) and Support Vector Machine (SVM) (Figure 5.4).

The classification was conducted in the GEE environment using the code developed by Tassi and Vizzari (2020) with necessary modifications. The object-based classification (also referred as Geographic Object-based Image Analysis (GEOBIA)) uses image segmentation and clustering techniques to make clusters of the same land uses and provides better results on high resolution data (Ren and Malik, 2003; Blaschke, 2010; Solano et al., 2019). On the other hand, the pixel-based classification approach is more suited to low resolution data and creates a "salt-pepper" effect with high resolution data (Messina et al., 2020). The object-based classification includes the Gray-Level Co-occurrence Matrix (GLCM) to calculate cluster textural indices and the Simple Non-Iterative Clustering (SNIC) algorithm to identify spatial clusters, which is widely used to improve the accuracy in land use and land cover (LULC) classification (Mahdianpari et al., 2020; Stromann et al., 2020).

Machine Learning (ML) classifiers such as RF and SVM have been shown to outperform the traditional maximum likelihood algorithms for land use and land cover classification (LULC) (Ghimire et al., 2012; Mondal et al., 2019). Being non-parametric methods, these classifiers have the advantage that they do not require any statistical assumptions for data distribution (Tassi and Vizzari, 2020). The RF classifier is a collection of multiple trees, where each tree casts a random vote to the most popular class by using a random vector sampled independently from training datasets (Breiman, 2001). This classifier uses 'bootstrap aggregating' or 'bagging' to select training data for each class and each pixel is assigned to a class according to the most popular vote from all tree predictors (Ghimire et al., 2012). RF generally performs better than other popular classifiers in LULC classification including in mangrove forests (Adam et al., 2014; Mondal et al., 2019). On the other hand, SVM, a non-linear classifier, identifies boundaries between classes rather than assigning points to a class (Pal and Mather, 2005). It separates classes based on a user defined kernel function and parameters that are optimised using machine-learning to maximise the margin from the closest point to the hyperplane. Therefore, it requires the choice and tuning of kernels and other input parameters (Huang et al., 2002). However, both classifiers require high quality training datasets to train the classifier.

The GEE code executes the pixel-based (PB) and object-based (OB) approach one after another either with RF or SVM classifiers with the same composite dataset, and training data. The flowchart of all datasets and methodologies is presented in Figure 5.4. The GEE codes for creating composites, classification and accuracy assessments are provided via the following two links-

1) https://code.earthengine.google.com/e56d1cab4e8cd9af89a4ead037189fd8

2) https://code.earthengine.google.com/62de8534047d05f27103b61c24031623

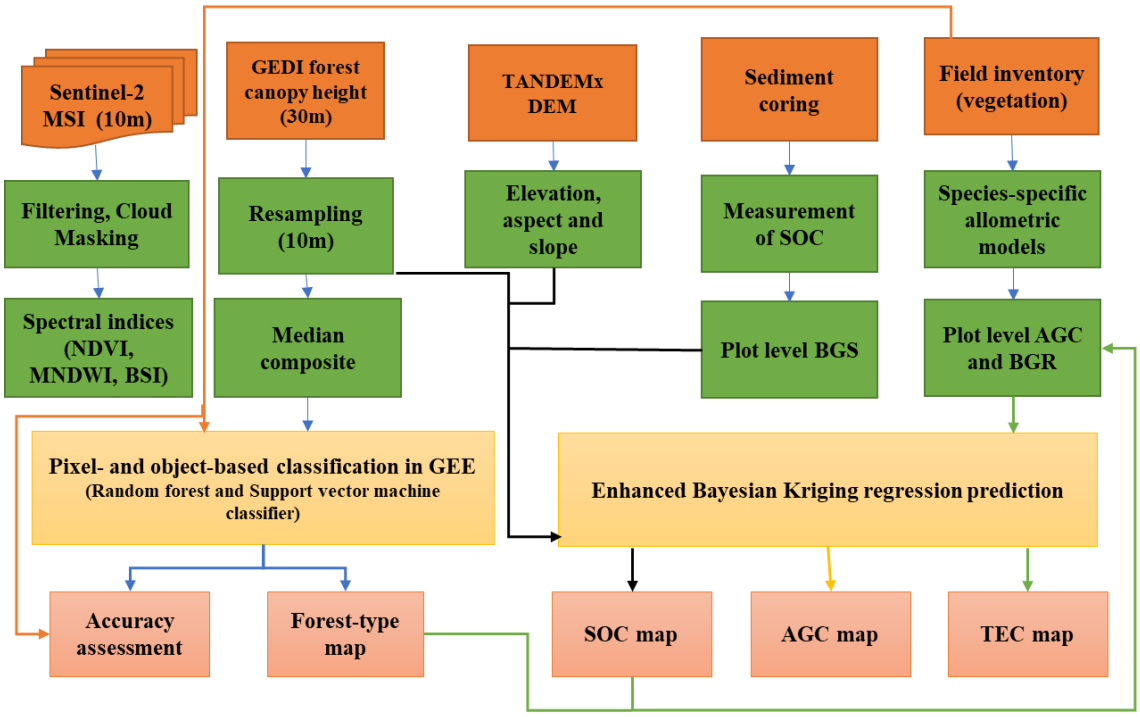

Figure 6.4: The methodological workflow implemented in Google Earth Engine (GEE) and GIS environment.

The PB approach followed quick classification of images with the desired forest-type and accuracy assessment. However, for SVM, a band normalisation of the input dataset was done before executing the code. A radial basis function kernel (RBF) was applied for SVM with gamma = 1 and cost = 10 following Tassi and Vizzari (2020). In case of RF classifier, the number of trees (DT) was set to 60. This is achieved by checking the lowest Out-Of-Bag error (OOB) in the GEE by using "Explain" function through increasing the number of trees from 10 to 200. In the pixel-based output map, a final morphological operation "focal mode" was performed with the default 1.5 m radius to reduce the "salt and pepper" effect. In the OB method, both SNIC and GLCM was applied together where SNIC requires a regular grid of seeds as input using the "Image.Segmentation.seedGrid" function. This

function requires to state the superpixel seed location spacing in pixels. Therefore, to run SNIC, various seed spacings such as 5, 10, 15, 20 were applied and the best combination was compared with accuracy assessment following Tassi and Vizzari (2020).

6.2.9. Validation

For validation, 30% of sample plots were used and the uncertainty in classification was measured by using an error matrix. The same training samples were run for each combination of methods and classifiers. Users, Producers and overall accuracy were calculated for each of the forest types according to Olofsson et al. (2014). Quantity disagreement and allocation disagreement were also calculated as described by Pontius and Millones (2011) and Warrens (2015). The quantity disagreement is the deviation from perfect agreement between the classified and training classes and the allocation disagreement reflects the error due to differences in the spatial allocation of each class.

6.2.10. Prediction of soil carbon and total ecosystem carbon stocks

Soil organic carbon, above-ground carbon and total ecosystem carbon stocks were predicted using co-kriging in GIS (ArcGIS Pro 2.9.1). Enhanced Bayesian Kriging Regression Prediction (EBKRP) was used to interpolate carbon stocks in places where measurements were not taken. This method is relatively new and is a hybrid interpolation method combining simple kriging and ordinary least squares (OLS) regression. EBKRP is the extension of Empirical Bayesian Kriging where an explanatory variable raster, such as a forest-type map is used that affect the dependent variable (Krivoruchko, 2012; ESRI, 2022b). The input raster acts as a prior distribution for the Bayesian analysis and the combination of regression analysis and kriging make interpolations more precise than estimated by only kriging or regression (Krivoruchko and Gribov, 2020; ESRI, 2022b). The combination of kriging and regression has the advantage of separating the mean and error of the dependent variable, whereas OLS with regression models, the mean value as a weighted sum of the explanatory variables and simple kriging models the error term using a semivariogram/covariance model (ESRI, 2022b). However, estimation of the mean value and error term are computed simultaneously.

In this study, soil organic carbon (SOC) was predicted with the forest-type map, Digital Elevation Model (DEM), aspect and slope (Figure 5.5). The forest-type map from this study was used to predict SOC using the data from 55 sample plots. The DEM of the Bangladesh Sundarbans was calculated by subtracting the GEDI canopy height map from the Digital Surface Model (DSM) taken from the TanDEM-X 12 m satellite data (Krieger et al., 2006; Hawker et al., 2019). In this case, both were resampled to 10 m resolution to match with forest-type map. From the DEM, aspect and slope were created by using ArcMap 10.7.1. For the prediction of TEC and AGC stocks, the plot level carbon stocks were combined with the forest-type map.

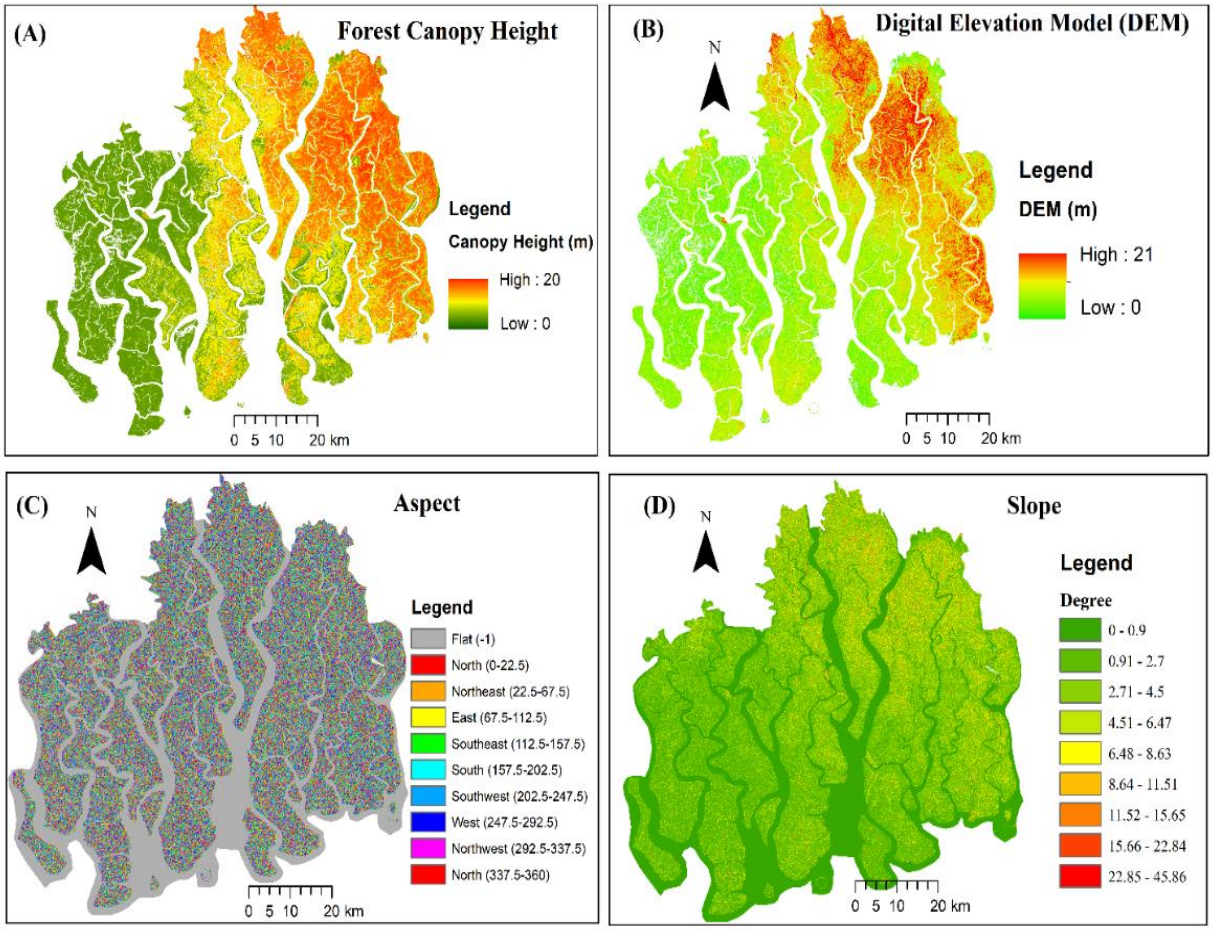

Figure 6.5: Remote sensing dataset used in classification of forest types and geostatistical interpolation. A) Canopy height map in the Sundarbans using Landsat 8 and GEDI by Potapov et al. (2021), B) Digital elevation model (DEM), C) Aspect and D) Slope in the Sundarbans from TanDEM-x (12.5 m) (Krieger et al., 2006).

In ArcGIS Pro 2.9.1, four available semivariogram models (Exponential, Nugget, Whittel and K-Bessel) were used to produce covariate surfaces and the model with least Residual Mean Squared

Error (RMSE) was used for the final prediction. The spatial autocorrelation of the error term diminishes relatively quickly for the Exponential model and slowly for Whittle model compared to other options. On the other hand, the Nugget model assumes the error term is spatially independent, whereas K-Bessel is quite flexible to reduce the error term either slowly or quickly or anywhere in between (ESRI, 2022b).

6.2.11. Error and uncertainty analysis

The measurement errors as a result of the combination of instrument errors and human errors propagate into the plot-level ecosystem carbon stocks through using allometric models to estimate individual tree AGC and below-ground root carbon from DBH, height and wood density (Réjou-Méchain et al., 2017; Réjou-Méchain et al., 2019). The plot-level error was estimated by using the "*AGBmonteCarlo"* function of the BIOMASS R package, where the overall error propagation is estimated by using the probability distributions of errors from trees and allometric model parameters by running 1000 Monte Carlo simulations (Réjou-Méchain et al., 2017). The package estimates AGC and SD (standard deviation) for each tree which is then scaled to plot-level. The accuracy of the height measuring instrument (Vertex-III hypsometer) is 1%, and so 1% of total height of each tree was considered as instrumental error. For diameter error, the default "chave 2004" was used in "*Dpropag"* argument representing large and small errors on 5 and 95% of all trees respectively (Chave et al., 2004). The error due to measurement of wood density was obtained as the SD of wood density for each species from the Table 4.3. The function was modified to employ species-specific allometric models and their respective residual standard errors from the Table 4.2. The plot-level above-ground error was used to interpolate spatial distribution of AGC error and the uncertainty of soil carbon (Standard Deviation) was combined to obtain a spatial distribution of TEC error in the Sundarbans.

6.2.12. Statistical analysis

All statistical analysis and graphics were accomplished in R 4.0.4 for Windows (R Core Team, 2021). The performance of each interpolation method was evaluated through the cross-validation statistics

produced by ArcGIS pro-2.9.1. In the cross-validation method, the observed value is removed one by one from the analysis to predict that value from the remaining values and the error is calculated from the difference of measured and estimated values. The default statistical diagnostics from ArcGIS Pro was used to compare the performance of each interpolation model such as Mean Error (ME), Root Mean Squared Error (RMSE), Average Standard Error (ASE), Mean Standardized Error (MSE), Root Mean Square Standardized Error (RMSSE) and average Continuous Ranked Probability Score (CRPS).

The Mean Error (ME) represents the arithmetic averaged difference between the measured and the predicted values. The positive and negative values represent overestimation and underestimation of predicted values (Li and Heap, 2011). The Root Mean Square Error (RMSE) is a commonly used cross-validation parameter which indicates the accuracy of prediction of measured values. The smallest RMSE signifies the best model in cross validation. The Average Standard Error (ASE) is the arithmetic average of prediction errors, whereas Mean Standardized Error (MSE) provides the average of the standardized errors. The value of MSE is closer to zero for better models. If the RMSE is similar to ASE then the model predicts the observed values well. On the other hand, when the ASE is greater than RMSE, this indicates overestimation, and when lower than the RMSE, this indicates underestimation. The Root Mean Square Standardized Error (RMSSE) is the square root of MSE which signifies a better model when close to 1. The RMSSE > 1 indicates a general underestimation, while the RMSSE < 1 indicates a general overestimation of predicted variables. The geostatistical wizard of EBKRP in ArcGIS Pro 2.9.1 has a separate statistical parameter called average Continuous Ranked Probability Score (CRPS), which measures predictive cumulative distribution function and calculates deviation to each observation. This parameter has the advantage over other parameters for comparing the full distribution rather than single values and the ideal value should be as small as possible (ESRI, 2022a). To facilitate selection of the best interpolation methods, both RMSE and CRPS were prioritised over other statistical parameters.

The Total Ecosystem Carbon stocks (TEC, Mg ha^{-1}) among different components (standing trees, pneumatophores, dead wood, below-ground root and soil) were compared with one-way analysis of

variance (ANOVA) using the ‘car’ package (Fox and Weisberg, 2019). Similarly, the TEC among three salinity zones and eight forest types were compared with a two-way ANOVA test. In all cases, data were logarithmic (natural) transformed to meet the assumptions of normality and equal variances by using Shapiro Wilk and Levene’s tests, respectively, and subsequently back-transformed to present graphically. All graphical output was generated using the ‘ggplot2’ package in R (Wickham, 2016) and maps were produced with ArcMap 10.7.1 and ArcGIS pro 2.9.1.

6.3. Results

6.3.1. Determination of forest type class

The composition of each species from all sample plots comprised 18 forest-types. These forest-types were used to extract surface reflectance, spectral index and height map values from the Sentinel-2 composite(Figure C.1 and C.2). The spectral reflectance of water and bare land showed strong discrimination in all 6 bands of Sentinel-2 MSI imagery. On the other hand, mangrove tree species showed different of spectral reflectance in the red edge, near infra-red and short-wave infra-red bands (Figure C.1). All spectral indices and the GEDI height map data showed differentiation for water and barren land, but there is not much differentiation among species type except for *Sonneratia* in the case of MNDWI (Figure C.2). However, forest species showed different canopy heights in the GEDI height map, which demonstrates the importance of these data for clustering different species. The 2 m average canopy height of water pixel in the GEDI height data and higher MNDWI of *Sonneratia* showed the influence of tidal current which can affect the classification for these two forest-types (Figure C.2). The Sonneratia spp. usually grows close proximity to the river, therefore it is difficult to separate this species with water from the spectral signatures during high tides.

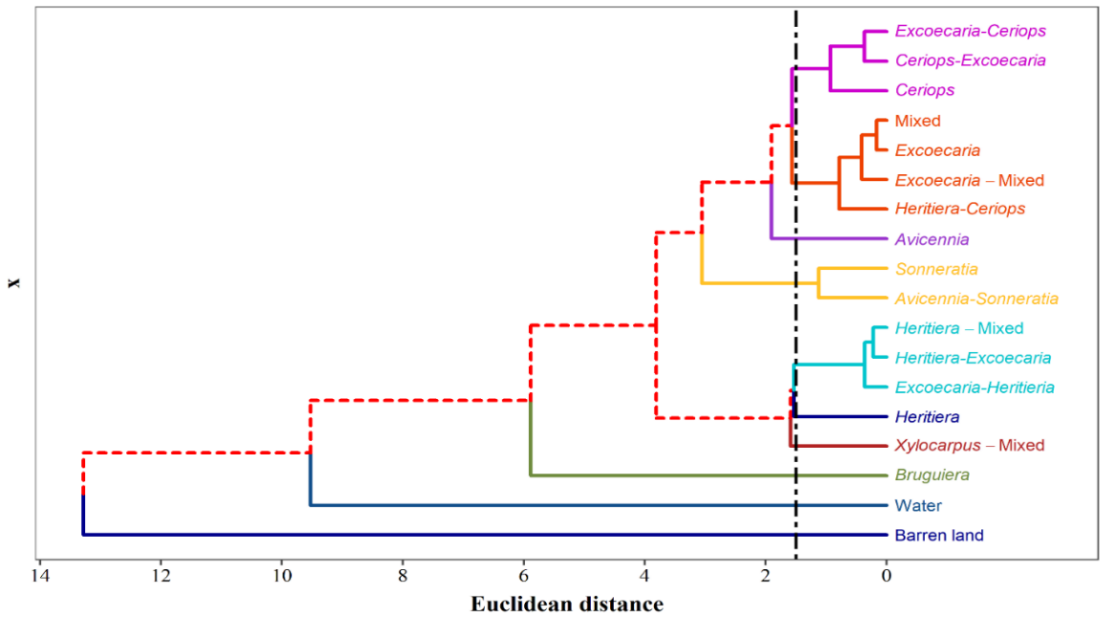

Figure 6.6: Dendogram showing hierarchical clustering analysis of different forest-type. The vertical lince was used to choose 10 forest-types from the clustering techniques.

The hierarchical clustering analysis showed that both barren land and water formed distinct clusters far from the vegetated forest-types (Figure 5.6). Among mangrove species, *Bruguiera*, *Xylocarpus*_Mixed, *Avicennia* and *Heritiera* formed distinct clusters. The other four clusters are mixed types which can be recognised as *Excoecaria_Heritiera*, *Avicennia_Sonneratia*, *Excoecaria*_Mixed and *Ceriops_Excoecaria*. The *Excoecaria_Heritiera* groups are mainly the combination of *Heritiera* and *Excoecaria* along with some *Sonneratia*_Mixed plots. *Avicennia_Sonneratia* forest-type is the combination of *Avicennia* and *Sonneratia* and some dominant *Sonneratia* plots. *Excoecaria*_Mixed includes plots where *Excoecaria* is the dominant species either alone or with mixed species and there is no dominant species such as Mixed and exceptionally *Heritiera_ceriops*. The last cluster includes both *Ceriops* and *Excoecaria* together or *Ceriops* alone.

6.3.2. Mapping forest-types in the Sundarbans

The Sentinel-2 MSI imagery composite of the Bangladesh Sundarbans was classified into ten forest-types. The best forest-type classification maps with both PB and OB along with RF and SVM classifier are presented in Figure 5.7. All maps show a gradient of forest-type with dominant *Heritiera* in the east and *Excoecaria* in the central part and the combination of *Ceriops* and *Excoecaria* in the

west. However, the map produced with the SVM classifier has more *Heritiera_Excoecaria* than only *Heritiera* in the eastern Sundarbans (Figure 5.7). In the case of the RF classifier, both PB and OB yielded a similar percentage of total area occupied by each forest-type. The biggest differences were observed when using the SVM classifier with the OB method, where *Bruguiera* is absent and the area of *Heritiera* and *Heritiera_Excoecaria* is decreased and increased by 6% and 9%, respectively, as compared to the classified map of OB with the RF method (Figure C.3). The total area of all classified maps is 865,691 ha including 54%, 53% and 52% water area in classified maps of PB_RF, OB_RF and OB_SVM methods, respectively.

Accuracy assessment was done using a confusion matrix according to the 30% of training samples kept for validation. Based on the overall accuracy of the confusion matrix, the pixel-based classification with the RF classifier showed the highest accuracy followed by OB (seed spacing 10) with SVM (Table 5.2). The forest-type map showed that the land area of Bangladesh Sundarbans is 396,675 ha. The *Hertiera_Excoecaria* type was the most dominant forest type (39.58%) in the central and eastern part of the Sundarbans followed by *Excoecaria*_Mixed (25.96%) and *Ceriops-Excoecaria* (17%). The *Heritiera fomes* alone constitutes about 13.61% of the total land area and is mostly concentrated in the eastern part of the Sundarbans (Figure C.3).

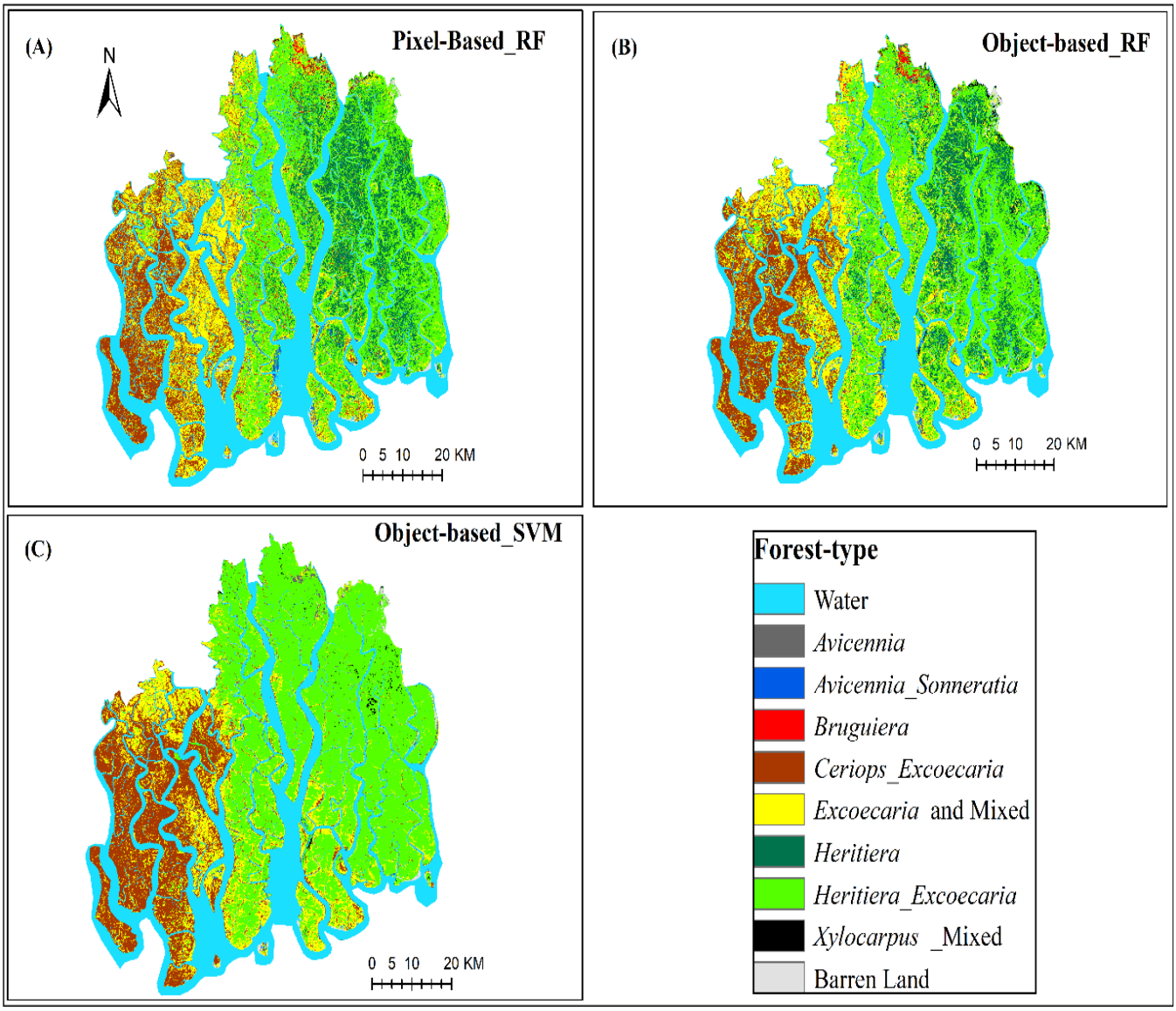

Figure 6.7: Forest-type map in the Sundarbans using A) Pixel-based classification with RF, B) Object-based classification with RF and C) Object-based classification with SVM.

Table 6.2: Comparison of overall accuracies (percentage) among PB and OB classification with RF and SVM classifiers. In case of OB method, difference seed spacing was compared.

Forest types	**Classifier**	**Pixel based Classification**	**Object-based classification**			
			Seed spacing (no. of pixels)			
			5	**10**	**15**	**20**
10 forest-types	Random Forest (RF)	66.3	53.8	57.7	48.1	52.9
	Support Vector Machine (SVM)	45.2	63.5	63.7	52.9	58.7

Good practice guideline was followed to the report accuracy assessment for the area estimation of all forest-types, according to Olofsson et al. (2014), and the detailed error matrix of pixel-based with RF classification is provided in the Table 5.3. The advantage of using the good practice guideline is that it implements a probability sampling design in order to quantify accuracy and area estimation, and reports the estimated error matrix in terms of the proportion of area and uncertainty by reporting confidence intervals for accuracy and area parameters (Olofsson et al., 2014).

Table 6.3: Confusion matrix of the most accurate forest-type classification in the Sundarbans.

	Water	***Avicennia***	***Avicennia_ Sonneratia***	***Bruguiera***	***Ceriops_ Excoecaria***	***Excoecaria* and Mixed**	***Heritiera***	***Heritiera_ Excoecaria***	***Xylocarpus_* Mixed**	**Barren land**	**Total**	**Users Accuracy (±95% CI)**	**Area proportion (Wi)**
Water	**0.4741**	0.0000	0.0677	0.0000	0.0000	0.0000	0.0000	0.0000	0.0000	0.0000	0.542	**0.88 (±0.23)**	0.5418
Avicennia	0.0000	**0.0014**	0.0000	0.0005	0.0000	0.0000	0.0000	0.0009	0.0000	0.0000	0.003	**0.50 (±0.31)**	0.0028
Avicennia_ Sonneratia	0.0000	0.0014	**0.0042**	0.0000	0.0028	0.0000	0.0000	0.0000	0.0000	0.0000	0.008	**0.50 (±0.31)**	0.0083
Bruguiera	0.0000	0.0000	0.0000	**0.0015**	0.0000	0.0000	0.0000	0.0000	0.0000	0.0000	0.001	**1.00 (±0.00)**	0.0015
Ceriops_ Excoecaria	0.0000	0.0000	0.0000	0.0000	**0.0659**	0.0120	0.0000	0.0000	0.0000	0.0000	0.078	**0.85 (±0.19)**	0.0779
Excoecaria* and *Mixed	0.0000	0.0000	0.0044	0.0000	0.0352	**0.0661**	0.0000	0.0044	0.0088	0.0000	0.119	**0.56 (±0.14)**	0.1190
Heritiera	0.0000	0.0000	0.0000	0.0000	0.0000	0.0208	**0.0416**	0.0000	0.0000	0.0000	0.062	**0.67 (±0.23)**	0.0624
Heritiera_ Excoecaria	0.0000	0.0000	0.0076	0.0000	0.0000	0.0756	0.0076	**0.0907**	0.0000	0.0000	0.181	**0.50 (±0.14)**	0.1813
***Xylocarpus_* Mixed**	0.0000	0.0000	0.0000	0.0004	0.0000	0.0000	0.0000	0.0000	**0.0011**	0.0000	0.001	**1.00 (±0.00)**	0.0014
Barren land	0.0000	0.0000	0.0000	0.0000	0.0000	0.0000	0.0000	0.0000	0.0000	**0.0036**	0.004	**1.00 (±0.00)**	0.0036
Total	0.474	0.003	0.084	0.002	0.104	0.174	0.049	0.096	0.010	0.004			
Producers accuracy (±95% CI)	**1.00 (±0.17)**	**0.50 (±0.21)**	**0.05 (±0.09)**	**0.64 (±0.09)**	**0.63 (±0.10)**	**0.38 (±0.08)**	**0.85 (±0.16)**	**0.94 (±0.16)**	**0.11 (±0.01)**	**1.00 (±0.17)**		**Overall Accuracy 0.75 (±0.09)**	

The confusion matrix with proportions of area of each class showed that the pixel-based (with RF) classification achieved an overall accuracy of 75% with a 95% confidence of being between 66% and 84% (Table 5.3). The quantity disagreement was 0.15 and allocation disagreement was 0.08.

6.3.3. Spatial distribution of soil organic carbon

By using the EBKRP kriging interpolation method, the SOC stocks were interpolated for the entire Bangladesh Sundarbans using the forest-type map and with a combination of elevation, slope and aspect. The interpolation result was checked and compared with different interpolation methods such as Exponential, Nugget, Whittle and K-Bessel. Different combinations of datasets and semivariograms provided different distributions of SOC. The statistics of cross-validation showed that the model with forest-type only (K-Bessel semivariogram) provided the lowest RMSE and CRPS (Table 5.4). However, the positive ME and RMSSE (lower than 1) indicates overestimation of the predicted values. The overestimation is also evident as ASE is greater than RMSE for the best interpolation model. However, the inclusion of the DEM, aspect and slope did not improve the prediction of SOC in the Sundarbans (Table 5.4).

Table 6.4: Cross-validation statistics of each Enhanced Bayesian Kriging Regression prediction (EBKRP) model for the prediction SOC in the Sundarbans. The bold value indicates the best value for all statistics.

Enhanced Bayesian Kriging Regression prediction (EBKRP) model parameter	SOC prediction with forest types				SOC prediction with forest types and DEM				SOC prediction with forest types, DEM, slope and aspect			
	Semivariogram type											
	Exponential	Nugget	Whittle	K-Bessel	Exponential	Nugget	Whittle	K-Bessel	Exponential	Nugget	Whittle	K-Bessel
Mean Error (ME)	-0.17	10.07	-0.14	0.2	-0.85	12.46	-0.84	-0.87	-0.2	3.16	-0.26	**0.13**
Root Mean Square error (RMSE)	11.32	23.27	11.48	**11.23**	13.19	20.71	13.68	12.77	12.61	19.56	13.21	12.31
Mean Standardized Error (MSE)	0.001	14.17	0.005	0.03	-0.05	14.4	-0.05	-0.05	-0.002	3.69	**-0.006**	0.02
Root-Mean-Square Standardized Error (RMSSE)	0.94	23.27	0.98	0.92	0.97	44.11	**0.99**	0.95	0.94	13.89	0.95	0.92
Average Standard Error (ASE)	12.7	**6.35**	12.91	12.89	14.29	**6.35**	14.99	13.93	14.30	**6.35**	15.26	13.87
Average Continuous Ranked Probability Score (CRPS)	6.41	17.36	6.53	**6.38**	7.23	15.79	7.55	7.03	7.06	13.36	7.38	6.86

The predicted SOC stocks in the Sundarbans varied between 17.87 to 99.44 Mg ha^{-1} with an average of 54.41 Mg ha-1. The central northern Sundarbans had higher SOC compared to western and southern areas (Figure 5.8). The standard error for SOC ranges from 1.15 Mg ha^{-1} to 15.57 Mg ha^{-1} with an average of 10.31 Mg ha^{-1}. The SOC stocks of the Bangladesh Sundarbans was 21.37 Teragram (Tg) with a 95% confidence of being between 13.20 Tg and 29.55 Tg.

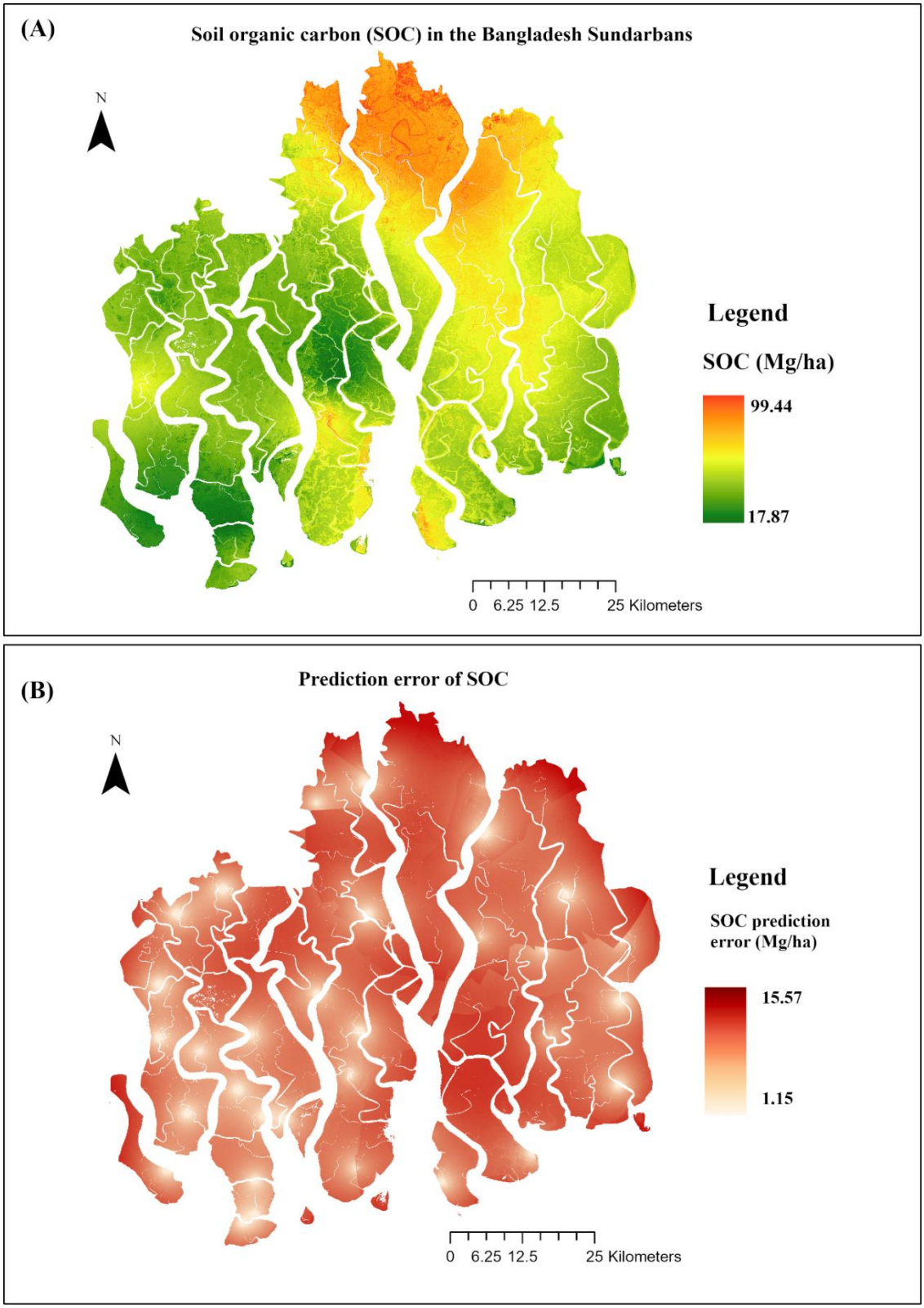

Figure 6.8: Spatial distribution of A) SOC stocks and B) SOC prediction standard errors in the Sundarbans.

6.3.4. Total ecosystem carbon stocks (TEC)

Above-ground carbon comprises the carbon stocks from living and dead standing trees, pneumatophores and dead lying wood on the forest floor. The standing trees included the non-tree species such as *Nypa fruticans* and *Phoenix paludosa* from which leaves and stems were harvested to measure the dry weight of each specimen. The average dry weight of a *N. fruticans* leaf is 1065.6 ± 342.68 gm (n = 9) and *P. paludosa* stem is 1813.24 ± 444.75 gm (n = 6). For dead wood, the mean diameter of different sized dead wood was measured. The mean diameters are as follows; fine dead wood (0.35 ± 0.10 cm, n = 51), small dead wood (1.86 ± 0.48 cm, n = 242), medium dead wood (4.47 ± 1.32 cm, n = 213) and large dead wood (12.75 ± 4.60 cm, N = 41). The quadratic mean of different dead wood comprises 0.37 cm for fine, 1.92 cm for small and 4.67 cm for medium dead wood. For measuring biomass of pneumatophores of different species, the average length, diameter, green weight and dry weight were measured and are presented in the Table C.1.

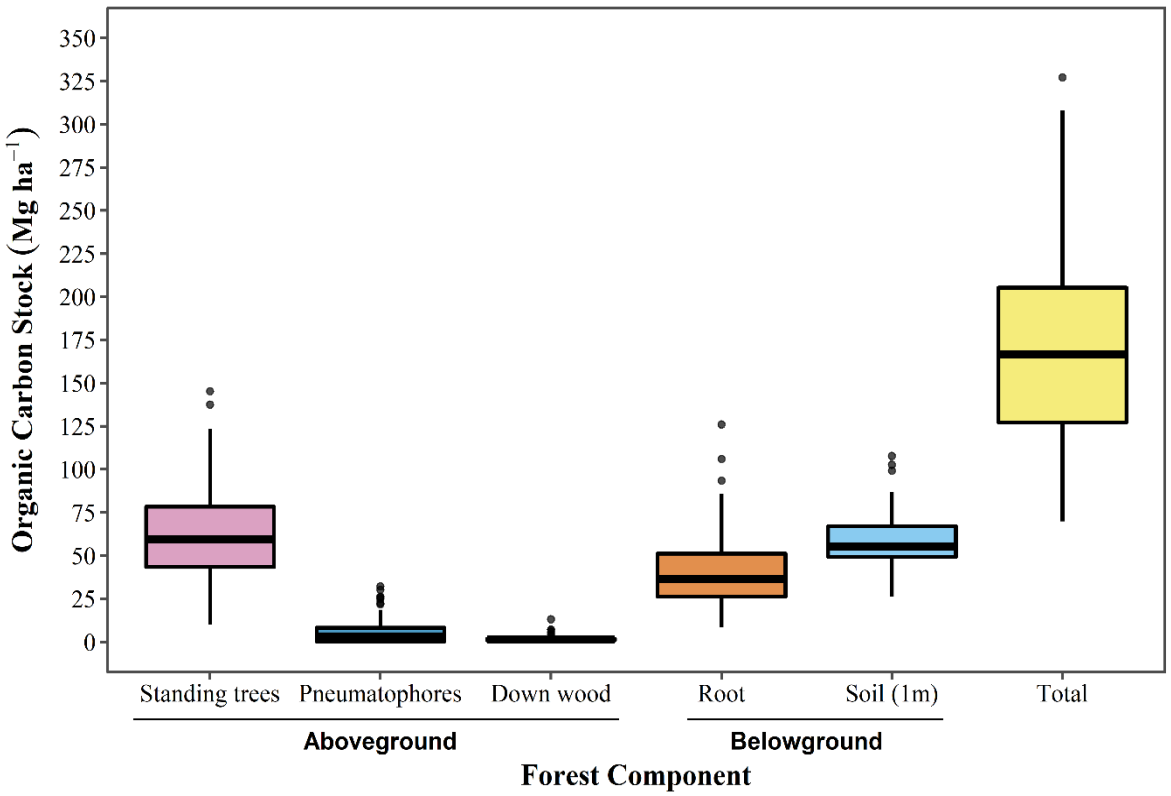

Figure 6.9: The ecosystem carbon stocks (Mg ha^{-1}) among different components in the Sundarbans. The black horizontal line of box plot represents the median and the black dot represents outliers.

The plot level above- and below-ground components were combined to estimate total ecosystem carbon stocks. The below-ground SOC were taken from the 55 measured plots and for the remaining plots, the predicted SOC was retrieved from Figure 5.8. The average TEC in the Sundarbans is 170 (± 51.7). One way ANOVA revealed that the carbon stocks varied significantly among different components. The average AGC was significantly higher (63.6 ± 27.6 Mg ha^{-1}) in standing live trees followed by below-ground soil (58.7 ± 14.3 Mg ha^{-1}), below-ground root (40.4 ± 18.9 Mg ha^{-1}), pneumatophores (5.5 ± 6.68 Mg ha^{-1}) and downed wood (1.65 ± 1.4 Mg ha^{-1}) ($p < 0.01$) (Figure 5.9).

The two-way ANOVA of natural logarithmic organic carbon stocks revealed that the TEC in the Sundarbans varied significantly with forest-type $F_{2, 123} = 55.6$, $p < 0.001$ and salinity zones $F_{7, 123} = 6.6$, $p < 0.001$ (Figure 5.10A, Table C.3). However, there was no interaction effect of both salinity zones and forest types on TEC in the Sundarbans ($p > 0.05$). The carbon stocks for each component varied significantly with salinity zones in the Sundarbans (Figure C.10). The TEC was significantly higher in the oligohaline zone (201.5 ± 42.5 Mg ha^{-1}) followed by the mesohaline zone (181.3 ± 48.3 Mg ha^{-1}) and the polyhaline zone (131.4 ± 35.6 Mg ha^{-1}) ($p < 0.01$) (Figure 5.10B).

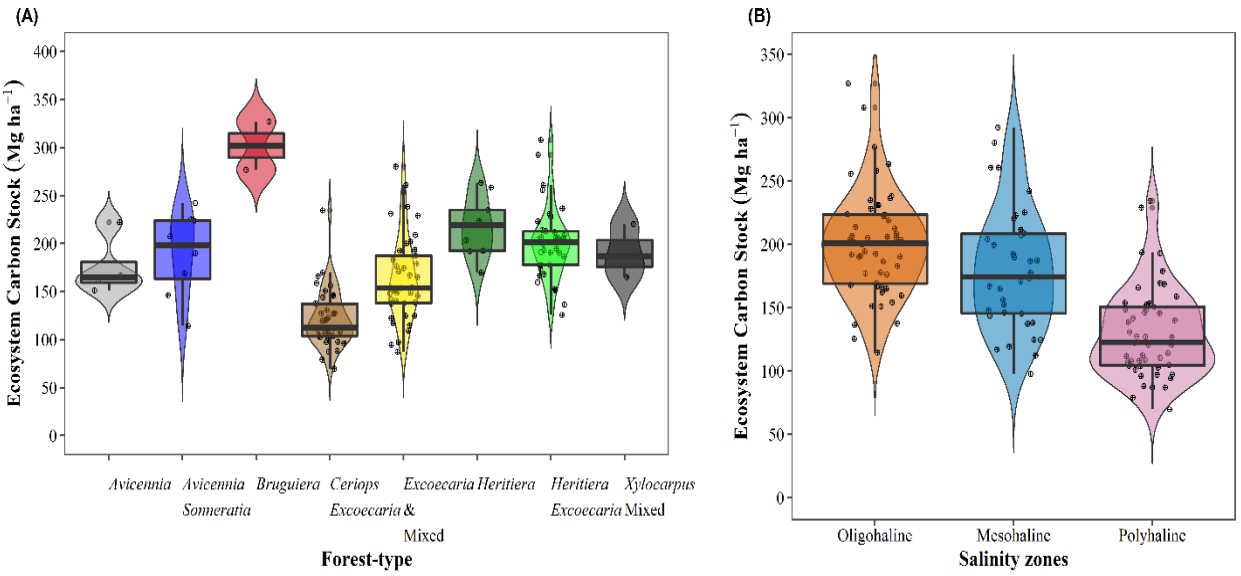

Figure 6.10: Integrated violin-box jitter plot shows the ecosystem carbon stocks (Mg ha^{-1}) among A) forest type and B) salinity zones. The black horizontal line of box plot represents the median and the width of violin plot represents the proportion of the data located there as a measure of kernel probability density. The black dots represent the data distributions.

6.3.5. Prediction of AGC and TEC

The plot level AGC and TEC stocks from 140 plots were interpolated using the EBKRP kriging interpolation method (Figure 5.11 and 5.12). In both cases the model with the K-Bessel semivariogram produced the lowest RMSE and CRPS (Table 5.5). The geostatistics parameter of crossvalidation for both AGC and TEC showed negative ME and RMSSE values greater than 1 indicating underestimation of predicted values. The underestimation is also evident as ASE is lower than the RMSE for the best interpolation model.

Table 6.5: Cross-validation statistics of each Enhanced Bayesian Kriging Regression prediction (EBKRP) model for the prediction AGC and TEC in the Sundarbans. The bold value indicates the best value for all statistics.

Enhanced Bayesian Kriging Regression prediction (EBKRP) model parameter	**Above-ground carbon with forest type**				**Total Ecosystem Carbon with forest type**			
	Semivariogram type							
	Exponential	**Nugget**	**Whittle**	**K-Bessel**	**Exponential**	**Nugget**	**Whittle**	**K-Bessel**
Mean Error (ME)	-10.36	-20.46	-10.80	**-9.69**	-9.54	-26.90	-10.11	**-8.86**
Root Mean Square Error (RMSE)	28.49	37.90	28.80	**28.19**	40.99	58.51	41.18	**40.72**
Mean Standardized Error	-0.23	-0.58	-0.25	**-0.21**	-0.14	-0.55	-0.16	**-0.12**
Root-Mean-Square Standardized Error (RMSSE)	1.09	1.75	1.13	**1.04**	1.15	1.99	1.21	**1.06**
Average Standard Error (ASE)	**23.48**	19.51	23.04	24.33	**34.38**	27.68	33.29	36.37
Average Continuous Ranked Probability Score (CRPS)	15.01	19.95	15.22	**14.85**	12.43	31.97	22.60	**12.19**

The AGC stocks in the Sundarbans ranges from 15.46 Mg ha^{-1} to 90.51 Mg ha^{-1} with an average of 60.29 Mg ha^{-1} (Figure 5.11). The higher TEC stocks is in the central north, north-eastern and south-eastern part of the Sundarbans, which is mostly dominated by *Heritiera*, *Heritiera-Excoecaria*, *Bruguiera* and *Xylocarpus* species. The prediction standard error for AGC ranges from 3.32 Mg ha^{-1}

to 19.80 Mg ha^{-1} with an average of 13.32 Mg ha^{-1}. The total AGC stocks in the Sundarbans comprises 23.91 Teragram (Tg) with a 95% confidence of being between 13.15 Tg and 34.27 Tg.

The TEC in the Sundarbans ranges from 83.63 Mg ha^{-1} to 240.14 Mg ha^{-1} with an average of 157.86 Mg ha^{-1} (Figure 5.12). The higher TEC stocks are distributed in the central north and north-eastern part of the Sundarbans, which is mostly dominated by *Heritiera*, *Bruguiera* and *Xylocarpus* species. The prediction standard error ranges from 9.31 Mg ha^{-1} to 35.46 Mg ha^{-1} with an average of 23.94 Mg ha^{-1}.

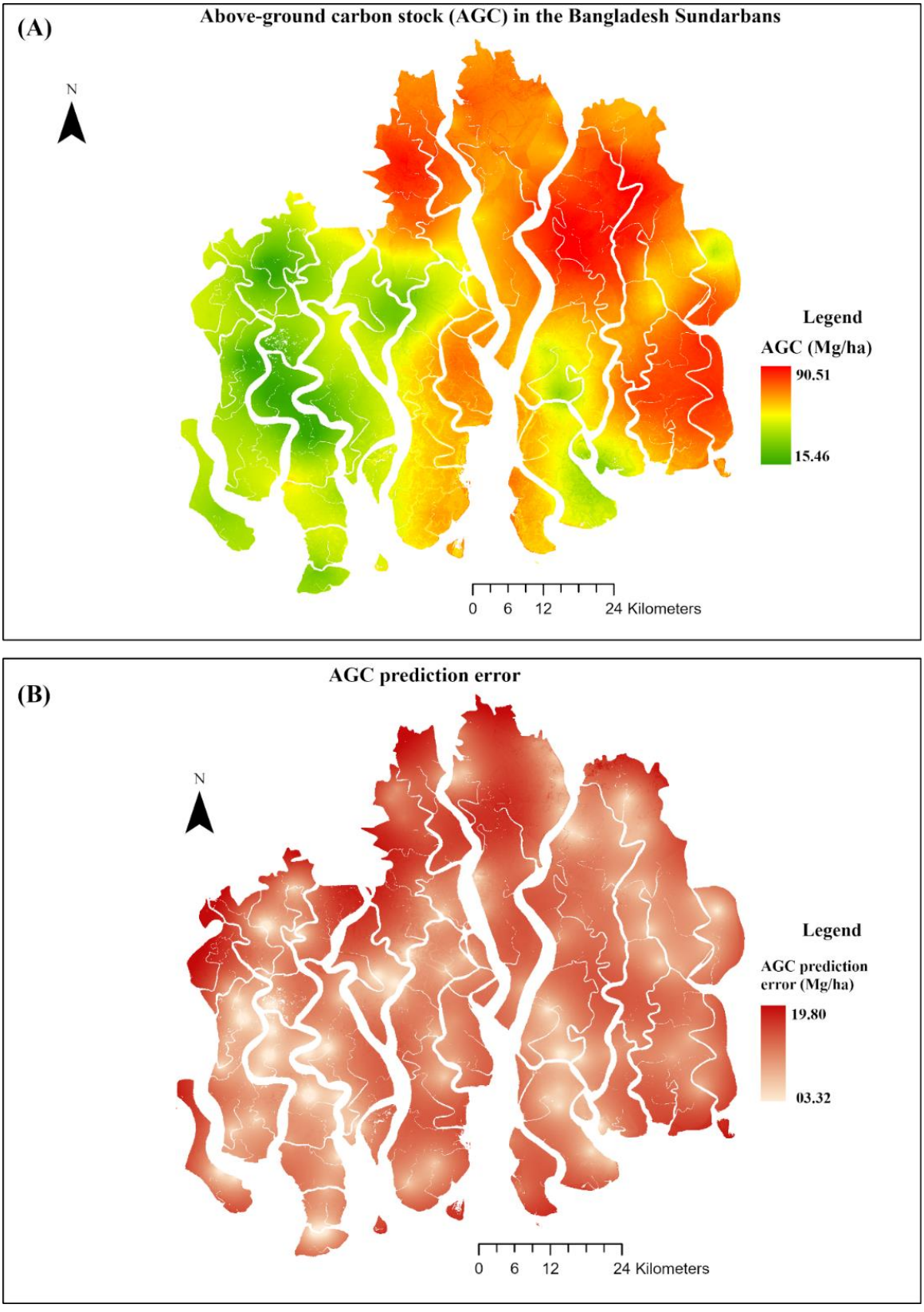

Figure 6.11: Spatial distribution of A) AGC stocks and B) AGC prediction standard errors in the Sundarbans.

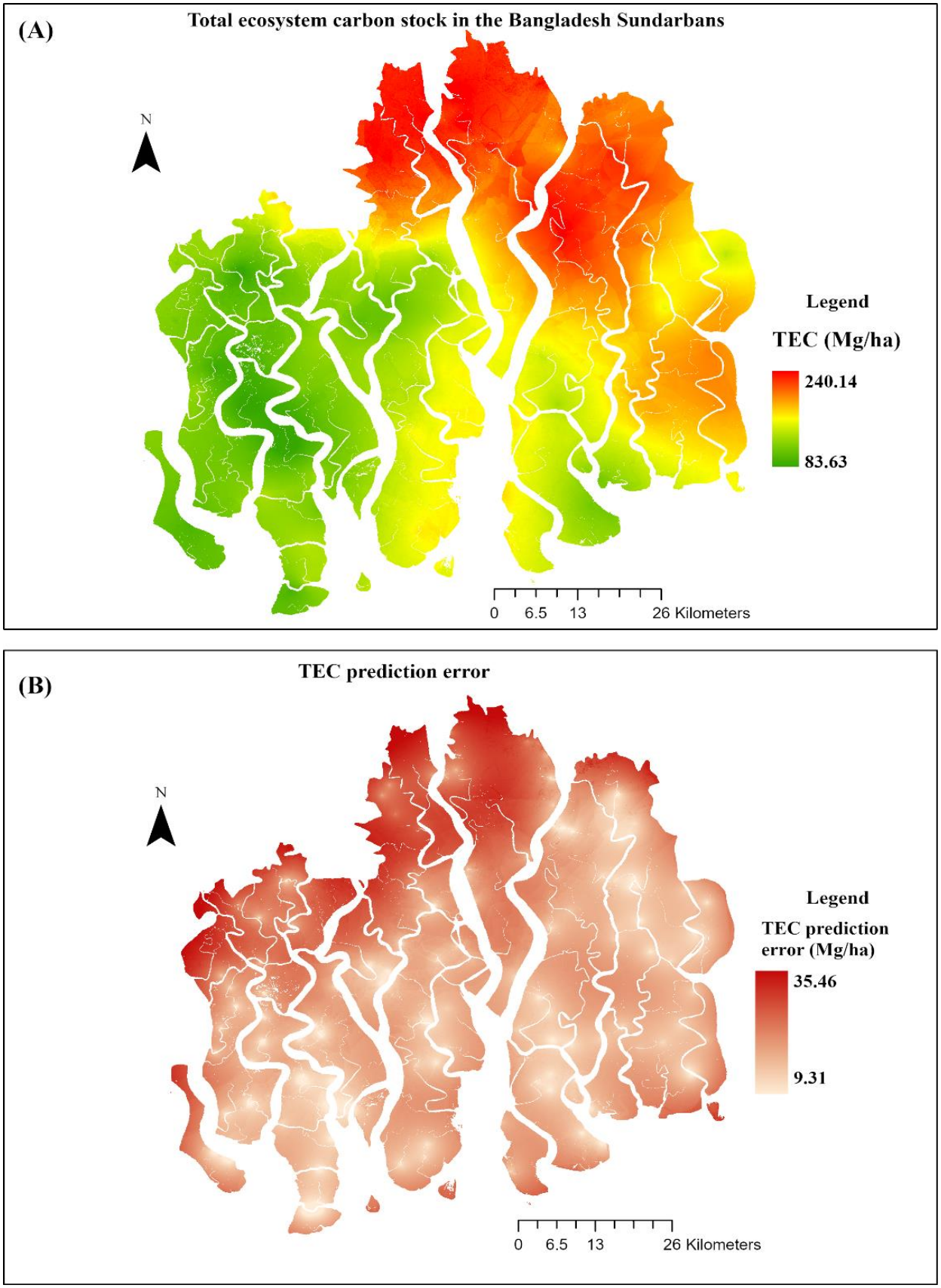

Figure 6.12: Spatial distribution of A) TEC stocks and B) TEC prediction standard errors in the Sundarbans.

The present study found 3,966.75 km^2 forest land area out of 6326.8 km^2 inside the Bangladesh Sundarbans which contributed 62.70 Teragram (Tg) TEC with a 95% confidence of being between 43.29 Tg and 81.14 Tg. Summing up the estimates of the respective species composition classes, it can be seen that 23.91 Tg C is locked in the above-ground compartments and 38.79 Tg C is stored in the below-ground compartments in the Bangladesh Sundarbans mangrove forest.

6.4. Discussions

By using a random forest classifier, the pixel-based classification provided the most accurate forest-type classification map in the Bangladesh Sundarbans showing a gradient of species mixture from *Heritiera fomes* in the east to the *Excoecaria agallocha* dominated in central and west along with *Ceriops decandra*. The forest-type map shows similar patterns of these three major species with a map developed by the Bangladesh Forest Department (BFD) showing 14 species groups based on aerial survey data from 1995 and 1 m pan-sharpened IKONOS images in 2013 (Dasgupta et al., 2017). Several forest inventories identified 24-27 species in the Sundarbans, however, these three species alone or their assemblages constitute 97% area of the Sundarbans (Rahman et al., 2015a; Dasgupta et al., 2017; GOB, 2019; Sarker et al., 2019a; Rahman et al., 2021c). The other species do not form sufficient mono-specific patches to capture with 10-30 m resolution satellite data. This study found that *Hertiera_Excoecaria* is the most dominant followed by *Excoecaria*_Mixed, *Ceriops-Excoecaria* (17%) and *Heritiera* only. On the other hand, Chanda et al. (2016b) found the same first two compositions as the most dominant followed by *Heritiera* and *Ceriops-Excoecaria*. This difference might be attributed to the use of different satellite data in different years.

Several studies have reliably classified major forest types of mangrove forests using Landsat imagery including the Sundarbans (Long and Giri, 2011; Ghosh et al., 2016; Kumar et al., 2021). Using maximum likelihood classifier, Ghosh et al. (2016) classified decadal composite images from Landsat 2, 5, 7 and 8 satellites between 1977 to 2015 and identified changes of vegetation composition for five species (*Heritiera fomes*, *Excoecaria agallocha*, *Ceriops decandra*, *Sonneratia apetala* and *Xylocarpus mekongensis*) in the Bangladesh Sundarbans with an accuracy between 72-89%. The

classification accuracy has increased in some studies while discriminating between forest and non-forest categories in the Sundarbans (for example: Awty-Carroll et al., 2019; Hasan et al., 2020). By using Continuous Change Detection and Classification (CCDC) methods on the Landsat (4, 5, 7 and 8) archive from 1988 to 2017, Awty-Carroll et al. (2019) classified mangrove to non-mangrove areas in the Sundarbans with an overall accuracy of 94.5%. Therefore, classification of detailed species assemblages with sufficient accuracy is still a challenge with Landsat imagery. However, the use of high-resolution data, vegetation indices, canopy height, DEMs and the use of machine learning algorithm has improved classification accuracies in many studies (Pham et al., 2019; Rahman et al., 2019). Sentinel-2 MSI has provided better resolution in shortwave bands (20 m) that have provided reliable classification of mangrove species in most mangrove forests (Baloloy et al., 2020; Cissell et al., 2021; Ghorbanian et al., 2021; Liu et al., 2021).

Using Sentinel-2 MSI imagery and machine learning classifiers, this study provided a forest-type map with a reasonable accuracy of 75%. The quantity disagreement was higher than allocation disagreement indicating that much disagreement arises from errors due to the quantity mapped for each class rather than the spatial distribution of forest types. As evident from the classification maps, forest-types comprising two or more species showed less users accuracy, such as *Excoecaria* and Mixed, *Avicennia_ Sonneratia* and *Heritiera_Excoecaria*. On the other hand, *Bruguiera*, *Xylocarpus* and non-vegetated types such as water and barren land showed the highest classification accuracy. The low producers accuracy indicates that classifiers failed to capture the forest-type of these reference point such as *Xylocarpus*_Mixed and *Avicennia_Sonneratia*. The confusion arises for these species due to similar spectral signatures, similar value of indices, or similar GEDI canopy height. The tidal influence on the spectral signatures especially close to river or canal banks is also an important source of classification error (Baloloy et al., 2020; Xia et al., 2021). Capturing seasonal variation or using knowledge of ecological zonation of each species benefits the classification accuracy. Moreover, using high-resolution data or adding LiDAR or RADAR data will produce better mangrove classification in the Sundarbans in future (Pham et al., 2019; Rahman et al., 2019).

The object-based classification combines pixels of similar spatial properties and provides meaningful objects of interest and therefore successfully classified mangroves in many regions (Conchedda et al., 2008; Pham et al., 2019). However, comparison of error matrices suggests that the pixel-based classifier captured the most accurate forest-type in the Sundarbans. The 10 m Sentinel-2 MSI is 25% of the area of the sample plots, therefore each sample plot is composed of mixed pixels. In case of the object-based approach, the information from multiple pixels smooths out across one object. On the other hand, the pixel-based approach retains the distribution of species-type and therefore showed greater accuracy compared to object-based approach. The diversity of species in the Sundarbans is not homogenous and is largely dependent on linear distance from the riverbank. For example, Sarker et al. (2019b) found that the alpha and beta diversity is the highest at a distance of 1500 m and gamma diversity at 800 m from the river bank. The pixel-based approach might better capture these variations in species types in the Sundarbans.

The above– and below-ground carbon stocks is largely dependent on a range of variables such as forest-type, salinity, water discharge, climatic and other environmental factors (Rahman et al., 2021a; Rahman et al., 2021b). Regression kriging is a widely used interpolation method to upscale plot level information to larger scales, where the predicted variables are dependent on a range of covariate variables (Keskin and Grunwald, 2018). Enhanced Bayesian Kriging Regression Prediction (EBKRP) is used in a few studies to interpolate SOC in many regions and proved to be the best interpolation method among all available alternatives (Mallik et al., 2020; Sahu et al., 2021). The interpolation of SOC with forest types did not improve by adding DEM data from the TanDEMx mission or slope or aspect. The DEM is actually the Digital Surface Model (DSM) representing the top of vegetation in the Sundarbans. From the forest-type map, it is evident that the Sundarbans has an east-west gradient of species-assemblages reflecting a variation of species height as evident in GEDI forest height map (Figure 5.5). Therefore, the forest type-map and the DEM might be correlated. On the other hand, the slope and aspect didn't have any marked impact on the SOC stocks as the Sundarbans is within 2-4 m above mean sea level (MSL) (Payo et al., 2016; Rahman et al., 2021b).

Results showed that the TEC and AGC stocks in the Sundarbans is higher in the central north and north-eastern part of the Sundarbans. Spatial modelling of biodiversity by Sarker et al. (2019b) revealed that the most species-rich mangrove species are confined to the northern and eastern regions in the Sundarbans. Species in these areas receive more freshwater due to proximity of two large rivers, the Baleshwar and Passur, ensuring suitable less-salty conditions for salt-intolerant plant species. The species-rich communities in these regions might encounter more above- and below-ground carbon in this region. The high carbon-rich area is mostly dominated by *Heritiera fomes* dominated areas along with *Excoecaria*, *Bruguiera* and *Xylocarpus* spp. Since the plot level mean AGC was significantly higher for *Bruguiera*, *Heritiera fomes* and *Heritiera-Excoecaria*, the below-ground root carbon is also expected to be higher for these species as used allometric models for root carbon are obtained from above-ground tree parameters. On the other hand, SOC is also higher in the north-eastern zone compared to other parts of the Sundarbans.

Results from this study show that the total ecosystem carbon stocks is 62.70 Teragram (Tg) in the Sundarbans, which is 55% lower than recent estimation by BFD using a recent national forest inventory (GOB, 2019). Chanda et al. (2016b) estimated TEC in the Sundarbans in 2016 is 91.19 Tg using the data and procedures from Rahman et al. (2015a). Both studies used common local and pan-tropical allometric models which might estimate higher TEC than this study. Moreover, these studies used a stratify & multiply (SM) approach which uses average values with the area of each species from remote sensing imagery, which can over- or underestimate carbon stocks. The uncertainty analysis of this study shows that the TEC can vary between 43.29 Tg and 81.14 Tg with a 95% confidence interval. The TEC varied significantly within salinity zones. Rahman et al. (2015) estimated ecosystem carbon stock for salinity zones which varies from 117 for polyhaline, 229 for mesohaline and 336 for oligohaline zone. Similarly, Chanda et al. (2016b) also found similar findings for three salinity zones, although the values are lower than Rahman et al. (2015) and higher than this study. The vegetation composition, growth and yield of mangroves is dependent on the salinity of the Sundarbans, which can affect the above- and below-ground biomass or carbon (Siddique et al., 2017; Rahman et al., 2020; Rahman et al., 2021b).

Table 6.6: Comparison of ecosystem carbon stocks in the Sundarbans

	Study	No, of sample plot & plot size/ Satellite	Salinity zones	Above-ground carbon (Mg ha^{-1})	Below-ground root carbon (Mg ha^{-1})	Below-ground soil carbon (1 m) (Mg ha^{-1})	Ecosystem carbon stocks (Mg ha^{-1})
The Sundarbans, Bangladesh World study	This study	140 (400 m^2)	All	60 (16 – 91)	41 (9 – 126)	54 (18 – 100)	158 (83 – 240)
	Ahmed et al. (2021)	50 (100 m^2)	All	128 (35 – 274)	79 (23 – 161), 9 (7-13) *	-	-
	Ahmed and Kamruzzaman (2021)	6 (400 m^2)	Oligohaline	122	66	-	-
	Azad et al. (2020)	18 (600 m^2)	Mesohaline	117 (58 – 195)	67 (35 – 99)	-	-
	GOB (2019)	1,653 (400) m^2	All	49	33	182	345
	Kamruzzaman et al. (2018)	6 (400) m^2	Oligohaline	77 (26 – 158)	42 (7 – 71)	-	-
	Sanderman et al. (2018)	Model based	All	-	-	127 (74-463)	-
	Atwood et al. (2017)	Literature based	All	-	-	118	-
	Kamruzzaman et al. (2017)	21, 100 m^2	Oligohaline	77	42	-	-
	Chanda et al. (2016b)	150, 1570 m^2	All	-	-	-	258 (172 – 343)
	Rahman et al. (2015a)	150, 1570 m^2	All	89 (25 – 153)	38 (12 – 63)	112 (90 – 134)	260 (160 – 360)
World average	Kauffman et al. (2020)	190 Plot data from five continents	Global	115	-	334 (33 – 789)	856
	Simard et al. (2019)	SRTM and ICESat/GLAS	Global	62	-	-	-
	Sanderman et al. (2018)	Model based	Global	-	-	361 (94-628)	-
	Atwood et al. (2017)	Literature based	Global	-	-	283 (15 – 1527)	-
	Jardine and Siikamäki (2014)	Model based	Global	-	-	369 (272 – 703)	-
	IPCC (2014)	Literature based	Global	83	-	428	511
	Donato et al. (2011)	field data from the Indo-Pacific	Indo-Pacific	159	-	864 **	1023

N.B: (*) * Fine root biomass (diameter <2 mm), (**) indicates soil carbon measurement for more than 1 m depth. SRTM: Shuttle Radar Topography Mission, ICESat/GLAS: Ice, Cloud and land Elevation Satellite / Geoscience Laser Altimeter System (GLAS). Studies presented as biomass value were converted into carbon assuming 50% biomass is carbon (Howard et al., 2014).

The estimated average above-ground carbon stocks in the Sundarbans is lower than all other local and global estimates, except the recent national forest inventory by GOB (2019) (Table 5.6). Using species-specific allometric models, the below-ground root carbon stocks is quite similar to many studies (for example, Kamruzzaman et al. (2017), Rahman et al. (2015a) and Kamruzzaman et al. (2018)), however the rest available studies estimated higher root carbon stocks. The difference arises due to the species composition since all studies used common allometric models as a relationship between above-ground tree structure to below-ground root carbon stocks. The major difference was found for below-ground soil carbon where this study is the lowest compared to all local and global studies. The 1 m soil carbon stocks was almost 25% of the latest national inventory estimation, and 50% than Rahman et al. (2015a). A range of factors are associated with lower carbon stocks in the Sundarbans compared to other mangroves or global average values. Such can be explained by high mineral sediment deposition (Sanderman et al., 2018; Twilley et al., 2018), low burial rate (Ray et al., 2011), rapid turnover rate (Ray et al., 2018), historical logging, stand age (Marchand, 2017), plant litter quality (Rovai et al., 2018) and biological processes.

Mangroves play a vital role in supporting biodiversity and also mitigating climate change through soaking up carbon dioxide and storing carbon in both above- and below-ground biomass and sediments. The present study used field inventories, species-specific allometric models and species-specific carbon fractions to estimate total ecosystem carbon stocks in the Bangladesh Sundarbans and upscale plot level carbon to ecosystem level through GIS-based interpolation. However, the study measured only 1 m depth of SOC despite the Sundarbans having organic carbon in 4-6 m depth of sediments (Allison et al., 2003). However, the 2013 IPCC Supplement to the 2006 IPCC Guidelines suggests that impact of forest management and anthropogenic activities is up to a depth of 1 m, below which the carbon stocks is almost intact (IPCC, 2014).

The study is intended to develop a tier 3 level assessment of ecosystem carbon stocks in the Bangladesh Sundarbans with increasing accuracy by using available models, cloud computing

platforms and software. Reducing uncertainties in carbon estimation is one of the key research agendas to reduce error at the global scale. However, carbon estimates often ignore error propagated from allometric models (Vorster et al., 2020). Therefore, the carbon maps produced in the study considered reducing errors from field data by developing species-specific and site-specific allometric models or generic models with species level structural information such as wood density and tree height. To reduce error from carbon maps, terrestrial LiDAR scanning could be an option for individual- and plot-level biomass estimates (Réjou-Méchain et al., 2019). The error propagation during upscaling local scale carbon estimates to the ecosystem scale can be minimised through using Airborne LiDAR and very fine-resolution optical satellite images. UAV-based LiDAR can also be used for improved accuracy of carbon estimation in forests. However, the recent advances of satellite missions such GEDI (Global Ecosystem Dynamics Investigation), Icesat-2 (Ice, Cloud, and Land Elevation Satellite-2) or NISAR (NASA-ISRO SAR) could reduce the error propagation if calibrated to the wide range of ground data collected from forests around the world. The accurate error propagation in biomass products and the pathways to overcome the uncertainties would then pave the way to meet requirements of international environmental policies and other applications (Herold et al., 2019; Réjou-Méchain et al., 2019).

6.5. Conclusions

The remote sensing pixel-based classification of Sentinel-2 MSI using the GEDI height map provided the most accurate forest-type classification with 10 forest-types across the Bangladesh Sundarbans. The *Hertiera_Excoecaria* type was the most dominant forest type followed by *Excoecaria*_Mixed and Ceriops-Excoecaria. The plot level TEC varied significantly within both salinity zones and by forest-type ($p < 0.05$). The interpolation of plot level data with forest-type maps revealed that the SOC and AGC in the Sundarbans was 21.37 Tg and 23.92 Tg, respectively. On the other hand, the total ecosystem carbon stocks comprised 62.70 Tg with a 95% confidence of being between 43.29 Tg and 81.14 Tg. The central-north and north-eastern part of the Bangladesh Sundarbans is the most carbon rich forest in both above- and below-ground components. Therefore, this carbon-rich area should be a

conservation priority. The uncertainty assessments from the field estimation, allometric models, classification to the interpolation all provide confidence in the estimates of total ecosystem carbon stocks in the Sundarbans. The methodology used in this study provides a robust approach for estimating ecosystem carbon stocks in any mangrove forest and the method can be extended to track and monitor carbon dioxide emissions.

Chapter 7

General Discussions and Conclusions

7.1. Overview of thesis findings

The overall aim of this thesis was to estimate total ecosystem carbon stocks, uncertainties behind carbon stocks estimation and to understand spatial variability of carbon stocks in the Bangladesh Sundarbans. In the chapter 2, a synthesis of peer-reviewed literature on carbon stocks in mangrove forests were compiled and analysed. The available methodologies, either field inventory or remote sensing or a combination for the estimation of ecosystem carbon stocks were discussed. A short description of the Bangladesh Sundarbans and used research methodologies are presented in the chapter 3. The methods for upscaling plot-level carbon stocks measurements to the ecosystem level through remote sensing, and the variety of remote sensing sensors for estimating carbon stocks were presented. Previous estimates of below- and above-ground carbon stocks in the Sundarbans were discussed and research gaps were identified which helped to inform the research design used in this study.

Chapter 4 introduced the use of sediment coring to quantify soil carbon stocks (SOC) up to 1 m soil depth at four narrow depth intervals. This study represents one of the first to quantify SOC using a CHN analyser, which is known to be more accurate than other methods. The study finds that levels of SOC in the Sundarbans are much lower than those reported in previously published work and those used in global models. Explanations for this low SOC were explored and these include high mineral sediment deposition, low burial rate, rapid turnover rate, historical logging, stand age, plant litter quality and biological processes are important. Soil salinity is key factor that influences the spatial variability of SOC in the Sundarbans along with the C: N ratio and diameter of trees. The study also found that SOC stocks is significantly different amongst vegetation types where *Bruguiera* spp. stands hold the maximum SOC measured, followed by two pioneer species *Sonneratia apetala* and *Avicennia* spp. The result from this chapter answers research question 2 and 4 with regards below-ground SOC stocks.

In response to research question 1, chapter 5 explored the variability of above-ground biomass (AGB) using different sets of allometric models and model parameters (wood density and height). The

biomass variability indicates uncertainties in biomass estimation using generic models or model parameters that do not closely represent the local conditions. Using independent datasets from Mahmood et al. (2019), the study developed and tested five species-specific and four genus-specific allometric models which explained a high percentage of the variance in tree AGB using measured diameter at breast height (DBH) and total height (H) data. The generic allometric models overestimated AGB between 22% to 167% compared to the species-specific models at the plot level. Using measured wood density (WD) in allometric models estimated 5-10% less biomass than WD from database and other sources, and AGB was overestimated when using plot top height and underestimated using plot average height data rather than individual tree heights.

In chapter 6, the study estimated the above- and below-ground carbon stocks in the Sundarbans in both plot and ecosystem level to satisfy research question 2, 3 and 4. Based on the forest-type classification map, *Hertiera_Excoecaria* was the most dominant forest type followed by *Excoecaria*_Mixed and *Ceriops-Excoecaria*. After analysing the field inventory, the estimated plot level TEC varied significantly with both salinity zone and forest-type. The interpolation of plot level data with the forest-type map revealed that the SOC and AGC in the Sundarbans was 21.37 Tg and 23.92 Tg, respectively. On the other hand, the total ecosystem carbon stocks comprised 62.70 Tg with a 95% confidence of being between 43.29 Tg and 81.14 Tg. The central-north and north-eastern part of the Bangladesh Sundarbans contains the most carbon rich forests for both the above- and below-ground components. Standard prediction error maps were also developed for AGC, SOC and TEC. The study demonstrated a systematic and easily replicable approach for estimating ecosystem carbon stocks that can be replicated in any mangrove forest.

Each data chapter (4, 5 and 6) had separate aims and specific questions. The main findings can be categorised as- 1) low SOC in the Sundarbans, 2) the importance of species-specific allometric models, 3) spatial variability of carbon stocks, and 4) carbon stocks responses to environmental drivers. The main findings are discussed below along with practical implications of the findings, limitations and potential improving areas are discussed below.

7.1.1. Low SOC in the Sundarbans

Despite mangroves having a high carbon density in the below-ground sediment, surprisingly this study reveals that the Sundarbans contains lower levels of soil organic carbon than has been reported in most mangroves in the world. Compared to direct estimates from 190 sites across the world by Kauffman et al. (2020), the Sundarbans contains higher SOC than only two other mangrove forests, the Porto Céu mangrove in Brazil (48 Mg ha^{-1}) and the Bu Tinah Janoub in the United Arab Emirates (33 Mg ha^{-1}), located at lower and higher latitudes respectively than the Sundarbans. However, the differences in sampling strategy and methodologies can also yield large differences in SOC stocks, which needs to be investigated further.

The low soil carbon in the Sundarbans is largely due to high mineral sediment deposition (Sanderman et al., 2018; Twilley et al., 2018), low burial rate (Ray et al., 2011), rapid turnover rate (Ray et al., 2018), historical logging, stand age (Marchand, 2017), plant litter quality (Rovai et al., 2018) and biological processes. Being both a tidal and river-dominated ecosystem, the carbon allocation in the above and below ground is very complex and highly dependent on the local and regional geomorphic and geophysical drivers (Twilley et al., 2018). Nonetheless, higher tidal amplitude in the Sundarbans leads to higher carbon export totalling 7.3 Tg C yr^{-1} to the adjacent Bay of Bengal, which is higher than any other mangrove system (Ray et al., 2018). This rapid carbon turnover results in reduced burial of organic matter (0.18%) in the soil (Ray et al., 2011). Moreover, the pronounced tidal cycle in the Sundarbans affects carbon burial process by altering soil water chemistry (Chatterjee et al., 2013; Spivak et al., 2019). Besides the high carbon turnover rate, the Sundarbans is believed to have become tidally active in the recent past due to reduced freshwater flow from the Ganges-Brahmaputra-Meghna river (Rogers et al., 2013; Hale et al., 2019). However, despite the historical reduction of sedimentation, the Sundarbans is itself still keeping pace with sea-level rise with the highest average surface elevation and vertical accretion rate (0.74 and 2.71 cm yr^{-1}) compared to the worldwide average (Bomer et al., 2020a; Bomer et al., 2020b). This high sedimentation rate is the outcome of the massive flux of clastic sediments which attenuates the amount of organic carbon per unit area.

The century-long historical exploitation in the Sundarbans before the felling moratorium in 1989 has largely decreased the populations of threatened tree species (Siddiqi, 2001; Sarker et al., 2011). This in turn is likely to have lessened the continuous autochthonous input of organic matter in the forest and reduced the overall stand age. Studies also showed that historical harvesting had altered the species composition in the Sundarbans, with decreasing abundances of *Heritiera fomes*, *Ceriops decandra* and *Xylocarpus mekongensis* and increasing for *Excoecaria agallocha* (Sarker et al., 2016).

7.1.2. The importance of species-specific allometric models in biomass estimation

Chapter 4 concludes that biomass estimates of mangrove forests are the most precise when species-specific models and individual tree measurements are used. Several studies have concluded that site-specific AGB models estimate biomass or carbon with less error than regional or pan-tropical models; for example, Sundarbans mangrove forest (Mahmood et al., 2019), lowland Dipterocarp forest in Indonesia (Basuki et al., 2009), degraded landscape in Northern Ethiopia (Mokria et al., 2018), central African forest (Ngomanda et al., 2014) and Mexican tropical humid forests (Martínez-Sánchez et al., 2020). Uncertainty in biomass estimation arises when the developed allometric model for one species is applied to another species. Similarly, site-specific allometric models are needed to represent forest heterogeneity (Weiskittel et al., 2015; Hickey et al., 2018). For example, De Souza Pereira et al. (2018) found AGB estimation errors between minus 18% and plus 14% when using biome-specific allometries rather than species-specific ones in Brazilian mangrove forests. Rovai et al. (2016) concluded that recently published global and continental AGB estimates contain errors due to an under representative sample size and the exclusion of the climatic regime, geophysical and geomorphological variables, which are key to understanding the spatial distribution of biomass. Therefore, inclusion of biophysical parameters such as wood density and tree height can help to capture geographical heterogeneity and also act as a suitable proxy of environmental drivers such as variation in salinity which affects the growth rate, wood density, species composition and tree height (Mahmood et al., 2019; Rahman et al., 2020; Virgulino-Júnior et al., 2020; Rahman et al., 2021b).

Species-specific allometric models are also important for estimating below-ground root biomass. After analysing the available global datasets on below-ground root biomass, Adame et al. (2017) concluded that using common allometric models overestimates root biomass up to 40% compared with using species-specific models. However, a few studies have shown that generic models can outcompete locally developed ones (Rutishauser et al., 2013; Stas et al., 2017). Aabeyir et al. (2020) also found better performance of regional or pan-tropical models as local models incurred large uncertainties in West Africa. The accuracy of these generic models for a particular forest depends on whether these models incorporate sufficient samples from that forest. Chave et al. (2014) point out that the discrepancy between local models and their own generic model in wet forests (including mangroves) is largely due to failure to address the wider variation of tree form and other characteristics like buttresses, which are common in the Sundarbans.

7.1.3. Spatial variability of carbon stocks in the Sundarbans

The developed SOC, AGC and TEC stocks map showed spatial variability of carbons stocks in the Sundarbans where the north-eastern part is the most carbon-rich forest in the Sundarbans (Figure 5.8; 5.11 and 5.12). A range of studies in the Sundarbans found that the total ecosystem carbon is significantly higher in the oligohaline zone followed by mesohaline and polyhaline (Rahman et al., 2015a; Chanda et al., 2016b; GOB, 2019). The oligohaline zone is mostly composed of north-eastern Sundarbans, while mesohaline is the central zone and the polyhaline zone consists of an area from western and southern part (Figure 3.1).

The area with the highest TEC stocks is dominated by *Heritiera, Heritiera-Excoecaria, Bruguiera* and *Xylocarpus* species. Spatial modelling of biodiversity by Sarker et al. (2019b) revealed that the most species-rich mangrove species are confined to the northern and eastern regions in the Sundarbans. Species in this area receive more freshwater due to proximity of two large rivers, the Baleshwar and Passur, ensuring suitable less-salty conditions for salt-intolerant plant species. The species-rich communities in these regions might encounter more above- and below-ground carbon in this region. The high carbon-rich area is mostly dominated by *Heritiera fomes* along with *Excoecaria*, *Bruguiera*

and *Xylocarpus* spp. Since the plot level mean AGC was significantly higher for *Bruguiera*, *Heritiera fomes* and *Heritiera-Excoecaria*, the below-ground root carbon is also expected to be higher for these species based on allometric models for root carbon obtained from above-ground tree parameters. Rahman et al. (2015a) also found that *Heritiera* dominated vegetation hold the highest carbon stocks, while Ahmed and Kamruzzaman (2021) found *Avicennia* contains the highest carbon stocks. Since the carbon stocks varies with forest type, the spatial variation of carbon is assumed from the distribution of species type in the Sundarbans.

7.1.4. Carbon stocks responses to environmental drivers

Results from the chapter 3 and chapter 5 highlight that the TEC and SOC stocks in the Sundarbans are largely influenced by the salinity zone and forest-type. In addition, the predictive model from chapter 3 indicates that the SOC is also affected by C: N and diameter of trees as a proxy. In the Sundarbans, hydro-geomorphological changes in rivers along the downstream-upstream gradient alter habitat quality that results in spatial variability in species distributions (Angiolini et al., 2011). The variation of the amount of freshwater flow in the Bangladesh Sundarbans also varies in an east-west direction, where major rivers and tributaries are located in the eastern part of the Sundarbans making the area a low saline zone (Aziz and Paul, 2015). Soil and water salinity is considered as the outcome of the combined impact of these climatic and environmental variables resulting in pronounced differences of SOC and TEC stocks among the three salinity zones (Sarker et al., 2016; Sarker et al., 2019b; Rahman et al., 2020). Several previous studies have confirmed that salinity determines a strong zonation of tree species and biodiversity in the Sundarbans, which in turn leads to comparatively higher diversity and taller tree species in the oligohaline, followed by mesohaline and polyhaline zone (Aziz and Paul, 2015; Sarker et al., 2016; Sarker et al., 2019a; Sarker et al., 2019b; Rahman et al., 2020). Comparatively higher productive trees (for example, higher DBH and higher height) promotes organic matter accumulation through producing higher litter mass and increases both AGC and SOC stocks by forming stable aggregates from roots and pneumatophores (Lange et al., 2015). The three salinity zones also comprise differential soil physical and chemical properties and vegetation characteristics

that usually affects SOC storage by influencing microbial decomposition, soil water chemistry, plant-microbe interaction, and plant litter quality.

Variation in SOC stocks among different forest types are often mediated by the primary productivity, resources allocation in different parts (for example, above- and below-ground) and microorganism activity is driven by a number of biological (for example, bioturbation and species composition) and physical (for example, soil texture, salinity, inundation and nutrients) factors (McLeod et al., 2011). Therefore, differing stand structure and composition in mangrove forests in different tidal regimes yield variable AGC and SOC stocks (Lacerda et al., 1995; Gleason and Ewel, 2002). Moreover, the long and short-term resilience and resistance of microbial communities are largely dependent on the structure and zonation of mangrove communities reflecting environmental gradients (Capdeville et al., 2019). In this study, species with higher TEC and SOC stocks, such as *Bruguiera* spp., *Sonneratia* spp. and *Avicennia* spp. are frequently inundated due to proximity to the river and low land elevation compared to other species in the Sundarbans (Siddiqi, 2001; Sarker et al., 2016). These high inundation regimes, in turn, may lead to increased microbial activity and a higher level of dissolved organic carbon (Wang et al., 2013; Chambers et al., 2014; Chambers et al., 2016). Regular tides also bring sediments along with high allochthonous input whereas the raised less-inundated areas foster autochthonous SOC and less microbial activity (Lovelock et al., 2015b; Woodroffe et al., 2016). Rao et al. (1994) found almost double the C: N ratio in fresh leaves of *Bruguiera* spp. compared with other mangrove species, suggesting higher input of autochthonous carbon. Being the pioneer species in the succession of the Sundarbans, both *Sonneratia* spp. and *Avicennia* spp. are resilient to disturbances leading to higher SOC than climax and seral species (Table A.1) and accumulate a large quantity of organic litter in the tidal channel close to the river or seafront (Sarker et al., 2016; Bomer et al., 2020a).

7.2. Practical implications

The study used robust methods to measure plot-level carbon stocks by using the best available methods for each component and subsequently upscaled estimates to the ecosystem level using remote

sensing imagery. Being a signatory of nationally determined contributions (NDCs) to the United Nations Framework Convention on Climate Change (UNFCCC), Bangladesh is committed to provide reports on greenhouse gas (GHG) emissions and projected scenarios. Bangladesh has recently completed a REDD+ readiness phase and the implementation phase will start in future (GOB, 2018). To satisfy the requirement of these international policy schemes, Bangladesh needs robust estimates of GHG emissions and their uncertainties from all sectors including forests. This study demonstrated an IPCC Tier 3 approach for estimating ecosystem carbon stocks in the Bangladesh Sundarbans which can be used to monitor ecosystem carbon stocks in mangroves and other forests in Bangladesh.

According to IPCC guidelines for the forestry sub-sector, Bangladesh has established a Forest Reference Level (FRL) for the historical reference period 2000-2015 (GOB, 2021). According to the report, the estimated emissions from the forestry sector is 1.19 $MtCO_2e$/year (metric tons of carbon dioxide equivalent), and the estimated removal is 0.81 $MtCO_2e$/year. On the other hand, the projected reduction is 409.41 Mt CO_2e along with reduction aim to reduce this by 22% by 2030. However, the report showed emissions in 2012 (0.37) which is projected the same in 2030. Keeping constant for this projected period indicates that the gain and loss would be counterbalanced by 2030 (GOB, 2021). However, as a signatory of the pledge to halt and reverse deforestation by 2030 at COP26 (Conference of Parties) in 2021, Bangladesh promised to curb deforestation. Additionally, protection of existing forests and planting targets in the degraded forest might mitigate more carbon loss by 2030. This study demonstrates the estimation and prediction of both above- and below-ground carbon stocks with greater accuracy which can be considered in the national greenhouse gas reporting and estimations. Including mangrove soil carbon in the report, especially the Sundarbans and coastal forests and adding the growth would achieve the 2030 target and can even act as a carbon credit to compensate other sectors like transportation or energy sectors.

The study developed five species-specific and four genus-specific allometric models to estimate above-ground biomass for nine species in the Sundarbans. These models only need diameter at breast height and height from the field survey to compute biomass. The study also calculated wood density

for most tree species which can be used in models. These site-specific wood density values will provide estimates of biomass with higher accuracy. Moreover, the spatial variation of wood density of the same species will provide better insights into the species-specific responses to environmental changes.

The use of remote sensing and cloud computing facilities in the study will allow us to monitor the Sundarbans and other forests and understand the carbon stocks changes. Time-series monitoring of changes in biomass or carbon provides the opportunity to estimate net gain and loss in carbon, which is important to calculate GHG emissions. Timely monitoring of GHG emissions is vital to satisfy the country's target to achieve for national and international policy goals. The GEE platform provides us opportunity to analyse imagery and store data in the cloud free of cost. Use of this cloud-based platform to monitor forest biomass is a good option for developing countries like Bangladesh.

The ecosystem carbon stocks maps provide us with spatial variability of both above- and below-ground carbon stocks in the Sundarbans. Since the most carbon-rich and biodiverse portions are in the North-Eastern part of the Sundarbans, these areas should get conservation priority. The dominant species in these areas is *Heritiera fomes*, which is the iconic species after which the Sundarbans is named. These are the home of many threatened species including the Irrawaddy dolphin. After assuming the importance of conserving these areas, the BFD declared three wildlife sanctuaries and three dolphin sanctuaries. However, establishing a coal plant near the Sundarbans is regarded as contentious policy by the Government of Bangladesh (Khan et al., 2020a). The study underlines the importance of spatial conservation planning measures and initiatives to conserve and maximise carbon accumulation in this carbon-rich area and to contribute to global climate change adaptation and mitigation strategies.

Reducing uncertainties in carbon estimation is one of the key research agendas to reduce error in carbon maps at the global scale. The present study used field inventories, species-specific allometric models and species-specific carbon fractions to estimate total ecosystem carbon stocks in a large mangrove forest and upscale plot level carbon to ecosystem level through GIS-based interpolation.

The study developed a tier 3 level assessment of ecosystem carbon stocks with increasing accuracy by using available models, cloud computing platforms and software. The use of remote sensing in cloud computing platforms showed the repeatable methodologies for carbon estimation in mangrove forests which satisfies the requirements of IPCC Tier 3 approach of carbon accounting. The uncertainty assessments from the field estimation, allometric models, forest-types classification and GIS-based interpolation provide confidence in the estimates of total ecosystem carbon stocks. The methodology used in this study provides a robust approach for estimating ecosystem carbon stocks in any mangrove forest and the method can be extended to track and monitor carbon dioxide emissions in any forests in the world.

7.3. Limitations and future directions

The study estimated ecosystem carbon stocks in the Sundarbans through field inventory and remote sensing. The estimation of carbon stocks at one time does not provide the changes in carbon stocks which is necessary for tracking greenhouse gas emissions from the Sundarbans. Estimation of carbon stocks at multiple times is necessary to understand CO_2 emissions from the Sundarbans. Therefore, time-series estimation is necessary to monitor changes. The present study did not estimate the carbon stocks in the past. Therefore, future research should consider back calculation of carbon stocks from previous decades that can act as a baseline or reference level for greenhouse emissions in the Sundarbans.

The study quantified SOC up to 1 m soil depth, however, the organic layer in the Sundarbans consists up to 4-6 m of sediments varied from landward to seaward zone (Allison et al., 2003). In order to capture the total SOC from the Sundarbans, future studies should expand carbon stocks measurement to include the whole organic layer. The assessment of complete soil organic carbon is necessary to fully understand the below-ground carbon dynamics in the Sundarbans including outwelling organic carbon to the Bay of Bengal.

The present study estimated below-ground root carbon with species-specific allometric models. However, Adame et al. (2017) found using allometric models overestimated root biomass by 40% compared to direct coring. Therefore, destructive methods are preferable to using models. Moreover, site-specific models are not available for root carbon. The present study used a coring method to measure root carbon, however, it only measured fine and medium roots. The bigger roots were largely excluded in the coring method. Using both coring and models will estimate fine and medium roots twice, therefore it will be double-counted. Therefore, only species-specific allometric models were used for root biomass. However, excavating large trenches or pits (for example, 1 m × 1 m) would be the best option compared to other methods to reduce uncertainty. After comparing root biomass measured from trenches and other methods such as allometric models and coring, Adame et al. (2017) found significantly higher root biomass in trenches from different mangrove forests. Therefore, future studies should improve estimation of root carbon through digging trenches or pits.

The forest type map in the Sundarbans showed that 54% of the Bangladesh Sundarbans is rivers, canals and low inundated areas. These areas also hold a high amount carbon in the sediments and macrophytes either exported from mangroves or that originate from the photosynthesis of algae and aquatic plants in the water (Cole et al., 2007). Estimating carbon stocks from rivers and canals is important for total budgeting of carbon stocks from the whole mangrove and also for understanding the outwelling dynamics of mangroves. Therefore, future studies should take these watery areas in to account to estimate ecosystem carbon stocks in the Sundarbans.

Satellite based biomass estimation programmes such as the GEDI (Global Ecosystem Dynamics Investigation, since 4/2019) and ICESat-2 (since 10/2018) missions provide near global coverage of forest heights and biomass products. Very recently the world GEDI biomass/carbon product was released. The study could not compare the locally-derived carbon map with the GEDI carbon map. Therefore, future studies should compare or use these satellite-based carbon products with the carbon estimation from field inventories.

Continuous monitoring of above-ground carbon is critical for forest management in support of climate impact mitigation. Therefore, several cloud-based platforms have been developed for continuous monitoring of tropical forest including mangroves such as Global Forest Watch and Global Mangrove Watch. However, these platforms monitor the coverage of forests and deforestation. Integrating ecosystem level carbon estimation from various forests is a prerequisite if these global platforms are to monitor global forest/mangrove carbon. The methodologies followed in this thesis can be integrated with cloud-based platforms to monitor mangrove forest carbon in the Sundarbans and other mangrove forests. Satellite based biomass/carbon missions (GEDI or ICESat-2) can be integrated with the existing coverage product to monitor carbon in forests. In such cases, the use of GEE apps could be a promising monitoring tool as it provides a platform for querying, analysing and publishing real-time apps free of cost.

7.4. Conclusions

Using field inventories and remote sensing data, the estimated total soil organic carbon and above-ground carbon in the Sundarbans was 21.37 Tg and 23.92 Tg, respectively. The total ecosystem carbon stocks comprised 62.70 Tg with a 95% confidence of being between 43.29 Tg and 81.14 Tg. The ecosystem carbon stocks in the Sundarbans are relatively low compared to most published estimates of carbon stocks levels from mangroves across the world. This is due to the fact that the top meter of soil organic carbon (SOC) per area is lower than most mangrove forest in the world. However, the SOC will be higher if complete organic depth of soil is measured. In terms of reducing GHG, mangrove forests should be conserved whatever the amount of carbon stored in the forest for its wide range of ecosystem services. In terms of climate change mitigation and adaptation, the conservation of the existing carbon stocks should receive much higher priority rather than the debates of high-low carbon stocks.

The forest-type classification showed that the *Hertiera_Excoecaria* type was the most dominant forest type followed by *Excoecaria*_Mixed and Ceriops-Excoecaria. The central-north and north-eastern part of the Bangladesh Sundarbans contains the most carbon rich forests in both above- and below-ground

components. Therefore, this carbon-rich part should be a conservation priority for forest management and policy development. However, this north-eastern area of the Sundarbans is highly vulnerable to tourism and economic development. Therefore, the study underlines the importance of spatial conservation planning measures and initiatives to conserve and maximize carbon accumulation and to contribute to global climate change adaptation and mitigation strategies.

This study developed five species-specific and four genus-specific allometric models for the nine most important species in the Sundarbans. At the individual tree level, the generic allometric models overestimated AGB between 22% to 167% compared to the species-specific models and at the plot level, they showed statistically significant AGB differences compared to the species-specific models. Measured wood density (WD) showed 5-10% less biomass than WD from databases and other sources, and AGB was overestimated by up to 20% when using plot top height and underestimated by 8% using plot average height data rather than individual tree heights. The study concludes that biomass estimation in mangroves forests always benefit from species-specific models and individual tree measurements when appropriate input data are available.

The uncertainty assessments from the field estimation, allometric models, classification to the interpolation all provide confidence in the estimates of total ecosystem carbon stocks in the Sundarbans. The methodology used in this study provides an approach for estimating ecosystem carbon stocks in any mangrove forest and the method can easily be extended to track and monitor carbon dioxide emissions.

The plot level total ecosystem carbon varied significantly with both salinity zones and forest-type. The soil organic carbon stocks (SOC) is also largely influenced by soil salinity, probably by amending the forest productivity and microbial activity. The results highlighted that increasing salinity as a result of predicted sea-level rise will likely have pronounced effects on future soil carbon accumulation rates by altering the soil environment and vegetation characteristics. The Bangladesh Sundarbans can act as an important blue carbon hotspot due to the high sedimentation and carbon sequestration rate and conservation priorities by the Bangladesh government. However, disturbances

such as sea-level rise, global warming, eutrophication, and landscape development might hinder this conservation activities in the future.

References

Aabeyir, R., Adu-Bredu, S., Agyare, W.A., Weir, M.J.C., 2020. Allometric models for estimating aboveground biomass in the tropical woodlands of Ghana, West Africa. Forest Ecosystems. 7, 41. https://doi.org/10.1186/s40663-020-00250-3.

Abdullah, A.N., Stacey, N., Garnett, S.T., Myers, B., 2016. Economic dependence on mangrove forest resources for livelihoods in the Sundarbans, Bangladesh. Forest Policy and Economics. 64, 15-24. https://doi.org/10.1016/j.forpol.2015.12.009.

Adam, E., Mutanga, O., Odindi, J., Abdel-Rahman, E.M., 2014. Land-use/cover classification in a heterogeneous coastal landscape using RapidEye imagery: evaluating the performance of random forest and support vector machines classifiers. International Journal of Remote Sensing. 35, 3440-3458. https://doi.org/10.1080/01431161.2014.903435.

Adame, M.F., Cherian, S., Reef, R., Stewart-Koster, B., 2017. Mangrove root biomass and the uncertainty of belowground carbon estimations. Forest Ecology and Management. 403, 52-60. https://doi.org/10.1016/j.foreco.2017.08.016.

Adame, M.F., Connolly, R.M., Turschwell, M.P., Lovelock, C.E., Fatoyinbo, T., Lagomasino, D., Goldberg, L.A., Holdorf, J., Friess, D.A., Sasmito, S.D., Sanderman, J., Sievers, M., Buelow, C., Kauffman, J.B., Bryan-Brown, D., Brown, C.J., 2021. Future carbon emissions from global mangrove forest loss. Global Change Biology. 27, 2856-2866. https://doi.org/10.1111/gcb.15571.

Ahmed, S., Kamruzzaman, M., 2021. Species-specific biomass and carbon flux in Sundarbans mangrove forest, Bangladesh: Response to stand and weather variables. Biomass and Bioenergy. 153, 106215. https://doi.org/10.1016/j.biombioe.2021.106215.

Ahmed, S., Kamruzzaman, M., Azad, M.S., Khan, M.N.I., 2021. Fine root biomass and its contribution to the mangrove communities in three saline zones of Sundarbans, Bangladesh. Rhizosphere. 17, 100294. https://doi.org/10.1016/j.rhisph.2020.100294.

Alam, M., 1989. Geology and depositional history of Cenozoic sediments of the Bengal Basin of Bangladesh. Palaeogeography, Palaeoclimatology, Palaeoecology. 69, 125-139. https://doi.org/10.1016/0031-0182(89)90159-4.

Allison, M., Kepple, E., 2001. Modern sediment supply to the lower delta plain of the Ganges-Brahmaputra River in Bangladesh. Geo-Marine Letters. 21, 66-74. https://doi.org/10.1007/s003670100069.

Allison, M.A., Khan, S.R., Goodbred, S.L., Kuehl, S.A., 2003. Stratigraphic evolution of the late Holocene Ganges–Brahmaputra lower delta plain. Sedimentary Geology. 155, 317-342. https://doi.org/10.1016/S0037-0738(02)00185-9.

Alongi, D., 2002. Present state and future of the world's mangrove forests. Environmental Conservation. 29, 331–349. https://doi.org/10.1017/S0376892902000231.

Alongi, D.M., 2011. Carbon payments for mangrove conservation: ecosystem constraints and uncertainties of sequestration potential. Environmental Science & Policy. 14, 462-470. https://doi.org/10.1016/j.envsci.2011.02.004.

Alongi, D.M., 2012. Carbon sequestration in mangrove forests. Carbon Management. 3, 313-322. https://doi.org/10.4155/cmt.12.20.

Alongi, D.M., 2014. Carbon Cycling and Storage in Mangrove Forests. Annual Review of Marine Science. 6, 195-219. https://doi.org/10.1146/annurev-marine-010213-135020.

Alongi, D.M., 2015. The Impact of Climate Change on Mangrove Forests. Current Climate Change Reports. 1, 30-39. https://doi.org/10.1007/s40641-015-0002-x.

Ameray, A., 2018. Climate change mitigation: Annual carbon balance accounting and mapping in the national Forest ecosystems (continental Portugal), Bragança, Portugal: Polytechnic Institute of Bragança. https://bibliotecadigital.ipb.pt/handle/10198/18257 (accessed 20/02/2022).

Angiolini, C., Nucci, A., Frignani, F., Landi, M., 2011. Using Multivariate Analyses to Assess Effects of Fluvial Type on Plant Species Distribution in a Mediterranean River. Wetlands. 31, 167-177. https://doi.org/10.1007/s13157-010-0118-7.

Anwar, M.S., Takewaka, S., 2014. Analyses on phenological and morphological variations of mangrove forests along the southwest coast of Bangladesh. Journal of Coastal Conservation. 18, 339-357. https://doi.org/10.1007/s11852-014-0321-4.

Asbridge, E., Lucas, R., Ticehurst, C., Bunting, P., 2016. Mangrove response to environmental change in Australia's Gulf of Carpentaria. Ecology and Evolution. 6, 3523-3539. https://doi.org/10.1002/ece3.2140.

Aslan, A., Rahman, A.F., Robeson, S.M., 2018. Investigating the use of Alos Prism data in detecting mangrove succession through canopy height estimation. Ecological Indicators. 87, 136-143. https://doi.org/10.1016/j.ecolind.2017.12.008.

Aslan, A., Rahman, A.F., Warren, M.W., Robeson, S.M., 2016. Mapping spatial distribution and biomass of coastal wetland vegetation in Indonesian Papua by combining active and passive

remotely sensed data. Remote Sensing of Environment. 183, 65-81. https://doi.org/10.1016/j.rse.2016.04.026.

Asner, G.P., Powell, G.V., Mascaro, J., Knapp, D.E., Clark, J.K., Jacobson, J., Kennedy-Bowdoin, T., Balaji, A., Paez-Acosta, G., Victoria, E., 2010. High-resolution forest carbon stocks and emissions in the Amazon. PNAS. 107, 16738-42. https://doi.org/10.1073/pnas.1004875107.

Atwood, T.B., Connolly, R.M., Almahasheer, H., Carnell, P.E., Duarte, C.M., Lewis, C.J.E., Irigoien, X., Kelleway, J.J., Lavery, P.S., Macreadie, P.I., Serrano, O., Sanders, C.J., Santos, I., Steven, A.D.L., Lovelock, C.E., 2017. Global patterns in mangrove soil carbon stocks and losses. Nature Climate Change. 7, 523-528. https://doi.org/10.1038/nclimate3326.

Avitabile, V., Herold, M., Heuvelink, G.B.M., Lewis, S.L., Phillips, O.L., Asner, G.P., Armston, J., Ashton, P.S., Banin, L., Bayol, N., Berry, N.J., Boeckx, P., de Jong, B.H.J., DeVries, B., Girardin, C.A.J., Kearsley, E., Lindsell, J.A., Lopez-Gonzalez, G., Lucas, R., Malhi, Y., Morel, A., Mitchard, E.T.A., Nagy, L., Qie, L., Quinones, M.J., Ryan, C.M., Ferry, S.J.W., Sunderland, T., Laurin, G.V., Gatti, R.C., Valentini, R., Verbeeck, H., Wijaya, A., Willcock, S., 2016. An integrated pan-tropical biomass map using multiple reference datasets. Global Change Biology. 22, 1406-1420. https://doi.org/10.1111/gcb.13139.

Awty-Carroll, K., Bunting, P., Hardy, A., Bell, G., 2019. Using Continuous Change Detection and Classification of Landsat Data to Investigate Long-Term Mangrove Dynamics in the Sundarbans Region. Remote Sensing. 11, 2833.

Azad, M.S., Kamruzzaman, M., Osawa, A., 2020. Quantification and Understanding of Above and Belowground Biomass in Medium Saline Zone of the Sundarbans, Bangladesh: The Relationships with Forest Attributes. Journal of Sustainable Forestry. 39, 331-345. https://doi.org/10.1080/10549811.2019.1664307.

Aziz, A., Paul, A.R., 2015. Bangladesh Sundarbans: Present status of the Environment and Biota. Diversity. 7, 242-269. https://doi.org/10.3390/d7030242.

Baccini, A., Goetz, S.J., Walker, W.S., Laporte, N.T., Sun, M., Sulla-Menashe, D., Hackler, J., Beck, P.S.A., Dubayah, R., Friedl, M.A., Samanta, S., Houghton, R.A., 2012. Estimated carbon dioxide emissions from tropical deforestation improved by carbon-density maps. Nature Climate Change. 2, 182. https://doi.org/10.1038/nclimate1354.

Baccini, A., Laporte, N., Goetz, S.J., Sun, M., Dong, H., 2008. A first map of tropical Africa's above-ground biomass derived from satellite imagery. Environmental Research Letters. 3, 045011.

Baccini, A., Walker, W., Carvalho, L., Farina, M., Sulla-Menashe, D., Houghton, R.A., 2017. Tropical forests are a net carbon source based on aboveground measurements of gain and loss. Science. https://doi.org/10.1126/science.aam5962.

Baldwin, D.S., Rees, G.N., Mitchell, A.M., Watson, G., Williams, J., 2006. The short-term effects of salinization on anaerobic nutrient cycling and microbial community structure in sediment from a freshwater wetland. Wetlands. 26, 455-464. https://doi.org/10.1672/0277-5212(2006)26[455:TSEOSO]2.0.CO;2.

Ball, M.C., Pidsley, S.M., 1995. Growth Responses to Salinity in Relation to Distribution of Two Mangrove Species, *Sonneratia alba* and *S. lanceolata*, in Northern Australia. Functional Ecology. 9, 77-85. https://doi.org/10.2307/2390093.

Baloloy, A.B., Blanco, A.C., Sta. Ana, R.R.C., Nadaoka, K., 2020. Development and application of a new mangrove vegetation index (MVI) for rapid and accurate mangrove mapping. ISPRS Journal of Photogrammetry and Remote Sensing. 166, 95-117. https://doi.org/10.1016/j.isprsjprs.2020.06.001.

Banerjee, K., Bal, G., Mitra, A., 2018. How Soil Texture Affects the Organic Carbon Load in the Mangrove Ecosystem? A Case Study from Bhitarkanika, Odisha. in: Singh, V.P., Yadav, S., Yadava, R.N. (Eds.), Environmental Pollution. Springer Singapore, Singapore, pp. 329-341.

Banerjee, K., Roy Chowdhury, M., Sengupta, K., Sett, S., Mitra, A., 2012. Influence of anthropogenic and natural factors on the mangrove soil of Indian Sundarbans wetland. Arch Environ Sci. 6, 80-91.

Banerjee, K., Sengupta, K., Raha, A., Mitra, A., 2013. Salinity based allometric equations for biomass estimation of Sundarban mangroves. Biomass and Bioenergy. 56, 382-391. https://doi.org/10.1016/j.biombioe.2013.05.010.

Bartholomé, E., Belward, A.S., 2005. GLC2000: a new approach to global land cover mapping from Earth observation data. International Journal of Remote Sensing. 26, 1959-1977. https://doi.org/10.1080/01431160412331291297.

Bartoń, K., 2020. MuMIn: multi-model inference. R package version 1.43.17. Retrieved from https://CRAN.R-project.org/package=MuMIn.(accessed 23/02/2020).

Barua, S.K., Boscolo, M., Animon, I., 2020. Valuing forest-based ecosystem services in Bangladesh: Implications for research and policies. Ecosystem Services. 42. https://doi.org/10.1016/j.ecoser.2020.101069.

Basuki, T.M., van Laake, P.E., Skidmore, A.K., Hussin, Y.A., 2009. Allometric equations for estimating the above-ground biomass in tropical lowland Dipterocarp forests. Forest Ecology and Management. 257, 1684-1694. https://doi.org/10.1016/j.foreco.2009.01.027.

BFD, 2010. Integrated resources management plans for the Sundarbans (2010-2020), Nishorgo Network, Forest Department, Government of Bangladesh, Dhaka. http://pdf.usaid.gov/pdf_docs/pnaec417.pdf (accessed 07/01/2018).

Bisutti, I., Hilke, I., Raessler, M., 2004. Determination of total organic carbon – an overview of current methods. TrAC Trends in Analytical Chemistry. 23, 716-726. https://doi.org/10.1016/j.trac.2004.09.003.

Blaschke, T., 2010. Object based image analysis for remote sensing. ISPRS Journal of Photogrammetry and Remote Sensing. 65, 2-16. https://doi.org/10.1016/j.isprsjprs.2009.06.004.

Bomer, E.J., Wilson, C.A., Elsey-Quirk, T., 2020a. Process Controls of the Live Root Zone and Carbon Sequestration Capacity of the Sundarbans Mangrove Forest, Bangladesh. Sci. 2, 35. https://doi.org/10.3390/sci2020035.

Bomer, E.J., Wilson, C.A., Hale, R.P., Hossain, A.N.M., Rahman, F.M.A., 2020b. Surface elevation and sedimentation dynamics in the Ganges-Brahmaputra tidal delta plain, Bangladesh: Evidence for mangrove adaptation to human-induced tidal amplification. CATENA, 104312. https://doi.org/10.1016/j.catena.2019.104312.

Bouillon, S., Boschker, H.T.S., 2006. Bacterial carbon sources in coastal sediments: a cross-system analysis based on stable isotope data of biomarkers. Biogeosciences. 3, 175-185. https://doi.org/10.5194/bg-3-175-2006.

Bouillon, S., Dahdouh-Guebas, F., Rao, A.V.V.S., Koedam, N., Dehairs, F., 2003. Sources of organic carbon in mangrove sediments: variability and possible ecological implications. Hydrobiologia. 495, 33-39. https://doi.org/10.1023/a:1025411506526.

Breiman, L., 2001. Random forests. Machine learning. 45, 5-32.

Brodersen, K.E., Trevathan-Tackett, S.M., Nielsen, D.A., Connolly, R.M., Lovelock, C.E., Atwood, T.B., Macreadie, P.I., 2019. Oxygen Consumption and Sulfate Reduction in Vegetated Coastal Habitats: Effects of Physical Disturbance. Frontiers in Marine Science. 6. https://doi.org/10.3389/fmars.2019.00014.

Brown, S., 1997. Estimating biomass and biomass change of tropical forests: A primer. FAO Forestry Paper 134, Rome, Italy.

Brown, S., Gillespie, A.J.R., Lugo, A.E., 1989. Biomass Estimation Methods for Tropical Forests with Applications to Forest Inventory Data. Forest Science. 35, 881-902. https://doi.org/10.1093/forestscience/35.4.881.

Bunting, P., Rosenqvist, A., Hilarides, L., Lucas, R.M., Thomas, N., 2022a. Global Mangrove Watch: Updated 2010 Mangrove Forest Extent (v2.5). Remote Sensing. 14, 1034.

Bunting, P., Rosenqvist, A., Hilarides, L., Lucas, R.M., Thomas, N., Tadono, T., Worthington, T.A., Spalding, M., Murray, N.J., Rebelo, L.-M., 2022b. Global Mangrove Extent Change 1996-2020: Global Mangrove Watch Version 3.0. Remote Sensing. 14, 3657.

Bunting, P., Rosenqvist, A., Lucas, R.M., Rebelo, L.-M., Hilarides, L., Thomas, N., Hardy, A., Itoh, T., Shimada, M., Finlayson, C.M., 2018. The Global Mangrove Watch—A New 2010 Global Baseline of Mangrove Extent. Remote Sensing. 10, 1669.

Burnham, K.P., Anderson, D.R., 2002. A practical information-theoretic approach. Model selection and multimodel inference, 2nd ed. Springer, New York. 2.

Bustamante, M.M.C., Roitman, I., Aide, T.M., Alencar, A., Anderson, L.O., Aragão, L., Asner, G.P., Barlow, J., Berenguer, E., Chambers, J., Costa, M.H., Fanin, T., Ferreira, L.G., Ferreira, J., Keller, M., Magnusson, W.E., Morales-Barquero, L., Morton, D., Ometto, J.P.H.B., Palace, M., Peres, C.A., Silvério, D., Trumbore, S., Vieira, I.C.G., 2016. Toward an integrated monitoring framework to assess the effects of tropical forest degradation and recovery on carbon stocks and biodiversity. Global Change Biology. 22, 92-109. https://doi.org/10.1111/gcb.13087.

Candra, E.D., Hartono, Wicaksono, P., 2016. Above Ground Carbon Stock Estimates of Mangrove Forest Using Worldview-2 Imagery in Teluk Benoa, Bali, IOP Conference Series: Earth and Environmental Science.

Capdeville, C., Pommier, T., Gervaix, J., Fromard, F., Rols, J.-L., Leflaive, J., 2019. Mangrove Facies Drives Resistance and Resilience of Sediment Microbes Exposed to Anthropic Disturbance. Frontiers in Microbiology. 9. https://doi.org/10.3389/fmicb.2018.03337.

Chaffey, D.R., Miller, F.R., Sandom, J.H., 1985. A forest inventory of the Sundarbans, Bangladesh. Project Report No.140, Overseas Development Authority (ODA), London(accessed 20/03/2019).

Chambers, L.G., Davis, S.E., Troxler, T., Boyer, J.N., Downey-Wall, A., Scinto, L.J., 2014. Biogeochemical effects of simulated sea level rise on carbon loss in an Everglades mangrove peat soil. Hydrobiologia. 726, 195-211. https://doi.org/10.1007/s10750-013-1764-6.

Chambers, L.G., Guevara, R., Boyer, J.N., Troxler, T.G., Davis, S.E., 2016. Effects of Salinity and Inundation on Microbial Community Structure and Function in a Mangrove Peat Soil. Wetlands. 36, 361-371. https://doi.org/10.1007/s13157-016-0745-8.

Chanda, A., Akhand, A., Manna, S., Das, S., Mukhopadhyay, A., Das, I., Hazra, S., Choudhury, S.B., Rao, K.H., Dadhwal, V.K., 2016a. Mangrove associates versus true mangroves: a comparative analysis of leaf litter decomposition in Sundarban. Wetlands Ecology and Management. 24, 293-315. https://doi.org/10.1007/s11273-015-9456-9.

Chanda, A., Mukhopadhyay, A., Ghosh, T., Akhand, A., Mondal, P., Ghosh, S., Mukherjee, S., Wolf, J., Lázár, A.N., Rahman, M.M., Salehin, M., Chowdhury, S.M., Hazra, S., 2016b. Blue Carbon Stock of the Bangladesh Sundarban Mangroves: What could Be the Scenario after a Century? Wetlands. 36, 1033-1045. https://doi.org/10.1007/s13157-016-0819-7.

Chatterjee, M., Shankar, D., Sen, G., Sanyal, P., Sundar, D., Michael, G., Chatterjee, A., Amol, P., Mukherjee, D., Suprit, K., 2013. Tidal variations in the Sundarbans estuarine system, India. Journal of Earth System Science. 122, 899-933.

Chave, J., Andalo, C., Brown, S., Cairns, M.A., Chambers, J.Q., Eamus, D., Fölster, H., Fromard, F., Higuchi, N., Kira, T., Lescure, J.-P., Nelson, B.W., Ogawa, H., Puig, H., Riéra, B., Yamakura, T., 2005. Tree allometry and improved estimation of carbon stocks and balance in tropical forests. Oecologia. 145, 87-99. https://doi.org/10.1007/s00442-005-0100-x.

Chave, J., Condit, R., Aguilar, S., Hernandez, A., Lao, S., Perez, R., 2004. Error propagation and scaling for tropical forest biomass estimates. Philosophical transactions of the Royal Society of London. Series B, Biological sciences. 359, 409-420. https://doi.org/10.1098/rstb.2003.1425.

Chave, J., Coomes, D., Jansen, S., Lewis, S.L., Swenson, N.G., Zanne, A.E., 2009. Towards a worldwide wood economics spectrum. Ecology Letters. 12, 351-366. https://doi.org/10.1111/j.1461-0248.2009.01285.x.

Chave, J., Davies, S.J., Phillips, O.L., Lewis, S.L., Sist, P., Schepaschenko, D., Armston, J., Baker, T.R., Coomes, D., Disney, M., Duncanson, L., Hérault, B., Labrière, N., Meyer, V., Réjou-Méchain, M., Scipal, K., Saatchi, S., 2019. Ground Data are Essential for Biomass Remote Sensing Missions. Surveys in Geophysics. 40, 863-880. https://doi.org/10.1007/s10712-019-09528-w.

Chave, J., Réjou-Méchain, M., Búrquez, A., Chidumayo, E., Colgan, M.S., Delitti, W.B.C., Duque, A., Eid, T., Fearnside, P.M., Goodman, R.C., Henry, M., Martínez-Yrízar, A., Mugasha, W.A., Muller-Landau, H.C., Mencuccini, M., Nelson, B.W., Ngomanda, A., Nogueira, E.M.,

Ortiz-Malavassi, E., Pélissier, R., Ploton, P., Ryan, C.M., Saldarriaga, J.G., Vieilledent, G., 2014. Improved allometric models to estimate the aboveground biomass of tropical trees. Global Change Biology. 20, 3177-3190. https://doi.org/10.1111/gcb.12629.

Chen, B.Q., Xiao, X.M., Li, X.P., Pan, L.H., Doughty, R., Ma, J., Dong, J.W., Qin, Y.W., Zhao, B., Wu, Z.X., Sun, R., Lan, G.Y., Xie, G.S., Clinton, N., Giri, C., 2017. A mangrove forest map of China in 2015: Analysis of time series Landsat 7/8 and Sentinel-1A imagery in Google Earth Engine cloud computing platform. ISPRS Journal of Photogrammetry and Remote Sensing. 131, 104-120. https://doi.org/10.1016/j.isprsjprs.2017.07.011.

Chen, D., Stow, D., 2002. The effect of training strategies on supervised classification at different spatial resolutions. Photogrammetric Engineering and Remote Sensing. 68, 1155-1162.

Chowdhury, M.Q., De Ridder, M., Beeckman, H., 2016. Climatic Signals in Tree Rings of *Heritiera fomes* Buch.-Ham. in the Sundarbans, Bangladesh. PloS one. 11, e0149788. https://doi.org/10.1371/journal.pone.0149788.

Church, J.A., Clark, P.U., Cazenave, A., J.M. Gregory, Jevrejeva, S., Levermann, A., Merrifield, M.A., Milne, G.A., Nerem, R.S., Nunn, P.D., Payne, A.J., Pfeffer, W.T., Stammer, D., Unnikrishnan, A.S. (Eds.), 2013. Sea Level Change. Cambridge University Press, New York, pp. 1137-1216.

Cissell, J.R., Canty, S.W.J., Steinberg, M.K., Simpson, L.T., 2021. Mapping National Mangrove Cover for Belize Using Google Earth Engine and Sentinel-2 Imagery. Applied Sciences. 11, 4258.

Clough, B.F., Dixon, P., Dalhaus, O., 1997. Allometric relationships for estimating biomass in multi-stemmed mangrove trees. Australian Journal of Botany. 45, 1023-1031. https://doi.org/10.1071/BT96075.

Cole, J.J., Prairie, Y.T., Caraco, N.F., McDowell, W.H., Tranvik, L.J., Striegl, R.G., Duarte, C.M., Kortelainen, P., Downing, J.A., Middelburg, J.J., Melack, J., 2007. Plumbing the Global Carbon Cycle: Integrating Inland Waters into the Terrestrial Carbon Budget. Ecosystems. 10, 172-185. https://doi.org/10.1007/s10021-006-9013-8.

Collins, M., Knutti, R., Arblaster, J., Dufresne, J., Fichefet, T., Friedlingstein, P., Gao, X., Gutowski, W., Johns, T., Krinner, G., 2013. Climate change 2013: the physical science basis. Contribution of Working Group I to the Fifth Assessment Report of the Intergovernmental Panel on Climate Change. Long-term Clim. Chang. Proj. Commitments Irreversibility, Cambridge Univ. Press. Cambridge, UK, New York.

Comley, B.W.T., McGuinness, K.A., 2005. Above- and below-ground biomass, and allometry, of four common northern Australian mangroves. Australian Journal of Botany. 53, 431-436. https://doi.org/10.1071/BT04162.

Conchedda, G., Durieux, L., Mayaux, P., 2008. An object-based method for mapping and change analysis in mangrove ecosystems. ISPRS Journal of Photogrammetry and Remote Sensing. 63, 578-589. https://doi.org/10.1016/j.isprsjprs.2008.04.002.

Couteron, P., 2002. Quantifying change in patterned semi-arid vegetation by Fourier analysis of digitized aerial photographs. International Journal of Remote Sensing. 23, 3407-3425. https://doi.org/10.1080/01431160110107699.

Craft, C., 2007. Freshwater input structures soil properties, vertical accretion, and nutrient accumulation of Georgia and U.S tidal marshes. Limnology and Oceanography. 52, 1220-1230. https://doi.org/10.4319/lo.2007.52.3.1220.

Danielson, T.M., Rivera-Monroy, V.H., Castañeda-Moya, E., Briceño, H., Travieso, R., Marx, B.D., Gaiser, E., Farfán, L.M., 2017. Assessment of Everglades mangrove forest resilience: Implications for above-ground net primary productivity and carbon dynamics. Forest Ecology and Management. 404, 115-125. https://doi.org/10.1016/j.foreco.2017.08.009.

Dasgupta, S., Sobhan, I., Wheeler, D., 2017. The impact of climate change and aquatic salinization on mangrove species in the Bangladesh Sundarbans. Ambio. 46, 680-694. https://doi.org/10.1007/s13280-017-0911-0.

De Souza Pereira, F.R., Kampel, M., Gomes Soares, M.L., Estrada, G.C.D., Bentz, C., Vincent, G., 2018. Reducing Uncertainty in Mapping of Mangrove Aboveground Biomass Using Airborne Discrete Return Lidar Data. Remote Sensing. 10, 637. https://doi.org/10.3390/rs10040637.

De Vos, B., Lettens, S., Muys, B., Deckers, J.A., 2007. Walkley–Black analysis of forest soil organic carbon: recovery, limitations and uncertainty. Soil Use and Management. 23, 221-229. https://doi.org/10.1111/j.1475-2743.2007.00084.x.

Donato, D.C., Kauffman, J.B., Murdiyarso, D., Kurnianto, S., Stidham, M., Kanninen, M., 2011. Mangroves among the most carbon-rich forests in the tropics. Nature Geoscience. 4, 293-297. https://doi.org/10.1038/ngeo1123.

Duarte, C.M., 2017. Reviews and syntheses: Hidden forests, the role of vegetated coastal habitats in the ocean carbon budget. Biogeosciences. 14, 301-310. https://doi.org/10.5194/bg-14-301-2017.

Duarte, C.M., Losada, I.J., Hendriks, I.E., Mazarrasa, I., Marbà, N., 2013. The role of coastal plant communities for climate change mitigation and adaptation. Nature Climate Change. 3, 961-968. https://doi.org/10.1038/nclimate1970.

Duke, N.C., Kovacs, J.M., Griffiths, A.D., Preece, L., Hill, D.J.E., van Oosterzee, P., Mackenzie, J., Morning, H.S., Burrows, D., 2017. Large-scale dieback of mangroves in Australia's Gulf of Carpentaria: a severe ecosystem response, coincidental with an unusually extreme weather event. Marine and Freshwater Research. 68, 1816-1829. https://doi.org/10.1071/MF16322.

Duke, N.C., Meynecke, J.-O., Dittmann, S., Ellison, A.M., Anger, K., Berger, U., Cannicci, S., Diele, K., Ewel, K.C., Field, C.D., Koedam, N., Lee, S.Y., Marchand, C., Nordhaus, I., Dahdouh-Guebas, F., 2007. A World Without Mangroves? Science. 317, 41-42. https://doi.org/10.1126/science.317.5834.41b.

Dutta, J., Banerjee, K., Agarwal, S., Mitra, A., 2019. Soil Organic Carbon (soc): A Proxy to Assess the Degree of Anthropogenic and Natural Stress. The Journal of Interrupted Studies. 2, 90-102.

Dutta, M.K., Chowdhury, C., Jana, T.K., Mukhopadhyay, S.K., 2013. Dynamics and exchange fluxes of methane in the estuarine mangrove environment of the Sundarbans, NE coast of India. Atmospheric Environment. 77, 631-639. https://doi.org/10.1016/j.atmosenv.2013.05.050.

Edwards, D.P., Socolar, J.B., Mills, S.C., Burivalova, Z., Koh, L.P., Wilcove, D.S., 2019. Conservation of Tropical Forests in the Anthropocene. Current Biology. 29, R1008-R1020. https://doi.org/10.1016/j.cub.2019.08.026.

Ellison, A.M., Mukherjee, B.B., Karim, A., 2000. Testing patterns of zonation in mangroves: scale dependence and environmental correlates in the Sundarbans of Bangladesh. Journal of Ecology. 88, 813-824. https://doi.org/10.1046/j.1365-2745.2000.00500.x.

Emach, M., Peterson, M., 2006. Mangrove forest cover change in Bangladesh Sundarbans from 1989-2000: a remote sensing approach. Geocarto International. 21, 5-12.

ESA, 2022. Sentinel-2 MSI User Guide. https://sentinel.esa.int/web/sentinel/user-guides/sentinel-2-msi (accessed 22/02/2022).

ESRI, 2022a. Cross Validation (Geostatistical Analyst), Environmental Systems Research Institute, USA. https://pro.arcgis.com/en/pro-app/latest/tool-reference/geostatistical-analyst/cross-validation.htm (accessed 11/03/2022).

ESRI, 2022b. What is EBK Regression Prediction?, Environmental Systems Research Institute, USA. https://pro.arcgis.com/en/pro-app/latest/help/analysis/geostatistical-analyst/what-is-ebk-regression-prediction-.htm (accessed 11/03/2022).

FAO, 2010. Global Forest Resources Assessment 2010. FAO Forestry Paper No. 163, UN Food and Agriculture Organization, Rome(accessed.

FAO, 2016. Map accuracy assessment, area estimation: A practical guide. National forest monitoring assessment working paper No.46/E. FAO: Roma, Italy, pp. 69.

FAO, 2020. Global Forest Resources Assessment 2020: Main report. FAO, Rome, https://doi.org/10.4060/ca9825en.

Fatoyinbo, T., Armston, J., Simard, M., Saatchi, S., Denbina, M., Lavalle, M., Hofton, M., Tang, H., Marselis, S., Pinto, N., Hancock, S., Hawkins, B., Duncanson, L., Blair, B., Hansen, C., Lou, Y., Dubayah, R., Hensley, S., Silva, C., Poulsen, J.R., Labrière, N., Barbier, N., Jeffery, K., Kenfack, D., Herve, M., Bissiengou, P., Alonso, A., Moussavou, G., White, L.T.J., Lewis, S., Hibbard, K., 2021. The NASA AfriSAR campaign: Airborne SAR and lidar measurements of tropical forest structure and biomass in support of current and future space missions. Remote Sensing of Environment. 264, 112533. https://doi.org/10.1016/j.rse.2021.112533.

Fatoyinbo, T., Feliciano, E.A., Lagomasino, D., Lee, S.K., Trettin, C., 2018. Estimating mangrove aboveground biomass from airborne LiDAR data: a case study from the Zambezi River delta. Environmental Research Letters. 13. https://doi.org/10.1088/1748-9326/aa9f03.

Fatoyinbo, T.E., Simard, M., 2013. Height and biomass of mangroves in Africa from ICESat/GLAS and SRTM. International Journal of Remote Sensing. 34, 668-681. https://doi.org/10.1080/01431161.2012.712224.

Fatoyinbo, T.E., Simard, M., Washington-Allen, R.A., Shugart, H.H., 2008. Landscape-scale extent, height, biomass, and carbon estimation of Mozambique's mangrove forests with Landsat ETM+ and Shuttle Radar Topography Mission elevation data. Journal of Geophysical Research: Biogeosciences. 113, 1-13. https://doi.org/10.1029/2007JG000551.

Feldpausch, T.R., Banin, L., Phillips, O.L., Baker, T.R., Lewis, S.L., Quesada, C.A., Affum-Baffoe, K., Arets, E.J.M.M., Berry, N.J., Bird, M., Brondizio, E.S., de Camargo, P., Chave, J., Djagbletey, G., Domingues, T.F., Drescher, M., Fearnside, P.M., França, M.B., Fyllas, N.M., Lopez-Gonzalez, G., Hladik, A., Higuchi, N., Hunter, M.O., Iida, Y., Salim, K.A., Kassim, A.R., Keller, M., Kemp, J., King, D.A., Lovett, J.C., Marimon, B.S., Marimon-Junior, B.H., Lenza, E., Marshall, A.R., Metcalfe, D.J., Mitchard, E.T.A., Moran, E.F., Nelson, B.W., Nilus, R., Nogueira, E.M., Palace, M., Patiño, S., Peh, K.S.H., Raventos, M.T., Reitsma, J.M.,

Saiz, G., Schrodt, F., Sonké, B., Taedoumg, H.E., Tan, S., White, L., Wöll, H., Lloyd, J., 2011. Height-diameter allometry of tropical forest trees. Biogeosciences. 8, 1081-1106. https://doi.org/10.5194/bg-8-1081-2011.

Feldpausch, T.R., Lloyd, J., Lewis, S.L., Brienen, R.J.W., Gloor, M., Monteagudo Mendoza, A., Lopez-Gonzalez, G., Banin, L., Abu Salim, K., Affum-Baffoe, K., Alexiades, M., Almeida, S., Amaral, I., Andrade, A., Aragão, L.E.O.C., Araujo Murakami, A., Arets, E.J.M.M., Arroyo, L., Aymard C, G.A., Baker, T.R., Bánki, O.S., Berry, N.J., Cardozo, N., Chave, J., Comiskey, J.A., Alvarez, E., de Oliveira, A., Di Fiore, A., Djagbletey, G., Domingues, T.F., Erwin, T.L., Fearnside, P.M., França, M.B., Freitas, M.A., Higuchi, N., C, E.H., Iida, Y., Jiménez, E., Kassim, A.R., Killeen, T.J., Laurance, W.F., Lovett, J.C., Malhi, Y., Marimon, B.S., Marimon-Junior, B.H., Lenza, E., Marshall, A.R., Mendoza, C., Metcalfe, D.J., Mitchard, E.T.A., Neill, D.A., Nelson, B.W., Nilus, R., Nogueira, E.M., Parada, A., Peh, K.S.H., Pena Cruz, A., Peñuela, M.C., Pitman, N.C.A., Prieto, A., Quesada, C.A., Ramírez, F., Ramírez-Angulo, H., Reitsma, J.M., Rudas, A., Saiz, G., Salomão, R.P., Schwarz, M., Silva, N., Silva-Espejo, J.E., Silveira, M., Sonké, B., Stropp, J., Taedoumg, H.E., Tan, S., ter Steege, H., Terborgh, J., Torello-Raventos, M., van der Heijden, G.M.F., Vásquez, R., Vilanova, E., Vos, V.A., White, L., Willcock, S., Woell, H., Phillips, O.L., 2012. Tree height integrated into pantropical forest biomass estimates. Biogeosciences. 9, 3381-3403. https://doi.org/10.5194/bg-9-3381-2012.

Feliciano, E.A., Wdowinski, S., Potts, M.D., Lee, S.K., Fatoyinbo, T.E., 2017. Estimating mangrove canopy height and above-ground biomass in the Everglades National Park with airborne LiDAR and TanDEM-X data. Remote Sensing. 9. https://doi.org/10.3390/rs9070702.

Feller, I.C., Friess, D.A., Krauss, K.W., Lewis, R.R., 2017. The state of the world's mangroves in the 21st century under climate change. Hydrobiologia. 803, 1-12. https://doi.org/10.1007/s10750-017-3331-z.

Feller, I.C., Lovelock, C.E., Berger, U., McKee, K.L., Joye, S.B., Ball, M.C., 2010. Biocomplexity in mangrove ecosystems. Ann Rev Mar Sci. 2, 395-417. https://doi.org/10.1146/annurev.marine.010908.163809.

Fontaine, S., Barot, S., Barré, P., Bdioui, N., Mary, B., Rumpel, C., 2007. Stability of organic carbon in deep soil layers controlled by fresh carbon supply. Nature. 450, 277-280. https://doi.org/10.1038/nature06275.

Fox, J., Weisberg, S., 2019. An {R} Companion to Applied Regression. Sage, Thousand Oaks CA.

Freeman, C., Ostle, N.J., Fenner, N., Kang, H., 2004. A regulatory role for phenol oxidase during decomposition in peatlands. Soil Biology and Biochemistry. 36, 1663-1667. https://doi.org/10.1016/j.soilbio.2004.07.012.

Friess, D.A., Rogers, K., Lovelock, C.E., Krauss, K.W., Hamilton, S.E., Lee, S.Y., Lucas, R., Primavera, J., Rajkaran, A., Shi, S., 2019. The State of the World's Mangrove Forests: Past, Present, and Future. Annual Review of Environment and Resources. 44, 89-115. https://doi.org/10.1146/annurev-environ-101718-033302.

Friess, D.A., Yando, E.S., Abuchahla, G.M.O., Adams, J.B., Cannicci, S., Canty, S.W.J., Cavanaugh, K.C., Connolly, R.M., Cormier, N., Dahdouh-Guebas, F., Diele, K., Feller, I.C., Fratini, S., Jennerjahn, T.C., Lee, S.Y., Ogurcak, D.E., Ouyang, X., Rogers, K., Rowntree, J.K., Sharma, S., Sloey, T.M., Wee, A.K.S., 2020a. Mangroves give cause for conservation optimism, for now. Current Biology. 30, R153-R154. https://doi.org/10.1016/j.cub.2019.12.054.

Friess, D.A., Yando, E.S., Alemu, J.B., Wong, L.-W., Soto, S.D., Bhatia, N., 2020b. Chapter 3 Ecosystem Services and Disservices of Mangrove Forests and Salt Marshesnull. Taylor & Francis.

GFOI, 2016. Integration of Remote-sensing and Ground-based Observations for Estimation of Emissions and Removals of Greenhouse Gases in Forests: Methods and Guidance from the Global Forest Observation Initiative, Edition 2.0. Food and Agriculture Organization, Rome.

Ghimire, B., Rogan, J., Galiano, V.R., Panday, P., Neeti, N., 2012. An Evaluation of Bagging, Boosting, and Random Forests for Land-Cover Classification in Cape Cod, Massachusetts, USA. GIScience & Remote Sensing. 49, 623-643. https://doi.org/10.2747/1548-1603.49.5.623.

Ghorbanian, A., Zaghian, S., Asiyabi, R.M., Amani, M., Mohammadzadeh, A., Jamali, S., 2021. Mangrove Ecosystem Mapping Using Sentinel-1 and Sentinel-2 Satellite Images and Random Forest Algorithm in Google Earth Engine. Remote Sensing. 13, 2565.

Ghosh, M.K., Kumar, L., Roy, C., 2016. Mapping long-term changes in mangrove species composition and distribution in the Sundarbans. Forests. 7, 1-17. https://doi.org/10.3390/f7120305.

Gibbs, H.K., Brown, S., Niles, J.O., Foley, J.A., 2007. Monitoring and estimating tropical forest carbon stocks: making REDD a reality. Environmental Research Letters. 2, 045023. https://doi.org/10.1088/1748-9326/2/4/045023.

Gilman, E.L., Ellison, J., Duke, N.C., Field, C., 2008. Threats to mangroves from climate change and adaptation options: A review. Aquatic Botany. 89, 237-250. https://doi.org/10.1016/j.aquabot.2007.12.009.

Giri, C., Ochieng, E., Tieszen, L.L., Zhu, Z., Singh, A., Loveland, T., Masek, J., Duke, N., 2011. Status and distribution of mangrove forests of the world using earth observation satellite data. Global Ecology and Biogeography. 20, 154-159. https://doi.org/10.1111/j.1466-8238.2010.00584.x.

Giri, C., Pengra, B., Zhu, Z., Singh, A., Tieszen, L.L., 2007. Monitoring mangrove forest dynamics of the Sundarbans in Bangladesh and India using multi-temporal satellite data from 1973 to 2000. Estuarine, Coastal and Shelf Science. 73, 91-100. https://doi.org/10.1016/j.ecss.2006.12.019.

Giri, C., Zhu, Z., Tieszen, L., Singh, A., Gillette, S., Kelmelis, J., 2008. Mangrove forest distributions and dynamics (1975–2005) of the tsunami-affected region of Asia. Journal of Biogeography. 35, 519-528. https://doi.org/10.1111/j.1365-2699.2007.01806.x.

Gleason, S.M., Ewel, K.C., 2002. Organic matter dynamics on the forest floor of a micronesian mangrove forest: An investigation of species composition shifts. Biotropica. 34, 190-198. https://doi.org/10.1111/j.1744-7429.2002.tb00530.x.

GOB, 2018. The submission of Bangladesh's Forest Reference Level for REDD+ under the UNFCCC. https://redd.unfccc.int/files/frl-report_revised_17_july2019_f.pdf (accessed 18/02/2022).

GOB, 2019. Tree and forest resources of Bangladesh: Report on the Bangladesh Forest Inventory, Forest Department, Ministry of Environment, Forest and Climate Change, Government of the People's Republic of Bangladesh, Dhaka, Bangladesh. http://bfis.bforest.gov.bd/bfi/wp-content/uploads/2021/02/BFI-Report_final_08_02_2021.pdf (accessed 31/03/2021).

GOB, 2021. Nationally determined contributions (NDCs) 2021: Bangladesh https://www4.unfccc.int/sites/ndcstaging/PublishedDocuments/Bangladesh%20First/NDC_submission_20210826revised.pdf (accessed 18/02/2022).

Goetz, S.J., Baccini, A., Laporte, N.T., Johns, T., Walker, W., Kellndorfer, J., Houghton, R.A., Sun, M., 2009. Mapping and monitoring carbon stocks with satellite observations: a comparison of methods. Carbon Balance and Management. 4, 2. https://doi.org/10.1186/1750-0680-4-2.

Goetz, S.J., Hansen, M., Houghton, R.A., Walker, W., Laporte, N., Busch, J., 2015. Measurement and monitoring needs, capabilities and potential for addressing reduced emissions from

deforestation and forest degradation under REDD+. Environ. Res. Lett. 10. https://doi.org/10.1088/1748-9326/10/12/123001.

GOFC-GOLD, 2016. A sourcebook of methods and procedures for monitoring and reporting anthropogenic greenhouse gas emissions and removals associated with deforestation, gains and losses of carbon stocks in forests remaining forests, and forestation, GOFC-GOLD Land Cover Project Office, Wageningen University, The Netherlands(accessed 21/02/2020).

Goldberg, L., Lagomasino, D., Thomas, N., Fatoyinbo, T., 2020. Global declines in human-driven mangrove loss. Global Change Biology. 26, 5844-5855. https://doi.org/10.1111/gcb.15275.

Goodbred, S.L., Kuehl, S.A., 2000. The significance of large sediment supply, active tectonism, and eustasy on margin sequence development: Late Quaternary stratigraphy and evolution of the Ganges–Brahmaputra delta. Sedimentary Geology. 133, 227-248. https://doi.org/10.1016/S0037-0738(00)00041-5.

Gorelick, N., Hancher, M., Dixon, M., Ilyushchenko, S., Thau, D., Moore, R., 2017. Google Earth Engine: Planetary-scale geospatial analysis for everyone. Remote Sensing of Environment. 202, 18-27. https://doi.org/10.1016/j.rse.2017.06.031.

Gross, C.D., Harrison, R.B., 2018. Quantifying and Comparing Soil Carbon Stocks: Underestimation with the Core Sampling Method. Soil Science Society of America Journal. 82, 949-959. https://doi.org/10.2136/sssaj2018.01.0015.

Hale, R., Bain, R., Goodbred Jr, S., Best, J., 2019. Observations and scaling of tidal mass transport across the lower Ganges–Brahmaputra delta plain: implications for delta management and sustainability. Earth Surface Dynamics. 7, 231-245. https://doi.org/10.5194/esurf-7-231-2019.

Hamdan, O., Khairunnisa, M.R., Ammar, A.A., Hasmadi, I.M., Aziz, H.K., 2013. Mangrove carbon stock assessment by optical satellite imagery. Journal of Tropical Forest Science. 25, 554-565.

Hamilton, S.E., Friess, D.A., 2018. Global carbon stocks and potential emissions due to mangrove deforestation from 2000 to 2012. Nature Climate Change. 8, 240-244. https://doi.org/10.1038/s41558-018-0090-4.

Hansen, M.C., Potapov, P.V., Moore, R., Hancher, M., Turubanova, S.A., Tyukavina, A., Thau, D., Stehman, S.V., Goetz, S.J., Loveland, T.R., Kommareddy, A., Egorov, A., Chini, L., Justice, C.O., Townshend, J.R.G., 2013. High-Resolution Global Maps of 21st-Century Forest Cover Change. Science. 342, 850-853. https://doi.org/10.1126/science.1244693.

Hardie, M., Doyle, R., 2012. Measuring Soil Salinity. in: Shabala, S., Cuin, T.A. (Eds.), Plant Salt Tolerance: Methods and Protocols. Humana Press, Totowa, NJ, pp. 415-425. https://doi.org/10.1007/978-1-61779-986-0_28.

Harmon, M.E., Phillips, D.L., Battles, J.J., Rassweiler, A., Hall Jr, R.O., Lauenroth, W.K., 2007. Quantifying uncertainty in net primary production measurements. Principles and standards for measuring primary production, 238-260.

Harris, N., 2016. Global Forest Watch Climate: Summary of Methods and Data. http://climate.globalforestwatch.org/downloads/about/technical-note/wri15_TECH_GFW-Climate-v3.pdf (accessed 03/04/2018).

Hasan, M.E., Nath, B., Sarker, A.H.M.R., Wang, Z., Zhang, L., Yang, X., Nobi, M.N., Røskaft, E., Chivers, D.J., Suza, M., 2020. Applying Multi-Temporal Landsat Satellite Data and Markov-Cellular Automata to Predict Forest Cover Change and Forest Degradation of Sundarban Reserve Forest, Bangladesh. Forests. 11, 1016.

Hawker, L., Neal, J., Bates, P., 2019. Accuracy assessment of the TanDEM-X 90 Digital Elevation Model for selected floodplain sites. Remote Sensing of Environment. 232, 111319. https://doi.org/10.1016/j.rse.2019.111319.

Henry, M., Besnard, A., Asante, W.A., Eshun, J., Adu-Bredu, S., Valentini, R., Bernoux, M., Saint-André, L., 2010. Wood density, phytomass variations within and among trees, and allometric equations in a tropical rainforest of Africa. Forest Ecology and Management. 260, 1375-1388. https://doi.org/10.1016/j.foreco.2010.07.040.

Henry, M., Iqbal, Z., Johnson, K., Akhter, M., Costello, L., Scott, C., Jalal, R., Hossain, M.A., Chakma, N., Kuegler, O., Mahmood, H., Mahamud, R., Siddique, M.R.H., Misbahuzzaman, K., Uddin, M.M., Al Amin, M., Ahmed, F.U., Sola, G., Siddiqui, M.B., Birigazzi, L., Rahman, M., Animon, I., Ritu, S., Rahman, L.M., Islam, A., Hayden, H., Sidik, F., Kumar, M.F., Mukul, R.H., Nishad, H., Belal, A.H., Anik, A.R., Khaleque, A., Shaheduzzaman, M., Hossain, S.S., Aziz, T., Rahaman, M.T., Mohaiman, R., Meyer, P., Chakma, P., Rashid, A.Z.M.M., Das, S., Hira, S., Jashimuddin, M., Rahman, M.M., Wurster, K., Uddin, S.N., Azad, A.K., Islam, S.M.Z., Saint-André, L., 2021. A multi-purpose National Forest Inventory in Bangladesh: design, operationalisation and key results. Forest Ecosystems. 8, 12. https://doi.org/10.1186/s40663-021-00284-1.

Herold, M., Carter, S., Avitabile, V., Espejo, A.B., Jonckheere, I., Lucas, R., McRoberts, R.E., Næsset, E., Nightingale, J., Petersen, R., Reiche, J., Romijn, E., Rosenqvist, A., Rozendaal, D.M.A., Seifert, F.M., Sanz, M.J., De Sy, V., 2019. The Role and Need for Space-Based

Forest Biomass-Related Measurements in Environmental Management and Policy. Surveys in Geophysics. 40, 757-778. https://doi.org/10.1007/s10712-019-09510-6.

Herold, M., Román-Cuesta, R.M., Mollicone, D., Hirata, Y., Van Laake, P., Asner, G.P., Souza, C., Skutsch, M., Avitabile, V., MacDicken, K., 2011. Options for monitoring and estimating historical carbon emissions from forest degradation in the context of REDD+. Carbon Balance and Management. 6, 13. https://doi.org/10.1186/1750-0680-6-13.

Hickey, S.M., Callow, N.J., Phinn, S., Lovelock, C.E., Duarte, C.M., 2018. Spatial complexities in aboveground carbon stocks of a semi-arid mangrove community: A remote sensing height-biomass-carbon approach. Estuarine, Coastal and Shelf Science. 200, 194-201. https://doi.org/10.1016/j.ecss.2017.11.004.

Himes-Cornell, A., Pendleton, L., Atiyah, P., 2018. Valuing ecosystem services from blue forests: A systematic review of the valuation of salt marshes, sea grass beds and mangrove forests. Ecosystem Services. 30, 36-48. https://doi.org/10.1016/j.ecoser.2018.01.006.

Hoque, A., Sharma, S., Hagihara, A., 2011. Above and belowground carbon acquisition of mangrove Kandelia obovata trees in Manko Wetland, Okinawa, Japan. International Journal of Environment. 1, 7-13.

Hoque, M., Sarkar, M., Khan, S., Moral, M., Khurram, A., 2006. Present status of salinity rise in Sundarbans area and its effect on Sundari (*Heritiera fomes*) species. Research Journal Of Agriculture And Biological Sciences. 2, 115-121.

Hossain, G.M., Bhuiyan, M.A.H., 2016. Spatial and temporal variations of organic matter contents and potential sediment nutrient index in the Sundarbans mangrove forest, Bangladesh. KSCE Journal of Civil Engineering. 20, 163-174. https://doi.org/10.1007/s12205-015-0333-0.

Hossain, M., Saha, C., Abdullah, S.M.R., Saha, S., Siddique, M.R.H., 2016. Allometric biomass, nutrient and carbon stock models for Kandelia candel of the Sundarbans, Bangladesh. Trees-Structure and Function. 30, 709-717. https://doi.org/10.1007/s00468-015-1314-0.

Hossain, M., Siddique, M.R.H., Bose, A., Limon, S.H., Chowdhury, M.R.K., Saha, S., 2012. Allometry, above-ground biomass and nutrient distribution in *Ceriops decandra* (Griffith) Ding Hou dominated forest types of the Sundarbans mangrove forest, Bangladesh. Wetlands Ecology and Management. 20, 539-548. https://doi.org/10.1007/s11273-012-9274-2.

Houghton, R.A., Lawrence, K.T., Hackler, J.L., Brown, S., 2001. The spatial distribution of forest biomass in the Brazilian Amazon: a comparison of estimates. Global Change Biology. 7, 731-746. https://doi.org/10.1111/j.1365-2486.2001.00426.x.

Howard, J., Hoyt, S., Isensee, K., Telszewski, M., Pidgeon, E. (Eds.), 2014. Coastal blue carbon: methods for assessing carbon stocks and emissions factors in mangroves, tidal salt marshes, and seagrasses. Conservation International, Intergovernmental Oceanographic Commission of UNESCO, International Union for Conservation of Nature, Arlington, Virginia, USA, pp. 184.

Hu, Y., Wang, L., Fu, X., Yan, J., Wu, J., Tsang, Y., Le, Y., Sun, Y., 2016. Salinity and nutrient contents of tidal water affects soil respiration and carbon sequestration of high and low tidal flats of Jiuduansha wetlands in different ways. Science of the Total Environment. 565, 637-648. https://doi.org/10.1016/j.scitotenv.2016.05.004.

Huang, C., Davis, L.S., Townshend, J.R.G., 2002. An assessment of support vector machines for land cover classification. International Journal of Remote Sensing. 23, 725-749. https://doi.org/10.1080/01431160110040323.

Hunter, M.O., Keller, M., Victoria, D., Morton, D.C., 2013. Tree height and tropical forest biomass estimation. Biogeosciences. 10, 8385-8399. https://doi.org/10.5194/bg-10-8385-2013.

Hurtt, G.C., Dubayah, R., Drake, J., Moorcroft, P.R., Pacala, S.W., Blair, J.B., Fearon, M.G., 2004. Beyond potential vegetation: Combining lidar data and a height-structured model for carbon studies. Ecological Applications. 14, 873-883. https://doi.org/10.1890/02-5317.

Hutchison, J., Manica, A., Swetnam, R., Balmford, A., Spalding, M., 2014. Predicting Global Patterns in Mangrove Forest Biomass. Conservation Letters. 7, 233-240. https://doi.org/10.1111/conl.12060.

ICRAF, 2016. Tree Functional and Ecological Databases. World Agroforestry Centre. http://db.worldagroforestry.org/ (accessed 24/11/2020).

Iftekhar, M., Saenger, P., 2008. Vegetation dynamics in the Bangladesh Sundarbans mangroves: a review of forest inventories. Wetlands Ecology and Management. 16, 291-312. https://doi.org/10.1007/s11273-007-9063-5.

IPCC (Ed.), 2006. 2006 IPCC guidelines for national greenhouse gas inventories. Prepared by the National Greenhouse Gas Inventories Programme, IGES, Japan.

IPCC, 2014. 2013 Supplement to the 2006 IPCC guidelines for national greenhouse gas inventories: Wetlands. in: Hiraishi, T. et al. (Eds.). IPCC, Geneva, Switzerland, pp. 354.

IPCC (Ed.), 2019. 2019 Refinement to the 2006 IPCC Guidelines for National Greenhouse Gas Inventories, IPCC, Switzerland.

Islam, A.K.M.N., 2016a. Germination Eco-Physiology and Plant Diversity in Halophytes of Sundarban Mangrove Forest in Bangladesh. in: Khan, M.A., Ozturk, M., Gul, B., Ahmed, M.Z. (Eds.), Halophytes for Food Security in Dry Lands. Academic Press, San Diego, pp. 277-289. https://doi.org/10.1016/B978-0-12-801854-5.00017-0.

Islam, M.R., Begum, S.F., Yamaguchi, Y., Ogawa, K., 1999. The Ganges and Brahmaputra rivers in Bangladesh: basin denudation and sedimentation. Hydrological Processes. 13, 2907-2923. https://doi.org/10.1002/(sici)1099-1085(19991215)13:17<2907::Aid-hyp906>3.0.Co;2-e.

Islam, S.N., 2016b. Deltaic floodplains development and wetland ecosystems management in the Ganges–Brahmaputra–Meghna Rivers Delta in Bangladesh. Sustainable Water Resources Management. 2, 237-256. https://doi.org/10.1007/s40899-016-0047-6.

Jachowski, N.R.A., Quak, M.S.Y., Friess, D.A., Duangnamon, D., Webb, E.L., Ziegler, A.D., 2013. Mangrove biomass estimation in Southwest Thailand using machine learning. Applied Geography. 45, 311-321. https://doi.org/10.1016/j.apgeog.2013.09.024.

Jackson, D.A., 1993. Stopping Rules in Principal Components Analysis: A Comparison of Heuristical and Statistical Approaches. Ecology. 74, 2204-2214. https://doi.org/10.2307/1939574.

James, G., Witten, D., Hastie, T., Tibshirani, R., 2013. An introduction to statistical learning. Springer, New York.

Jandl, R., Rodeghiero, M., Martinez, C., Cotrufo, M.F., Bampa, F., van Wesemael, B., Harrison, R.B., Guerrini, I.A., Richter, D.d., Rustad, L., Lorenz, K., Chabbi, A., Miglietta, F., 2014. Current status, uncertainty and future needs in soil organic carbon monitoring. Science of the Total Environment. 468-469, 376-383. https://doi.org/10.1016/j.scitotenv.2013.08.026.

Jardine, S.L., Siikamäki, J.V., 2014. A global predictive model of carbon in mangrove soils. Environmental Research Letters. 9, 104013. https://doi.org/10.1088/1748-9326/9/10/104013.

Joshi, N., Mitchard, E.T.A., Brolly, M., Schumacher, J., Fernández-Landa, A., Johannsen, V.K., Marchamalo, M., Fensholt, R., 2017. Understanding ‘saturation’ of radar signals over forests. Scientific Reports. 7, 3505. https://doi.org/10.1038/s41598-017-03469-3.

Kamruzzaman, M., Ahmed, S., Osawa, A., 2017. Biomass and net primary productivity of mangrove communities along the Oligohaline zone of Sundarbans, Bangladesh. Forest Ecosystems. 4, 16. https://doi.org/10.1186/s40663-017-0104-0.

Kamruzzaman, M., Ahmed, S., Paul, S., Rahman, M.M., Osawa, A., 2018. Stand structure and carbon storage in the oligohaline zone of the Sundarbans mangrove forest, Bangladesh. Forest Science and Technology. 14, 23-28. https://doi.org/10.1080/21580103.2017.1417920.

Kamruzzaman, M., Basak, K., Paul, S.K., Ahmed, S., Osawa, A., 2019. Litterfall production, decomposition and nutrient accumulation in Sundarbans mangrove forests, Bangladesh. Forest Science and Technology. 15, 24-32. https://doi.org/10.1080/21580103.2018.1557566.

Kangkuso, A., Jamili, J., Septiana, A., Raya, R., Sahidin, I., Rianse, U., Rahim, S., Alfirman, A., Sharma, S., Nadaoka, K., 2016. Allometric models and aboveground biomass of Lumnitzera racemosa Willd. forest in Rawa Aopa Watumohai National Park, Southeast Sulawesi, Indonesia. Forest Science and Technology. 12, 43-50. https://doi.org/10.1080/21580103.2015.1034191.

Kassambara, A., 2020. Rstatix: pipe-friendly framework for basic statistical tests. R package version 0.6. 0.

Kauffman, J.B., Adame, M.F., Arifanti, V.B., Schile-Beers, L.M., Bernardino, A.F., Bhomia, R.K., Donato, D.C., Feller, I.C., Ferreira, T.O., del Carmen Jesus Garcia, M., MacKenzie, R.A., Megonigal, J.P., Murdiyarso, D., Simpson, L., Hernández Trejo, H., 2020. Total ecosystem carbon stocks of mangroves across broad global environmental and physical gradients. Ecological Monographs. n/a. https://doi.org/10.1002/ecm.1405.

Kauffman, J.B., Bhomia, R.K., 2017. Ecosystem carbon stocks of mangroves across broad environmental gradients in West-Central Africa: Global and regional comparisons. PloS one. 12, e0187749. https://doi.org/10.1371/journal.pone.0187749.

Kauffman, J.B., Donato, D., 2012. Protocols for the measurement, monitoring and reporting of structure, biomass and carbon stocks in mangrove forests. Working Paper 86. Center for International Forestry Research (CIFOR), Bogor, Indonesia, pp. 50.

Kauffman, J.B., Heider, C., Cole, T.G., Dwire, K.A., Donato, D.C., 2011. Ecosystem Carbon Stocks of Micronesian Mangrove Forests. Wetlands. 31, 343-352. https://doi.org/10.1007/s13157-011-0148-9.

Kearsley, E., de Haulleville, T., Hufkens, K., Kidimbu, A., Toirambe, B., Baert, G., Huygens, D., Kebede, Y., Defourny, P., Bogaert, J., Beeckman, H., Steppe, K., Boeckx, P., Verbeeck, H., 2013. Conventional tree height–diameter relationships significantly overestimate aboveground carbon stocks in the Central Congo Basin. Nature Communications. 4, 2269. https://doi.org/10.1038/ncomms3269.

Kenzo, T., Ichie, T., Hattori, D., Itioka, T., Handa, C., Ohkubo, T., Kendawang, J.J., Nakamura, M., Sakaguchi, M., Takahashi, N., Okamoto, M., Tanaka-Oda, A., Sakurai, K., Ninomiya, I., 2009. Development of Allometric Relationships for Accurate Estimation of above- and

Below-Ground Biomass in Tropical Secondary Forests in Sarawak, Malaysia. Journal of Tropical Ecology. 25, 371-386.

Keskin, H., Grunwald, S., 2018. Regression kriging as a workhorse in the digital soil mapper's toolbox. Geoderma. 326, 22-41. https://doi.org/10.1016/j.geoderma.2018.04.004.

Khan, M., Amin, M., 2019. Macro nutrient status of Sundarbans forest soils in Southern region of Bangladesh. Bangladesh Journal of Scientific and Industrial Research. 54, 67-72. https://doi.org/10.3329/bjsir.v54i1.40732.

Khan, M.F.A., Rahman, M.S., Giessen, L., 2020a. Mangrove forest policy and management: Prevailing policy issues, actors' public claims and informal interests in the Sundarbans of Bangladesh. Ocean & Coastal Management. 186, 105090. https://doi.org/10.1016/j.ocecoaman.2019.105090.

Khan, M.N.I., Khatun, S., Azad, M.S., Mollick, A.S., 2020b. Leaf morphological and anatomical plasticity in Sundri (Heritiera fomes Buch.-Ham.) along different canopy light and salinity zones in the Sundarbans mangrove forest, Bangladesh. Global Ecology and Conservation. 23, e01127. https://doi.org/10.1016/j.gecco.2020.e01127.

Kominoski, J.S., Gaiser, E.E., Baer, S.G., 2018. Advancing Theories of Ecosystem Development through Long-Term Ecological Research. Bioscience. 68, 554-562. https://doi.org/10.1093/biosci/biy070.

Komiyama, A., Ong, J.E., Poungparn, S., 2008. Allometry, biomass, and productivity of mangrove forests: A review. Aquatic Botany. 89, 128-137. https://doi.org/10.1016/j.aquabot.2007.12.006.

Komiyama, A., Poungparn, S., Kato, S., 2005. Common allometric equations for estimating the tree weight of mangroves. Journal of Tropical Ecology. 21, 471-477. https://doi.org/10.1017/S0266467405002476.

Krauss, K.W., McKee, K.L., Lovelock, C.E., Cahoon, D.R., Saintilan, N., Reef, R., Chen, L., 2014. How mangrove forests adjust to rising sea level. New Phytologist. 202, 19-34. https://doi.org/10.1111/nph.12605.

Krieger, G., Moreira, A., Fiedler, H., Hajnsek, I., Zink, M., Werner, M., Eineder, M., 2006. TanDEM-X: Mission concept, product definition and performance prediction, European Conference on Synthetic Aperture Radar (EUSAR). VDE Verlag GmbH, pp. 1-4.

Kristensen, E., Bouillon, S., Dittmar, T., Marchand, C., 2008. Organic carbon dynamics in mangrove ecosystems: A review. Aquatic Botany. 89, 201-219. https://doi.org/10.1016/j.aquabot.2007.12.005.

Krivoruchko, K., 2012. (a) Empirical Bayesian kriging and (b) Modeling contamination using empirical Bayesian kriging, ESRI. https://www.esri.com/news/arcuser/1012/fall2012.html (accessed 11/03/2022).

Krivoruchko, K., Gribov, A., 2020. Distance metrics for data interpolation over large areas on Earth's surface. Spatial Statistics. 35, 100396. https://doi.org/10.1016/j.spasta.2019.100396.

Kuhn, M., 2008. Building predictive models in R using the caret package. J Stat Softw. 28, 1-26.

Kumar, M., Mondal, I., Pham, Q.B., 2021. Monitoring forest landcover changes in the Eastern Sundarban of Bangladesh from 1989 to 2019. Acta Geophysica. 69, 561-577. https://doi.org/10.1007/s11600-021-00551-3.

Kusmana, C., Hidayat, T., Tiryana, T., Rusdiana, O., Istomo, 2018. Allometric models for above- and below-ground biomass of *Sonneratia* spp. Global Ecology and Conservation. 15, e00417. https://doi.org/10.1016/j.gecco.2018.e00417.

Lacerda, L.D., Ittekkot, V., Patchineelam, S.R., 1995. Biogeochemistry of mangrove soil organic matter: a comparison between *Rhizophora* and *Avicennia* soils in south-eastern Brazil. Estuarine, Coastal and Shelf Science. 40, 713-720. https://doi.org/10.1006/ecss.1995.0048.

Lagomasino, D., Fatoyinbo, T., Lee, S., Feliciano, E., Trettin, C., Shapiro, A., Mangora, M.M., 2019. Measuring mangrove carbon loss and gain in deltas. Environmental Research Letters. 14, 025002. https://doi.org/10.1088/1748-9326/aaf0de.

Lange, M., Eisenhauer, N., Sierra, C.A., Bessler, H., Engels, C., Griffiths, R.I., Mellado-Vázquez, P.G., Malik, A.A., Roy, J., Scheu, S., Steinbeiss, S., Thomson, B.C., Trumbore, S.E., Gleixner, G., 2015. Plant diversity increases soil microbial activity and soil carbon storage. Nature Communications. 6, 6707. https://doi.org/10.1038/ncomms7707.

Larjavaara, M., Muller-Landau, H.C., 2013. Measuring tree height: a quantitative comparison of two common field methods in a moist tropical forest. Methods in Ecology and Evolution. 4, 793-801. https://doi.org/10.1111/2041-210X.12071.

Laurin, G.V., Pirotti, F., Callegari, M., Chen, Q., Cuozzo, G., Lingua, E., Notarnicola, C., Papale, D., 2017. Potential of ALOS2 and NDVI to Estimate Forest Above-Ground Biomass, and Comparison with Lidar-Derived Estimates. Remote Sensing. 9. https://doi.org/10.3390/rs9010018.

Lee, S.K., Fatoyinbo, T., Lagomasino, D., Osmanoglu, B., Simard, M., Trettin, C., Rahman, M., Ahmed, I., 2015. Large-scale mangrove canopy height map generation from TanDEM-X data by means of Pol-InSAR techniques, International Geoscience and Remote Sensing Symposium (IGARSS), pp. 2895-2898.

Lee, S.K., Fatoyinbo, T.E., 2015. TanDEM-X Pol-InSAR Inversion for Mangrove Canopy Height Estimation. Ieee Journal of Selected Topics in Applied Earth Observations and Remote Sensing. 8, 3608-3618. https://doi.org/10.1109/jstars.2015.2431646.

Legendre, P., Legendre, L.F., 2012. Numerical ecology. Elsevier, UK.

Li, J., Heap, A.D., 2011. A review of comparative studies of spatial interpolation methods in environmental sciences: Performance and impact factors. Ecological Informatics. 6, 228-241. https://doi.org/10.1016/j.ecoinf.2010.12.003.

Liu, X., Fatoyinbo, T.E., Thomas, N.M., Guan, W.W., Zhan, Y., Mondal, P., Lagomasino, D., Simard, M., Trettin, C.C., Deo, R., Barenblitt, A., 2021. Large-Scale High-Resolution Coastal Mangrove Forests Mapping Across West Africa With Machine Learning Ensemble and Satellite Big Data. Frontiers in Earth Science. 8. https://doi.org/10.3389/feart.2020.560933.

Liu, X., Ruecker, A., Song, B., Xing, J., Conner, W.H., Chow, A.T., 2017. Effects of salinity and wet–dry treatments on C and N dynamics in coastal-forested wetland soils: Implications of sea level rise. Soil Biology and Biochemistry. 112, 56-67. https://doi.org/10.1016/j.soilbio.2017.04.002.

Liu, Z., Lee, C., 2006. Drying effects on sorption capacity of coastal sediment: The importance of architecture and polarity of organic matter. Geochimica et Cosmochimica Acta. 70, 3313-3324. https://doi.org/10.1016/j.gca.2006.04.017.

Locatelli, T., Binet, T., Kairo, J.G., King, L., Madden, S., Patenaude, G., Upton, C., Huxham, M., 2014. Turning the Tide: How Blue Carbon and Payments for Ecosystem Services (PES) Might Help Save Mangrove Forests. Ambio. 43, 981-995. https://doi.org/10.1007/s13280-014-0530-y.

Long, J.B., Giri, C., 2011. Mapping the Philippines' mangrove forests using Landsat imagery. Sensors (Basel). 11, 2972-81. https://doi.org/10.3390/s110302972

sensors-11-02972 [pii].

Lovelock, C.E., Cahoon, D.R., Friess, D.A., Guntenspergen, G.R., Krauss, K.W., Reef, R., Rogers, K., Saunders, M.L., Sidik, F., Swales, A., Saintilan, N., Thuyen le, X., Triet, T., 2015a. The

vulnerability of Indo-Pacific mangrove forests to sea-level rise. Nature. 526, 559-63. https://doi.org/10.1038/nature15538.

Lovelock, C.E., Cahoon, D.R., Friess, D.A., Guntenspergen, G.R., Krauss, K.W., Reef, R., Rogers, K., Saunders, M.L., Sidik, F., Swales, A., Saintilan, N., Thuyen, L.X., Triet, T., 2015b. The vulnerability of Indo-Pacific mangrove forests to sea-level rise. Nature. 526, 559-563. https://doi.org/10.1038/nature15538.

Lovelock, C.E., Duarte, C.M., 2019. Dimensions of Blue Carbon and emerging perspectives. Biology Letters. 15, 20180781. https://doi.org/10.1098/rsbl.2018.0781.

Lovelock, C.E., Feller, I.C., Reef, R., Hickey, S., Ball, M.C., 2017. Mangrove dieback during fluctuating sea levels. Scientific Reports. 7. https://doi.org/10.1038/s41598-017-01927-6.

Lovelock, C.E., Sorrell, B.K., Hancock, N., Hua, Q., Swales, A., 2010. Mangrove Forest and Soil Development on a Rapidly Accreting Shore in New Zealand. Ecosystems. 13, 437-451. https://doi.org/10.1007/s10021-010-9329-2.

Lucas, R., Rebelo, L.-M., Fatoyinbo, L., Rosenqvist, A., Itoh, T., Shimada, M., Simard, M., Souza-Filho, P.W., Thomas, N., Trettin, C., 2014. Contribution of L-band SAR to systematic global mangrove monitoring. Marine and Freshwater Research. 65, 589-603. https://doi.org/10.1071/MF13177.

Lucas, R.M., Mitchell, A.L., Armston, J., 2015. Measurement of Forest Above-Ground Biomass Using Active and Passive Remote Sensing at Large (Subnational to Global) Scales. Current Forestry Reports. 1, 162-177. https://doi.org/10.1007/s40725-015-0021-9.

Lucas, R.M., Mitchell, A.L., Rosenqvist, A., Proisy, C., Melius, A., Ticehurst, C., 2007. The potential of L-band SAR for quantifying mangrove characteristics and change: case studies from the tropics. Aquatic Conservation: Marine and Freshwater Ecosystems. 17, 245-264. https://doi.org/10.1002/aqc.833.

Lüdecke, D., 2018. ggeffects: Tidy data frames of marginal effects from regression models. Journal of Open Source Software. 3, 772.

Luo, M., Huang, J.-F., Zhu, W.-F., Tong, C., 2019. Impacts of increasing salinity and inundation on rates and pathways of organic carbon mineralization in tidal wetlands: a review. Hydrobiologia. 827, 31-49. https://doi.org/10.1007/s10750-017-3416-8.

Macreadie, P.I., Anton, A., Raven, J.A., Beaumont, N., Connolly, R.M., Friess, D.A., Kelleway, J.J., Kennedy, H., Kuwae, T., Lavery, P.S., Lovelock, C.E., Smale, D.A., Apostolaki, E.T., Atwood, T.B., Baldock, J., Bianchi, T.S., Chmura, G.L., Eyre, B.D., Fourqurean, J.W., Hall-

Spencer, J.M., Huxham, M., Hendriks, I.E., Krause-Jensen, D., Laffoley, D., Luisetti, T., Marbà, N., Masque, P., McGlathery, K.J., Megonigal, J.P., Murdiyarso, D., Russell, B.D., Santos, R., Serrano, O., Silliman, B.R., Watanabe, K., Duarte, C.M., 2019. The future of Blue Carbon science. Nature Communications. 10, 3998. https://doi.org/10.1038/s41467-019-11693-w.

Macreadie, P.I., Costa, M.D.P., Atwood, T.B., Friess, D.A., Kelleway, J.J., Kennedy, H., Lovelock, C.E., Serrano, O., Duarte, C.M., 2021. Blue carbon as a natural climate solution. Nature Reviews Earth & Environment. 2, 826-839. https://doi.org/10.1038/s43017-021-00224-1.

Magalhães, T.M., Seifert, T., 2015. Tree component biomass expansion factors and root-to-shoot ratio of Lebombo ironwood: measurement uncertainty. Carbon Balance and Management. 10, 9. https://doi.org/10.1186/s13021-015-0019-4.

Mahdianpari, M., Salehi, B., Mohammadimanesh, F., Brisco, B., Homayouni, S., Gill, E., DeLancey, E.R., Bourgeau-Chavez, L., 2020. Big Data for a Big Country: The First Generation of Canadian Wetland Inventory Map at a Spatial Resolution of 10-m Using Sentinel-1 and Sentinel-2 Data on the Google Earth Engine Cloud Computing Platform. Canadian Journal of Remote Sensing. 46, 15-33. https://doi.org/10.1080/07038992.2019.1711366.

Mahmood, A.R.J., 2015a. Forest Change in the Mangroves of the Ganges-Brahmaputra Delta 1906-2014., Durham University.

Mahmood, H., 2015b. Handbook of selected plant and species of the Sundarbans and the embankment ecosystem, Sustainable Development and Biodiversity Conservation in Coastal Protection Forests, Bangladesh (SDBC-Sundarbans) Project implemented by the Deutsche Gesellschaft für Internationale Zusammenarbeit (GIZ) GmbH on behalf of the German Federal Ministry for Economic Cooperation and Development (BMZ), Dhaka(accessed.

Mahmood, H., Saha, C., Rubaiot Abdullah, S.M., Saha, S., Siddique, M.R.H., 2016a. Allometric biomass, nutrient and carbon stock models for Kandelia candel of the Sundarbans, Bangladesh. Trees. 30, 709-717. https://doi.org/10.1007/s00468-015-1314-0.

Mahmood, H., Shaikh, M.A.A., Saha, C., Abdullah, S.M.R., Saha, S., Siddique, M.R.H., 2016b. Above-Ground Biomass, Nutrients and Carbon in *Aegiceras corniculatum* of the Sundarbans. Open Journal of Forestry. 06, 72-81. https://doi.org/10.4236/ojf.2016.62007.

Mahmood, H., Siddique, M.R.H., Abdullah, S.M.R., Islam, S.M.Z., Matieu, H., Iqbal, M.Z., Akhter, M., 2020. Semi-destructive method to derive allometric aboveground biomass model for village forest of Bangladesh: comparison of regional and pantropical models. Journal of Tropical Forest Science. 32, 246-256. https://doi.org/10.2307/26921872.

Mahmood, H., Siddique, M.R.H., Bose, A., Limon, S.H., Chowdhury, M.R.K., Saha, S., 2012. Allometry, above-ground biomass and nutrient distribution in *Ceriops decandra* (Griffith) Ding Hou dominated forest types of the Sundarbans mangrove forest, Bangladesh. Wetlands Ecology and Management. 20, 539-548. https://doi.org/10.1007/s11273-012-9274-2.

Mahmood, H., Siddique, M.R.H., Rubaiot Abdullah, S.M., Costello, L., Matieu, H., Iqbal, M.Z., Akhter, M., 2019. Which option best estimates the above-ground biomass of mangroves of Bangladesh: pantropical or site- and species-specific models? Wetlands Ecology and Management. https://doi.org/10.1007/s11273-019-09677-0.

Mallik, S., Bhowmik, T., Mishra, U., Paul, N., 2020. Mapping and prediction of soil organic carbon by an advanced geostatistical technique using remote sensing and terrain data. Geocarto International, 1-17. https://doi.org/10.1080/10106049.2020.1815864.

Marchand, C., 2017. Soil carbon stocks and burial rates along a mangrove forest chronosequence (French Guiana). Forest Ecology and Management. 384, 92-99. https://doi.org/10.1016/j.foreco.2016.10.030.

Martínez-Sánchez, J.L., Martínez-Garza, C., Cámara, L., Castillo, O., 2020. Species-specific or generic allometric equations: which option is better when estimating the biomass of Mexican tropical humid forests? Carbon Management. 11, 241-249. https://doi.org/10.1080/17583004.2020.1738823.

Marton, J.M., Herbert, E.R., Craft, C.B., 2012. Effects of Salinity on Denitrification and Greenhouse Gas Production from Laboratory-incubated Tidal Forest Soils. Wetlands. 32, 347-357. https://doi.org/10.1007/s13157-012-0270-3.

Martone, M., Rizzoli, P., Wecklich, C., González, C., Bueso-Bello, J.-L., Valdo, P., Schulze, D., Zink, M., Krieger, G., Moreira, A., 2018. The global forest/non-forest map from TanDEM-X interferometric SAR data. Remote Sensing of Environment. 205, 352-373. https://doi.org/10.1016/j.rse.2017.12.002.

Matsui, N., Meepol, W., Chukwamdee, J., 2015. Soil Organic Carbon in Mangrove Ecosystems with Different Vegetation and Sedimentological Conditions. Journal of Marine Science and Engineering. 3, 1404-1424. https://doi.org/10.3390/jmse3041404.

McGill, R., Tukey, J.W., Larsen, W.A., 1978. Variations of Box Plots. The American Statistician. 32, 12-16. https://doi.org/10.2307/2683468.

McLeod, E., Chmura, G.L., Bouillon, S., Salm, R., Björk, M., Duarte, C.M., Lovelock, C.E., Schlesinger, W.H., Silliman, B.R., 2011. A blueprint for blue carbon: toward an improved

understanding of the role of vegetated coastal habitats in sequestering CO2. Frontiers in Ecology and the Environment. 9, 552-560. https://doi.org/10.1890/110004.

McLeod, E., Salm, R.V., 2006. Managing Mangroves for Resilience to Climate Change. IUCN, Gland, Switzerland, pp. 64.

Messina, G., Peña, J.M., Vizzari, M., Modica, G., 2020. A Comparison of UAV and Satellites Multispectral Imagery in Monitoring Onion Crop. An Application in the 'Cipolla Rossa di Tropea' (Italy). Remote Sensing. 12, 3424.

Mitchard, E.T., Saatchi, S.S., Baccini, A., Asner, G.P., Goetz, S.J., Harris, N.L., Brown, S., 2013. Uncertainty in the spatial distribution of tropical forest biomass: a comparison of pan-tropical maps. Carbon Balance and Management. 8, 10. https://doi.org/10.1186/1750-0680-8-10.

Mitra, A., Banerjee, K., Sett, S., 2012. Spatial Variation in Organic Carbon Density of Mangrove Soil in Indian Sundarbans. National Academy Science Letters. 35, 147-154. https://doi.org/10.1007/s40009-012-0046-6.

Mokria, M., Mekuria, W., Gebrekirstos, A., Aynekulu, E., Belay, B., Gashaw, T., Bräuning, A., 2018. Mixed-species allometric equations and estimation of aboveground biomass and carbon stocks in restoring degraded landscape in northern Ethiopia. Environmental Research Letters. 13, 024022. https://doi.org/10.1088/1748-9326/aaa495.

Mondal, P., Liu, X., Fatoyinbo, T.E., Lagomasino, D., 2019. Evaluating Combinations of Sentinel-2 Data and Machine-Learning Algorithms for Mangrove Mapping in West Africa. Remote Sensing. 11, 2928.

Morrissey, E.M., Gillespie, J.L., Morina, J.C., Franklin, R.B., 2014. Salinity affects microbial activity and soil organic matter content in tidal wetlands. Global Change Biology. 20, 1351-1362. https://doi.org/10.1111/gcb.12431.

Murtagh, F., Legendre, P., 2014. Ward's Hierarchical Agglomerative Clustering Method: Which Algorithms Implement Ward's Criterion? Journal of Classification. 31, 274-295. https://doi.org/10.1007/s00357-014-9161-z.

Nasrin, S., Hossain, M., Rahman, M.M., 2019. Adaptive responses to salinity: nutrient resorption efficiency of Sonneratia apetala (Buch.-Ham.) along the salinity gradient in the Sundarbans of Bangladesh. Wetlands Ecology and Management. 27, 343-351. https://doi.org/10.1007/s11273-019-09663-6.

Nayak, A.K., Rahman, M.M., Naidu, R., Dhal, B., Swain, C.K., Nayak, A.D., Tripathi, R., Shahid, M., Islam, M.R., Pathak, H., 2019. Current and emerging methodologies for estimating

carbon sequestration in agricultural soils: A review. Science of the Total Environment. 665, 890-912. https://doi.org/10.1016/j.scitotenv.2019.02.125.

Nayak, B., Zaman, S., Gadi, S.D., Raha, A.K., Mitra, A., 2014. Dominant gastropods of Indian Sundarbans: A major sink of carbon. International Journal of Advances in Pharmacy, Biology and Chemistry. 3, 282-289.

Nellemann, C., Corcoran, E., Duarte, C., Valdés, L., De Young, C., Fonseca, L., Grimsditch, G., 2009. Blue Carbon: The Role of Healthy Oceans in Binding Carbon. UN Environment, GRID-Arendal.

Nelson, D.W., Sommers, L.E., 1996. Total carbon, organic carbon, and organic matter. in: Sparks, D. et al. (Eds.), Methods of soil analysis: Part 3 Chemical methods, pp. 961-1010. https://doi.org/10.2136/sssabookser5.3.c34.

Ngomanda, A., Engone Obiang, N.L., Lebamba, J., Moundounga Mavouroulou, Q., Gomat, H., Mankou, G.S., Loumeto, J., Midoko Iponga, D., Kossi Ditsouga, F., Zinga Koumba, R., Botsika Bobé, K.H., Mikala Okouyi, C., Nyangadouma, R., Lépengué, N., Mbatchi, B., Picard, N., 2014. Site-specific versus pantropical allometric equations: Which option to estimate the biomass of a moist central African forest? Forest Ecology and Management. 312, 1-9. https://doi.org/10.1016/j.foreco.2013.10.029.

Ni-Meister, W., 2015. Aboveground terrestrial biomass and carbon stock estimations from multisensor remote sensing. in: Thenkabail, P.S. (Ed.), Land resources monitoring, modeling, and mapping with remote sensing. CRC Press, Boca Raton.

Njana, M.A., Meilby, H., Eid, T., Zahabu, E., Malimbwi, R.E., 2016. Importance of tree basic density in biomass estimation and associated uncertainties: a case of three mangrove species in Tanzania. Annals of Forest Science. 73, 1073-1087. https://doi.org/10.1007/s13595-016-0583-0.

Nóbrega, G.N., Ferreira, T.O., Artur, A.G., de Mendonça, E.S., de O. Leão, R.A., Teixeira, A.S., Otero, X.L., 2015. Evaluation of methods for quantifying organic carbon in mangrove soils from semi-arid region. Journal of Soils and Sediments. 15, 282-291. https://doi.org/10.1007/s11368-014-1019-9.

Nyman, J.A., Delaune, R.D., Patrick, W.H., 1990. Wetland soil formation in the rapidly subsiding Mississippi River Deltaic Plain: Mineral and organic matter relationships. Estuarine, Coastal and Shelf Science. 31, 57-69. https://doi.org/10.1016/0272-7714(90)90028-P.

Odum, E.P., 1969. The strategy of ecosystem development. Science. 164, 262-270. https://doi.org/10.1126/science.164.3877.262.

Olofsson, P., Foody, G.M., Herold, M., Stehman, S.V., Woodcock, C.E., Wulder, M.A., 2014. Good practices for estimating area and assessing accuracy of land change. Remote Sensing of Environment. 148, 42-57. https://doi.org/10.1016/j.rse.2014.02.015.

Omar, H., Chuah, N.M.J., Parlan, I., Musa, S., 2016. Assessing rate of deforestation and changes of carbon stock on mangroves in Pahang, Malaysia. Malaysian Forester. 79, 174-179.

Ong, J.E., Gong, W.K., Wong, C.H., 2004. Allometry and partitioning of the mangrove, Rhizophora apiculata. Forest Ecology and Management. 188, 395-408. https://doi.org/10.1016/j.foreco.2003.08.002.

Otero, V., Van De Kerchove, R., Satyanarayana, B., Martínez-Espinosa, C., Fisol, M.A.B., Ibrahim, M.R.B., Sulong, I., Mohd-Lokman, H., Lucas, R., Dahdouh-Guebas, F., 2018. Managing mangrove forests from the sky: Forest inventory using field data and Unmanned Aerial Vehicle (UAV) imagery in the Matang Mangrove Forest Reserve, peninsular Malaysia. Forest Ecology and Management. 411, 35-45. https://doi.org/10.1016/j.foreco.2017.12.049.

Ouyang, X., Lee, S.Y., 2020. Improved estimates on global carbon stock and carbon pools in tidal wetlands. Nature Communications. 11, 317. https://doi.org/10.1038/s41467-019-14120-2.

Owers, C.J., Rogers, K., Woodroffe, C.D., 2018. Spatial variation of above-ground carbon storage in temperate coastal wetlands. Estuarine, Coastal and Shelf Science. 210, 55-67. https://doi.org/10.1016/j.ecss.2018.06.002.

Pal, M., Mather, P.M., 2005. Support vector machines for classification in remote sensing. International Journal of Remote Sensing. 26, 1007-1011. https://doi.org/10.1080/01431160512331314083.

Passos, T.R.G., Artur, A.G., Nóbrega, G.N., Otero, X.L., Ferreira, T.O., 2016. Comparison of the quantitative determination of soil organic carbon in coastal wetlands containing reduced forms of Fe and S. Geo-Marine Letters. 36, 223-233. https://doi.org/10.1007/s00367-016-0437-7.

Payo, A., Mukhopadhyay, A., Hazra, S., Ghosh, T., Ghosh, S., Brown, S., Nicholls, R.J., Bricheno, L., Wolf, J., Kay, S., Lázár, A.N., Haque, A., 2016. Projected changes in area of the Sundarban mangrove forest in Bangladesh due to SLR by 2100. Climatic Change. 139, 279-291. https://doi.org/10.1007/s10584-016-1769-z.

Pendleton, L., Donato, D.C., Murray, B.C., Crooks, S., Jenkins, W.A., Sifleet, S., Craft, C., Fourqurean, J.W., Kauffman, J.B., Marbà, N., Megonigal, P., Pidgeon, E., Herr, D., Gordon, D., Baldera, A., 2012. Estimating Global “Blue Carbon” Emissions from Conversion and

Degradation of Vegetated Coastal Ecosystems. PloS one. 7, e43542. https://doi.org/10.1371/journal.pone.0043542.

Peng, Y., Zheng, M., Zheng, Z., Wu, G., Chen, Y., Xu, H., Tian, G., Peng, S., Chen, G., Lee, S.Y., 2016. Virtual increase or latent loss? A reassessment of mangrove populations and their conservation in Guangdong, southern China. Marine Pollution Bulletin. 109, 691-699. https://doi.org/10.1016/j.marpolbul.2016.06.083.

Penman, J., Gytarsky, M., Hiraishi, T., Krug, T., Kruger, D., Pipatti, R., Buendia, L., Miwa, K., Ngara, T., Tanabe, K. (Eds.), 2003. Good practice guidance for land use, land-use change and forestry. The Intergovernmental Panel on Climate Change (IPCC), Japan, pp. 590.

Petrokofsky, G., Kanamaru, H., Achard, F., Goetz, S.J., Joosten, H., Holmgren, P., Lehtonen, A., Menton, M.C.S., Pullin, A.S., Wattenbach, M., 2012. Comparison of methods for measuring and assessing carbon stocks and carbon stock changes in terrestrial carbon pools. How do the accuracy and precision of current methods compare? A systematic review protocol. Environmental Evidence. 1, 6. https://doi.org/10.1186/2047-2382-1-6.

Pham, T.D., Xia, J., Baier, G., Le, N.N., Yokoya, N., 2019. Mangrove Species Mapping Using Sentinel-1 and Sentinel-2 Data in North Vietnam, IGARSS 2019 - 2019 IEEE International Geoscience and Remote Sensing Symposium, pp. 6102-6105.

Pham, T.D., Yoshino, K., 2017. Aboveground biomass estimation of mangrove species using ALOS-2 PALSAR imagery in Hai Phong City, Vietnam. Journal of Applied Remote Sensing. 11. https://doi.org/10.1117/1.jrs.11.026010.

Pham, T.D., Yoshino, K., Bui, D.T., 2017. Biomass estimation of *Sonneratia caseolaris* (l.) Engler at a coastal area of Hai Phong city (Vietnam) using ALOS-2 PALSAR imagery and GIS-based multi-layer perceptron neural networks. GIScience & Remote Sensing. 54, 329-353. https://doi.org/10.1080/15481603.2016.1269869.

Phillips, O.L., Sullivan, M.J.P., Baker, T.R., Monteagudo Mendoza, A., Vargas, P.N., Vásquez, R., 2019. Species Matter: Wood Density Influences Tropical Forest Biomass at Multiple Scales. Surveys in Geophysics. 40, 913-935. https://doi.org/10.1007/s10712-019-09540-0.

Picard, N., Saint-André, L., Henry, M., 2012. Manual for building tree volume and biomass allometric equations: from field measurement to prediction. Food and Agricultural Organization of the United Nations, Rome, and Centre de Coopération Internationale en Recherche Agronomique pour le éveloppement, Montpellier, pp. 215.

Pontius, R.G., Millones, M., 2011. Death to Kappa: birth of quantity disagreement and allocation disagreement for accuracy assessment. International Journal of Remote Sensing. 32, 4407-4429. https://doi.org/10.1080/01431161.2011.552923.

Potapov, P., Li, X., Hernandez-Serna, A., Tyukavina, A., Hansen, M.C., Kommareddy, A., Pickens, A., Turubanova, S., Tang, H., Silva, C.E., Armston, J., Dubayah, R., Blair, J.B., Hofton, M., 2021. Mapping global forest canopy height through integration of GEDI and Landsat data. Remote Sensing of Environment. 253, 112165. https://doi.org/10.1016/j.rse.2020.112165.

Potapov, P., Siddiqui, B.N., Iqbal, Z., Aziz, T., Zzaman, B., Islam, A., Pickens, A., Talero, Y., Tyukavina, A., Turubanova, S., Hansen, M.C., 2017. Comprehensive monitoring of Bangladesh tree cover inside and outside of forests, 2000–2014. Environmental Research Letters. 12, 104015. https://doi.org/10.1088/1748-9326/aa84bb.

Poungparn, S., Komiyama, A., Intana, V., Piriyaota, S., Sangtiean, T., Tanapermpool, P., Patanaponpaiboon, P., Kato, S., 2002. A quantitative analysis on the root system of a mangrove, Xylocarpus granatum Koenig. Tropics. 12, 35-42.

Prasad, M.B.K., Kumar, A., Ramanathan, A.L., Datta, D.K., 2017. Sources and dynamics of sedimentary organic matter in Sundarban mangrove estuary from Indo-Gangetic delta. Ecological Processes. 6, 8. https://doi.org/10.1186/s13717-017-0076-6.

Primavera, J.H., 2006. Overcoming the impacts of aquaculture on the coastal zone. Ocean & Coastal Management. 49, 531-545. https://doi.org/10.1016/j.ocecoaman.2006.06.018.

Proisy, C., Couteron, P., Fromard, F., 2007. Predicting and mapping mangrove biomass from canopy grain analysis using Fourier-based textural ordination of IKONOS images. Remote Sensing of Environment. 109, 379-392. https://doi.org/10.1016/j.rse.2007.01.009.

R Core Team, 2019. R: A language and environment for statistical computing. R Foundation for Statistical Computing, Vienna, Austria.

R Core Team, 2020. R: A language and environment for statistical computing. R Foundation for Statistical Computing, Vienna, Austria.

R Core Team, 2021. R: A language and environment for statistical computing. R Foundation for Statistical Computing, Vienna, Austria.

Rahman, M.M., Khan, M.N.I., Hoque, A.K.F., Ahmed, I., 2015a. Carbon stock in the Sundarbans mangrove forest: spatial variations in vegetation types and salinity zones. Wetlands Ecology and Management. 23, 269-283. https://doi.org/10.1007/s11273-014-9379-x.

Rahman, M.M., Lagomasino, D., Lee, S., Fatoyinbo, T., Ahmed, I., Kanzaki, M., 2019. Improved assessment of mangrove forests in Sundarbans East Wildlife Sanctuary using WorldView 2 and TanDEM-X high resolution imagery. Remote Sensing in Ecology and Conservation. 5, 136-149. https://doi.org/10.1002/rse2.105.

Rahman, M.M., Zimmer, M., Ahmed, I., Donato, D., Kanzaki, M., Xu, M., 2021a. Co-benefits of protecting mangroves for biodiversity conservation and carbon storage. Nature Communications. 12, 3875. https://doi.org/10.1038/s41467-021-24207-4.

Rahman, M.S., Donoghue, D.N.M., Bracken, L.J., 2021b. Is soil organic carbon underestimated in the largest mangrove forest ecosystems? Evidence from the Bangladesh Sundarbans. CATENA. 200, 105159. https://doi.org/10.1016/j.catena.2021.105159.

Rahman, M.S., Donoghue, D.N.M., Bracken, L.J., Mahmood, H., 2021c. Biomass estimation in mangrove forests: a comparison of allometric models incorporating species and structural information. Environmental Research Letters.

Rahman, M.S., Hossain, G.M., Khan, S.A., Uddin, S.N., 2015b. An annotated checklist of the vascular plants of Sundarban Mangrove Forest of Bangladesh. Bangladesh Journal of Plant Taxonomy. 22, 17-41. https://doi.org/10.3329/bjpt.v22i1.23862.

Rahman, M.S., Sass-Klaassen, U., Zuidema, P.A., Chowdhury, M.Q., Beeckman, H., 2020. Salinity drives growth dynamics of the mangrove tree Sonneratia apetala Buch. -Ham. in the Sundarbans, Bangladesh. Dendrochronologia. 62, 125711. https://doi.org/10.1016/j.dendro.2020.125711.

Ramsar Convention on Wetlands, 2018. Global Wetland Outlook: State of the World's Wetlands and their Services to People. , Ramsar Convention Secretariat., Gland, Switzerland(accessed.

Rao, R.G., Woitchik, A.F., Goeyens, L., van Riet, A., Kazungu, J., Dehairs, F., 1994. Carbon, nitrogen contents and stable carbon isotope abundance in mangrove leaves from an east African coastal lagoon (Kenya). Aquatic Botany. 47, 175-183. https://doi.org/10.1016/0304-3770(94)90012-4.

Rath, K.M., Rousk, J., 2015. Salt effects on the soil microbial decomposer community and their role in organic carbon cycling: A review. Soil Biology and Biochemistry. 81, 108-123. https://doi.org/10.1016/j.soilbio.2014.11.001.

Rau, B.M., Melvin, A.M., Johnson, D.W., Goodale, C.L., Blank, R.R., Fredriksen, G., Miller, W.W., Murphy, J.D., Todd, D.E.J., Walker, R.F., 2011. Revisiting Soil Carbon and Nitrogen Sampling: Quantitative Pits Versus Rotary Cores. Soil Science. 176, 273-279. https://doi.org/10.1097/SS.0b013e31821d6d4a.

Ray, R., Baum, A., Rixen, T., Gleixner, G., Jana, T.K., 2018. Exportation of dissolved (inorganic and organic) and particulate carbon from mangroves and its implication to the carbon budget in the Indian Sundarbans. Science of the Total Environment. 621, 535-547. https://doi.org/10.1016/j.scitotenv.2017.11.225.

Ray, R., Ganguly, D., Chowdhury, C., Dey, M., Das, S., Dutta, M.K., Mandal, S.K., Majumder, N., De, T.K., Mukhopadhyay, S.K., Jana, T.K., 2011. Carbon sequestration and annual increase of carbon stock in a mangrove forest. Atmospheric Environment. 45, 5016-5024. https://doi.org/10.1016/j.atmosenv.2011.04.074.

Reddy, C.S., Pasha, S.V., Jha, C.S., Diwakar, P.G., Dadhwal, V.K., 2016. Development of national database on long-term deforestation (1930-2014) in Bangladesh. Global and Planetary Change. 139, 173-182. https://doi.org/10.1016/j.gloplacha.2016.02.003.

Réjou-Méchain, M., Barbier, N., Couteron, P., Ploton, P., Vincent, G., Herold, M., Mermoz, S., Saatchi, S., Chave, J., de Boissieu, F., Féret, J.-B., Takoudjou, S.M., Pélissier, R., 2019. Upscaling Forest Biomass from Field to Satellite Measurements: Sources of Errors and Ways to Reduce Them. Surveys in Geophysics. 40, 881-911. https://doi.org/10.1007/s10712-019-09532-0.

Réjou-Méchain, M., Tanguy, A., Piponiot, C., Chave, J., Hérault, B., 2017. biomass: an r package for estimating above-ground biomass and its uncertainty in tropical forests. Methods in Ecology and Evolution. 8, 1163-1167. https://doi.org/10.1111/2041-210X.12753.

Ren, Malik, 2003. Learning a classification model for segmentation, Proceedings Ninth IEEE International Conference on Computer Vision, pp. 10-17 vol.1.

Ren, H., Jian, S., Lu, H., Zhang, Q., Shen, W., Han, W., Yin, Z., Guo, Q., 2008. Restoration of mangrove plantations and colonisation by native species in Leizhou bay, South China. Ecological Research. 23, 401-407. https://doi.org/10.1007/s11284-007-0393-9.

Richards, D.R., Friess, D.A., 2016. Rates and drivers of mangrove deforestation in Southeast Asia, 2000-2012. Proceedings of the National Academy of Sciences of the United States of America. 113, 344-349. https://doi.org/10.1073/pnas.1510272113.

Rikimaru, A., Roy, P.S., Miyatake, S., 2002. Tropical forest cover density mapping. Tropical Ecology. 43, 39-47.

Rogers, K., Kelleway, J.J., Saintilan, N., Megonigal, J.P., Adams, J.B., Holmquist, J.R., Lu, M., Schile-Beers, L., Zawadzki, A., Mazumder, D., Woodroffe, C.D., 2019. Wetland carbon storage controlled by millennial-scale variation in relative sea-level rise. Nature. 567, 91-95. https://doi.org/10.1038/s41586-019-0951-7.

Rogers, K.G., Goodbred, S.L., Mondal, D.R., 2013. Monsoon sedimentation on the 'abandoned' tide-influenced Ganges–Brahmaputra delta plain. Estuarine, Coastal and Shelf Science. 131, 297-309. https://doi.org/10.1016/j.ecss.2013.07.014.

Rouse, J., Haas, J., Schell, J., Deering, D., 1974. Monitoring vegetation systemsin the Great Plains witherts, Proceedings of the 3rd ERTS Symposium, Washington, DC, USA.

Rovai, A.S., Riul, P., Twilley, R.R., Castañeda-Moya, E., Rivera-Monroy, V.H., Williams, A.A., Simard, M., Cifuentes-Jara, M., Lewis, R.R., Crooks, S., Horta, P.A., Schaeffer-Novelli, Y., Cintrón, G., Pozo-Cajas, M., Pagliosa, P.R., Currie, D., 2016. Scaling mangrove aboveground biomass from site-level to continental-scale. Global Ecology and Biogeography. 25, 286-298. https://doi.org/doi:10.1111/geb.12409.

Rovai, A.S., Twilley, R.R., Castañeda-Moya, E., Riul, P., Cifuentes-Jara, M., Manrow-Villalobos, M., Horta, P.A., Simonassi, J.C., Fonseca, A.L., Pagliosa, P.R., 2018. Global controls on carbon storage in mangrove soils. Nature Climate Change. 8, 534-538. https://doi.org/10.1038/s41558-018-0162-5.

Rudra, K., 2014. Changing river courses in the western part of the Ganga–Brahmaputra delta. Geomorphology. 227, 87-100. https://doi.org/10.1016/j.geomorph.2014.05.013.

Rutishauser, E., Noor'an, F., Laumonier, Y., Halperin, J., Rufi'ie, Hergoualc'h, K., Verchot, L., 2013. Generic allometric models including height best estimate forest biomass and carbon stocks in Indonesia. Forest Ecology and Management. 307, 219-225. https://doi.org/10.1016/j.foreco.2013.07.013.

Saatchi, S.S., Harris, N.L., Brown, S., Lefsky, M., Mitchard, E.T.A., Salas, W., Zutta, B.R., Buermann, W., Lewis, S.L., Hagen, S., Petrova, S., White, L., Silman, M., Morel, A., 2011. Benchmark map of forest carbon stocks in tropical regions across three continents. Proceedings of the National Academy of Sciences. 108, 9899-9904. https://doi.org/10.1073/pnas.1019576108.

Saenger, P., 2002. Introduction: The Mangrove Environment, Mangrove Ecology, Silviculture and Conservation. Springer, Dordrecht, pp. 1-10.

Saenger, P., Snedaker, S., 1993. Pan-tropical trends in mangrove above-ground biomass and annual litter fall. Oecologia. 96, 293-299. https://doi.org/10.1007/BF00317496.

Sahu, B., Ghosh, A.K., Seema, 2021. Deterministic and geostatistical models for predicting soil organic carbon in a 60 ha farm on Inceptisol in Varanasi, India. Geoderma Regional. 26, e00413. https://doi.org/10.1016/j.geodrs.2021.e00413.

Sanderman, J., Hengl, T., Fiske, G., Solvik, K., Adame, M.F., Benson, L., Bukoski, J.J., Carnell, P., Cifuentes-Jara, M., Donato, D., Duncan, C., Eid, E.M., Ermgassen, P.z., Lewis, C.J.E., Macreadie, P.I., Glass, L., Gress, S., Jardine, S.L., Jones, T.G., Nsombo, E.N., Rahman, M.M., Sanders, C.J., Spalding, M., Landis, E., 2018. A global map of mangrove forest soil carbon at 30 m spatial resolution. Environmental Research Letters. 13. https://doi.org/10.1088/1748-9326/aabe1c.

Sarker, S.K., Deb, J.C., Halim, M.A., 2011. A diagnosis of existing logging bans in Bangladesh. International Forestry Review. 13, 461-475. https://doi.org/10.1505/146554811798811344.

Sarker, S.K., Matthiopoulos, J., Mitchell, S.N., Ahmed, Z.U., Mamun, M.B.A., Reeve, R., 2019a. 1980s–2010s: The world's largest mangrove ecosystem is becoming homogeneous. Biological Conservation. 236, 79-91. https://doi.org/10.1016/j.biocon.2019.05.011.

Sarker, S.K., Reeve, R., Paul, N.K., Matthiopoulos, J., 2019b. Modelling spatial biodiversity in the world's largest mangrove ecosystem—The Bangladesh Sundarbans: A baseline for conservation. Diversity and Distributions. 25, 729-742. https://doi.org/10.1111/ddi.12887.

Sarker, S.K., Reeve, R., Thompson, J., Paul, N.K., Matthiopoulos, J., 2016. Are we failing to protect threatened mangroves in the Sundarbans world heritage ecosystem? Scientific Reports. 6. https://doi.org/10.1038/srep21234.

Sattar, M.A., Bhattacharjee, D.K., Sarker, S.B., 1995. Physical, mechanical and seasoning properties of 45 lesser used or unused forest timbers of Bangladesh and their uses. Bangladesh Journal of Forest Science. 24, 11-21.

Setia, R., Gottschalk, P., Smith, P., Marschner, P., Baldock, J., Setia, D., Smith, J., 2013. Soil salinity decreases global soil organic carbon stocks. Science of the Total Environment. 465, 267-272. https://doi.org/10.1016/j.scitotenv.2012.08.028.

Shimada, M., Itoh, T., Motooka, T., Watanabe, M., Shiraishi, T., Thapa, R., Lucas, R., 2014. New global forest/non-forest maps from ALOS PALSAR data (2007–2010). Remote Sensing of Environment. 155, 13-31. https://doi.org/10.1016/j.rse.2014.04.014.

Siddiqi, N.A., 2001. Mangrove forestry in Bangladesh. Institute of Forestry & Environmental Sciences, University of Chittagong, Chittagong, pp. 301.

Siddique, M.R.H., Mahmood, H., Chowdhury, M.R.K., 2012. Allometric relationship for estimating above-ground biomass of *Aegialitis rotundifolia* Roxb. of Sundarbans mangrove forest, in Bangladesh. Journal of Forestry Research. 23, 23-28. https://doi.org/10.1007/s11676-012-0229-5.

Siddique, M.R.H., Saha, S., Salekin, S., Mahmood, H., 2017. Salinity strongly drives the survival, growth, leaf demography, and nutrient partitioning in seedlings of xylocarpus granatum J. König. IForest. 10, 851-856. https://doi.org/10.3832/ifor2382-010.

Sileshi, G.W., 2014. A critical review of forest biomass estimation models, common mistakes and corrective measures. Forest Ecology and Management. 329, 237-254. https://doi.org/10.1016/j.foreco.2014.06.026.

Simard, M., Fatoyinbo, L., Smetanka, C., Rivera-Monroy, V.H., Castañeda-Moya, E., Thomas, N., Van der Stocken, T., 2019. Mangrove canopy height globally related to precipitation, temperature and cyclone frequency. Nature Geoscience. 12, 40-45. https://doi.org/10.1038/s41561-018-0279-1.

Simard, M., Fatoyinbo, L.E., Pinto, N., 2010. Mangrove canopy 3D structure and ecosystem productivity using active remote sensing. in: Wang, Y. (Ed.), Remote Sensing of Coastal Environment. CRC Press, pp. 61-78.

Simard, M., Rivera-Monroy, V.H., Mancera-Pineda, J.E., Castañeda-Moya, E., Twilley, R.R., 2008. A systematic method for 3D mapping of mangrove forests based on Shuttle Radar Topography Mission elevation data, ICEsat/GLAS waveforms and field data: Application to Ciénaga Grande de Santa Marta, Colombia. Remote Sensing of Environment. 112, 2131-2144. https://doi.org/10.1016/j.rse.2007.10.012.

Simard, M., Zhang, K., Rivera-Monroy, V.H., Ross, M.S., Ruiz, P.L., Castañeda-Moya, E., Twilley, R.R., Rodriguez, E., 2006. Mapping height and biomass of mangrove forests in Everglades National Park with SRTM elevation data. Photogrammetric Engineering & Remote Sensing. 72, 299-311. https://doi.org/10.14358/PERS.72.3.299.

Slik, J.W.F., Arroyo-Rodríguez, V., Aiba, S.-I., Alvarez-Loayza, P., Alves, L.F., Ashton, P., Balvanera, P., Bastian, M.L., Bellingham, P.J., van den Berg, E., Bernacci, L., da Conceição Bispo, P., Blanc, L., Böhning-Gaese, K., Boeckx, P., Bongers, F., Boyle, B., Bradford, M., Brearley, F.Q., Breuer-Ndoundou Hockemba, M., Bunyavejchewin, S., Calderado Leal Matos, D., Castillo-Santiago, M., Catharino, E.L.M., Chai, S.-L., Chen, Y., Colwell, R.K., Chazdon, R.L., Clark, C., Clark, D.B., Clark, D.A., Culmsee, H., Damas, K., Dattaraja, H.S., Dauby, G., Davidar, P., DeWalt, S.J., Doucet, J.-L., Duque, A., Durigan, G., Eichhorn, K.A.O., Eisenlohr, P.V., Eler, E., Ewango, C., Farwig, N., Feeley, K.J., Ferreira, L., Field, R., de Oliveira Filho, A.T., Fletcher, C., Forshed, O., Franco, G., Fredriksson, G., Gillespie, T., Gillet, J.-F., Amarnath, G., Griffith, D.M., Grogan, J., Gunatilleke, N., Harris, D., Harrison, R., Hector, A., Homeier, J., Imai, N., Itoh, A., Jansen, P.A., Joly, C.A., de Jong, B.H.J., Kartawinata, K., Kearsley, E., Kelly, D.L., Kenfack, D., Kessler, M., Kitayama, K.,

Kooyman, R., Larney, E., Laumonier, Y., Laurance, S., Laurance, W.F., Lawes, M.J., Amaral, I.L.d., Letcher, S.G., Lindsell, J., Lu, X., Mansor, A., Marjokorpi, A., Martin, E.H., Meilby, H., Melo, F.P.L., Metcalfe, D.J., Medjibe, V.P., Metzger, J.P., Millet, J., Mohandass, D., Montero, J.C., de Morisson Valeriano, M., Mugerwa, B., Nagamasu, H., Nilus, R., Ochoa-Gaona, S., Onrizal, Page, N., Parolin, P., Parren, M., Parthasarathy, N., Paudel, E., Permana, A., Piedade, M.T.F., Pitman, N.C.A., Poorter, L., Poulsen, A.D., Poulsen, J., Powers, J., Prasad, R.C., Puyravaud, J.-P., Razafimahaimodison, J.-C., Reitsma, J., dos Santos, J.R., Roberto Spironello, W., Romero-Saltos, H., Rovero, F., Rozak, A.H., Ruokolainen, K., Rutishauser, E., Saiter, F., Saner, P., Santos, B.A., Santos, F., Sarker, S.K., Satdichanh, M., Schmitt, C.B., Schöngart, J., Schulze, M., Suganuma, M.S., Sheil, D., da Silva Pinheiro, E., Sist, P., Stevart, T., Sukumar, R., Sun, I.-F., Sunderland, T., Suresh, H.S., Suzuki, E., Tabarelli, M., Tang, J., Targhetta, N., Theilade, I., Thomas, D.W., Tchouto, P., Hurtado, J., Valencia, R., van Valkenburg, J.L.C.H., Van Do, T., Vasquez, R., Verbeeck, H., Adekunle, V., Vieira, S.A., Webb, C.O., Whitfeld, T., Wich, S.A., Williams, J., Wittmann, F., Wöll, H., Yang, X., Adou Yao, C.Y., Yap, S.L., Yoneda, T., Zahawi, R.A., Zakaria, R., Zang, R., de Assis, R.L., Garcia Luize, B., Venticinque, E.M., 2015. An estimate of the number of tropical tree species. Proceedings of the National Academy of Sciences. 112, 7472-7477. https://doi.org/10.1073/pnas.1423147112.

Slik, J.W.F., Bernard, C.S., Breman, F.C., Van Beek, M., Salim, A., Sheil, D., 2008. Wood Density as a Conservation Tool: Quantification of Disturbance and Identification of Conservation-Priority Areas in Tropical Forests. Conservation Biology. 22, 1299-1308. https://doi.org/10.1111/j.1523-1739.2008.00986.x.

Soares, M.L.G., Schaeffer-Novelli, Y., 2005. Above-ground biomass of mangrove species. I. Analysis of models. Estuarine, Coastal and Shelf Science. 65, 1-18. https://doi.org/10.1016/j.ecss.2005.05.001.

Solano, F., Di Fazio, S., Modica, G., 2019. A methodology based on GEOBIA and WorldView-3 imagery to derive vegetation indices at tree crown detail in olive orchards. International Journal of Applied Earth Observation and Geoinformation. 83, 101912. https://doi.org/10.1016/j.jag.2019.101912.

Spalding, M., Blasco, F., Field, C. (Eds.), 1997. World mangrove atlas. The International Society for Mangrove Ecosystems, Okinawa, pp. 178.

Spalding, M.D., Kainuma, M., Collins, L. (Eds.), 2010. World atlas of mangroves. Earthscan, London, pp. 336.

Spivak, A.C., Sanderman, J., Bowen, J.L., Canuel, E.A., Hopkinson, C.S., 2019. Global-change controls on soil-carbon accumulation and loss in coastal vegetated ecosystems. Nature Geoscience. 12, 685-692. https://doi.org/10.1038/s41561-019-0435-2.

Sprugel, D.G., 1983. Correcting for bias in log-transformed allometric equations. Ecology. 64, 209-210. https://doi.org/10.2307/1937343.

Stas, S.M., Rutishauser, E., Chave, J., Anten, N.P.R., Laumonier, Y., 2017. Estimating the aboveground biomass in an old secondary forest on limestone in the Moluccas, Indonesia: Comparing locally developed versus existing allometric models. Forest Ecology and Management. 389, 27-34. https://doi.org/10.1016/j.foreco.2016.12.010.

Stibig, H.J., Beuchle, R., Achard, F., 2003. Mapping of the tropical forest cover of insular Southeast Asia from SPOT4-Vegetation images. International Journal of Remote Sensing. 24, 3651-3662. https://doi.org/10.1080/0143116021000024113.

Stromann, O., Nascetti, A., Yousif, O., Ban, Y., 2020. Dimensionality Reduction and Feature Selection for Object-Based Land Cover Classification based on Sentinel-1 and Sentinel-2 Time Series Using Google Earth Engine. Remote Sensing. 12, 76.

Su, J., Friess, D.A., Gasparatos, A., 2021. A meta-analysis of the ecological and economic outcomes of mangrove restoration. Nature Communications. 12, 5050. https://doi.org/10.1038/s41467-021-25349-1.

Suhaili, A., Lawen, J., 2017. Estimation of plant biomass and carbon stock for a juvenile reforested mangrove stand using high resolution imaging spectrometer. Workshop on Hyperspectral Image and Signal Processing, Evolution in Remote Sensing. 2013-June. https://doi.org/10.1109/WHISPERS.2013.8080666.

Syvitski, J.P.M., Milliman, J.D., 2007. Geology, Geography, and Humans Battle for Dominance over the Delivery of Fluvial Sediment to the Coastal Ocean. The Journal of Geology. 115, 1-19. https://doi.org/10.1086/509246.

Taillardat, P., Friess, D.A., Lupascu, M., 2018. Mangrove blue carbon strategies for climate change mitigation are most effective at the national scale. Biology Letters. 14, 20180251. https://doi.org/doi:10.1098/rsbl.2018.0251.

Tamai, S., Nakasuga, T., Tabuchi, R., Ogino, K., 1986. Standing biomass of mangrove forests in southern Thailand. Journal of the Japanese Forestry Society. 68, 384-388.

Tang, W., Zheng, M., Zhao, X., Shi, J., Yang, J., Trettin, C., 2018. Big Geospatial Data Analytics for Global Mangrove Biomass and Carbon Estimation. Sustainability. 10, 472. https://doi.org/10.3390/su10020472.

Tassi, A., Vizzari, M., 2020. Object-Oriented LULC Classification in Google Earth Engine Combining SNIC, GLCM, and Machine Learning Algorithms. Remote Sensing. 12, 3776.

Thomas, N., Lucas, R., Bunting, P., Hardy, A., Rosenqvist, A., Simard, M., 2017. Distribution and drivers of global mangrove forest change, 1996-2010. PloS one. 12. https://doi.org/10.1371/journal.pone.0179302.

Tomlinson, P.B., 2016. The Botany of Mangroves, 2nd ed. Cambridge University Press, Cambridge.

Twilley, R.R., Castañeda-Moya, E., Rivera-Monroy, V.H., Rovai, A., 2017. Productivity and Carbon Dynamics in Mangrove Wetlands. in: Rivera-Monroy, V.H., Lee, S.Y., Kristensen, E., Twilley, R.R. (Eds.), Mangrove Ecosystems: A Global Biogeographic Perspective: Structure, Function, and Services. Springer International Publishing, Cham, pp. 113-162. https://doi.org/10.1007/978-3-319-62206-4_5.

Twilley, R.R., Chen, R.H., Hargis, T., 1992. Carbon sinks in mangroves and their implications to carbon budget of tropical coastal ecosystems. Water, Air, and Soil Pollution. 64, 265-288. https://doi.org/10.1007/bf00477106.

Twilley, R.R., Rovai, A.S., Riul, P., 2018. Coastal morphology explains global blue carbon distributions. Frontiers in Ecology and the Environment. 16, 503-508. https://doi.org/10.1002/fee.1937.

Tyagi, N.K., Sen, H.S., 2019. Development of Sundarbans through Estuary Management for Augmenting Freshwater Supply, Improved Drainage and Reduced Bank Erosion. in: Sen, H.S. (Ed.), The Sundarbans: A Disaster-Prone Eco-Region: Increasing Livelihood Security. Springer International Publishing, Cham, pp. 375-402. https://doi.org/10.1007/978-3-030-00680-8_13.

Tyukavina, A., Baccini, A., Hansen, M.C., Potapov, P.V., Stehman, S.V., Houghton, R.A., Krylov, A.M., Turubanova, S., Goetz, S.J., 2015. Aboveground carbon loss in natural and managed tropical forests from 2000 to 2012. Environmental Research Letters. 10, 074002. https://doi.org/10.1088/1748-9326/10/7/074002.

UNEP, 2014. The importance of mangroves to people: A call to action. United Nations Environment Programme, World Conservation Monitoring Centre, Cambridge, pp. 128.

van Breugel, M., Ransijn, J., Craven, D., Bongers, F., Hall, J.S., 2011. Estimating carbon stock in secondary forests: Decisions and uncertainties associated with allometric biomass models. Forest Ecology and Management. 262, 1648-1657. https://doi.org/10.1016/j.foreco.2011.07.018.

VCS, 2020. Verified Carbon Standard Methodology VD0007. REDD+ Methodology Framework (REDD+ MF) Version 1.6. https://verra.org/wp-content/uploads/2020/09/VM0007-REDDMF_v1.6.pdf (accessed 17/02/2022).

Vieilledent, G., Vaudry, R., Andriamanohisoa, S.F.D., Rakotonarivo, O.S., Randrianasolo, H.Z., Razafindrabe, H.N., Rakotoarivony, C.B., Ebeling, J., Rasamoelina, M., 2012. A universal approach to estimate biomass and carbon stock in tropical forests using generic allometric models. Ecological Applications. 22, 572-583. https://doi.org/10.1890/11-0039.1.

Virgulino-Júnior, P.C.C., Carneiro, D.N., Nascimento, W.R., Jr., Cougo, M.F., Fernandes, M.E.B., 2020. Biomass and carbon estimation for scrub mangrove forests and examination of their allometric associated uncertainties. PloS one. 15, e0230008. https://doi.org/10.1371/journal.pone.0230008.

Vorster, A.G., Evangelista, P.H., Stovall, A.E.L., Ex, S., 2020. Variability and uncertainty in forest biomass estimates from the tree to landscape scale: the role of allometric equations. Carbon Balance and Management. 15, 8. https://doi.org/10.1186/s13021-020-00143-6.

Wahid, S.M., Babel, M.S., Bhuiyan, A.R., 2007. Hydrologic monitoring and analysis in the Sundarbans mangrove ecosystem, Bangladesh. Journal of Hydrology. 332, 381-395. https://doi.org/10.1016/j.jhydrol.2006.07.016.

Wang, G., Guan, D., Peart, M.R., Chen, Y., Peng, Y., 2013. Ecosystem carbon stocks of mangrove forest in Yingluo Bay, Guangdong Province of South China. Forest Ecology and Management. 310, 539-546. https://doi.org/10.1016/j.foreco.2013.08.045.

Ward, R.D., Friess, D.A., Day, R.H., MacKenzie, R.A., 2016. Impacts of climate change on mangrove ecosystems: a region by region overview. Ecosystem Health and Sustainability 2, 1-25. https://doi.org/10.1002/ehs2.1211.

Warrens, M.J., 2015. Properties of the quantity disagreement and the allocation disagreement. International Journal of Remote Sensing. 36, 1439-1446. https://doi.org/10.1080/01431161.2015.1011794.

Weiskittel, A.R., MacFarlane, D.W., Radtke, P.J., Affleck, D.L.R., Temesgen, H., Woodall, C.W., Westfall, J.A., Coulston, J.W., 2015. A Call to Improve Methods for Estimating Tree

Biomass for Regional and National Assessments. Journal of Forestry. 113, 414-424. https://doi.org/10.5849/jof.14-091.

Weiss, C., Weiss, J., Boy, J., Iskandar, I., Mikutta, R., Guggenberger, G., 2016. Soil organic carbon stocks in estuarine and marine mangrove ecosystems are driven by nutrient colimitation of P and N. Ecol Evol. 6, 5043-56. https://doi.org/10.1002/ece3.2258.

Wicaksono, P., 2017. Mangrove above-ground carbon stock mapping of multi-resolution passive remote-sensing systems. International Journal of Remote Sensing. 38, 1551-1578. https://doi.org/10.1080/01431161.2017.1283072.

Wicaksono, P., Danoedoro, P., Hartono, Nehren, U., 2016. Mangrove biomass carbon stock mapping of the Karimunjawa Islands using multispectral remote sensing. International Journal of Remote Sensing. 37, 26-52. https://doi.org/10.1080/01431161.2015.1117679.

Wickham, H., 2016. ggplot2: Elegant Graphics for Data Analysis. Springer-Verlag, New York.

Wiemann, M.C., Williamson, G.B., 2013. Biomass determination using wood specific gravity from increment cores. USDA Forest Service, Forest Products Laboratory, General Technical Report, FPL-GTR-225, 2013: 9 p. 225, 1-9.

Więski, K., Guo, H., Craft, C.B., Pennings, S.C., 2010. Ecosystem Functions of Tidal Fresh, Brackish, and Salt Marshes on the Georgia Coast. Estuaries and Coasts. 33, 161-169. https://doi.org/10.1007/s12237-009-9230-4.

Wilke, C.O., Wickham, H., Wilke, M.C.O., 2019. Package 'cowplot'. Streamlined Plot Theme and Plot Annotations for 'ggplot2.

Wong, V.N.L., Dalal, R.C., Greene, R.S.B., 2009. Carbon dynamics of sodic and saline soils following gypsum and organic material additions: A laboratory incubation. Applied Soil Ecology. 41, 29-40. https://doi.org/10.1016/j.apsoil.2008.08.006.

Wong, V.N.L., Greene, R.S.B., Dalal, R.C., Murphy, B.W., 2010. Soil carbon dynamics in saline and sodic soils: a review. Soil Use and Management. 26, 2-11. https://doi.org/10.1111/j.1475-2743.2009.00251.x.

Woodroffe, C.D., Rogers, K., McKee, K.L., Lovelock, C.E., Mendelssohn, I.A., Saintilan, N., 2016. Mangrove Sedimentation and Response to Relative Sea-Level Rise. Annual Review of Marine Science. 8, 243-266. https://doi.org/10.1146/annurev-marine-122414-034025.

Worthington, T.A., Andradi-Brown, D.A., Bhargava, R., Buelow, C., Bunting, P., Duncan, C., Fatoyinbo, L., Friess, D.A., Goldberg, L., Hilarides, L., Lagomasino, D., Landis, E., Longley-Wood, K., Lovelock, C.E., Murray, N.J., Narayan, S., Rosenqvist, A., Sievers, M., Simard,

M., Thomas, N., van Eijk, P., Zganjar, C., Spalding, M., 2020. Harnessing Big Data to Support the Conservation and Rehabilitation of Mangrove Forests Globally. One Earth. 2, 429-443. https://doi.org/10.1016/j.oneear.2020.04.018.

Wuest, S.B., 2009. Correction of Bulk Density and Sampling Method Biases Using Soil Mass per Unit Area. Soil Science Society of America Journal. 73, 312-316. https://doi.org/10.2136/sssaj2008.0063.

Xia, Q., Jia, M., He, T., Xing, X., Zhu, L., 2021. Effect of tide level on submerged mangrove recognition index using multi-temporal remotely-sensed data. Ecological Indicators. 131, 108169. https://doi.org/10.1016/j.ecolind.2021.108169.

Xiao, X., White, E.P., Hooten, M.B., Durham, S.L., 2011. On the use of log-transformation vs. nonlinear regression for analyzing biological power laws. Ecology. 92, 1887-1894. https://doi.org/10.1890/11-0538.1.

Xu, H., 2006. Modification of normalised difference water index (NDWI) to enhance open water features in remotely sensed imagery. International Journal of Remote Sensing. 27, 3025-3033. https://doi.org/10.1080/01431160600589179.

Yando, E.S., Osland, M.J., Willis, J.M., Day, R.H., Krauss, K.W., Hester, M.W., 2016. Salt marsh-mangrove ecotones: using structural gradients to investigate the effects of woody plant encroachment on plant–soil interactions and ecosystem carbon pools. Journal of Ecology. 104, 1020-1031. https://doi.org/10.1111/1365-2745.12571.

Yang, J., Gao, J., Liu, B., Zhang, W., 2014. Sediment deposits and organic carbon sequestration along mangrove coasts of the Leizhou Peninsula, southern China. Estuarine, Coastal and Shelf Science. 136, 3-10. https://doi.org/10.1016/j.ecss.2013.11.020.

Yuen, J.Q., Fung, T., Ziegler, A.D., 2016. Review of allometric equations for major land covers in SE Asia: Uncertainty and implications for above- and below-ground carbon estimates. Forest Ecology and Management. 360, 323-340. https://doi.org/10.1016/j.foreco.2015.09.016.

Zanne, A.E., Lopez-Gonzalez, G., Coomes, D.A., Ilic, J., Jansen, S., Lewis, S.L., Miller, R.B., Swenson, N.G., Wiemann, M.C., Chave, J., 2009. Data from: Towards a worldwide wood economics spectrum, Dryad, Dataset, https://doi.org/10.5061/dryad.234. (accessed 20/03/2020).

Zeileis, A., Hothorn, T., 2002. Diagnostic checking in regression relationships. R News 2: 7–10. https://CRAN.R-project.org/doc/Rnews/. (accessed 22/03/2021).

Zhao, Q., Bai, J., Lu, Q., Zhang, G., 2017. Effects of salinity on dynamics of soil carbon in degraded coastal wetlands: Implications on wetland restoration. Physics and Chemistry of the Earth, Parts A/B/C. 97, 12-18. https://doi.org/10.1016/j.pce.2016.08.008.

Zhou, G., Xu, S., Ciais, P., Manzoni, S., Fang, J., Yu, G., Tang, X., Zhou, P., Wang, W., Yan, J., Wang, G., Ma, K., Li, S., Du, S., Han, S., Ma, Y., Zhang, D., Liu, J., Liu, S., Chu, G., Zhang, Q., Li, Y., Huang, W., Ren, H., Lu, X., Chen, X., 2019. Climate and litter C/N ratio constrain soil organic carbon accumulation. National Science Review. 6, 746-757. https://doi.org/10.1093/nsr/nwz045.

Appendix A

Is soil organic carbon underestimated in the largest mangrove forest ecosystems? Evidence from the Bangladesh Sundarbans

Catena 200 (2021) 105159

Contents lists available at ScienceDirect

Catena

journal homepage: www.elsevier.com/locate/catena

Is soil organic carbon underestimated in the largest mangrove forest ecosystems? Evidence from the Bangladesh Sundarbans

Md. Saidur Rahman [a,b,*], Daniel N.M. Donoghue [a], Louise J. Bracken [a]

[a] Department of Geography, Durham University, South Road, Durham DH1 3LE, United Kingdom
[b] Forestry and Wood Technology Discipline, Khulna University, Khulna 9208, Bangladesh

ARTICLE INFO

Keywords:
Soil organic carbon
Salinity zones
Soil depth
Mangrove forest
The Sundarbans

ABSTRACT

Globally, mangroves sequester a large amount of carbon into the sediments, although spatial heterogeneity exists owing to a wide variety of local, regional, and global controls. Rapid environmental and climate change, including increasing sea-level rise, global warming, reduced upstream discharge and anthropogenic activities, are predicted to increase salinity in the mangroves, especially in the Bangladesh Sundarbans, thereby disrupting this blue carbon reservoir. Nevertheless, it remains unclear how salinity affects the belowground soil carbon despite the recognised effect on above ground productivity. To address this gap, research was undertaken in the Bangladesh Sundarbans to compare total soil organic carbon (SOC) across three salinity zones and to explore any potential predictive relationships with other physical, chemical properties and vegetation characteristics. Total SOC was significantly higher in the oligohaline zone (74.8 ± 14.9 Mg ha^{-1}), followed by the mesohaline (59.3 ± 15.8 Mg ha^{-1}), and polyhaline zone (48.3 ± 10.3 Mg ha^{-1}) (ANOVA, $F_{2,\ 500} = 118.9$, $p < 0.001$). At all sites, the topmost 10 cm of soil contained higher SOC density than the bottom depths (ANOVA, $F_{3,\ 500} = 30.1$, $p < 0.001$). On average, *Bruguiera* sp. stand holds the maximum SOC measured, followed by two pioneer species *Sonneratia apetala* and *Avicennia* sp. Multiple regression results indicated that soil salinity, organic C:N and tree diameter were the best predictor for the variability of the SOC in the Sundarbans ($R^2 = 0.62$). Despite lower carbon in the soil, the study highlights that the conservation priorities and low deforestation rate have led to less CO_2 emissions than most sediment carbon-rich mangroves in the world. The study also emphasised the importance of spatial conservation planning to safeguard the soil carbon-rich zones in the Bangladesh Sundarbans from anthropogenic tourism and development activities to support climate change adaptation and mitigation strategies.

1. Introduction

Mangroves are recognised as one of the most carbon-dense forest types in the world due to their efficient carbon sequestration capacity into both above and below ground carbon pools (Donato et al., 2011; Alongi, 2012; Sanderman et al., 2018). Recent assessments of soil carbon suggest that mangrove ecosystems contain, on an average, between 856 and 1023 Mg of carbon per hectare, with the majority (~85%) of this carbon stored in the soil (Donato et al., 2011; Pendleton et al., 2012; Sanderman et al., 2018; Kauffman et al., 2020). This large amount of soil carbon is of global importance due to its potential to store sequestered CO_2 emissions for the long term and help mitigate adverse effects of climate change (McLeod et al., 2011; Duarte et al., 2013; Abdullah et al., 2016). To recognise the importance of mangrove forests for carbon sequestration, United Nations Environmental Programme (UNEP) designated this ecosystem as "Blue Carbon" along with other coastal vegetated ecosystems such as seagrass meadows and saltmarshes (Nellemann et al., 2009; Lovelock and Duarte, 2019; Macreadie et al., 2019). This growing worldwide importance of mangroves has led to a substantial reduction of mangrove loss leading to reductions in CO_2 emissions in the last three decades (Friess et al., 2019). At the same time, mangroves have gained substantial traction in being managed, protected and restored as part of national and global climate change mitigation policies and actions including Nationally Determined Contributions (NDC) towards the Paris Agreement and climate action goal (goal 13) under United Nations Sustainable Development Goals (SDG) (Taillardat et al., 2018; Friess et al., 2020). However, variability and uncertainty in SOC estimation is a key barrier to the inclusion of mangroves (and other

* Corresponding author at: Department of Geography, Durham University, South Road, Durham DH1 3LE, United Kingdom.
E-mail address: msrahman@fwt.ku.ac.bd (Md.S. Rahman).

https://doi.org/10.1016/j.catena.2021.105159
Received 1 July 2020; Received in revised form 3 November 2020; Accepted 7 January 2021
Available online 21 January 2021
0341-8162/

blue carbon) in national and international policy tools and frameworks.

Despite covering only 0.1% of the world's total landmass, mangroves sequester more carbon per unit area than any other natural ecosystems (Atwood et al., 2017; Lovelock and Duarte, 2019). With autochthonous inputs from the productive above-ground, mangrove soils store large quantities of carbon as a result of the low decomposition rate resulting from anoxic conditions (Donato et al., 2011; Alongi, 2012). Mangroves are also highly efficient traps for allochthonous inputs through their dense network of above ground roots. The rising elevation of mangroves in response to sea-level rise allows large accommodation spaces to sequester more carbon in the soil, which barely reaches saturation (Krauss et al., 2014; Rogers et al., 2019). Therefore, mangroves act as an efficient carbon store despite continuous threats from deforestation, land-use change, sea-level rise, and climate change.

Blue carbon research across the globe has highlighted considerable spatial heterogeneity in soil organic carbon (SOC) at multiple scales (Atwood et al., 2017; Sanderman et al., 2018). At a regional and global scale, SOC variability has been linked to net primary productivity (Alongi, 2012; Twilley et al., 2017), latitude/climate (Rovai et al., 2018; Twilley et al., 2018; Kauffman et al., 2020), coastal geomorphology (Rovai et al., 2018; Twilley et al., 2018) and Holocene sea-level trends (Rogers et al., 2019). These physical and biological factors and geomorphic evolutionary processes promote and develop unique coastal environmental settings, which ultimately drive macroscale variation in SOC (Rovai et al., 2018). The site-specific variability in SOC is largely attributed to differences in species composition (Ren et al., 2008), stand age (Lovelock et al., 2010; Donato et al., 2011), sources of allochthonous particles (Bouillon and Boschker, 2006; Yang et al., 2014), soil physical and chemical properties (Freeman et al., 2004; Kristensen et al., 2008; Banerjee et al., 2018), elevation and tidal regimes (Liu and Lee, 2006; Spivak et al., 2019), plant-litter biochemistry (Kristensen et al., 2008; Brodersen et al., 2019) and plant–microbe interactions (Fontaine et al., 2007; Alongi, 2014). Several soils and environmental characteristics such as pH, salinity, organic matter, precipitation and tidal inundation influence the mangrove productivity and can also directly or indirectly influence SOC (Yando et al., 2016). Therefore, careful consideration of relevant factors is vital for reliable estimation of SOC at a particular spatial scale.

The Sundarbans is the largest contiguous mangrove forest in the world and is situated in the lower delta plain of the Ganges-Brahmaputra-Meghna (GBM) delta, and stretches across political boundaries between Bangladesh and India (Giri et al., 2011; Sarker

Table 1
Comparison of Soil Organic Carbon (SOC) density and stock among studies in the Sundarbans and globally.

Study area		Study	Sample size	Depth (cm)	Methods	Mean Soil organic carbon percentage (%) (range)	Mean Soil organic carbon density (gm/cm^3) (range)	Mean top m Soil Organic Carbon Storage (Mg/ha) (range)
Sundarbans	**Bangladesh**	Bomer et al. (2020a)	56	100 cm	Coring, CHN analyser	0.9 (0.6–1.5)	0.010 (0.008–0.011)	–
		Khan and Amin (2019)	35	15 cm (0–15)	Coring, wet oxidation	0.6 (0.4–1.0)	–	–
		Sanderman et al. (2018)	–	100 cm	Literature and Model based	–	–	127 (74–463)
		Atwood et al. (2017)	–	100 cm	Literature and Model based	–	–	118
		Prasad et al. (2017)	400	100 cm (1 cm interval)	Coring, CN analyser	1.25 (0.8–2.4)	–	–
		Hossain and Bhuiyan (2016)	96	5 cm (0–5)	Coring, wet oxidation	1.2 (0.6–2.0)	–	–
		Rahman et al. (2015)	150	100 cm (0–30, 30–100)	Coring, wet oxidation	–	0.011 (0.007–0.014)	112 (90–134)
		Donato et al., (2011)	4	100 cm (0–30, 30–100)	Coring, wet oxidation	1.7 (1.6–1.7)	0.016 (0.015– 0.016)	–
		Allison et al. (2003)	4	600 cm (0–600)	Coring, CHN analyser	0.5–1.1	–	–
	India	Dutta et al. (2019)	48	40 cm (0–10, 10–20, 20–30, 30–40)	Coring, wet oxidation	1.25 (0.8–1.6)	–	–
		Prasad et al. (2017)	300	100 cm (1 cm interval)	Coring, CN analyser	0.8–5.2	–	–
		Dutta et al. (2013)	15	25 cm (0–5, 5–10, 10–15,15–20, 20–25)	Coring, TOC analyser	1.8 (1.2–2.1)	0.017 (0.013–0.019)	–
		Banerjee et al. (2012)	140	40 cm (0–10, 10–20, 20–30, 30–40)	Coring, wet oxidation	1.0 (0.5–1.4)	0.011 (0.007–0.015)	–
		Mitra et al. (2012)	120	40 cm (0–10, 10–20, 20–30, 30–40) cm	Coring, wet oxidation	0.7 (0.4–1.1)	0.009 (0.006–0.012)	–
		Ray et al. (2011)	16	30 cm (0–30)	Coring, wet oxidation	0.6 (0.5–0.7)	–	–
Global studies		Kauffman et al. (2020)	190 sample plot data from 5 continents in different soil depth			–	–	334 (33–789)
		Sanderman et al. (2018)	Model based estimation of carbon from literature values of 1812 samples			–	–	361 (94–628)
		Rovai et al. (2018)	Model based estimation of carbon from literature values of 932 samples			–	0.033 (0.001–0.153)	–
		Atwood et al. (2017)	Literature based estimation from 1230 sampling locations			–	–	283 (15–1527)
		IPCC (2014)	Literature based estimation			–	–	428
		Jardine and Siikamäki (2014)	Model based estimation of carbon from literature values of 932 samples			5.7 (0.1–43.3)	0.032 (0.014–0.115)	369 (272–703)
		Donato et al. (2011)	Field based data from Indo-pacific area of 25 samples			11.9 (1.7–21.5)	0.043 (0.016–0.076)	–

et al., 2016). It is either mostly excluded from the global estimates of mangrove SOC (Table 1), or is underrepresented due to a limited number of samples or perceived poor data quality (Donato et al., 2011; Jardine and Siikamäki, 2014; Atwood et al., 2017; Sanderman et al., 2018; Twilley et al., 2018; Kauffman et al., 2020). A range of studies into SOC content in mangrove soils of the Sundarbans have been carried out (Table 1), but these all have limitations. The first comprehensive carbon inventory throughout the Sundarbans was completed by the Bangladesh Forest Department (BFD) in 2009–10; however, the wider vertical sample depth might have an effect on the SOC estimation within the top meter (Rahman et al., 2015). Allison et al. (2003) and Donato et al. (2011) investigated soil organic carbon at greater depth (>1 m) in the Bangladesh Sundarbans, however, the number of samples (2 and 6 respectively) was not sufficient to address the variability inside the forests. Studies by Khan and Amin (2019) and Hossain and Bhuiyan (2016) measured SOC from different parts of the Sundarbans, however, the sampling was only performed within the top 15 cm. These all the previous studies of SOC in the Sundarbans have limitations resulting from low spatial sampling intensity and limited analysis of soil depth range. Moreover, some global studies like Rovai et al. (2018) argued that past climate-based estimation overestimated SOC by up to 86% for deltaic settings like the Sundarbans. Therefore, accurate investigation on the spatial variation of soil organic carbon and the identification of major controls for such variation in the Bangladesh Sundarbans is urgently needed.

Increasing salinity in the inundated mangroves stimulate a wide range of biogeochemical reactions- including enhancing sulphate concentrations, cation exchange, ionic and osmotic stress, acidity, and turbidity and at the same time reducing soil redox potential and oxygen levels (Setia et al., 2013; Luo et al., 2019). These soil biogeochemical changes in turn alter sediment characteristics and modify plant and microbe communities, which ultimately affect both the soil organic carbon pool and quality. Increased soil salinity affects organic matter solubility by altering flocculation of different soil particles (Wong et al., 2009; Wong et al., 2010; Rath and Rousk, 2015). The Investigations of tidal wetlands across the world reveals a significant negative relationship between the soil organic carbon pool with salinity (Nyman et al., 1990; Craft, 2007; Więski et al., 2010; Morrissey et al., 2014; Hu et al., 2016). High soil salinity decreases decomposition rates by lowering microbial activities in the soil and lowers autochthonous carbon input by reducing plant productivity leading to lower organic carbon in the soil (Baldwin et al., 2006; Marton et al., 2012; Setia et al., 2013; Liu et al., 2017; Zhao et al., 2017). High salinity in general acts as an inhibitor of carbon mineralisation, however the opposite is also evident in some studies suggesting that a small increase in salinity promotes mineralisation process in the oligohaline zone, while in the mesohaline and polyhaline zones, elevated salinity reduces the mineralisation rate (Luo et al., 2019). Therefore, the impact of salinity on the soil organic carbon pool and quality is not uniform in all wetland settings in the world, rather it depends on the local geomorphology and hydrological characteristics.

The aim of the present study is to estimate soil organic carbon (SOC) in the Bangladesh part of the Sundarbans mangrove forest and to better understand the relationship of SOC with three salinity zones (oligohaline, mesohaline and polyhaline) and major forest types. The study hypothesises that higher salinity zones (polyhaline) would yield a lower organic soil carbon stock as a reflection of lower productive vegetation and altered soil physical and biological processes compared with the lower salinity zone (oligohaline). The relationships between physical, chemical properties and vegetation characteristics with SOC are also investigated to develop dependable predictive models for this forest. The novelty of this study lies in the extensive stratified random sampling from all over Bangladesh Sundarbans combined with vertical investigation of soil depth up to 1 m.

2. Material and methods

2.1. Study area

The Sundarbans is the largest single block of mangrove forest in the world and a Ramsar and UNESCO World Heritage site (Fig. 1) (Giri et al., 2011; Sarker et al., 2016). The Bangladesh Sundarbans is situated between 21°30′N and 22°30′N and 89°00′E and 89°55′E. The climate of the Sundarbans is warm, humid, and tropical, where annual precipitation varies from 1474 to 2265 mm and mean annual minimum and maximum temperature is between 29 °C and 31 °C (Chowdhury et al., 2016; Sarker et al., 2016). Based on the salinity variation, the Sundarbans naturally divides into three distinct zones based on the soil salinity; i) Oligohaline (LSZ) (<2 dS/m, ii) Mesohaline (2–4 dS/m) and iii) Polyhaline (>4 dS/m) (Siddiqi, 2001; Chanda et al., 2016b). Several studies have identified a relationship between tree species abundance along the east–west salinity gradient (Iftekhar and Saenger, 2008; Aziz and Paul, 2015; Sarker et al., 2016; Sarker et al., 2019a). Although *Excoecaria agallocha* is abundant in all three salinity zones, *Heritiera fomes* (characteristic species in Bangladesh Sundarbans) is dominant in both the oligohaline and mesohaline zones, whereas *Ceriops decandra* is abundant in the polyhaline zone (Sarker et al., 2019a). Some pioneer species, such as *Avicenna* spp. and *Sonneratia apetala* are also present in the mudflats all over the Sundarbans. A short description of all 23 tree species from 10 families found in this study is presented in Table A.1.

2.2. Geology and soils of the Sundarbans

The Sundarbans mangrove forest lies in the south-western part of the Bengal Basin, one of the most extensive sediment reservoirs in the world composed of unconsolidated Quaternary deposits (Rudra, 2014). The rapid sedimentation followed by the tectonic collision of the Indian plate with the Tibetan plate and the Burmese plate in the Miocene triggered the formation of the Bengal Basin (Alam, 1989). Since the Holocene, the dynamic Ganges-Brahmaputra river system has been discharging sediments from the Sub-Himalaya and is still delivering >1 Gt of sediment to the delta plain of India and Bangladesh (Islam et al., 1999; Syvitski and Milliman, 2007). The Sundarbans is of relatively recent origin (3000-year B.P.) and this mangrove has developed as a result of both fluvial and tidal forces depositing sediments to the GBM river mouth (Goodbred and Kuehl, 2000; Allison and Kepple, 2001; Rogers et al., 2013). Previously, the Ganges was the main source of sediments in the Sundarbans, however, recent changes have resulted from the merging of the Ganges and Brahmaputra which have now migrated to the eastward, far away from the Sundarbans (Rudra, 2014; Islam, 2016). Together with the eastward migration of the primary GBM delta, the construction of the Farakka barrage in the main Ganges River and earthen embankments surrounding the Sundarbans have reduced freshwater flow, resulting in reduced fluvial sedimentation in the Bangladesh Sundarbans. This geomorphological change, in turn, has led to increased remobilisation of sediments by tidal forces (Rogers et al., 2013; Hale et al., 2019; Bomer et al., 2020b). The changed pattern of freshwater flow has resulted in a salinity gradient increasing from the east to the west of the Sundarbans.

The soil is mainly fine-grained, grey coloured, slightly calcareous, and mostly composed of silts to clayey silts (Allison et al., 2003; Bomer et al., 2020a). The subsurface sediment extends up to 6 m in depth in the landward direction and up to 4 m in depth in the seaward direction (Allison et al., 2003). The median grain size ranges between 16 and 32 μm reflecting the medium silt range. The average dry bulk density (0.81 g cm ^{3}) is higher in the Sundarbans in comparison to other mangroves in the world (Bomer et al., 2020a). The soil physical and chemical properties are varied from the eastern to the western part of Bangladesh Sundarbans, the eastern part is softer, more fertile and receives more fresh sediments than the western part (Siddiqi, 2001). Soils are mostly neutral to alkaline (pH 6.5–8.0), whereas the polyhaline zone is more alkaline than the oligohaline zone. Soils of the western and southern

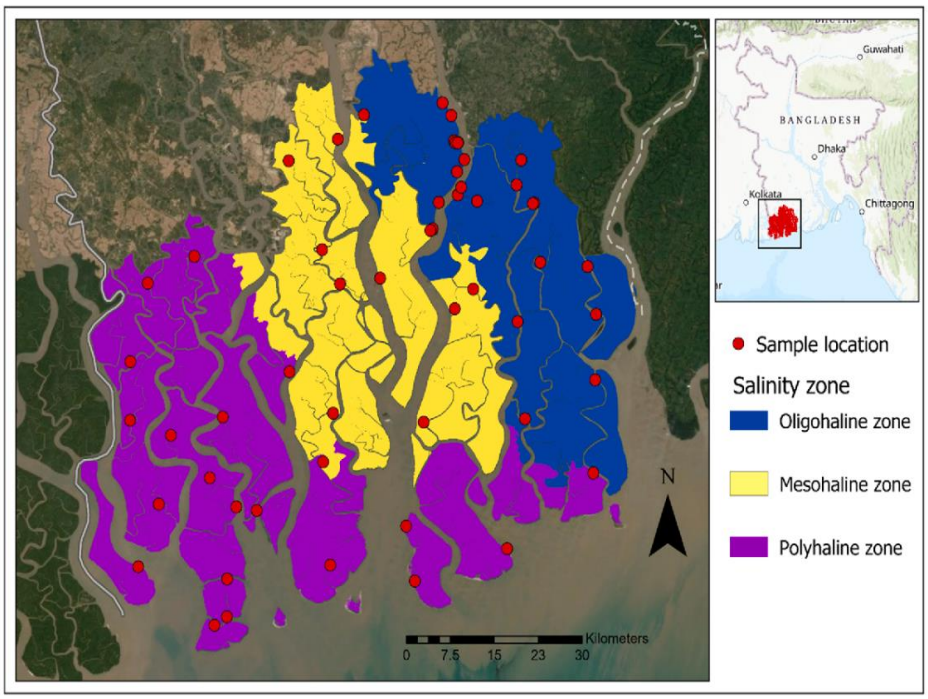

Fig. 1. Sundarbans mangrove forest, Bangladesh. Legend colour represents three major salinity zones (Chanda et al., 2016b). ESRI Basemap Sources: Esri, HERE, Garmin, FAO, NOAA, USGS, © OpenStreetMap contributors, and the GIS User Community.

polyhaline zone are comparatively richer in P, K, Na, Mg, Cl^- and Fe, but lower in soil NH^{4-} and Na than the eastern oligohaline zone (Siddiqi, 2001; Sarker et al., 2016). This pronounced differences in soil nutrients and salinity trigger the diversity of vegetation composition in different parts of the Sundarbans.

2.3. Sediment and tree data collection

In the Bangladesh Sundarbans, permanent sample plots (PSP) were established in 1986 by the ODA (Overseas Development Administration) for monitoring growth, regeneration, and long-term ecological changes (Chaffey et al., 1985). A total of 120 PSPs (20 m × 100 m) were established to assess growth rate, regeneration, stocking, and crop composition based on salinity, forest type and accessibility (Iftekhar and Saenger, 2008; Sarker et al., 2019b) (Fig. 1). In this study, sediment samples were collected from 55 plots, of which 50 plots are from PSPs selected at random, and the remaining five plots are from outside PSPs to represent areas outside PSP. Sampling was undertaken in two phases: In the first phase, three sediment cores of 50 cm depth were taken from 18 PSPs. After laboratory analysis of the samples from the first 18 PSPs, it was decided to extend the sediment sampling depth to 1 m and take two core samples from each plot because of little within-plot variation among the initial 54 core samples. In the second phase, an additional 37 PSPs were sampled with two cores sampled at each plot. Altogether, 126 sediment cores from 55 plots were sampled across the whole of the Bangladesh Sundarbans (Fig. 1).

The location of the cores within a PSP was decided by establishing a random circular plot with a radius of 11.3 m (an area of 400 m^2). Within each plot, a small circular plot was laid with 5 m radius and sediment cores were taken from east, west and south side (east and west for two cores) from the centre, which is perpendicular to each other. The cores were taken using an open-faced auger (6 cm diameter), which was further subdivided into four depths (0–10, 10–30, 30–50 and 50–100 cm), following the method of Kauffman and Donato (2012). Sediment sub-samples were taken from the middle of each core section with fixed 2.5 cm length, sealed in plastic and subsequently placed in an icebox to reduce oxidation. The sub-samples were kept below 4 °C in zip-sealed plastic bags until laboratory processing.

For vegetation data, the Diameter at Breast Height (DBH) and height were measured for all trees within the 11.3 m radius plot. DBH was measured at 1.3 m and height was measured with a Vertex-III hypsometer. For small trees with a DBH < 14.5 cm, a smaller circular plot (radius 5 m) was nested within the 11.3 m plot. The elevation of each plot was calculated by subtracting the mean tree height of the plot from the Digital Surface Model (DSM) taken from the TanDEM-X 90 m satellite data (Hawker et al., 2019). For major forest types, single-species dominance was determined when the relative composition is >75%, and the remaining forest types are termed as mixed type.

2.4. Laboratory analysis

2.4.1. Soil physical and chemical properties

For each core sub-samples, samples were freeze-dried and re-weighted to determine the bulk density. Bulk density was calculated by dividing the dry mass of the soil by the volume of the soil. Soil pH and soil salinity (as soil conductivity) were measured from a portion of the homogenised dry soil for each core. Dried soils were diluted with distilled water (1:5 ratio), and subsequently, soil pH was measured using a Jenway 3510 Standard Digital pH Meter and soil salinity by a hand-held Jenway 470 Conductivity Meter (Hardie and Doyle, 2012).

2.4.2. Total soil organic carbon (SOC)

To determine the soil organic carbon (SOC) and nitrogen content of the soil, any large stones or twigs were removed from the sample and subsequently homogenised and ground with a ball mill. A few milligrams (~40 mg) of the sediment was then passed through an elemental analyser (Thermo Scientific Flash 2000-NC Soil Analyzer) to derive the total carbon and nitrogen as a percentage. Inorganic carbon

content was deducted from the total carbon to get organic carbon percentage, according to Howard et al. (2014). The inorganic carbon content was measured from some random samples across all salinity zones using an Analytik Jena Multi EA (Elemental Analyser) 4000. Soil organic carbon density (gm cm ^{3}) for each sample and total organic carbon content (Mg ha ^{1}) of each depth and core were measured according to Howard et al. (2014).

2.5. Statistical analysis

All statistical analysis and graphics used R 3.6.1 for Windows (R Core Team, 2019). Total organic carbon (Mg ha ^{1}), organic carbon density (gm cm ^{3}) and bulk density (gm cm ^{3}) among three salinity zones and four depths were compared with two-way analysis of variance (ANOVA) test using the 'car' package (Fox and Weisberg, 2019). In order to compare soil organic carbon among vegetation types, total organic carbon (Mg ha ^{1}) was compared with one-way analysis of variance (ANOVA). The results of ANOVA are summarized in Supplementary Information. To derive the relationship among organic carbon density (g cm ^{3}), bulk density and total nitrogen content, data from all the core subsections (n = 512) were used. To examine the relationship among SOC and soil physical and chemical parameters (soil salinity, pH, bulk density, Total N, organic C:N, elevation, latitude and longitude) and vegetation characteristics (species richness, tree density, mean DBH and mean height), stepwise multiple linear regression analysis was undertaken. SOC was considered as the dependant variable, whereas all the selected parameters were independent variables. Correlation analysis and principal component analysis (PCA) were carried out to decrease the number of explanatory variables and to reduce collinearity in the regression model. All the variables were standardised before PCA according to Legendre and Legendre (2012). Eigenvalues greater than one were retained and variables with factor loadings >0.35 were treated as potential explanatory variables for the regression model (Jackson, 1993). In all cases, the data were logarithmic (natural) transformed (if needed) to meet the assumptions of normality and equal variances by using Shapiro Wilk and Levene's tests, respectively and subsequently back-transformed to present graphically. The graphical output of the linear model was generated using the 'ggplot2' package (Wickham, 2016).

3. Results

3.1. Soil organic carbon, salinity zones and soil depth

The average soil organic carbon (SOC) density significantly varied from 0.003 gm cm ^{3} to 0.009 gm cm ^{3} in different salinity zones and soil depths (two-way ANOVA for Ln (SOC density), salinity zones, $F_{2,\ 500} = 112.3$, $p < 0.001$ and soil depths, $F_{3,\ 500} = 30.1$, $p < 0.001$) (Fig. 2, Table A.2). Both salinity zone and soil depth had a significant interaction effect on the variability of SOC density in the Sundarbans ($F_{6,\ 500} = 3.5$, $p < 0.01$) (Table A.1). Significantly higher SOC density was found in the topmost depth followed by the subsequent three depths; however, SOC density in the intermediate depths (between 10–30 cm and 30–50 cm) are not significantly different (Fig. 2b), which indicates the unequal variability of SOC with soil depth. The oligohaline zone comprises higher SOC density (gm cm ^{3}) followed by mesohaline and polyhaline zone indicating higher soil organic carbon in the low salinity areas.

The bulk density (BD) of the soil revealed an opposite trend as significantly higher bulk density was observed in the higher salinity zones and in the 50–100 cm soil depth (two-way ANOVA for Ln (bulk density (gm cm ^{3})), salinity zones, $F_{2,\ 500} = 22.2$, $p < 0.001$ and soil depth, $F_{3,\ 500} = 46.2$, $p < 0.001$) (Fig. A.1, Table A.3). Likewise, SOC density, the soil organic carbon storage (SOC) for the different depths was significantly different among the three salinity zones and the four soil depths (two-way ANOVA for Ln (SOC), salinity zones, $F_{2,\ 500} = 118.9$, $p < 0.001$ and soil depth, $F_{3,\ 500} = 526.2$, $p < 0.001$) (Fig. 3 & Fig. 4, Table A.4). However, higher amounts of SOC were found in the 50–100 cm depth in comparison to the top three depths (Fig. 4). The top meter SOC ranges from 26.2 Mg ha ^{1} to 107.9 Mg ha ^{1} in the Sundarbans, where oligohaline zone comprises the highest SOC (74.8 Mg ha ^{1}), followed by the mesohaline (59.3 Mg ha ^{1}), and the polyhaline zone (48.3 Mg ha ^{1}) (Table 2).

3.2. Soil organic carbon and forest types

One-way ANOVA revealed that SOC varied with major forest types in the Sundarbans ($F_{7,\ 47} = 3.3$, $p < 0.01$) (Table A.5). As shown in Fig. 5, the average SOC content in the *Bruguiera* sp. stand was the highest, with an average of 105.3 Mg ha ^{1}, followed by *Sonneratia* sp. and *Avicennia* sp., with an average of 68.7 Mg ha ^{1} and 67.1 Mg ha ^{1}, respectively. The Tukey HSD test showed that the other forest types had no significant

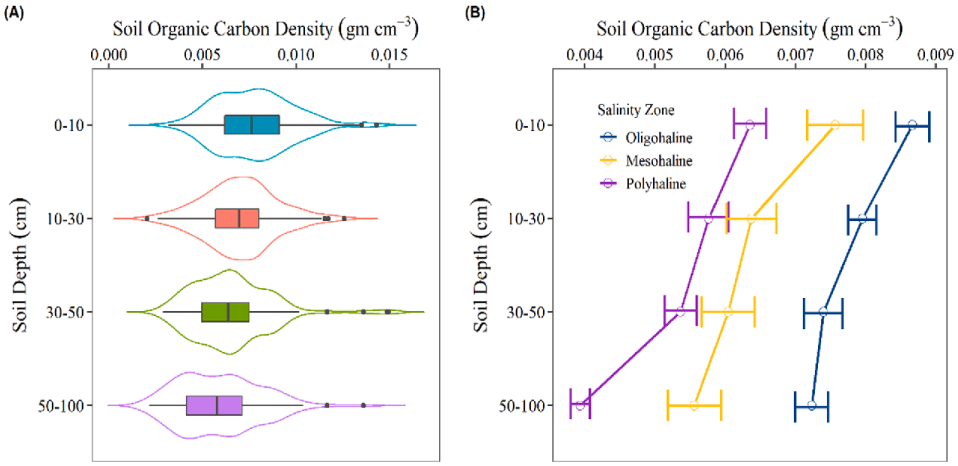

Fig. 2. (A) The distribution of soil organic carbon (SOC) density (gm cm^{-3}) in four soil depths presented as violin-box plot, where the black vertical line represents the median and black dots are outliers. Here, the width of violin plot represents the proportion of the data located there as a measure of kernel probability density. (B) Average SOC density (gm cm^{-3}) in three salinity zones and four soil depths.

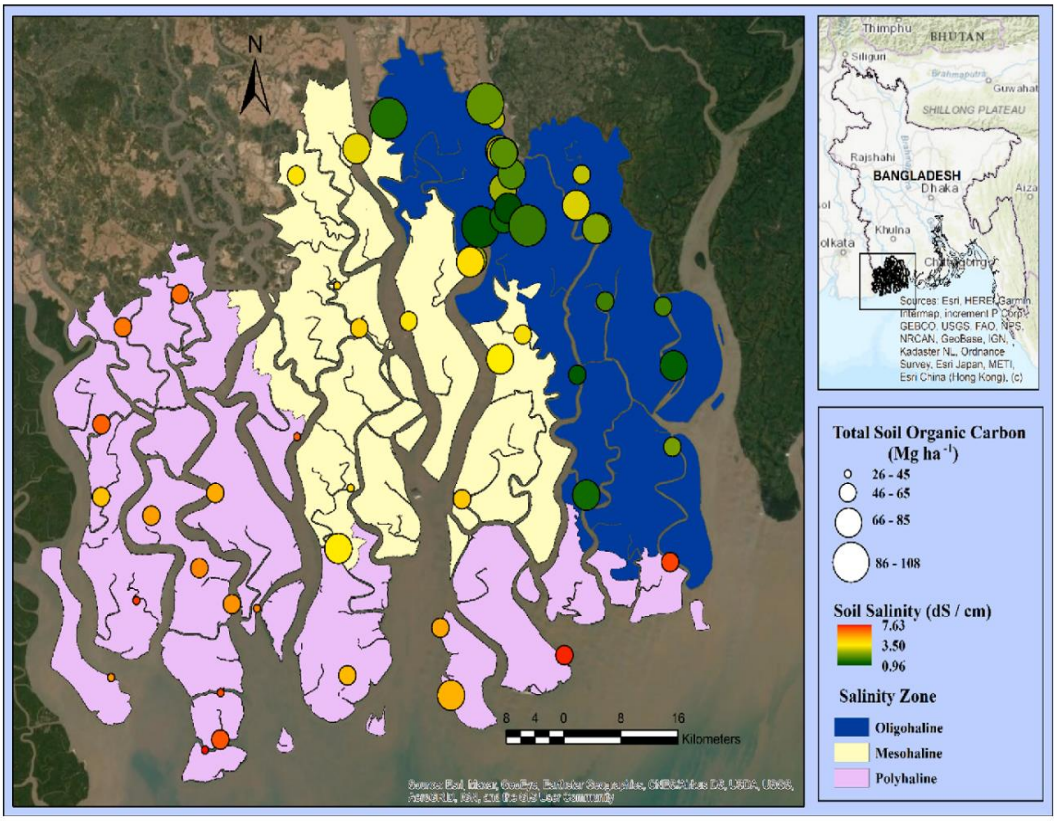

Fig. 3. Spatial distribution of total soil organic carbon (SOC) (Mg ha^{-1}) and soil salinity (dS/cm) in the Sundarbans. Note that circle represents the amount of SOC and gradual colour ramp reveals soil salinity indicating green to red as from low to high salinity. Three major salinity zones are represented according to Chanda et al., (2016b). (For interpretation of the references to colour in this figure legend, the reader is referred to the web version of this article.)

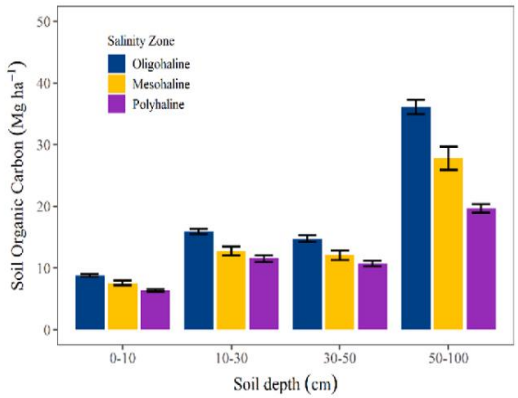

Fig. 4. Average soil organic carbon (Mg ha^{-1}) in different soil depths in three salinity zones.

effect on SOC content, which ranges from 50.2 Mg ha ^{1} to 67.0 Mg ha ^{1} for *Ceriops* and *Heritiera* forest types, respectively (Table A.6).

3.3. Soil physical, chemical properties and vegetation characteristics

The soil physical, chemical properties and vegetation characteristics varied considerably among the three salinity zones (Table 2). As expected, oligohaline zones had relatively low average soil bulk density, pH, and soil salinity, in comparison to higher salinity zones. Additionally, significantly higher SOC and lower total N contributes higher organic C:N in the oligohaline zone, although it is similar to the mesohaline zone ($p < 0.05$). BD and SOC density showed a statistically significant negative relationship ($r = -0.47$, $p < 0.001$) (Fig. 6A). However, the soil organic carbon (SOC) density and soil nitrogen density is significantly positively correlated with soil nitrogen density across the Sundarbans ($r = 0.66$, $p < 0.001$) (Fig. 6B). Analysis from the satellite and tree height data reveals that the average elevation is higher in the polyhaline zone. The average DBH and height of the trees were statistically significantly higher in both the oligohaline and mesohaline zone, whereas the average stem density was higher in both the mesohaline and polyhaline zone ($p < 0.05$). Bivariate relationship between SOC and other soil physical, chemical properties and vegetation characteristics are presented in the supplementary Fig. A.2.

3.4. Relationship of SOC with soil and vegetation properties

SOC content was positively correlated with tree DBH, tree height, organic C:N, latitude, and longitude, but negatively correlated with soil salinity, bulk density, soil pH, tree density and elevation ($p < 0.05$) (Fig. 7). As total nitrogen and species richness did not show any significant correlation with SOC content, these two parameters were discarded from the subsequent PCA analysis. The measured properties also showed a significant positive and negative correlation among themselves, which indicates a source of multicollinearity, a phenomenon which makes multiple regression unreliable. Therefore, principal

Table 2
Overview of measured soil parameters and vegetation characteristics. Values are presented as mean (±SD), where n ≥ 3. Lowercase letters indicate significant variability among salinity zones, according to least-significant difference (LSD) test at α = 0.05.

Salinity zone	Bulk density (gm cm^{-3})	Soil pH	Soil salinity (EC dS/cm)	Total Soil Organic Carbon (Mg ha^{-1})	Total Nitrogen (Mg ha^{-1})	Organic C:N	Elevation (m)	Stem Density (ha^{-1})	Height (m)	DBH (Diameter at Breast Height) (cm)
Oligohaline	0.58 (0.07) ^{b}	7.06 (0.26) ^{c}	1.49 (0.32) ^{c}	74.77 (14.93) ^{a}	2.66 (1.19) ^{b}	21.30 (7.23) ^{a}	3.39 (1.78) ^{b}	5,009 (2,485) ^{b}	7.98 (2.03) ^{a}	8.12 (2.41) ^{a}
Mesohaline	0.62 (0.04) ^{ab}	7.43 (0.19) ^{b}	3.07 (0.56) ^{b}	59.30 (15.80) ^{b}	3.52 (1.08) ^{a}	17.30 (6.87) ^{a}	3.67 (1.01) ^{ab}	6,876 (3,290) ^{ab}	7.88 (2.63) ^{a}	8.60 (5.36) ^{ab}
Polyhaline	0.63 (0.05) ^{a}	7.80 (0.26) ^{a}	5.56 (0.85) ^{a}	48.25 (10.32) ^{c}	3.81 (0.98) ^{a}	13.08 (3.00) ^{b}	4.79 (1.52) ^{a}	8,750 (4,798) ^{a}	5.98 (1.66) ^{b}	6.72 (4.12) ^{b}

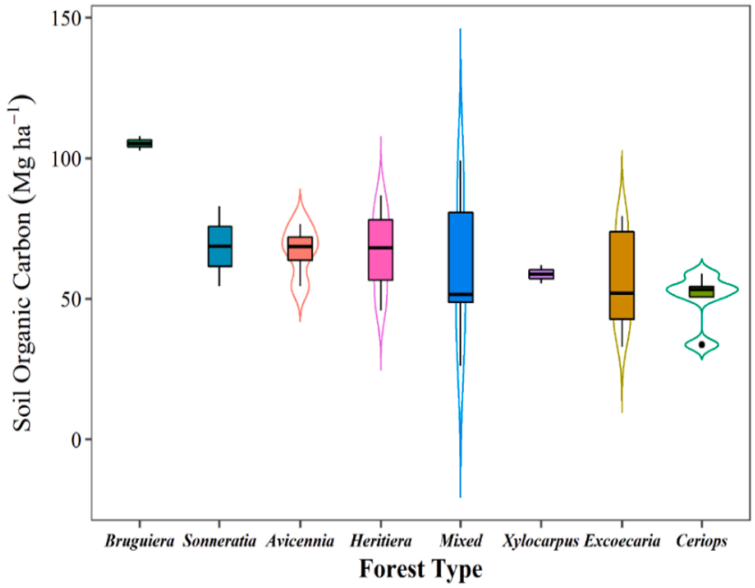

Fig. 5. Integrated violin-box plot shows average soil organic carbon (SOC) in major forest types in the Sundarbans. The black vertical line of box plot represents the median and the width of violin plot represents the proportion of the data located there as a measure of kernel probability density.

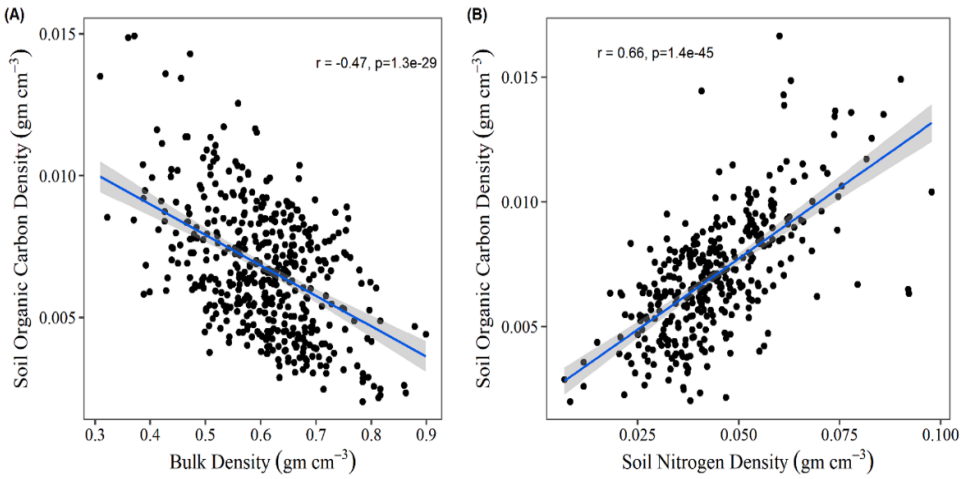

Fig. 6. (A) Relationship between bulk density and soil organic carbon density. (B) Relationship between soil nitrogen density and soil organic carbon density.

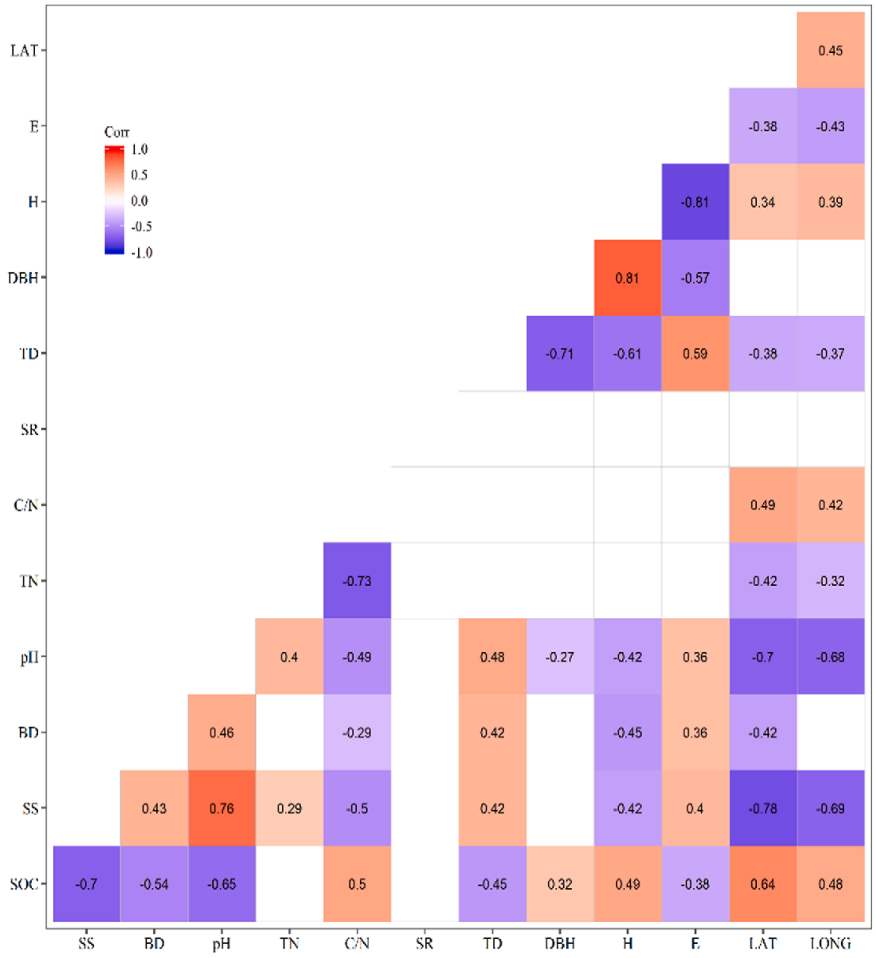

Fig. 7. Correlation matrix among SOC and other physicochemical, geophysical and vegetation properties. The number of each block shows the Spearman's rank correlation coefficients at $p < 0.05$, where red and violet colour represents respective positive and negative correlations. The white block indicates the correlation coefficient is statistically insignificant. The soil properties: SOC Soil organic carbon, SS soil salinity, BD Bulk density, pH soil pH, TN Total Nitrogen, C:N organic C- total Nitrogen ratio, the vegetation characteristics: SR Species richness, TD Tree density, DBH mean Diameter at Breast Height, H Mean height and geophysical properties: E Elevation, LAT Latitude and LONG Longitude. (For interpretation of the references to colour in this figure legend, the reader is referred to the web version of this article.)

component analysis was used to identify and group those properties that influence SOC the most and to overcome the influence of multicollinearity.

Principal component analysis (PCA) was performed with ten variables to assemble and isolate the smallest possible of subsets to explain the variation of the dataset (Fig. 8). The PCA result indicates that the first two principal components explained more than two-thirds of the total variation with an eigenvalue greater than 1. The most important component (PC1) explained 49.5% with the highest loadings (>0.35) for soil SS (soil salinity) and pH. On the other hand, the second component showed higher leadings for tree H, DBH and soil C:N with 20% explained variation (Table A.7). As soil SS and pH are highly correlated with each other ($r = 0.76$, $p < 0.05$) (Fig. 7), the variable with the highest loading, soil SS, was selected from the first component for the regression model. Similarly, tree H was discarded due to collinearity with tree DBH and therefore, tree DBH and soil C:N was selected from the second component.

By using the PCA-derived subset of variables, the relationship between SOC and soil and vegetation properties was obtained by using stepwise multiple linear regression (MLR). The regression results showed that soil salinity alone could explain 50% SOC variability in the Sundarbans, however, the percentage increases to 57% and 62% when soil C:N or soil C:N and tree DBH are added to the model (Table 3). Although all three regression models are highly significant (Table A.8), the best subset of MLR model was selected based on the largest adjusted R^2 value and the smallest Mallow's Cp, AIC (Akaike Information Criteria) and RMSE (Root Mean Squared Error) and presented in Eq. (1).

$$\mathrm{Ln}\ (\mathrm{SOC}) = 3.439 - 0.077\ \mathrm{SS} + 0.274\ \mathrm{Ln}\ (\mathrm{C:N}) + 0.017\ \mathrm{DBH} \quad (1)$$

4. Discussion

The reported average soil organic carbon (SOC) density in this study is lower than previous estimates from the Sundarbans and far lower than average estimates of SOC density from global mangroves (Table 1). SOC density, the standardized carbon stock measurement with depth, is the most useful parameter to compare SOC between different forests (Donato et al., 2011; Weiss et al., 2016). However, due to unreported bulk density, it was not possible to convert from the reported organic

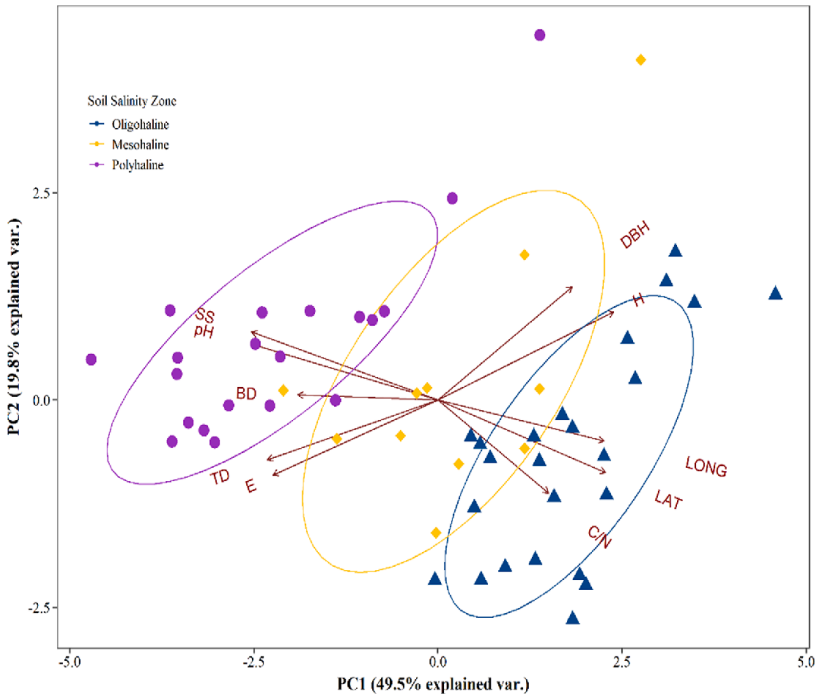

Fig. 8. Principal component analysis (PCA) biplot of soil physicochemical, geophysical and vegetation characteristics as vectors (n 10) and mangroves areas are coloured coded as three salinity zones (n 55). The soil physicochemical properties included SS soil salinity, pH soil pH, BD Bulk density, C:N organic C-total Nitrogen ratio, geophysical properties comprised LAT Latitude, LONG Longitude, E Elevation, and the vegetation characteristics included TD Tree density, DBH mean Diameter at Breast Height, H Mean height. Here, perpendicular direction signifies uncorrelated relationship, while negative and positive correlated vectors are presented in the opposite vectors and small angle vectors, respectively.

Table 3
Summary statistics of regression model. Here, SS Soil salinity, C:N Soil organic carbon: Nitrogen and DBH tree Diameter at breast height.

Model	R^2	Adjusted R^2	C(p)	AIC	RMSE
1. SS	0.508	0.498	18.217	−10.457	0.212
2. SS and C:N	0.590	0.574	8.650	−18.513	0.196
3. SS, C:N and DBH	0.637	0.616	4.00	−23.255	0.186

carbon (%) to SOC density for most of the local and world studies. Despite a greater range of soil organic carbon (SOC) percentage in this study (0.3–4.4%), the average value (1.2%) is in line with most previous studies, although higher than estimates published by Ray et al. (2011), Banerjee et al. (2012), and Allison et al. (2003). These differences are likely to be attributed to variable sampling strategies along with variable soil depth or different methods used for carbon estimation. Likewise SOC density, the average top 1 m SOC storage in the Bangladesh Sundarbans (50.9 ± 15.2 Mg ha ^{1}) is almost half of the previous estimate by Rahman et al. (2015), Sanderman et al. (2018) and Atwood et al. (2017). Estimates of soil organic carbon could fluctuate based on the differences in sampling design, choice of analytical method and soil depth (Howard et al., 2014; Nayak et al., 2019). In the case of mangroves, Passos et al. (2016) found overestimation of organic carbon measured with the oxidation method in comparison to the elemental analyser. Anaerobic microbial decomposition yields reduced soil compounds (i.e., Fe^{2+}, S^{2} , Mn^{2+}, and Cl) in mangroves, which might interfere with organic carbon determination with chemical oxidation method (Nelson and Sommers, 1996; Bisutti et al., 2004; De Vos et al., 2007; Nóbrega et al., 2015). Apart from using different methods, the SOC variation originates from the consideration of soil depth in sample design as the SOC concentration is a function of soil depth and shows considerable variability (Wuest, 2009; Kauffman and Donato, 2012; Jandl et al., 2014). Moreover, using coring for sampling might have an influence on soil bulk density estimation leading to lower SOC stock estimation in deeper soils (Rau et al., 2011; Gross and Harrison, 2018).

In comparison to global studies, the estimated top 1 m SOC stock is lower in the Sundarbans than the reported average from sites distributed all over the world (Table 1). Based on model-based georeferenced database of mangrove SOC, the global SOC map showed that the Sundarbans contains the lowest SOC stocks per ha in the world (Sanderman et al., 2018). Compared to direct estimates from 190 sites across the world by Kauffman et al. (2020), the Sundarbans contains higher SOC than only two other mangrove forests, the Porto Céu mangrove in Brazil (48 Mg ha ^{1}) and the Bu Tinah Janoub in the United Arab Emirates (33 Mg ha ^{1}), located in lower and higher latitudes respectively than the Sundarbans. However, global comparison in soil carbon among tropical, subtropical and temperate mangroves showed a contrasting relationship with latitudes (Atwood et al., 2017; Twilley et al., 2018; Kauffman et al., 2020; Ouyang and Lee, 2020). Both Kauffman et al. (2020) and Ouyang and Lee (2020) found significantly lower soil carbon in mangroves >20°N, although the former study had fewer samples largely limited to the middle east hyper arid mangroves. On the other hand, Atwood et al. (2017) and Twilley et al. (2018) documented the poor relationship between latitude and SOC stocks. This poor relationship might be attributed due to the poor representation of samples in the studies from the subtropical mangroves like the Sundarbans.

The low soil carbon in the Sundarbans is largely due to high mineral sediment deposition (Sanderman et al., 2018; Twilley et al., 2018), low burial rate (Ray et al., 2011), rapid turnover rate (Ray et al., 2018), historical logging, stand age (Marchand, 2017), plant litter quality

(Rovai et al., 2018) and biological processes. Being both a tide and river-dominated ecosystem, the carbon allocation in the above and below ground is very complex, largely dependent on the local and regional geomorphic and geophysical drivers (Twilley et al., 2018). In riverine deltas, trees invest much of the carbon to the above ground to keep pace with sedimentation and sea-level rise, which is evident in the oligohaline zone with greater forest productivity (Twilley et al., 2018; Sarker et al., 2019a; Sarker et al., 2019b). Moreover, research has highlighted that mangroves subjected to frequent cyclones leading to temporary losses of above ground carbon are usually followed by rapid below ground carbon gains during recovery process according to the 'Ecosystem Development' theory (Odum, 1969; Danielson et al., 2017; Kominoski et al., 2018). These rapid carbon gains in the above ground and the disturbance from the catastrophic cyclones could be the source of higher autochthonous input to the below ground. Nonetheless, higher tidal amplitude in the Sundarbans leads to higher carbon export totalling 7.3 Tg C yr^{-1} to the adjacent Bay of Bengal, which is higher than any other mangroves in the world (Ray et al., 2018). This rapid carbon turnover results in reduced burial of organic matter (0.18%) in the soil (Ray et al., 2011). Moreover, the pronounced tidal cycles in the Sundarbans affects carbon burial process by altering soil water chemistry (Chatterjee et al., 2013; Spivak et al., 2019). Besides high carbon turnover rate, the Sundarbans is believed to have become tidally active in the recent past due to reduced freshwater flow from the Ganges-Brahmaputra-Meghna river (Rogers et al., 2013; Hale et al., 2019). However, despite the historical reduction of sedimentation, the Sundarbans is itself still keeping pace with sea-level rise with the highest average surface elevation and vertical accretion rate (0.74 and 2.71 cm yr^{-1}) compared to the worldwide average (Bomer et al., 2020a; Bomer et al., 2020b). This high sedimentation rate is the outcome of the massive flux of clastic sediments which attenuates the amount of organic carbon per unit area.

The century-long historical exploitation in the Sundarbans before the felling moratorium in 1989 has largely decreased the populations of threatened tree species (Siddiqi, 2001; Sarker et al., 2011). This in turn is likely to have lessened the continuous autochthonous input of organic matter in the forest and reduced the overall stand age. Studies also showed that historical harvesting had altered the species composition in the Sundarbans, with decreasing abundances of *Heritiera fomes*, *Ceriops decandra* and *Xylocarpus mekongensis* and increasing for *Excoecaria agallocha* (Sarker et al., 2016). The SOC stock also depends on the age of the stands as evident in the Chrono sequence study on SOC stocks in French Guiana which revealed that the SOC varied from 4 to 107 Mg ha^{-1} from young stand to senescent stage (Marchand, 2017). In addition, studies have suggested that lower organic carbon in the soil is mostly associated with higher C:N of the plant litter which has resulted from lowering decomposition speed and decreasing carbon-use efficiency of the decomposer (Bouillon et al., 2003; Zhou et al., 2019). Compared to mangrove associates, the senescent leaves of true mangroves contain considerably higher C:N (~33) in the Indian part of Sundarbans (Chanda et al., 2016a). Kamruzzaman et al. (2019) observed a decreasing trend of C:N of the leaf litter in both forest floor and buried condition starting from 40, but barely reached below 30 after 196 days of decomposition study, suggesting N limitation in the oligohaline zone of the Bangladesh Sundarbans. The low organic carbon can also be attributed by the abundance of leaf-consuming organisms ingesting organic litter detritus both at surface and subsurface in burrows. The Sundarbans encompasses a wide range of gastropod species (e.g., *Cerithedia cingulata*, *Cymia lacera*) that predominantly consume mangrove detritus (Nayak et al., 2014).

Variation in SOC stocks among different forest types is often mediated by the primary productivity, resources allocation in different parts (e.g. above and below ground) and microorganism activity is driven by a number of biological (e.g. bioturbation and species composition) and physical (e.g. soil texture, salinity, inundation and nutrients) factors (McLeod et al., 2011). Therefore, differing stand structure and composition of mangrove forests in different tidal regimes yield variable SOC stock (Lacerda et al., 1995; Gleason and Ewel, 2002). Moreover, the long and short-term resilience and resistance of microbial communities are largely dependent on the structure and zonation of mangrove communities reflecting environmental gradients (Capdeville et al., 2019). In this study, the species with higher SOC stock such as *Bruguiera* sp., *Sonneratia* sp. and *Avicennia* sp. are frequently inundated due to proximity to the river and low land than other species in the Sundarbans (Siddiqi, 2001; Sarker et al., 2016). These high inundation regimes, in turn, lead to increased microbial activity and a higher level of dissolved organic carbon in the sediment (Wang et al., 2013; Chambers et al., 2014; Chambers et al., 2016). Regular tides also bring sediments along with high allochthonous input whereas the raised less-inundated areas foster autochthonous SOC and less microbial activity (Lovelock et al., 2015; Woodroffe et al., 2016). Rao et al. (1994) found almost double C:N ratio in fresh leaves of *Bruguiera* sp. compared with other mangrove species, suggesting higher input of autochthonous carbon. Being the pioneer species in the succession of the Sundarbans, both *Sonneratia* sp. and *Avicennia* sp. are resilient to disturbances leading to higher SOC than climax and seral species (Table A.1) and accumulate a large quantity of organic litter in the tidal channel close to the river or seafront (Sarker et al., 2016; Bomer et al., 2020a). The variability of SOC stocks among forest types followed a similar pattern to the global studies by Atwood et al. (2017), except for *Sonneratia* sp. which was found to hold less SOC stock than *Heritiera* and *Ceriops*. On the other hand, Kauffman et al. (2020) found significantly lower below ground carbon stocks in *Avicennia* sp., especially in the arid mangroves of Middle-East Asia, which is solely occupied by this species. Therefore, the impact of above ground vegetation of below ground is largely site-specific, and it depends on a wide range of factors.

The unexplained variation of the best multiple regression models (R^2 = 0.64) highlights the necessity of including other soil and environmental parameters such as soil cations and anions, clay characteristics and texture, precipitation, temperature, and river discharge. This study did not address these properties and suggests future studies incorporate a wider range of parameters to gain a better understating of organic carbon dynamics in the Sundarbans. In particular, for better ecosystem management, future research should include information relating to contextualising soil (e.g. soil texture, grain size and minerology), biogeochemical (e.g. important properties of soil and pore-water chemistry such as sulphate, oxygen, nitrate, ferric oxides in case of mangroves) and ecological (e.g. vegetation and plat-microbe interaction) properties (Luo et al., 2019; Spivak et al., 2019). However, soil salinity is considered as the outcome of the combined impact of these climatic and environmental variables in the Sundarbans resulting pronounced differences of SOC stock among the three salinity zones (Sarker et al., 2016; Sarker et al., 2019b; Rahman et al., 2020). Several previous studies have confirmed that salinity determines the strong zonation of tree species and diversity in the Sundarbans, which in turn leads to comparatively higher diversity and taller tree species in the oligohaline followed by mesohaline and polyhaline zone (Aziz and Paul, 2015; Sarker et al., 2016; Sarker et al., 2019a; Sarker et al., 2019b; Rahman et al., 2020). Comparatively higher productive trees (e.g. higher DBH and higher height) promotes organic matter accumulation through producing higher litter mass and increases SOC stock by forming stable aggregates from roots and pneumatophores (Lange et al., 2015). The three salinity zones also comprise differential soil physical, chemical properties and vegetation characteristics that usually affects SOC storage by influencing microbial decomposition, soil water chemistry, plant–microbe interaction, and plant litter quality. While comparing nutrient concentration in the leaf litter of *Sonneratia apetala*, one of the major pioneer species in the Sundarbans, Nasrin et al. (2019) found lowest concentrations of N, P and K and the highest concentrations of Na in the polyhaline zone, reflecting higher C:N in the leaf litter. However, the low SOC in the polyhaline zone is also coincided with the low C:N indicting inwelling of marine and terrestrial suspended particulate

materials (Bouillon et al., 2003). The strong positive correlation ($r = 0.66$, $p < 0.001$) between carbon and nitrogen density indicates that the source of carbon and nitrogen is likely to be same and can vary spatially (Matsui et al., 2015).

Although the Sundarbans is considered to be of recent origin, the large accommodation space exists due to accretion and erosion with historical relative sea-level variability (Goodbred and Kuehl, 2000; Tyagi and Sen, 2019). Therefore, the Sundarbans might have a 3 m organic layer in the seaward direction and much more in the landward (Allison et al., 2003). By considering this vertical depth and the area covered by mangrove forest, the Sundarbans are likely to contain considerable volumes of soil organic carbon. Previous research has demonstrated that mangroves holding higher carbon storage also have a higher rate of deforestation with 50% mangrove loss attributed to Indonesia, which holds about 25% of soil carbon in the world's mangroves; the figure increases to 75% when Malaysia and Myanmar are considered (Atwood et al., 2017). Therefore, mangroves from these countries are considered as a significant source of emissions due to high deforestation and forest conversion (Hamilton and Friess, 2018). On the other hand, in Bangladesh, despite the lower SOC stock in the Sundarbans mangrove forest demonstrated by this paper, recent positive trends in forest cover demonstrate the value of blue carbon conservation and an improved understanding of carbon storage will be of benefit to the inclusion of mangroves in national and international climate strategies and policies.

5. Conclusion

The top meter of soil organic carbon (SOC) per area in the Bangladesh Sundarbans is lower than has previously been reported. However, the total SOC will likely to be greater if total vertical depth is considered. The soil organic carbon stock (SOC) in the Sundarbans is largely influenced by soil salinity, probably by amending the forest productivity and microbial activity. The results highlighted that increasing salinity as result of predicted sea-level rise will likely have pronounced effects on future soil carbon accumulation rates by altering the soil environment and vegetation characteristics. The study underlines the importance of spatial conservation planning measures and initiatives to conserve and maximize carbon accumulation and to contribute to global climate change adaptation and mitigation strategies. Results suggest that high sediment carbon zone in the eastern part of the Sundarbans is highly vulnerable to tourism and economic development activities. In terms of climate change mitigation and adaptation, the conservation of the existing carbon stock should receive much higher priority rather than the debates of high-low carbon stock. The Bangladesh Sundarbans can act as an important blue carbon hotspot due to the high sedimentation and carbon sequestration rate and conservation priority by the government. However, disturbances such as sea-level rise, global warming, eutrophication, and landscape development might hinder this conservation activities in the future.

Funding

The study was funded by Commonwealth Scholarship Commission in the UK (Grant number: BDCS-2017-55).

Declaration of Competing Interest

The authors declare that they have no known competing financial interests or personal relationships that could have appeared to influence the work reported in this paper.

Acknowledgements

We are grateful to Commonwealth Scholarship Commission in the UK for the PhD scholarship to the first author. We want to extend our gratitude to the Bangladesh Forest Department for giving permission for fieldwork in the Sundarbans and Forestry and Wood Technology Discipline, Khulna University for allowing study leave to the first author. We also thank everyone involved the fieldwork in the Sundarbans and we recognised that without their help, this work could not have been completed. We are also grateful to the Institute of Hazard, Risk and Resilience for a small research grant and the Department of Geography, Durham University for allowing laboratory analysis and to Ustinov College, Durham University for a travel grant. Lastly, we give thanks to Ms. Robyn Shilland for her brilliant comments in the manuscript.

Appendix A. Supplementary material

Supplementary data to this article can be found online at https://doi.org/10.1016/j.catena.2021.105159.

References

Abdullah, A.N., Stacey, N., Garnett, S.T., Myers, B., 2016. Economic dependence on mangrove forest resources for livelihoods in the Sundarbans, Bangladesh. For. Policy Econ. 64, 15–24. https://doi.org/10.1016/j.forpol.2015.12.009.

Alam, M., 1989. Geology and depositional history of Cenozoic sediments of the Bengal Basin of Bangladesh. Palaeogeogr., Palaeoclimatol Palaeoecol. 69, 125–139. https://doi.org/10.1016/0031-0182(89)90159-4.

Allison, M., Kepple, E., 2001. Modern sediment supply to the lower delta plain of the Ganges-Brahmaputra River in Bangladesh. Geo-Mar. Lett. 21, 66–74. https://doi.org/10.1007/s003670100069.

Allison, M.A., Khan, S.R., Goodbred, S.L., Kuehl, S.A., 2003. Stratigraphic evolution of the late Holocene Ganges-Brahmaputra lower delta plain. Sediment. Geol. 155, 317–342. https://doi.org/10.1016/S0037-0738(02)00185-9.

Alongi, D.M., 2012. Carbon sequestration in mangrove forests. Carbon Manage. 3, 313–322. https://doi.org/10.4155/cmt.12.20.

Alongi, D.M., 2014. Carbon cycling and storage in mangrove forests. Ann. Rev. Mar. Sci. 6, 195–219. https://doi.org/10.1146/annurev-marine-010213-135020.

Atwood, T.B., Connolly, R.M., Almahasheer, H., Carnell, P.E., Duarte, C.M., Lewis, C.J.E., Irigoien, X., Kelleway, J.J., Lavery, P.S., Macreadie, P.I., Serrano, O., Sanders, C.J., Santos, I., Steven, A.D.L., Lovelock, C.E., 2017. Global patterns in mangrove soil carbon stocks and losses. Nat. Climate Change. 7, 523–528. https://doi.org/10.1038/nclimate3326.

Aziz, A., Paul, A.R., 2015. Bangladesh Sundarbans: present status of the environment and biota. Diversity. 7, 242–269. https://doi.org/10.3390/d7030242.

Baldwin, D.S., Rees, G.N., Mitchell, A.M., Watson, G., Williams, J., 2006. The short-term effects of salinization on anaerobic nutrient cycling and microbial community structure in sediment from a freshwater wetland. Wetlands. 26, 455–464. https://doi.org/10.1672/0277-5212(2006)26[455:TSEOSO]2.0.CO;2.

Banerjee, K., Bal, G., Mitra, A., 2018. How soil texture affects the organic carbon load in the mangrove ecosystem? A case study from Bhitarkanika, Odisha. In: Singh, V.P., Yadav, S., Yadava, R.N. (Eds.), Environmental Pollution. Springer Singapore, Singapore, pp. 329–341.

Banerjee, K., Roy Chowdhury, M., Sengupta, K., Sett, S., Mitra, A., 2012. Influence of anthropogenic and natural factors on the mangrove soil of Indian Sundarbans wetland. Arch. Environ. Sci. 6, 80–91.

Bisutti, I., Hilke, I., Raessler, M., 2004. Determination of total organic carbon – an overview of current methods. TrAC Trends Anal. Chem. 23, 716–726. https://doi.org/10.1016/j.trac.2004.09.003.

Bomer, E.J., Wilson, C.A., Elsey-Quirk, T., 2020a. Process controls of the live root zone and carbon sequestration capacity of the Sundarbans mangrove forest, Bangladesh. Sci. 2, 35. https://doi.org/10.3390/sci2020035.

Bomer, E.J., Wilson, C.A., Hale, R.P., Hossain, A.N.M., Rahman, F.M.A., 2020b. Surface elevation and sedimentation dynamics in the Ganges-Brahmaputra tidal delta plain, Bangladesh: evidence for mangrove adaptation to human-induced tidal amplification. Catena. 187, 104312 https://doi.org/10.1016/j.catena.2019.104312.

Bouillon, S., Boschker, H.T.S., 2006. Bacterial carbon sources in coastal sediments: a cross-system analysis based on stable isotope data of biomarkers. Biogeosciences. 3, 175–185. https://doi.org/10.5194/bg-3-175-2006.

Bouillon, S., Dahdouh-Guebas, F., Rao, A.V.V.S., Koedam, N., Dehairs, F., 2003. Sources of organic carbon in mangrove sediments: variability and possible ecological implications. Hydrobiologia. 495, 33–39. https://doi.org/10.1023/a:1025411506526.

Brodersen, K.E., Trevathan-Tackett, S.M., Nielsen, D.A., Connolly, R.M., Lovelock, C.E., Atwood, T.B., Macreadie, P.I., 2019. Oxygen consumption and sulfate reduction in vegetated coastal habitats: effects of physical disturbance. Front. Mar. Sci. 6, 00014. https://doi.org/10.3389/fmars.2019.00014.

Capdeville, C., Pommier, T., Gervaix, J., Promard, F., Rols, J.-L., Leflaive, J., 2019. Mangrove facies drives resistance and resilience of sediment microbes exposed to anthropic disturbance. Front. Microbiol. 9 https://doi.org/10.3389/fmicb.2018.03337.

Chaffey, D.R., Miller, F.R., Sandom, J.H., 1985. A forest inventory of the Sundarbans, Bangladesh. Project Report No.140, Overseas Development Authority (ODA), London.

Chambers, L.G., Davis, S.E., Troxler, T., Boyer, J.N., Downey-Wall, A., Scinto, L.J., 2014. Biogeochemical effects of simulated sea level rise on carbon loss in an Everglades mangrove peat soil. Hydrobiologia. 726, 195–211. https://doi.org/10.1007/s10750-013-1764-6.

Chambers, L.G., Guevara, R., Boyer, J.N., Troxler, T.G., Davis, S.E., 2016. Effects of salinity and inundation on microbial community structure and function in a mangrove peat soil. Wetlands. 36, 361–371. https://doi.org/10.1007/s13157-016-0745-8.

Chanda, A., Akhand, A., Manna, S., Das, S., Mukhopadhyay, A., Das, I., Hazra, S., Choudhury, S.B., Rao, K.H., Dadhwal, V.K., 2016a. Mangrove associates versus true mangroves: a comparative analysis of leaf litter decomposition in Sundarban. Wetlands Ecol. Manage. 24, 293–315. https://doi.org/10.1007/s11273-015-9456-9.

Chanda, A., Mukhopadhyay, A., Ghosh, T., Akhand, A., Mondal, P., Ghosh, S., Mukherjee, S., Wolf, J., Lázár, A.N., Rahman, M.M., Salehin, M., Chowdhury, S.M., Hazra, S., 2016b. Blue carbon stock of the Bangladesh Sundarban mangroves: what could be the scenario after a century? Wetlands. 36, 1033–1045. https://doi.org/10.1007/s13157-016-0819-7.

Chatterjee, M., Shankar, D., Sen, G., Sanyal, P., Sundar, D., Michael, G., Chatterjee, A., Amol, P., Mukherjee, D., Suprit, K., 2013. Tidal variations in the Sundarbans estuarine system, India. J. Earth Syst. Sci. 122, 899–933.

Chowdhury, M.Q., De Ridder, M., Beeckman, H., 2016. Climatic signals in tree rings of *Heritiera fomes* Buch.-Ham. in the Sundarbans, Bangladesh. Plos One. 11, e0149788 https://doi.org/10.1371/journal.pone.0149788.

Craft, C., 2007. Freshwater input structures soil properties, vertical accretion, and nutrient accumulation of Georgia and U.S tidal marshes. Limnol. Oceanogr. 52, 1220–1230. https://doi.org/10.4319/lo.2007.52.3.1220.

Danielson, T.M., Rivera-Monroy, V.H., Castañeda-Moya, E., Briceño, H., Travieso, R., Marx, B.D., Gaiser, E., Farfán, L.M., 2017. Assessment of Everglades mangrove forest resilience: implications for above-ground net primary productivity and carbon dynamics. For. Ecol. Manage. 404, 115–125. https://doi.org/10.1016/j.foreco.2017.08.009.

De Vos, B., Lettens, S., Muys, B., Deckers, J.A., 2007. Walkley-Black analysis of forest soil organic carbon: recovery, limitations and uncertainty. Soil Use Manage. 23, 221–229. https://doi.org/10.1111/j.1475-2743.2007.00084.x.

Donato, D.C., Kauffman, J.B., Murdiyarso, D., Kurnianto, S., Stidham, M., Kanninen, M., 2011. Mangroves among the most carbon-rich forests in the tropics. Nat. Geosci. 4, 293–297. https://doi.org/10.1038/ngeo1123.

Duarte, C.M., Losada, I.J., Hendriks, I.E., Mazarrasa, I., Marbà, N., 2013. The role of coastal plant communities for climate change mitigation and adaptation. Nat. Climate Change. 3, 961–968. https://doi.org/10.1038/nclimate1970.

Dutta, J., Banerjee, K., Agarwal, S., Mitra, A., 2019. Soil Organic Carbon (soc): a proxy to assess the degree of anthropogenic and natural stress. J. Interrupted Stud. 2, 90–102.

Dutta, M.K., Chowdhury, C., Jana, T.K., Mukhopadhyay, S.K., 2013. Dynamics and exchange fluxes of methane in the estuarine mangrove environment of the Sundarbans, NE coast of India. Atmos. Environ. 77, 631–639. https://doi.org/10.1016/j.atmosenv.2013.05.050.

Fontaine, S., Barot, S., Barré, P., Bdioui, N., Mary, B., Rumpel, C., 2007. Stability of organic carbon in deep soil layers controlled by fresh carbon supply. Nature 450, 277–280. https://doi.org/10.1038/nature06275.

Fox, J., Weisberg, S., 2019. An R companion to applied regression, third ed. Sage, Thousand Oaks CA.

Freeman, C., Ostle, N.J., Fenner, N., Kang, H., 2004. A regulatory role for phenol oxidase during decomposition in peatlands. Soil Biol. Biochem. 36, 1663–1667. https://doi.org/10.1016/j.soilbio.2004.07.012.

Friess, D.A., Rogers, K., Lovelock, C.E., Krauss, K.W., Hamilton, S.E., Lee, S.Y., Lucas, R., Primavera, J., Rajkaran, A., Shi, S., 2019. The state of the world's mangrove forests: past, present, and future. Annu. Rev. Env. Resour. 44, 89–115. https://doi.org/10.1146/annurev-environ-101718-033302.

Friess, D.A., Yando, E.S., Abuchahla, G.M.O., Adams, J.B., Cannicci, S., Canty, S.W.J., Cavanaugh, K.C., Connolly, R.M., Cormier, N., Dahdouh-Guebas, F., Diele, K., Feller, I.C., Fratini, S., Jennerjahn, T.C., Lee, S.Y., Ogurcak, D.E., Ouyang, X., Rogers, K., Rowntree, J.K., Sharma, S., Sloey, T.M., Wee, A.K.S., 2020. Mangroves give cause for conservation optimism, for now. Curr. Biol. 30, R153–R154. https://doi.org/10.1016/j.cub.2019.12.054.

Giri, C., Ochieng, E., Tieszen, L.L., Zhu, Z., Singh, A., Loveland, T., Masek, J., Duke, N., 2011. Status and distribution of mangrove forests of the world using earth observation satellite data. Global Ecol. Biogeogr. 20, 154–159. https://doi.org/10.1111/j.1466-8238.2010.00584.x.

Gleason, S.M., Ewel, K.C., 2002. Organic matter dynamics on the forest floor of a micronesian mangrove forest: an investigation of species composition shifts. Biotropica. 34, 190–198. https://doi.org/10.1111/j.1744-7429.2002.tb00530.x.

Goodbred, S.L., Kuehl, S.A., 2000. The significance of large sediment supply, active tectonism, and eustasy on margin sequence development: late Quaternary stratigraphy and evolution of the Ganges-Brahmaputra delta. Sediment. Geol. 133, 227–248. https://doi.org/10.1016/S0037-0738(00)00041-5.

Gross, C.D., Harrison, R.B., 2018. Quantifying and comparing soil carbon stocks: underestimation with the core sampling method. Soil Sci. Soc. Am. J. 82, 949–959. https://doi.org/10.2136/sssaj2018.01.0015.

Hale, R., Bain, R., Goodbred Jr, S., Best, J., 2019. Observations and scaling of tidal mass transport across the lower Ganges-Brahmaputra delta plain: implications for delta management and sustainability. Earth Surface Dyn. 7, 231–245. https://doi.org/10.5194/esurf-7-231-2019.

Hamilton, S.E., Friess, D.A., 2018. Global carbon stocks and potential emissions due to mangrove deforestation from 2000 to 2012. Nat. Climate Change. 8, 240–244. https://doi.org/10.1038/s41558-018-0090-4.

Hardie, M., Doyle, R., 2012. Measuring soil salinity. In: Shabala, S., Cuin, T.A. (Eds.), Plant Salt Tolerance: Methods and Protocols. Humana Press, Totowa, NJ, pp. 415–425. https://doi.org/10.1007/978-1-61779-986-0_28.

Hawker, L., Neal, J., Bates, P., 2019. Accuracy assessment of the TanDEM-X 90 Digital Elevation Model for selected floodplain sites. Remote Sens. Environ. 232, 111319 https://doi.org/10.1016/j.rse.2019.111319.

Hossain, G.M., Bhuiyan, M.A.H., 2016. Spatial and temporal variations of organic matter contents and potential sediment nutrient index in the Sundarbans mangrove forest, Bangladesh. KSCE J. Civil Eng. 20, 163–174. https://doi.org/10.1007/s12205-015-0333-0.

Howard, J., Hoyt, S., Isensee, K., Telszewski, M., Pidgeon, E. (Eds.), 2014. Coastal blue carbon: methods for assessing carbon stocks and emissions factors in mangroves, tidal salt marshes, and seagrasses. Conservation International, Intergovernmental Oceanographic Commission of UNESCO, International Union for Conservation of Nature, Arlington, Virginia, USA, pp. 184.

Hu, Y., Wang, L., Fu, X., Yan, J., Wu, J., Tsang, Y., Le, Y., Sun, Y., 2016. Salinity and nutrient contents of tidal water affects soil respiration and carbon sequestration of high and low tidal flats of Jiuduansha wetlands in different ways. Sci. Total Environ. 565, 637–648. https://doi.org/10.1016/j.scitotenv.2016.05.004.

Iftekhar, M., Saenger, P., 2008. Vegetation dynamics in the Bangladesh Sundarbans mangroves: a review of forest inventories. Wetlands Ecol. Manage. 16, 291–312. https://doi.org/10.1007/s11273-007-9063-5.

IPCC, 2014. 2013 Supplement to the 2006 IPCC guidelines for national greenhouse gas inventories: Wetlands. IPCC, Geneva, p. 354.

Islam, M.R., Begum, S.F., Yamaguchi, Y., Ogawa, K., 1999. The Ganges and Brahmaputra rivers in Bangladesh: basin denudation and sedimentation. Hydrol. Process. 13, 2907–2923. https://doi.org/10.1002/(sici)1099-1085(19991215)13:17<2907::Aid-hyp906>3.0.Co;2-e.

Islam, S.N., 2016. Deltaic floodplains development and wetland ecosystems management in the Ganges–Brahmaputra–Meghna Rivers Delta in Bangladesh. Sustainable Water Resour. Manage. 2, 237–256. https://doi.org/10.1007/s40899-016-0047-6.

Jackson, D.A., 1993. Stopping rules in principal components analysis: a comparison of heuristical and statistical approaches. Ecology. 74, 2204–2214. https://doi.org/10.2307/1939574.

Jandl, R., Rodeghiero, M., Martinez, C., Cotrufo, M.F., Bampa, F., van Wesemael, B., Harrison, R.B., Guerrini, I.A., Richter, D.d., Rustad, L., Lorenz, K., Chabbi, A., Miglietta, F., 2014. Current status, uncertainty and future needs in soil organic carbon monitoring. Sci. Total Environ. 468–469, 376–383. https://doi.org/10.1016/j.scitotenv.2013.08.026.

Jardine, S.L., Siikamäki, J.V., 2014. A global predictive model of carbon in mangrove soils. Environ. Res. Lett. 9, 104013 https://doi.org/10.1088/1748-9326/9/10/104013.

Kamruzzaman, M., Basak, K., Paul, S.K., Ahmed, S., Osawa, A., 2019. Litterfall production, decomposition and nutrient accumulation in Sundarbans mangrove forests, Bangladesh. Forest Sci. Technol. 15, 24–32. https://doi.org/10.1080/21580103.2018.1557566.

Kauffman, J.B., Adame, M.F., Arifanti, V.B., Schile-Beers, L.M., Bernardino, A.F., Bhomia, R.K., Donato, D.C., Feller, I.C., Ferreira, T.O., Jesus Garcia, M.d.C., MacKenzie, R.A., Megonigal, J.P., Murdiyarso, D., Simpson, L., Hernández Trejo, H., 2020. Total ecosystem carbon stocks of mangroves across broad global environmental and physical gradients. Ecol. Monogr. 90 https://doi.org/10.1002/ecm.1405.

Kauffman, J.B., Donato, D., 2012. Protocols for the measurement, monitoring and reporting of structure, biomass and carbon stocks in mangrove forests. Working Paper 86. Center for International Forestry Research (CIFOR), Bogor, Indonesia, pp. 50.

Khan, M., Amin, M., 2019. Macro nutrient status of Sundarbans forest soils in southern region of Bangladesh. Bangladesh J. Sci. Ind. Res. 54, 67–72. https://doi.org/10.3329/bjsir.v54i1.40732.

Kominoski, J.S., Gaiser, E.E., Baer, S.G., 2018. Advancing theories of ecosystem development through long-term ecological research. Bioscience. 68, 554–562. https://doi.org/10.1093/biosci/biy070.

Krauss, K.W., McKee, K.L., Lovelock, C.E., Cahoon, D.R., Saintilan, N., Reef, R., Chen, L., 2014. How mangrove forests adjust to rising sea level. New Phytol. 202, 19–34. https://doi.org/10.1111/nph.12605.

Kristensen, E., Bouillon, S., Dittmar, T., Marchand, C., 2008. Organic carbon dynamics in mangrove ecosystems: a review. Aquat. Bot. 89, 201–219. https://doi.org/10.1016/j.aquabot.2007.12.005.

Lacerda, L.D., Ittekkot, V., Patchineelam, S.R., 1995. Biogeochemistry of mangrove soil organic matter: a comparison between *Rhizophora* and *Avicennia* soils in south-eastern Brazil. Estuar. Coast. Shelf Sci. 40, 713–720. https://doi.org/10.1006/ecss.1995.0048.

Lange, M., Eisenhauer, N., Sierra, C.A., Bessler, H., Engels, C., Griffiths, R.I., Mellado-Vázquez, P.G., Malik, A.A., Roy, J., Scheu, S., Steinbeiss, S., Thomson, B.C., Trumbore, S.E., Gleixner, G., 2015. Plant diversity increases soil microbial activity and soil carbon storage. Nat. Commun. 6, 6707. https://doi.org/10.1038/ncomms7707.

Legendre, P., Legendre, L.F., 2012. Numerical ecology, third ed. Elsevier, Great Britain, p. 1006.

Liu, X., Ruecker, A., Song, B., Xing, J., Conner, W.H., Chow, A.T., 2017. Effects of salinity and wet–dry treatments on C and N dynamics in coastal-forested wetland soils: Implications of sea level rise. Soil Biol. Biochem. 112, 56–67. https://doi.org/10.1016/j.soilbio.2017.04.002.

Liu, Z., Lee, C., 2006. Drying effects on sorption capacity of coastal sediment: the importance of architecture and polarity of organic matter. Geochim. Cosmochim. Acta. 70, 3313–3324. https://doi.org/10.1016/j.gca.2006.04.017.

Lovelock, C.E., Cahoon, D.R., Friess, D.A., Guntenspergen, G.R., Krauss, K.W., Reef, R., Rogers, K., Saunders, M.L., Sidik, F., Swales, A., Saintilan, N., Thuyen, L.X., Triet, T., 2015. The vulnerability of Indo-Pacific mangrove forests to sea-level rise. Nature. 526, 559–563. https://doi.org/10.1038/nature15538.

Lovelock, C.E., Duarte, C.M., 2019. Dimensions of Blue Carbon and emerging perspectives. Biol. Lett. 15, 20180781. https://doi.org/10.1098/rsbl.2018.0781.

Lovelock, C.E., Sorrell, B.K., Hancock, N., Hua, Q., Swales, A., 2010. Mangrove forest and soil development on a rapidly accreting shore in New Zealand. Ecosystems. 13, 437–451. https://doi.org/10.1007/s10021-010-9329-2.

Luo, M., Huang, J.-F., Zhu, W.-F., Tong, C., 2019. Impacts of increasing salinity and inundation on rates and pathways of organic carbon mineralization in tidal wetlands: a review. Hydrobiologia. 827, 31–49. https://doi.org/10.1007/s10750-017-3416-8.

Macreadie, P.I., Anton, A., Raven, J.A., Beaumont, N., Connolly, R.M., Friess, D.A., Kelleway, J.J., Kennedy, H., Kuwae, T., Lavery, P.S., Lovelock, C.E., Smale, D.A., Apostolaki, E.T., Atwood, T.B., Baldock, J., Bianchi, T.S., Chmura, G.L., Eyre, B.D., Fourqurean, J.W., Hall-Spencer, J.M., Huxham, M., Hendriks, I.E., Krause-Jensen, D., Laffoley, D., Luisetti, T., Marbà, N., Masque, P., McGlathery, K.J., Megonigal, J.P., Murdiyarso, D., Russell, B.D., Santos, R., Serrano, O., Silliman, B.R., Watanabe, K., Duarte, C.M., 2019. The future of Blue Carbon science. Nat. Commun. 10, 3998. https://doi.org/10.1038/s41467-019-11693-w.

Marchand, C., 2017. Soil carbon stocks and burial rates along a mangrove forest chronosequence (French Guiana). For. Ecol. Manage. 384, 92–99. https://doi.org/10.1016/j.foreco.2016.10.030.

Marton, J.M., Herbert, E.R., Craft, C.B., 2012. Effects of salinity on denitrification and greenhouse gas production from laboratory-incubated tidal forest soils. Wetlands. 32, 347–357. https://doi.org/10.1007/s13157-012-0270-3.

Matsui, N., Meepol, W., Chukwamdee, J., 2015. Soil organic carbon in mangrove ecosystems with different vegetation and sedimentological conditions. J. Marine Sci. Eng. 3, 1404–1424. https://doi.org/10.3390/jmse3041404.

McLeod, E., Chmura, G.L., Bouillon, S., Salm, R., Björk, M., Duarte, C.M., Lovelock, C.E., Schlesinger, W.H., Silliman, B.R., 2011. A blueprint for blue carbon: toward an improved understanding of the role of vegetated coastal habitats in sequestering CO_2. Front. Ecol. Environ. 9, 552–560. https://doi.org/10.1890/110004.

Mitra, A., Banerjee, K., Sett, S., 2012. Spatial variation in organic carbon density of mangrove soil in Indian Sundarbans. Natl. Acad. Sci. Lett. 35, 147–154. https://doi.org/10.1007/s40009-012-0046-6.

Morrissey, E.M., Gillespie, J.L., Morina, J.C., Franklin, R.B., 2014. Salinity affects microbial activity and soil organic matter content in tidal wetlands. Global Change Biol. 20, 1351–1362. https://doi.org/10.1111/gcb.12431.

Nasrin, S., Hossain, M., Rahman, M.M., 2019. Adaptive responses to salinity: nutrient resorption efficiency of Sonneratia apetala (Buch.-Ham.) along the salinity gradient in the Sundarbans of Bangladesh. Wetlands Ecol. Manage. 27, 343–351. https://doi.org/10.1007/s11273-019-09663-6.

Nayak, A.K., Rahman, M.M., Naidu, R., Dhal, B., Swain, C.K., Nayak, A.D., Tripathi, R., Shahid, M., Islam, M.R., Pathak, H., 2019. Current and emerging methodologies for estimating carbon sequestration in agricultural soils: a review. Sci. Total Environ. 665, 890–912. https://doi.org/10.1016/j.scitotenv.2019.02.125.

Nayak, B., Zaman, S., Gadi, S.D., Raha, A.K., Mitra, A., 2014. Dominant gastropods of Indian Sundarbans: a major sink of carbon. Int. J. Adv. Pharm. Biol. Chem. 3, 282–289.

Nellemann, C., Corcoran, E., Duarte, C., Valdés, L., De Young, C., Fonseca, L., Grimsditch, G. (Eds.), 2009. Blue carbon. A rapid response assessment. United Nations Environment Programme (UNEP), GRID-Arendal, pp. 78.

Nelson, D.W., Sommers, L.E., 1996. Total carbon, organic carbon, and organic matter. In: Sparks, D. et al. (Eds.), Methods of soil analysis: Part 3 Chemical methods, pp. 961–1010. https://doi.org/10.2136/sssabookser5.3.c34.

Nóbrega, G.N., Ferreira, T.O., Artur, A.G., de Mendonça, E.S., Leão, R.A. de O., Teixeira, A.S., Otero, X.L., 2015. Evaluation of methods for quantifying organic carbon in mangrove soils from semi-arid region. J. Soils Sed. 15, 282–291. https://doi.org/10.1007/s11368-014-1019-9.

Nyman, J.A., Delaune, R.D., Patrick, W.H., 1990. Wetland soil formation in the rapidly subsiding Mississippi River Deltaic Plain: mineral and organic matter relationships. Estuar. Coast. Shelf Sci. 31, 57–69. https://doi.org/10.1016/0272-7714(90)90028-P.

Odum, E.P., 1969. The strategy of ecosystem development. Science. 164, 262–270. https://doi.org/10.1126/science.164.3877.262.

Ouyang, X., Lee, S.Y., 2020. Improved estimates on global carbon stock and carbon pools in tidal wetlands. Nat. Commun. 11, 317. https://doi.org/10.1038/s41467-019-14120-2.

Passos, T.R.G., Artur, A.G., Nóbrega, G.N., Otero, X.L., Ferreira, T.O., 2016. Comparison of the quantitative determination of soil organic carbon in coastal wetlands containing reduced forms of Fe and S. Geo-Mar. Lett. 36, 223–233. https://doi.org/10.1007/s00367-016-0437-7.

Pendleton, L., Donato, D.C., Murray, B.C., Crooks, S., Jenkins, W.A., Sifleet, S., Craft, C., Fourqurean, J.W., Kauffman, J.B., Marbà, N., Megonigal, P., Pidgeon, E., Herr, D., Gordon, D., Baldera, A., 2012. Estimating global "blue carbon" emissions from conversion and degradation of vegetated coastal ecosystems. PLOS ONE. 7, e43542 https://doi.org/10.1371/journal.pone.0043542.

Prasad, M.B.K., Kumar, A., Ramanathan, A.L., Datta, D.K., 2017. Sources and dynamics of sedimentary organic matter in Sundarban mangrove estuary from Indo-Gangetic delta. Ecol. Process. 6, 8. https://doi.org/10.1186/s13717-017-0076-6.

R Core Team, 2019. R: A Language and Environment for Statistical Computing. R Foundation for Statistical Computing, Vienna, Austria.

Rahman, M.M., Khan, M.N.I., Hoque, A.K.F., Ahmed, I., 2015. Carbon stock in the Sundarbans mangrove forest: spatial variations in vegetation types and salinity zones. Wetlands Ecol. Manage. 23, 269–283. https://doi.org/10.1007/s11273-014-9379-x.

Rahman, M.S., Sass-Klaassen, U., Zuidema, P.A., Chowdhury, M.Q., Beeckman, H., 2020. Salinity drives growth dynamics of the mangrove tree Sonneratia apetala Buch.-Ham. in the Sundarbans, Bangladesh. Dendrochronologia. 62, 125711 https://doi.org/10.1016/j.dendro.2020.125711.

Rao, R.G., Woitchik, A.F., Goeyens, L., van Riet, A., Kazungu, J., Dehairs, F., 1994. Carbon, nitrogen contents and stable carbon isotope abundance in mangrove leaves from an east African coastal lagoon (Kenya). Aquat. Bot. 47, 175–183. https://doi.org/10.1016/0304-3770(94)90012-4.

Rath, K.M., Rousk, J., 2015. Salt effects on the soil microbial decomposer community and their role in organic carbon cycling: a review. Soil Biol. Biochem. 81, 108–123. https://doi.org/10.1016/j.soilbio.2014.11.001.

Rau, B.M., Melvin, A.M., Johnson, D.W., Goodale, C.L., Blank, R.R., Fredriksen, G., Miller, W.W., Murphy, J.D., Todd, D.E.J., Walker, R.F., 2011. Revisiting soil carbon and nitrogen sampling: quantitative pits versus rotary cores. Soil Science. 176, 273–279. https://doi.org/10.1097/SS.0b013e31821d6d4a.

Ray, R., Baum, A., Rixen, T., Gleixner, G., Jana, T.K., 2018. Exportation of dissolved (inorganic and organic) and particulate carbon from mangroves and its implication to the carbon budget in the Indian Sundarbans. Sci. Total Environ. 621, 535–547. https://doi.org/10.1016/j.scitotenv.2017.11.225.

Ray, R., Ganguly, D., Chowdhury, C., Dey, M., Das, S., Dutta, M.K., Mandal, S.K., Majumder, N., De, T.K., Mukhopadhyay, S.K., Jana, T.K., 2011. Carbon sequestration and annual increase of carbon stock in a mangrove forest. Atmos. Environ. 45, 5016–5024. https://doi.org/10.1016/j.atmosenv.2011.04.074.

Ren, H., Jian, S., Lu, H., Zhang, Q., Shen, W., Han, W., Yin, Z., Guo, Q., 2008. Restoration of mangrove plantations and colonisation by native species in Leizhou bay, South China. Ecol. Res. 23, 401–407. https://doi.org/10.1007/s11284-007-0393-9.

Rogers, K., Kelleway, J.J., Saintilan, N., Megonigal, J.P., Adams, J.B., Holmquist, J.R., Lu, M., Schile-Beers, L., Zawadzki, A., Mazumder, D., Woodroffe, C.D., 2019. Wetland carbon storage controlled by millennial-scale variation in relative sea-level rise. Nature. 567, 91–95. https://doi.org/10.1038/s41586-019-0951-7.

Rogers, K.G., Goodbred, S.L., Mondal, D.R., 2013. Monsoon sedimentation on the 'abandoned' tide-influenced Ganges-Brahmaputra delta plain. Estuar. Coast. Shelf Sci. 131, 297–309. https://doi.org/10.1016/j.ecss.2013.07.014.

Rovai, A.S., Twilley, R.R., Castañeda-Moya, E., Riul, P., Cifuentes-Jara, M., Manrow-Villalobos, M., Horta, P.A., Simonassi, J.C., Fonseca, A.L., Pagliosa, P.R., 2018. Global controls on carbon storage in mangrove soils. Nat. Climate Change. 8, 534–538. https://doi.org/10.1038/s41558-018-0162-5.

Rudra, K., 2014. Changing river courses in the western part of the Ganga-Brahmaputra delta. Geomorphology. 227, 87–100. https://doi.org/10.1016/j.geomorph.2014.05.013.

Sanderman, J., Hengl, T., Fiske, G., Solvik, K., Adame, M.F., Benson, L., Bukoski, J.J., Carnell, P., Cifuentes-Jara, M., Donato, D., Duncan, C., Eid, E.M., Ermgassen, P.Z., Lewis, C.J.E., Macreadie, P.I., Glass, L., Gress, S., Jardine, S.L., Jones, T.G., Nsombo, E.N., Rahman, M.M., Sanders, C.J., Spalding, M., Landis, E., 2018. A global map of mangrove forest soil carbon at 30 m spatial resolution. Environ. Res. Lett. 13 https://doi.org/10.1088/1748-9326/aabe1c.

Sarker, S.K., Deb, J.C., Halim, M.A., 2011. A diagnosis of existing logging bans in Bangladesh. Int. For. Rev. 13, 461–475. https://doi.org/10.1505/146554811798811344.

Sarker, S.K., Matthiopoulos, J., Mitchell, S.N., Ahmed, Z.U., Mamun, M.B.A., Reeve, R., 2019a. 1980s–2010s: The world's largest mangrove ecosystem is becoming homogeneous. Biol. Conserv. 236, 79–91. https://doi.org/10.1016/j.biocon.2019.05.011.

Sarker, S.K., Reeve, R., Paul, N.K., Matthiopoulos, J., 2019b. Modelling spatial biodiversity in the world's largest mangrove ecosystem—The Bangladesh Sundarbans: a baseline for conservation. Divers. Distrib. 25, 729–742. https://doi.org/10.1111/ddi.12887.

Sarker, S.K., Reeve, R., Thompson, J., Paul, N.K., Matthiopoulos, J., 2016. Are we failing to protect threatened mangroves in the Sundarbans world heritage ecosystem? Sci. Rep. 6 https://doi.org/10.1038/srep21234.

Setia, R., Gottschalk, P., Smith, P., Marschner, P., Baldock, J., Setia, D., Smith, J., 2013. Soil salinity decreases global soil organic carbon stocks. Sci. Total Environ. 465, 267–272. https://doi.org/10.1016/j.scitotenv.2012.08.028.

Siddiqi, N.A., 2001. Mangrove forestry in Bangladesh. Institute of Forestry & Environmental Sciences, University of Chittagong, Chittagong, Bangladesh, pp. 301.

Spivak, A.C., Sanderman, J., Bowen, J.L., Canuel, E.A., Hopkinson, C.S., 2019. Global-change controls on soil-carbon accumulation and loss in coastal vegetated ecosystems. Nat. Geosci. 12, 685–692. https://doi.org/10.1038/s41561-019-0435-2.

Syvitski, J.P.M., Milliman, J.D., 2007. Geology, geography, and humans battle for dominance over the delivery of fluvial sediment to the coastal ocean. J. Geol. 115, 1–19. https://doi.org/10.1086/509246.

Taillardat, P., Friess, D.A., Lupascu, M., 2018. Mangrove blue carbon strategies for climate change mitigation are most effective at the national scale. Biol. Lett. 14, 20180251. https://doi.org/10.1098/rsbl.2018.0251.

Twilley, R.R., Castañeda-Moya, E., Rivera-Monroy, V.H., Rovai, A., 2017. Productivity and carbon dynamics in mangrove wetlands. In: Rivera-Monroy, V.H., Lee, S.Y., Kristensen, E., Twilley, R.R. (Eds.), Mangrove Ecosystems: A Global Biogeographic Perspective: Structure, Function, and Services. Springer International Publishing, Cham, pp. 113–162. https://doi.org/10.1007/978-3-319-62206-4_5.

Twilley, R.R., Rovai, A.S., Riul, P., 2018. Coastal morphology explains global blue carbon distributions. Front. Ecol. Environ. 16, 503–508. https://doi.org/10.1002/fee.1937.

Tyagi, N.K., Sen, H.S., 2019. Development of Sundarbans through estuary management for augmenting freshwater supply, improved drainage and reduced bank erosion. In: Sen, H.S. (Ed.), The Sundarbans: A Disaster-Prone Eco-Region: Increasing Livelihood

Security. Springer International Publishing, Cham, pp. 375–402. https://doi.org/10.1007/978-3-030-00680-8_13.
Wang, G., Guan, D., Peart, M.R., Chen, Y., Peng, Y., 2013. Ecosystem carbon stocks of mangrove forest in Yingluo Bay, Guangdong Province of South China. For. Ecol. Manage. 310, 539–546. https://doi.org/10.1016/j.foreco.2013.08.045.
Weiss, C., Weiss, J., Boy, J., Iskandar, I., Mikutta, R., Guggenberger, G., 2016. Soil organic carbon stocks in estuarine and marine mangrove ecosystems are driven by nutrient colimitation of P and N. Ecol. Evol. 6, 5043–5056. https://doi.org/10.1002/ece3.2258.
Wickham, H., 2016. ggplot2: Elegant Graphics for Data Analysis. Springer-Verlag, New York.
Więski, K., Guo, H., Craft, C.B., Pennings, S.C., 2010. Ecosystem functions of tidal fresh, brackish, and salt marshes on the Georgia coast. Estuaries Coasts. 33, 161–169. https://doi.org/10.1007/s12237-009-9230-4.
Wong, V.N.L., Dalal, R.C., Greene, R.S.B., 2009. Carbon dynamics of sodic and saline soils following gypsum and organic material additions: a laboratory incubation. Appl. Soil Ecol. 41, 29–40. https://doi.org/10.1016/j.apsoil.2008.08.006.
Wong, V.N.L., Greene, R.S.B., Dalal, R.C., Murphy, B.W., 2010. Soil carbon dynamics in saline and sodic soils: a review. Soil Use Manage. 26, 2–11. https://doi.org/10.1111/j.1475-2743.2009.00251.x.
Woodroffe, C.D., Rogers, K., McKee, K.L., Lovelock, C.E., Mendelssohn, I.A., Saintilan, N., 2016. Mangrove sedimentation and response to relative sea-level rise. Ann. Rev. Mar. Sci. 8, 243–266. https://doi.org/10.1146/annurev-marine-122414-034025.
Wuest, S.B., 2009. Correction of bulk density and sampling method biases using soil mass per unit area. Soil Sci. Soc. Am. J. 73, 312–316. https://doi.org/10.2136/sssaj2008.0063.
Yando, E.S., Osland, M.J., Willis, J.M., Day, R.H., Krauss, K.W., Hester, M.W., 2016. Salt marsh-mangrove ecotones: using structural gradients to investigate the effects of woody plant encroachment on plant–soil interactions and ecosystem carbon pools. J. Ecol. 104, 1020–1031. https://doi.org/10.1111/1365-2745.12571.
Yang, J., Gao, J., Liu, B., Zhang, W., 2014. Sediment deposits and organic carbon sequestration along mangrove coasts of the Leizhou Peninsula, southern China. Estuar. Coast. Shelf Sci. 136, 3–10. https://doi.org/10.1016/j.ecss.2013.11.020.
Zhao, Q., Bai, J., Lu, Q., Zhang, G., 2017. Effects of salinity on dynamics of soil carbon in degraded coastal wetlands: Implications on wetland restoration. Phys. Chem. Earth, Parts A/B/C. 97, 12–18. https://doi.org/10.1016/j.pce.2016.08.008.
Zhou, G., Xu, S., Ciais, P., Manzoni, S., Fang, J., Yu, G., Tang, X., Zhou, P., Wang, W., Yan, J., Wang, G., Ma, K., Li, S., Du, S., Han, S., Ma, Y., Zhang, D., Liu, J., Liu, S., Chu, G., Zhang, Q., Li, Y., Huang, W., Ren, H., Lu, X., Chen, X., 2019. Climate and litter C/N ratio constrain soil organic carbon accumulation. Natl. Sci. Rev. 6, 746–757. https://doi.org/10.1093/nsr/nwz045.

Table A.1. List of tree species found in the Sundarbans with taxonomy, distribution in salinity zones, inundation condition and succession stage.

Latin name	Local name	Family	Salinity zone	Inundation condition	Succession stage
***Aegiceras corniculatum* (L.) Blanco**	Kholshi	*Primulaceae*	M, P	WL, WH	S
***Aglaia piculate* (Roxb.) Pellegr. ***	Amoor	*Meliace*	O	WH	S
***Avicennia alba* Blume.**	Sada Baen	*Avicenniaceae*	P	WL	Pr
***Avicennia marina* (Forssk.) Vierh.**	Moricha Baen	*Avicenniaceae*	P	WL	Pr
Avicennia officinalis L.	Kala Baen	*Avicenniaceae*	O, M, P	WL	Pr
***Bruguiera gymnorrhiza* (L.) Lam.**	Lal Kakra	*Rhizophoraceae*	O, M, P	WL	S, C
***Bruguiera piculate* (Lour.) Poir.**	Holud Kakra	*Rhizophoraceae*	O, M, P	WL	S, C
***Cerbera manghas* L. ***	Dakur	*Apocynaceae*	O	WO	S
***Ceriops decandra* (Griff.) Ding Hou**	Goran	*Rhizophoraceae*	O, M, P	WO	C
***Cynometra ramiflora* L. ***	Singra	*Fabaceae*	O	WH	S
***Excoecaria agallocha* L.**	Gewa	*Euphorbiaceae*	O, M, P	WH, WO	S
***Excoecaria indica* (Willd.) Muell. Arg. ***	Batul	*Euphorbiaceae*	O	WH	S
***Heritiera fomes* Buch. -Ham.**	Sundri	*Malvaceae*	O, M, P	WO	C
***Hibiscus tiliaceus* L. ***	Bola	*Malvaceae*	O, M	WH	S
***Intsia bijuga* (Colebr.) Kuntze ***	Bhaila	*Fabaceae*	O, M	WH	S
***Kandelia candel* (L.) Druce**	Vatkathi	*Rhizophoraceae*	M, P	WL	S
***Lumnitzera piculat* Willd.**	Kirpa	*Combretaceae*	P	WH, WO	S
Millettia pinnata* (L.) Panigrahi	Karanj	*Fabaceae*	O	WL	S
***Rhizophora piculate* Blume.**	Bhora Jhana	*Rhizophoraceae*	M, P	WL	S
***Rhizophora mucronata* Lamk.**	Jhana Garjan	*Rhizophoraceae*	M, P	WL	S
***Sonneratia apetala* Buch. -Ham.**	Keora	*Lythraceae*	O, M, P	WL	Pr
***Xylocarpus granatum* K.D. Koen.**	Dhundul	*Meliaceae*	M, P	WH	S
***Xylocarpus mekongensis* Pierre.**	Passur	*Meliaceae*	O, M, P	WH, WO	S

*** Indicates mangrove associates according to Tomlinson (2016). Abbreviation: Salinity zone- O = oligohaline, M = Mesohaline, P = Polyhaline. Inundation: WL = Waterlogged during Low tide, WH= Waterlogged during High tide, WO = Waterlogged Occasionally. Successional stage: Pr = Pioneer, S = seral and C = Climax. Source: Siddiqi (2001); Mahmood (2015b); Rahman et al. (2015b); Islam (2016a); Sarker et al. (2016)**

Table A.2 Two-way ANOVA results for SOCD (gm cm^{-3}) in different salinity zones and soil depths.

Source	DF	SS	MSS	F	p
Soil Depth	3	6.4	2.1	30.1	<0.0001
Salinity Zone	2	15.9	7.9	112.3	<0.0001
Soil Depth*Salinity Zone	6	1.5	0.2	3.5	<0.01
Residuals	500	35.5	0.07		

Table A.3 Two-way ANOVA results for Bulk density (gm cm^{-3}) in different salinity zones and soil depths.

Source	DF	SS	MSS	F	p
Soil Depth	3	0.9	0.3	46.2	<0.0001
Salinity Zone	2	0.3	0.2	22.2	<0.0001
Soil Depth*Salinity Zone	6	0.01	0.003	0.5	>0.5
Residuals	500	3.5	0.007		

Table A.4 Two-way ANOVA results for SOC (Mg ha^{-1}) storage in different salinity zones and soil depths.

Source	DF	SS	MSS	F	p
Soil Depth	3	108.7	36.2	526.2	<0.0001
Salinity Zone	2	16.4	8.2	118.9	<0.0001
Soil Depth*Salinity Zone	6	1.4	0.2	3.3	<0.003
Residuals	500	34.4	0.07		

Table A.5 One-way ANOVA result for SOC in different forest types.

Source	DF	SS	MSS	F	p
Forest types	7	5704	8149	3.3	<0.01
Residuals	47	11715	249.3		

Table A.6 Tukey HSD Post-hoc test for the average soil organic carbon (SOC) (Mg ha^{-1}) in different forest types. Different letters indicate significant differences at P<0.05. Data are mean ±Standard Deviation (SD).

Forest Types	SOC (Mg ha^{-1})		
	Mean	± SD	HSD rank
***Bruguiera* spp.**	105.3	3.6	a
***Sonneratia* spp.**	68.7	20.1	ab
***Avicennia* spp.**	67.1	9.3	ab
***Heritiera* spp.**	67.0	13.2	b
MIXED	61.3	28.7	b
***Xylocarpus* spp.**	58.8	4.6	b
***Excoecaria* spp.**	56.3	15.9	b
***Ceriops* spp.**	50.2	9.7	b

Table A.7 PCA (Principal Component Analysis) results based on soil physical and chemical properties and vegetation properties. Bold values correspond highly correlated values (PCs > 0.35) and underlined values represent non-correlated variables with the respective PCs highest loading.

Principal Component	PC1	PC2
Eigenvalue	4.95	1.97
Percentage of total variance (%)	49.5	19.8
Cumulative percentage (%)	49.5	69.3
BD	-0.27	0.02
pH	**-0.36**	0.24
SS	**-0.37**	0.29
TD	-0.33	-0.25
DBH	0.26	**0.49**
H	0.34	**0.38**
E	-0.32	-0.32
C/N	0.21	**-0.40**
LAT	0.33	-0.31
LONG	0.32	-0.17

Table A.8 Step-wise multiple linear regression

Model		Unstandardized coefficient		Standardized coefficient	t	Significance	Lower	Upper
		β	Standard error	Beta				
1	(Intercept)	4.449	0.057		78.161	0.000	4.335	4.563
	Soil Salinity	-0.111	0.015	-0.712	-7.391	0.000	-0.141	-0.081
2	(Intercept)	3.594	0.270		13.330	0.000	3.053	4.135
	Soil Salinity	-0.083	0.016	-0.534	-5.106	0.000	-0.116	-0.050
	Ln (C: N)	0.273	0.085	0.338	3.230	0.002	0.103	0.443
3	(Intercept)	3.439	0.263		13.072	0.000	2.911	3.967
	Soil Salinity	-0.077	0.016	-0.499	-4.972	0.000	-0.109	-0.046
	Ln (C: N)	0.274	0.080	0.339	3.415	0.001	0.113	0.436
	Mean DBH	0.017	0.007	0.220	2.579	0.013	0.004	0.031

Dependent variable: Ln (SOC)

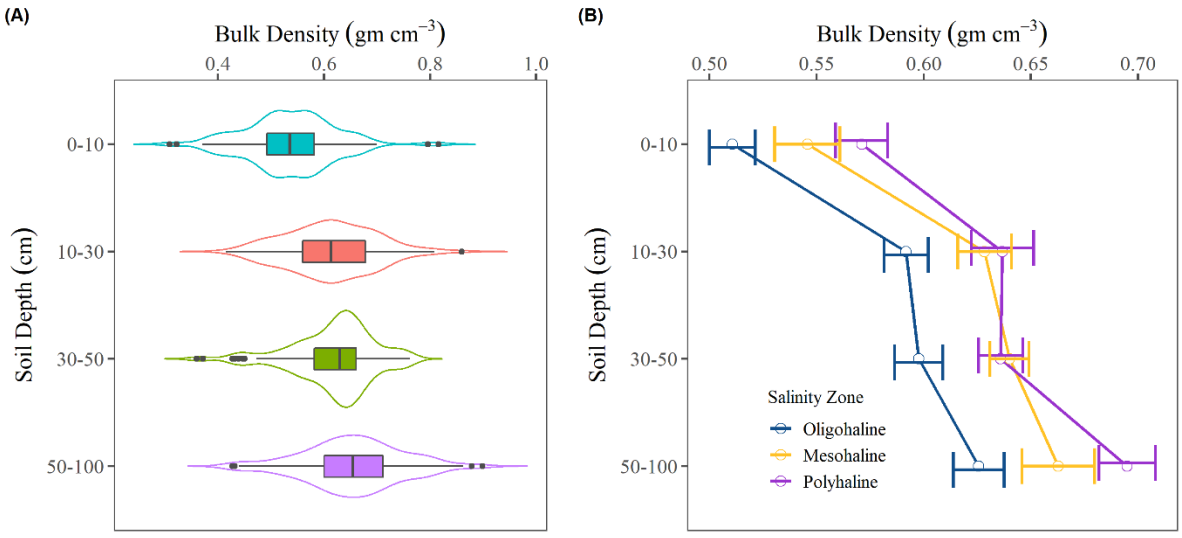

Figure A.1. (A) Integrated violin-box plot shows the distribution of bulk density in four soil depth, where the black dots are outliers. (B) Average bulk density in three salinity zones and four soil depths.

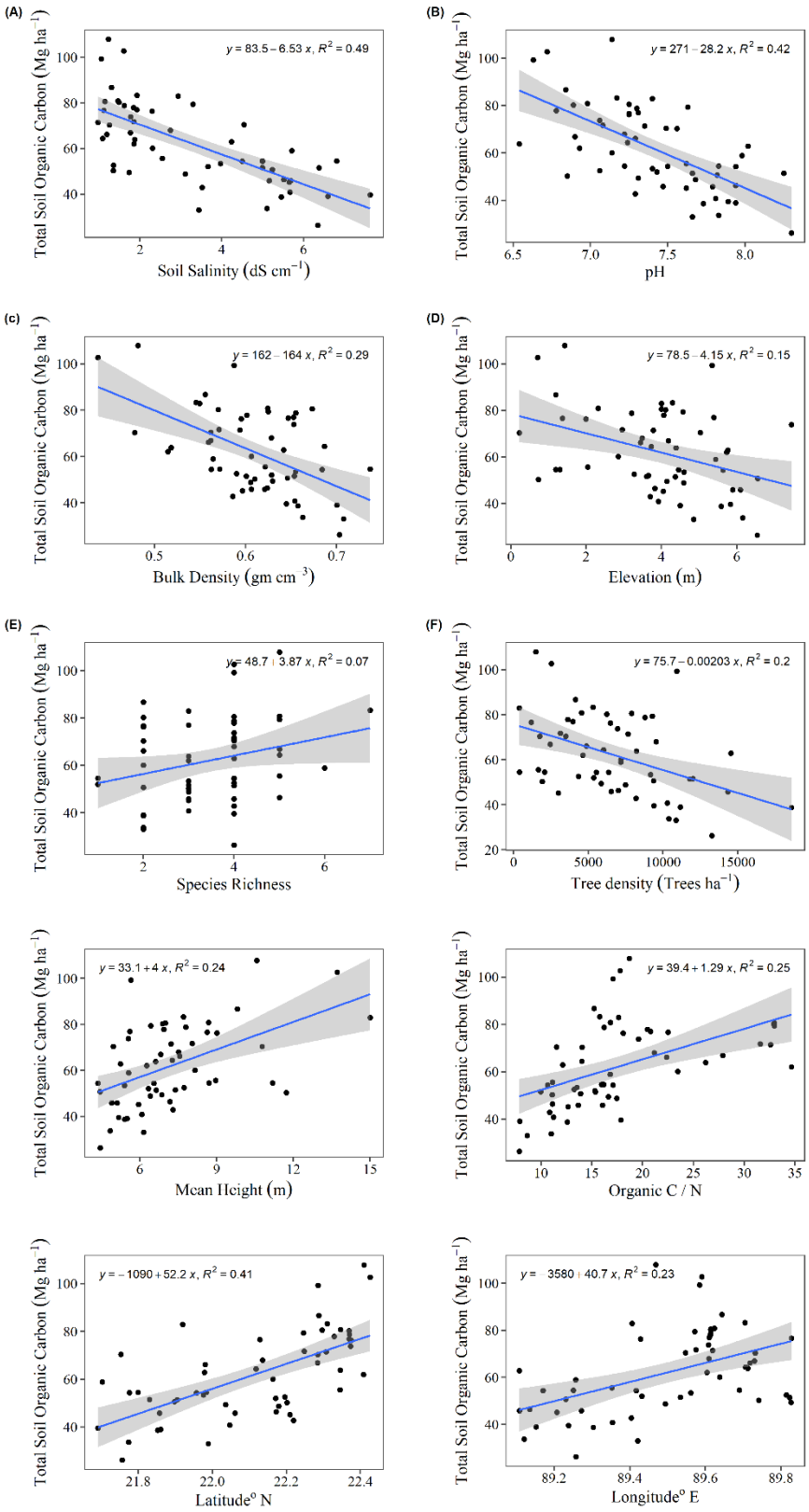

Figure A.2. Bivariate relationship between soil organic carbon with different soil physicochemical, geophysical properties and vegetation characteristics in the Sundarbans.

Appendix B

Biomass estimation in mangrove forests: a comparison of allometric models incorporating species and structural information

IOP Publishing Environ. Res. Lett. 16 (2021) 124002 https://doi.org/10.1088/1748-9326/ac31ee

ENVIRONMENTAL RESEARCH
LETTERS

LETTER

Biomass estimation in mangrove forests: a comparison of allometric models incorporating species and structural information

Md Saidur Rahman[1,2,*], Daniel N M Donoghue[2], Louise J Bracken[3] and Hossain Mahmood[1]

[1] Forestry and Wood Technology Discipline, Khulna University, Khulna 9208, Bangladesh
[2] Department of Geography, Durham University, South Road, DH1 3LE Durham, United Kingdom
[3] Northumbria University, Sutherland Building, Newcastle-upon-Tyne, NE1 8ST, United Kingdom
[*] Author to whom any correspondence should be addressed.

E-mail: msrahman@fwt.ku.ac.bd

Keywords: allometric models, wood density, tree height, aboveground biomass, mangrove forest, Sundarbans

Supplementary material for this article is available online

OPEN ACCESS

RECEIVED
6 July 2021

REVISED
12 October 2021

ACCEPTED FOR PUBLICATION
21 October 2021

PUBLISHED
15 November 2021

Abstract

Improved estimates of aboveground biomass (AGB) are required to improve our understanding of the productivity of mangrove forests to support the long-term conservation of these fragile ecosystems which are under threat from many natural and anthropogenic pressures. To understand how individual species affects biomass estimates in mangrove forests, five species-specific and four genus-specific allometric models were developed. Independent tree inventory data were collected from 140 sample plots to compare the AGB among the species-specific models and seven frequently used pan-tropical and Sundarbans-specific generic models. The effect of individual tree species was also evaluated using model parameters for wood densities (from individual trees to the whole Sundarbans) and tree heights (individual, plot average and plot top height). All nine developed models explained a high percentage of the variance in tree AGB ($R^2 = 0.97$–0.99) with the diameter at breast height and total height (H). At the individual tree level, the generic allometric models overestimated AGB from 22% to 167% compared to the species-specific models. At the plot level, mean AGB varied from 111.36 Mg ha^{-1} to 299.48 Mg ha^{-1}, where AGB significantly differed in all generic models compared to the species-specific models ($p < 0.05$). Using measured species wood density (WD) in the allometric model showed 4.5%–9.7% less biomass than WD from published databases and other sources. When using plot top height and plot average height rather than measured individual tree height, the AGB was overestimated by 19.5% and underestimated by 8.3% ($p < 0.05$). The study demonstrates that species-specific allometric models and individual tree measurements benefit biomass estimation in mangrove forests. Tree level measurement from the inventory plots, if available, should be included in allometric models to improve the accuracy of forest biomass estimates, particularly when upscaling individual trees up to the ecosystem level.

1. Introduction

There has been a global effort to develop accurate and efficient methods to quantify aboveground carbon (measured as biomass) in mangrove forests (Hutchison *et al* 2014, Ni-Meister 2015, Baccini *et al* 2017, Lagomasino *et al* 2019). A range of remote sensing (RS) technologies can indirectly infer forest biomass but field data are needed to calibrate and validate products (Gibbs *et al* 2007, Chave *et al* 2019, Réjou-Méchain *et al* 2019). Destructive harvesting of trees provides the most precise estimates of aboveground biomass (AGB), yet is impractical, laborious, costly and often illegal (Komiyama *et al* 2008, Edwards *et al* 2019) and so mathematical models have been developed to estimate tree biomass from easily measured biophysical parameters (tree diameter at breast height (DBH), height (H), or wood density (WD)) (Brown 1997, Komiyama *et al* 2005, Picard *et al* 2012, Chave *et al* 2014). These models are known

as allometric models. However, this method of estimation can yield a large degree of uncertainty scaling up from individual tree biomass to plot and forest-level as uncertainties associated with individual trees are propagated (van Breugel *et al* 2011, Petrokofsky *et al* 2012, Réjou-Méchain *et al* 2019). The choice of appropriate allometric model is therefore critical to reduce uncertainties in the estimation of forest biomass.

All allometric models have limitations since they are based on a limited number of destructively sampled trees and often the sample locations are unrepresentative of forest heterogeneity (Weiskittel *et al* 2015, Hickey *et al* 2018). These models also introduce an uncertainty when applied to species without the destructive sample (Mitchard *et al* 2013, Ngomanda *et al* 2014, Mahmood *et al* 2019). For example, de Souza Pereira *et al* (2018) found AGB estimation errors between minus 18% and plus 14% when using biome-specific allometries rather than species-specific ones in Brazilian mangrove forests. On the other hand, a few studies have shown that generic models can outcompete locally developed ones (Rutishauser *et al* 2013, Stas *et al* 2017). Uncertainties also arise from inappropriate use of regression models without considering collinearity of parameters, uncritical use of model dredging and inappropriate criteria for model selection (Sileshi 2014, Vorster *et al* 2020). Recently published global and continental AGB estimates contain errors due to an under representative sample size and the exclusion of the climatic regime, geophysical and geomorphological variables, which are key to understanding the spatial distribution of biomass (Rovai *et al* 2016). Inclusion of biophysical parameters such as WD and tree height can help to capture geographical heterogeneity and also act as a suitable proxy of environmental drivers such as variation in salinity which affects the growth rate, WD, species composition and tree height (Mahmood *et al* 2019, Rahman *et al* 2020, 2021, Virgulino-Júnior *et al* 2020).

Although WD is an important variable for assessing carbon content, it is rarely measured during field inventories. Most studies identify species and then use published WD values from a database of generic values (Njana *et al* 2016, Réjou-Méchain *et al* 2019). Using the same, or grouped, WD in the allometric model tends to smooth species-level variations in AGB (Mitchard *et al* 2013, Ni-Meister 2015). The inclusion of tree height has a large effect on individual tree and forest AGB (Feldpausch *et al* 2012). Any errors introduced during individual tree height measurements can originate from the choice of methods and/or instruments and can be propagated as estimates are scaled up (Larjavaara and Muller-Landau 2013). For example, the use of height–diameter (*H–D*) models, developed from the height and stem diameter of individual trees, often exhibit uncertainty due to wider height-variation at different spatial scales (Feldpausch *et al* 2011, Vieilledent *et al* 2012). Space-borne and air-borne LiDAR and RADAR technologies can improve the accuracy of the height measurement and have been used to develop canopy height models (Fatoyinbo *et al* 2021).

The Sundarbans mangrove forest is one of the largest and most bio-diverse mangroves in the world, located between Bangladesh and India. It contains the highest carbon densities (345 Mg ha^{-1}) in both above- and below-ground among all forests in Bangladesh (GOB 2019, Henry *et al* 2021). The Bangladesh Forest Department estimated carbon stocks in the Sundarbans in 2009 and 2015 using pan-tropical allometric models and Sundarbans-specific generic models (BFD 2010, Rahman *et al* 2015, Mahmood *et al* 2019, Henry *et al* 2021). Other studies such as Kamruzzaman *et al* (2017) and Azad *et al* (2020) used pan-tropical generic models to estimate AGB in selected areas. However, species-specific allometric models are not yet available to estimate AGB in the Sundarbans. Therefore, it is timely to examine whether species-specific allometric models using measured wood densities and tree heights can yield more accurate estimates of AGB in the Sundarbans and in mangrove forests more generally. The aim of this paper is to report research that compares a range of sources of uncertainty in allometric models, WD, and height measurement for AGB in the Sundarbans mangrove forest, Bangladesh. First, the study compares site- and species-specific AGB between the Sundarbans and pan-tropical generic allometric models for variability of aboveground tree biomass. Secondly, the study determines variability of AGB in the Sundarbans by comparing measured and published WD values at multiple spatial scales. Thirdly, the study quantifies the impact of different methods of tree height determination on estimates of AGB in mangrove forests.

2. Material and methods

2.1. Study area

The Bangladesh Sundarbans is situated between 21°30′ N and 22°30′ N and 89°00′ E and 89°55′ E in the lower delta plain of the Ganges–Brahmaputra–Meghna delta covering an area of 6017 km^2 (figure 1) (Giri *et al* 2011, Aziz and Paul 2015, Sarker *et al* 2016). The forest is of international significance as a Ramsar and UNESCO World Heritage site. It provides a number of valuable ecosystem services such as protecting inland areas from storms and tidal surges (Barua *et al* 2020). The near-constant mean annual minimum and maximum temperature (29 °C–31 °C) and high annual rainfall (1474–2265 mm) made the climate of the Sundarbans warm and humid between 1948 and 2011 (Chowdhury *et al* 2016, Sarker *et al* 2016). The soil is fine-gained silt and clay and slightly calcareous (Siddiqi 2001). The Sundarbans has a distinct salinity zonation with the high salinity zone in the

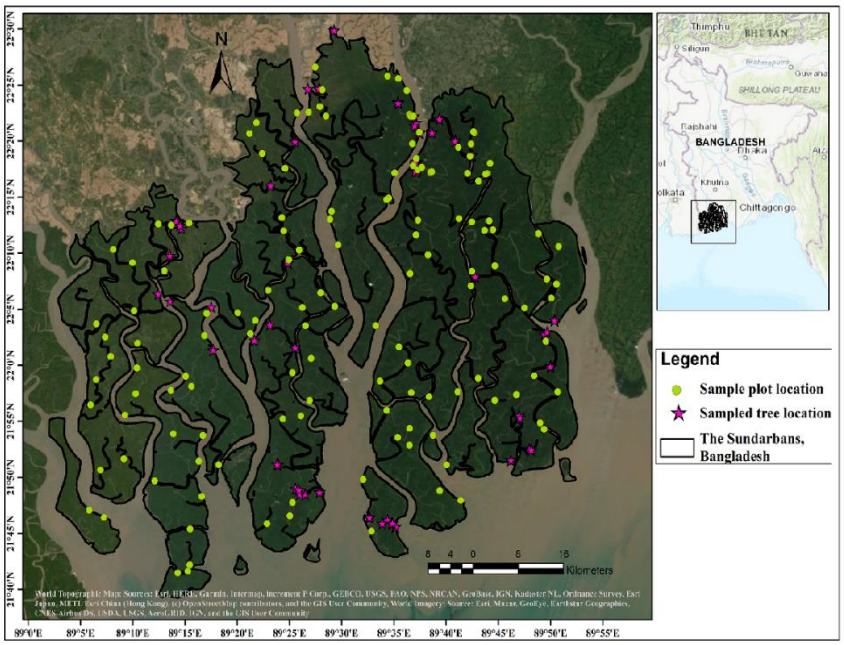

Figure 1. Sample plot location in the Sundarbans mangrove forest, Bangladesh. The pink star indicates tree location by Mahmood *et al* (2019).

west (polyhaline) to low salinity zone (oligohaline) in the east along with medium salinity zone (mesohaline) between (Siddiqi 2001, Chanda *et al* 2016). Salinity regulates the geomorphology and hydrological characteristics and also the morphology, growth and distribution of plant species (Sarker *et al* 2016, 2019a, Rahman *et al* 2020, 2021).

2.2. Allometric models in the Sundarbans

Species-specific allometric models are not available for all species in the Sundarbans as destructive sampling was not permitted due to an imposed felling moratorium of all species since 1989 (Mahmood *et al* 2019). However, four species-specific models were developed through destructive sampling in the Bangladesh Sundarbans (table 1). Three generic allometric models were recently developed for 14 species by using semi-destructive sampling methods where biomass of stems and larger branches were measured through volume and WD, and small branches and foliage through weighing after pruning (Mahmood *et al* 2019). Published pan-tropical models have also been used to estimate biomass in the Sundarbans (Rahman *et al* 2015, Kamruzzaman *et al* 2017, 2018).

2.3. Development of species-specific allometric model

A conceptual diagram of the research methodology is presented in the figure 2. The species-specific allometric models were developed from the semi-destructive sampling data (324 individuals, 13 species, except *Sonneratia caseolaris*) from Mahmood *et al* (2019), where AGB (kg/tree) was presented along with DBH and total height (H) (figure 1). Species-specific models for *S. caseolaris* were not developed as the independent tree inventory data did not have any individuals of this species. Out of 13 species, eight species (*Avicennia officinalis, Avicennia marina, Bruguiera gymnorrhiza, Bruguiera sexangula, Rhizophora apiculata, Rhizophora mucronata, Xylocarpus granatum* and *Xylocarpus moluccensis*) were merged into genus level to yield sufficient data for model fitting. Therefore, nine allometric models were developed for *Aglaia cucullata, Avicennia* sp., *Bruguiera* sp., *Excoecaria agallocha, Heritiera fomes, Lumnitzera racemosa, Rhizophora* sp., *Sonneratia apetala*, and *Xylocarpus* sp.

Log-linear ordinary least square regression was used to fit models to predict AGB for each species. The choice of log-linear regression over nonlinear regression was done by comparing error distribution of biomass. According to Xiao *et al* (2011), the linear regression of log-transformed data better characterizes multiplicative, heteroscedastic and lognormal error, whereas the nonlinear regression performs additive, homoscedastic, normal error. The goodness of fit of two models were compared and the lower value of Akaike's information criterion (AIC)

Table 1. Allometric models used for measuring aboveground biomass in the Sundarbans.

Model no.	Site, species	Allometric model	*N*	Identity in this paper and source
Bangladesh Sundarbans and species-specific				
1	*Aegialitis rotundifolia*	$AGB = 5.49GCH^2 - 251.36\,H - 0.07\,HCH + 0.75(GCH \times H \times HCH)$	29	Siddique *et al* (2012)
2	*Aegiceras corniculatum*	$\sqrt{AGB} = 0.48\,DBH - 0.13$	50	Mahmood *et al* (2016b)
3	*Ceriops decandra*	$AGB = 4.70\,GCH^{2.41}$	48	Mahmood *et al* (2012)
4	*Kandelia candel*	$AGB = 0.21\,DBH^2 + 0.12$	25	(Mahmood *et al* 2016a)
Bangladesh Sundarbans and generic model				
5	For 14 species *Aglaia cucullata*, *Avicennia officinalis*, *Avicennia marina*, *Bruguiera gymnorrhiza*, *Bruguiera sexangula*, *Excoecaria agallocha*, *Heritiera fomes*, *Lumnitzera racemosa*, *Rhizophora apiculata*, *Rhizophora mucronata*, *Sonneratia apetala*, *Sonneratia caseolaris*, *Xylocarpus granatum*, *Xylocarpus moluccensis*	$\ln(AGB) = -1.9272 + 2.3517\ln(DBH)$	260	Mahmood_2019_D (Mahmood *et al* 2019)
6		$\ln(AGB) = -2.4317 + 2.1341\ln(DBH) + 0.4953\ln(H)$	260	Mahmood_2019_DH (Mahmood *et al* 2019)
7		$\ln(AGB) = -6.7189 + 2.1634\ln(DBH) + 0.3752\ln(H) + 0.6895\ln(WD)$	260	Mahmood_2019_DHW (Mahmood *et al* 2019)
World or pantropical and generic model				
8	Pantropical, all species	$AGB = 0.0673 \times (WD \times DBH^2 \times H)^{0.976}$	4004	Chave_2014_DHW (Chave *et al* 2014)
9	Pan-tropical, mangrove species	$AGB = 0.0509 \times (WD \times DBH^2 \times H)$	84	Chave_2005_DHW (Chave *et al* 2005)
10	Pan-tropical, mangrove species	$AGB = WD \times \exp(-1.349 + 1.980\ln(DBH) + 0.207(\ln(DBH))^2 - 0.0281(\ln(DBH))^3)$	84	Chave_2005_DW (Chave *et al* 2005)
11	South-east Asia, mangrove species	$AGB = 0.251 \times WD \times DBH^{2.46}$	104	Komiyama_2005_DW (Komiyama *et al* 2005)

Here AGB = total above ground biomass (kg), *N* = number of destructive/semi-destructive samples, DBH = diameter at breast height (cm), H = total height (m), WD = wood density (gm cm^{-3}, model-7: kg m^{-3}), GCH = girth at collar height (cm), HCH = height of collar girth point (m).

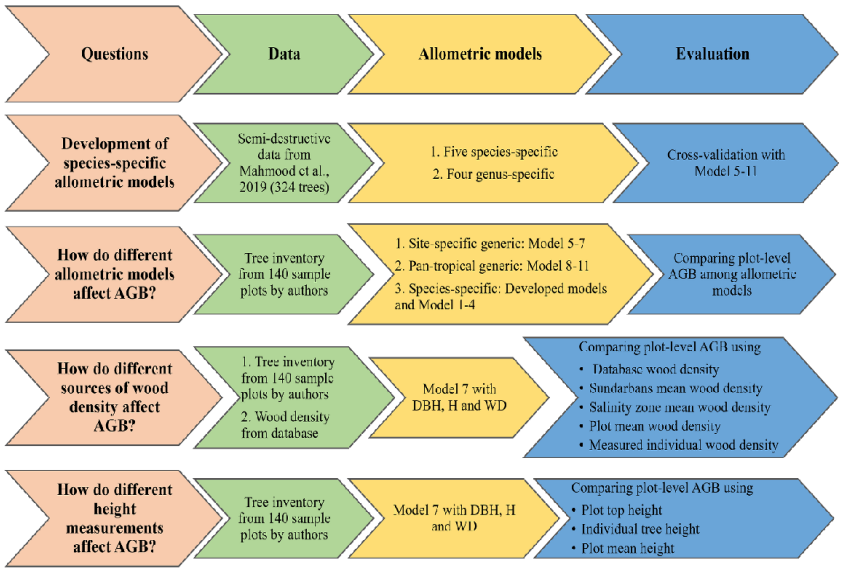

Figure 2. Conceptual diagram of the research methodology. The model numbers are labeled according to table 1. Here, DBH: diameter at breast height, H: height and WD: wood density.

provides significantly better fit when the magnitude of the difference of AIC is greater than 2 (Burnham and Anderson 2002). These two models were compared for all species following Xiao *et al* (2011). In all cases, the log-linear regression provided significantly better fit (table A.1 available online at stacks.iop.org/ERL/16/124002/mmedia). Therefore, the following six log-linear regression models were used to fit AGB as the dependent variable, and DBH and tree height (H) as independent variables

$$\text{E1: } \ln(\text{AGB}) = \ln(a) + \text{bln}(\text{DBH})$$
$$\text{E2: } \ln(\text{AGB}) = \ln(a) + \text{bln}(\text{H})$$
$$\text{E3: } \ln(\text{AGB}) = \ln(a) + \text{bln}(\text{DBH} \times \text{H})$$
$$\text{E4: } \ln(\text{AGB}) = \ln(a) + \text{bln}(\text{DBH}^2 \times \text{H})$$
$$\text{E5: } \ln(\text{AGB}) = \ln(a) + \text{bln}(\text{DBH} \times \text{H}^2)$$
$$\text{E6: } \ln(\text{AGB}) = \ln(a) + \text{bln}(\text{DBH}) + \text{cln}(\text{H}).$$

The underlying assumptions for the regression analysis such as normality of residuals and heteroscedasticity were used to judge the suitability of each regression model. Percent relative standard errors (PRSEs) of each regression coefficient was measured according to Sileshi (2014), where PRSE > 25 is considered an unreliable model. The multicollinearity of each model was measured with the variance inflation factor (VIF), where VIF > 5 indicates high collinearity among independent variables. Due to high multicollinearity, complex models with more independent variables were not considered in this study. After obtaining the eligible potential models for each species, the best models were selected by the lowest second-order Akaike information criterion (AICc) and residual standard error (RSE), and the highest Akaike information criterion weight (AICw) and coefficient of determination (R^2) values (Picard *et al* 2012, Sileshi 2014, Mahmood *et al* 2019, 2020). Models with non-significant parameter of estimates were not considered regardless of meeting the criteria outlined. Since, the AICw provides the likelihood of each model to be the best, it was given highest priority compared with other parameters (Sileshi 2014). For all models, the correction factor was calculated to minimize systematic bias while converting biomass from ln scale to normal scale (Sprugel 1983). The K-fold cross-validation technique was used to validate the best model. This technique randomly divides the original dataset into K subsets (ten in this case) of equal sizes, where each subset is validated with $K - 1$ subsets (James *et al* 2013). The K-fold validation technique was also run for Sundarbans-specific and pantropical generic model (Model no. 7–11 in table 1) to measure tree level variability in AGB in the Sundarbans.

2.4. Tree inventory

Aboveground tree data were collected from 140 random sample plots within the Bangladesh Sundarbans (figure 1). Out of 140 sample plots, 120 plots were randomly placed within permanent sample plot (PSP) (20 × 100 m) established by the Bangladesh Forest Department whilst the remaining 20 plots were outside of the PSP. These sample plots are distributed to all 55 compartments in the Bangladesh Sundarbans covering all three salinity zones (oligohaline, mesohaline and polyhaline) and forest types (Iftekhar and

Saenger 2008, Sarker *et al* 2019b). Each plot consists of a circular plot with the radius of 11.3 m (400 m^2) for measuring bigger trees (DBH > 14.5 cm) and a smaller circular plot within this of 5 m radius (79 m^2) for smaller trees (DBH > 2.5–14.5 cm) (figure A.1). After establishing the plots, all individual trees (DBH > 2.5 cm) were marked, and DBH and total height (H) measured by using a diameter tape and a Vertex III hypsometer (Haglöf, Sweden), respectively. Haglöf wood increment borer (5.15 mm diameter and 300 mm bit length) was used to collect woody specimen at DBH point to determine the WD of studied species according to Wiemann and Williamson (2013). The WD (gm cm^{-3}) was then measured from the volume and dry mass of the specimen. The cylindrical volume was measured in the field from the diameter and length of the specimen and brought to the laboratory for oven-drying at 105 °C until constant weight.

2.5. Variability of AGB in the Sundarbans

The magnitude and patterns of differences in AGB at plot level in the Sundarbans were compared by using different allometric models with an independent set of collected inventory data from the Sundarbans. Plot level AGB variability was measured by actual AGB difference (Mg ha^{-1}), absolute difference (Mg ha^{-1}) and relative absolute difference (%) among different allometric models.

2.5.1. AGB variability with allometric models

Measured DBH, H and WD were used in the species-specific allometric models and other site-specific and pan-tropical generic models (Model 7–11 in table 1) to assess AGB at the individual tree level. In order to compute plot-level AGB estimation per hectare (Mg ha^{-1}), a hectare expansion factor (HEF) for each stem was used according to the size of the sample plot (i.e. HEF = 25 for bigger plots, and HEF = 126.58 for smaller sub-plot) and subsequently summed up all tree biomass in each plot to get plot biomass. To estimate biomass from the species-specific models, the developed nine species-specific models were used alongside four published species-specific models (Model 1–4 in table 1). If no species-specific allometric model was available, models for similar genus or family level were applied. Since measuring the girth at collar height (GCH) for *Ceriops decandra* and *Aegialitis rotundifolia* is laborious and time consuming, DBH was measured in the field and subsequently converted to GCH from the developed relationship between DBH and GCH of 50 individuals (figure A.2).

2.5.2. AGB variability with WD

Variation of tree AGB was compared with measured and databases-sourced WD obtained from published WD databases including the global WD database (Chave *et al* 2009, Zanne *et al* 2009), World Agroforestry's tree functional attributes and ecological databases (ICRAF 2016) and from Bangladesh Forest Research Institute (Sattar *et al* 1995). The Sundarbans-specific generic allometric model (Model 7: Mahmood_2019_DHW) was used for comparison of AGB from multiple WD sources. If there was no measured WD for any species, the WD from the same genus or family was used. Instead of applying species WD, plot-level mean WD, salinity zone WD and Sundarbans level WD were used to investigate how the spatial scale of WD variation on AGB estimates in the Sundarbans. To measure salinity zone mean WD, measured WD were averaged according to three salinity zones in the Sundarbans according to Rahman *et al* (2021).

2.5.3. AGB variability with tree height

To derive the variation of AGB from different height measurement, mean height and maximum height from each plot was used in Model 7 (Mahmood_2019_DHW). The Model 7 was used in this case as it is originated from the Sundarbans and it contains both H and WD parameters.

2.6. Statistical analysis

All statistical analysis and graphics used R4.0.4 for Windows in RStudio Version-1.4.1106 (R Core Team 2020). The normality of residuals, heteroscedasticity and multicollinearity of each regression model were tested with Shapiro–Wilk normality test by using 'R stats' base package, studentized Breusch–Pagan test by using 'lmtest' package and VIF test using 'car' package, respectively (Zeileis and Hothorn 2002, Fox and Weisberg 2019). AICc for fitted regression model was assessed by 'MuMIn' package (Bartoń 2020). *K*-fold cross validation was run using 'caret' package and model accuracy was compared with mean absolute error (MAE) and root mean squared error (Kuhn 2008). Pairwise comparison of tree AGB between the species-specific and other models were tested either by paired *t*-test if the underlying assumptions such as normality and heteroscedasticity were met; otherwise, Wilcoxon signed-rank non-parametric test was used. The 'rstatix' package was used for Wilcoxon signed-rant test and 'R stats' base package was used for paired *t*-test (Kassambara 2020). The graphical output was generated using the 'ggplot2' 'ggeffects' and 'cowplot' package (Wickham 2016, Lüdecke 2018, Wilke *et al* 2019).

3. Results

3.1. Species-specific allometric model

Out of 54 log-linear regression models for nine species, 26 models passed all four criteria including normality of residuals, heteroscedasticity, PRSE and VIF (table A.2). These 26 models were then fitted species-wise to the 324 semi-destructively harvested tree dataset with DBH and H: *A. cucullata* (19),

Table 2. Regression results for all species-specific allometric models in the Sundarbans.

Species	Eq. no.	Model, ln (AGB) =	a^*	b	c	Adj. R^2	RSE	AICc	AIC_W	CF
Aglaia cucullata	**E1**	**$\ln(a) + b \ln$ (DBH)**	−1.9066	2.3784	—	0.9915	0.1047	−26.3501	1.00	1.0055
	E5	$\ln(a) + b \ln$ (DBH × H^2)	3.7114	1.0918	—	0.9585	0.2316	3.8164	0.00	1.0980
	E2	$\ln(a) + b \ln$ (H)	4.5892	3.7109	—	0.8554	0.4324	27.5502	0.00	1.0272
Avicennia sp.	**E1**	**$\ln(a) + b \ln$ (DBH)**	−1.5554	2.2069	—	0.9781	0.2287	0.0103	0.81	1.0265
	E4	$\ln(a) + b \ln$ (DBH^2 × H)	−2.7625	0.9520	—	0.9765	0.237	2.8854	0.19	1.0285
Bruguiera sp.	**E1**	**$\ln(a) + b \ln$ (DBH)**	−1.4473	2.2870	—	0.9845	0.1926	−9.3234	1.00	1.0187
	E3	$\ln(a) + b \ln$ (DBH × H)	−2.7982	1.5246	—	0.9649	0.2901	16.0743	0.00	1.0430
	E5	$\ln(a) + b \ln$ (DBH × H^2)	−3.1823	1.1004	—	0.9178	0.4439	42.4386	0.00	1.1035
Excoecaria agallocha	**E4**	**$\ln(a) + b \ln$ (DBH^2 × H)**	−2.5721	0.8623	—	0.9903	0.1539	−26.9780	1.00	1.0119
	E3	$\ln(a) + b \ln$ (DBH × H)	−2.9335	1.4173	—	0.9801	0.2200	−1.9475	0.00	1.0245
	E5	$\ln(a) + b \ln$ (DBH × H^2)	−3.3198	1.0359	—	0.9591	0.3152	50.1953	0.00	1.0509
	E2	$\ln(a) + b \ln$ (H)	−4.0227	3.6582	—	0.8558	0.5919	67.3342	0.00	1.1915
Heritiera fomes	**E1**	**$\ln(a) + b \ln$ (DBH)**	−1.9944	2.4603	—	0.9931	0.1434	−97.2721	1.00	1.0103
Lumnitzera racemosa	**E1**	**$\ln(a) + b \ln$ (DBH)**	−2.1151	2.4187	—	0.9858	0.1342	−8.8255	0.94	1.0090
	E4	$\ln(a) + b \ln$ (DBH^2 × H)	−3.2562	1.0631	—	0.9783	0.1663	−3.2570	0.06	1.0139
	E3	$\ln(a) + b \ln$ (DBH × H)	−4.0458	1.8671	—	0.9558	0.2373	5.9931	0.00	1.0286
	E5	$\ln(a) + b \ln$ (DBH × H^2)	−4.9734	1.4650	—	0.8994	0.3579	16.6722	0.00	1.0661
Rhizophora sp.	**E4**	**$\ln(a) + b \ln$ (DBH^2 × H)**	−2.3744	0.8953	—	0.9467	0.2226	2.8788	0.82	1.0251
	E3	$\ln(a) + b \ln$ (DBH × H)	−2.8960	1.5009	—	0.9358	0.2443	6.0407	0.17	1.0303
	E5	$\ln(a) + b \ln$ (DBH × H^2)	−3.4321	1.1161	—	0.9065	0.2948	12.4334	0.01	1.0444
Sonneratia apetala	**E4**	**$\ln(a) + b \ln$ (DBH^2 × H)**	−2.8869	0.9170	—	0.9938	0.1633	−10.3304	0.71	1.0134
	E6	$\ln(a) + b \ln$ (DBH) + $c \ln$(H)	−2.6715	1.9068	0.7430	0.9939	0.1625	−8.5123	0.29	1.0133
	E3	$\ln(a) + b \ln$ (DBH × H)	−3.6314	1.5533	—	0.9854	0.2518	6.9904	0.00	1.0322
	E5	$\ln(a) + b \ln$ (DBH × H^2)	−4.4509	1.1706	—	0.9582	0.4256	27.9819	0.00	1.0948
	E2	$\ln(a) + b \ln$ (H)	−5.6705	4.2261	—	0.7723	0.9932	61.8759	0.00	1.6375
Xylocarpus sp.	**E1**	**$\ln(a) + b \ln$ (DBH)**	−1.9174	2.3100	—	0.9720	0.1989	−15.5152	1.00	1.0200

Here bold and light grey shaded models are the best model for each species, a^* stands for ln (a), all parameters of estimates (a, b and c) are significant at $p < 0.05$. R^2: coefficient of determination, RSE: residual standard error, AICc: with small sample bias adjustment, AICw: weighted AIC, CF = correction factor for converting log scale in to normal scale.

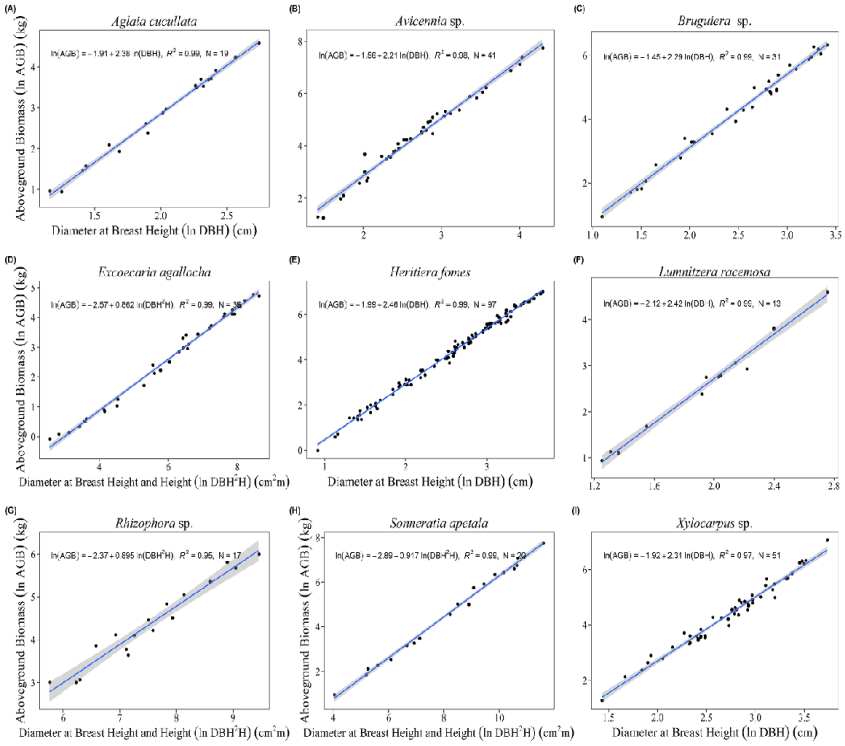

Figure 3. Best species-specific allometric model aboveground biomass in the Sundarbans.

Avicennia sp. (41), *Bruguiera* sp. (31), *E. agallocha* (35), *H. fomes* (97), *L. racemosa* (13), *Rhizophora* sp. (17), *S. apetala* (20), and *Xylocarpus* sp. (51).

Out of 26 models, the best nine species-specific models are presented for each species group (table 2; figure 3). The AICw shows that the best-chosen models for *A. cucullata, Bruguiera* sp., *E. agallocha, H. fomes*, and *Xylocarpus* sp. have 100% chance for being the best model, while *Avicennia* sp., *L. racemosa, Rhizophora* sp. and *S. apetala* have respectively 81%, 94%, 82%, and 71% chance to be the best model (table 3). In the case of *S. apetala*, while E6 models had the highest and lowest RSE and AIC value, the E4 model was chosen based on higher AICw for its greater chance for being the best model. The adjusted coefficient of determination (R^2) varied from 0.77 to 0.99 for all models. All species-specific models comprised single predictor value with only DBH for six species: *A. cucullata, Avicennia* sp., *Bruguiera* sp., *H. fomes, L. racemosa*, and *Xylocarpus* sp. and with combination of DBH and H ($DBH^2 \times H$) for *E. agallocha, S. apetala*, and *Rhizophora* sp.

The ten-fold cross validation showed that the species-specific model gives the lowest average MAE of all species in comparison to three Sundarbans-specific and four pan-tropical generic allometric models (figure 4, table A.4). The lowest average MAE revealed that the species-specific models performed well to predict the AGB in the Sundarbans. AGB estimation at tree level had mean relative absolute difference in MAE between 21.85% with Mahmood_2019_DHW model to the maximum 167.43% with Komiyama_2005_DW model followed by Chave_2005_DHW and Chave_2014_DHW (table A.4). The paired *t*-test of MAE for species-specific models with generic models showed that there is no significant difference of MAE with three Sundarbans-specific models ($p > 0.05$); however, all four pan-tropical models showed significantly higher MAE than the species specific-model ($p < 0.05$). The largest error was obtained for *E. agallocha* with Komiyama_2005_DW.

3.2. Aboveground tree biomass in the Sundarbans

The tree inventory in the Bangladesh Sundarbans indicates a total of 24 tree species. The mean DBH, height, measured and database-sourced WD of all tree species are presented in the table 3. The DBH and H distribution are presented in the supplementary figures A.3 and A.4. Frequency distribution of the topmost ten species based on basal area (m^2 ha^{-1}) and tree density (trees ha^{-1}) showed that *E. agallocha, H. fomes* and *C. decandra* comprise 90% of the stems in the Sundarbans, although they represent 60% in

Table 3. List of tree species found in the Sundarbans with taxonomy and structural parameters.

Sl No.	Latin name	Local name	Family	Mean DBH (cm ± s.d.)	Mean height (m ± s.d.)	Measured mean wood density (gm cm^{-3} ± s.d.)	Mean wood density from database (gm cm^{-3} ± s.d.)[b]
1.	*Aegialitis rotundifolia* Roxb.	Nunia	*Plumbaginaceae*	6.86 (±2.85)	3.94 (±1.71)	—	0.50 (±0.05)
2.	*Aegiceras corniculatum* (L.) Blanco	Kholshi	*Primulaceae*	5.69 (±2.67)	5.73 (±2.18)	0.74	0.60 (±0.08)
3.	*Aglaia cucullata* (Roxb.) Pellegr.[a]	Amur	*Meliace*	3.58 (±1.16)	4.70 (±1.62)	0.50	0.62 (±0.12)
4.	*Avicennia alba* Blume.	Sada Baen	*Avicenniaceae*	14.10 (±0.85)	8.70 (±2.40)	0.72 (±0.08)	0.70 (±0.12)
5.	*Avicennia marina* (Forssk.) Vierh.	Moricha Baen	*Avicenniaceae*	10.40 (±5.26)	10.87 (±5.77)	0.55	0.64 (±0.09)
6.	*Avicennia officinalis* L.	Kala Baen	*Avicenniaceae*	21.20 (±13.40)	11.56 (±5.13)	0.61 (±0.07)	0.65 (±0.08)
7.	*Bruguiera gymnorrhiza* (L.) Lam.	Lal Kakra	*Rhizophoraceae*	7.40	5.80	—	0.76 (±0.08)
8.	*Bruguiera sexangula* (Lour.) Poir.	Holud Kakra	*Rhizophoraceae*	15.75 (±3.95)	6.96 (±3.02)	0.69 (±0.03)	0.83 (±0.12)
9.	*Cerbera manghas* L.[a]	Dakur	*Apocynaceae*	8.92 (±0.08)	0.72 (±0.08)	0.35 (±0.01)	0.47 (±0.05)
10.	*Ceriops decandra* (Griff.) Ding Hou	Goran	*Rhizophoraceae*	3.31 (±0.80)	3.97 (±0.95)	0.73 (±0.07)	0.73 (±0.25)
11.	*Cynometra ramiflora* L.[a]	Singra	*Fabaceae*	4.25 (±1.55)	5.05 (±1.47)	0.66 (±0.05)	0.84 (±0.10)
12.	*Excoecaria agallocha* L.	Gewa	*Euphorbiaceae*	6.93 (±4.04)	6.71 (±2.49)	0.42 (±0.08)	0.43 (±0.06)
13.	*Excoecaria indica* (Willd.) Muell. Arg.[a]	Batul	*Euphorbiaceae*	6.60	6.80	0.41	0.50 (±0.02)
14.	*Heritiera fomes* Buch.-Ham.	Sundri	*Malvaceae*	8.57 (±6.58)	8.03 (±4.16)	0.75 (±0.07)	0.88 (±0.11)
15.	*Hibiscus tiliaceus* L.[a]	Bola	*Malvaceae*	3.90	5.00	—	0.48 (±0.06)
16.	*Intsia bijuga* (Colebr.) Kuntze[a]	Bhaila/Bhola	*Fabaceae*	4.40 (±0.79)	5.17 (±0.81)	—	0.71 (±0.20)
17.	*Kandelia candel* (L.) Druce	Vatkathi	*Rhizophoraceae*	11.87 (±5.09)	7.77 (±1.15)	0.58 (±0.05)	0.52 (±0.05)
18.	*Lumnitzera racemosa* Willd.	Kirpa	*Combretaceae*	5.23 (±1.84)	5.99 (±1.13)	0.82 (±0.13)	0.83 (±0.08)
19.	*Millettia pinnata* (L.) Panigrahi[a]	Karanj	*Fabaceae*	5.70	6.30	0.55	0.61 (±0.05)
20.	*Rhizophora apiculata* Blume.	Bhora Jhana	*Rhizophoraceae*	13.54	0.72	—	0.88 (±0.21)
21.	*Rhizophora mucronata* Lamk.	Jhana Garjan	*Rhizophoraceae*	15.42 (±3.72)	10.38 (±2.65)	0.95 (±0.05)	0.85 (±0.10)
22.	*Sonneratia apetala* Buch.-Ham.	Keora	*Lythraceae*	29.35 (±12.84)	17.97 (±5.90)	0.54 (±0.07)	0.53 (±0.11)
23.	*Xylocarpus granatum* K.D. Koen.	Dhundul	*Meliaceae*	18.77 (±12.03)	8.08 (±2.66)	0.58 (±0.05)	0.67 (±0.14)
24.	*Xylocarpus moluccensis* (Lam.) M. Roem	Passur	*Meliaceae*	15.51 (±10.80)	9.39 (±3.95)	0.65 (±0.09)	0.65 (±0.09)

[a] Indicates mangrove associates according to Tomlinson (2016). Abbreviation: DBH = diameter at breast height. Values without s.d. indicates single observation.
[b] Multiple wood density values from different sources.

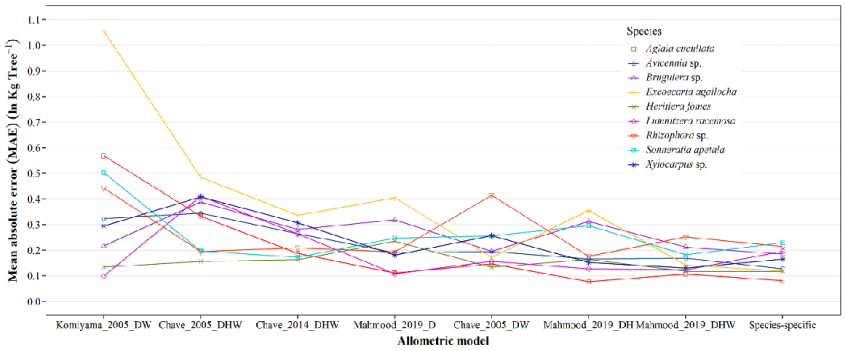

Figure 4. Species-wise mean absolute error (MAE) of tree AGB with all allometric models after ten-fold cross validation. The models are arranged from highest average MAE to minimum.

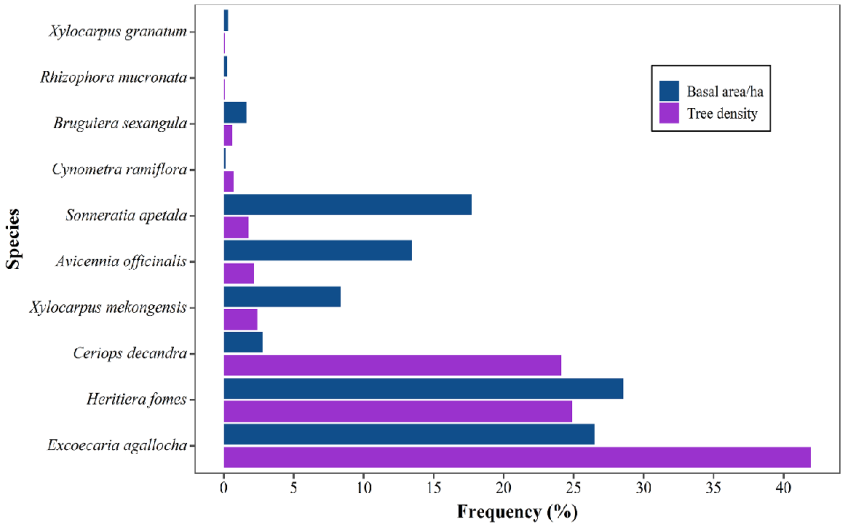

Figure 5. Frequency distribution of the ten most frequently occurring species based on basal area (m^2 ha^{-1}) and tree density (tree ha^{-1}).

terms of basal area (figure 5). *E. agallocha* and *H. fomes* was within the top two species in both categories; *C. decandra* was the third in terms of tree density, however, the sixth in case of basal area for its lower DBH.

The mean AGB varied from 111.36 Mg ha^{-1} with the Chave_2005_DHW model to the highest 299.48 Mg ha^{-1} for Chave_2005_DW model (figure 6). Except for Chave_2005_DHW and Chave_2014_DHW, all other models yielded higher AGB than the species-specific model (123 Mg ha^{-1}). The mean relative absolute difference in AGB ranged from 9% with Mahmood_2019_DHW to 142% with Chave_2005_DW. Pairwise comparison with the Wilcoxon signed-rank test between species-specific and other models showed that all generic models measured significantly different AGB than the species-specific model in the Sundarbans ($p < 0.05$). Both Chave_2005_DW and Komiyama_2005_DW overestimated AGB (supplementary table A.5). The absolute difference between allometric models tended to increase with DBH in all species, suggesting that larger trees are crucial for estimating AGB with a variety of available allometric model leading to a greater error and uncertainty.

AGB was significantly higher when models used published WD compared to species-specific measured WD (Wilcoxon signed-rank test, $p < 0.05$) (figure 7(A), table 4). The maximum mean relative difference biomass was for Sundarbans mean WD

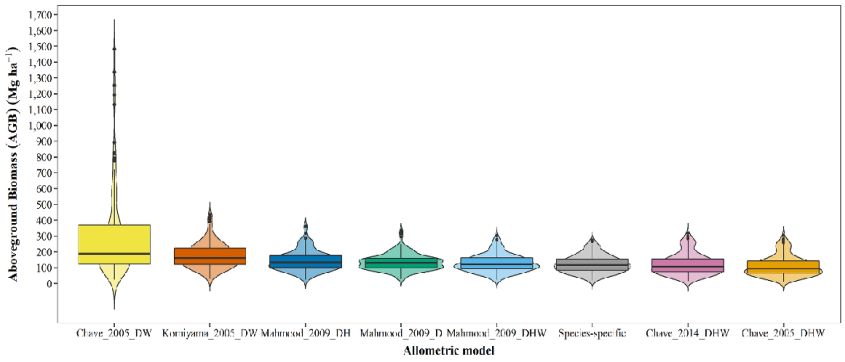

Figure 6. Comparison of aboveground biomass (Mg ha^{-1}) with different allometric models. The models are arranged from the highest median AGB to the lowest. The black horizontal line of box plot for each model represents the median and the width of violin plot represents the proportion of the data located there as a measure of kernel probability density. The black dots represent the outliers, which are 1.5 times of the interquartile range above the upper quartile and below the lower quartile (McGill *et al* 1978).

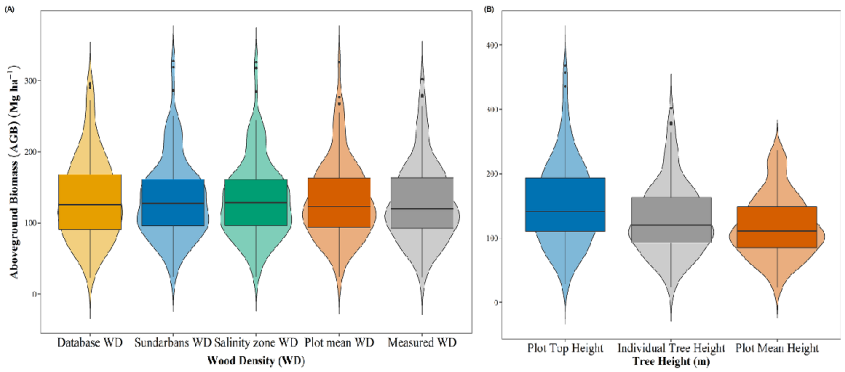

Figure 7. Comparison of aboveground biomass with (A) different wood density and (B) different height parameters. The parameters are arranged from the highest median AGB to the lowest. For details of the violin-box plot, see figure 6.

followed by salinity zone mean WD and database-derived WD. Looking at different sources of height data, using plot top height tended to be overestimate AGB by 19.46%, while using average height underestimated AGB by 8.31% compared to the measurements from individual species (figure 7(B), table 4).

4. Discussion

The results show that the species-specific allometric models provide the lowest average MAE for all species in the Sundarbans (figure 4, table A.4). However, the three Sundarbans-specific generic models showed no significant difference of mean MAE at tree-level compared with the species-specific models (table A.4). At plot-level, all local and pan-tropical generic models either overestimated or underestimated AGB when compared to local species-specific models (figure 6). Several studies have concluded that site-specific AGB models estimate biomass or carbon with less error than regional or pan-tropical models; for example, Sundarbans mangrove forest (Mahmood *et al* 2019), lowland Dipterocarp forest in Indonesia (Basuki *et al* 2009), degraded landscape in Northern Ethiopia (Mokria *et al* 2018), central African forest (Ngomanda *et al* 2014) and Mexican tropical humid forests (Martínez-Sánchez *et al* 2020). In contrast, only a few studies report better performance from regional or pan-tropical models and these appear result from large uncertainties in the data used to build the local model; for example, West Africa (Aabeyir *et al* 2020). The accuracy of these generic models for a particular forest depends on whether these models incorporate sufficient samples from that forest. Chave *et al* (2014) point out that the discrepancy between local models and their own model (Chave_2014_DHW) in wet forests (including mangroves) is largely due to failure to address the wider variation of tree form and other characteristics like

Table 4. Pairwise comparison test of plot-level AGB from species-specific and other allometric models.

Model comparison	Mean difference biomass ($Mg\,ha^{-1}$)	Mean absolute difference biomass ($Mg\,ha^{-1}$)	Mean relative absolute difference (%)	Wilcoxon signed-rank test (Z), p-value
Comparison of different allometric model				
Species-specific—Mahmood_2019_DHW	−5.18	11.38	9.21	$Z = -5.13$, $p < 0.05$
Species-specific—Chave_2014_DHW	0.79	17.38	14.07	$Z = -2.89$, $p < 0.05$
Species-specific—Mahmood_2019_D	−12.66	19.66	15.92	$Z = -6.40$, $p < 0.05$
Species-specific—Chave_2005_DHW	12.59	21.07	17.06	$Z = -6.51$, $p < 0.05$
Species-specific—Mahmood_2019_DH	−21.27	23.37	18.92	$Z = -7.95$, $p < 0.05$
Species-specific—Komiyama_2005_DW	−52.47	52.57	42.57	$Z = -10.26$, $p < 0.05$
Species-specific—Chave_2005_DW	−175.67	175.75	142.31	$Z = -10.26$, $p < 0.05$
Comparison from different wood density (WD)				
Measured WD—plot mean WD	−3.16	5.83	4.53	$Z = -5.86$, $p < 0.05$
Measured WD—database WD	−4.82	9.91	7.70	$Z = -3.83$, $p < 0.05$
Measured WD—salinity zone mean WD	−4.08	12.46	9.68	$Z = -3.54$, $p < 0.05$
Measured WD—Sundarbans mean WD	−4.29	12.47	9.69	$Z = -3.59$, $p < 0.05$
Comparison from different Tree Height (m)				
Individual height—plot mean height	10.70	10.70	8.31	$Z = -13.68$, $p < 0.05$
Individual height—plot top height	−25.04	25.04	19.46	$Z = -13.68$, $p < 0.05$

buttresses, which are common in the Sundarbans. Their previous model (Chave_2005_DW) overestimated AGB in the Sundarbans because of its inability to estimate biomass from larger trees (DBH > 42 cm) (Chave *et al* 2005). However, surprisingly, the worldwide generic models for mangroves also overestimate AGB, possibly because of the samples drawn from the mangroves of Asia-Pacific and Australia (Komiyama *et al* 2008).

The structure and morphological characteristics of all mangroves vary according to their ability to adapt to environmental conditions such as salinity, which is less pronounced in other wet and dry tropical areas (Ball and Pidsley 1995, Tomlinson 2016). Environmental drivers such as salinity and water deficit are considered the main stressors for the growth and development of mangroves, including the Sundarbans. For example, the third most abundant species in the Sundarbans, *C. decandra*, is a multi-stemmed bushy species, on the other hand, the top two, *H. fomes* and *E. agallocha* are tree-like structures. The pantropical models yielded a large error in the dwarf, bushy species and other true mangrove species in the Sundarbans (table A.5). Moreover, the extreme salinity has reduced the stature (Rahman *et al* 2015), trunk diameter (Rahman *et al* 2020) and the leaf area (Khan *et al* 2020) of *H. fomes* and *S. apetala*, present in all three salinity zones in the Sundarbans. Due to these wider morphological variation, Banerjee *et al* (2013) highlighted the importance of developing models based on salinity zonation.

This study demonstrates that when using measured wood densities and individual tree heights, generic equations yield accurate estimates of AGB in mangroves at the plot scale (figure 7). Most species had a higher published WD than the measured value seen in table 3 (Henry *et al* 2010). The use of WD from different databases such as the Global WD database resulted in a 9% variation for species having multiple values, which could provide a significant variation in AGB if upscaled (Réjou-Méchain *et al* 2019). Averaging WD at the plot scale, salinity zone scale or ecosystem scale also introduces errors. While WD is considered an important variable to capture a range of characteristics such as high density versus low density timber species, climax versus pioneer species or primary versus secondary species, the use of WD value from the secondary sources or averaging them in the higher scales might not reflect the true biomass (Slik *et al* 2008, Kenzo *et al* 2009). Phillips *et al* (2019) noted significant AGB error in the Amazon rainforest while scaling up from the plot level to forest and amazon-wide level. Yuen *et al* (2016) observed 31 Mg ha^{-1} higher AGB with the difference of measured and published WD of only 0.13 gm cm^{-3}.

Among nine developed models, six models showed that DBH alone is a strong predictor of AGB across the Bangladesh Sundarbans. The remaining three models of *E. agallocha, S. apetala*, and *Rhizophora* sp. showed sensitivity to height. However, the inclusion of top height or average height instead of using individual tree height can increase the error at the plot level and above. Kearsley *et al* (2013) observed 24% overestimation of AGB in the central Congo Basin by using a regional height–diameter relationship developed by Feldpausch *et al* (2012) compared to the local relationship. On the other hand, using mean height could reduce the difficulty of taking height measurements in dense forests, yet may lead to a significant underestimation of AGB (Hunter *et al* 2013). The difficulty of measuring height under a dense forest canopy allows researchers to use H-D relationship or to use bioclimatic variables in allometric models. However, these also lead to non-uniform bias in biomass estimation (Réjou-Méchain *et al* 2019).

Although species-specific WD and individual height data can be used to accurately estimate AGB at the plot and ecosystem level, collecting species information is impractical in highly diverse mixed tropical forests such as in Amazonia, Southeast Asia and the Congo basin, which comprise of more than 53 000 tree species (Feldpausch *et al* 2012, Slik *et al* 2015). Mangroves, by comparison exhibit less diversity. Developing allometric models for dominant species could improve the biomass inventory. For example, in the Sundarbans only 28 species were recorded (24 in this survey) and just three species (*E. agallocha, H. fomes* and *C. decandra*) constitute about 90% of stand density (figure 5), which implies that developing three allometric models is enough to produce acceptable AGB estimates in the Sundarbans (GOB 2019). The model used for *C. decandra* was developed by destructive sampling from Hossain *et al* (2012) and so this study recommends developing models with destructive samples from all salinity zones for *H. fomes* and *E. agallocha*.

The errors and uncertainties in the individual tree and plot level AGB estimates will result in large errors when scaling up to the ecosystem, region or country level by RS techniques. Réjou-Méchain *et al* (2019) described the errors due to poor choice of allometric models and failure to capture variabilities of WD and H as uniform and non-uniform bias. Uniform bias systematically propagates over- or underestimation whereas non-uniform bias is related to an inability to capture the variabilities across landscapes, for example, WD and H variation among successional stages or environmental gradients such as the salinity in the Sundarbans (Rahman *et al* 2020). These two types of bias, in addition to mapping errors resulting from the use of RS, may result in serious anomalies in national and global carbon budgets and result in poor understanding of species contribution to ecosystem processes and function in mangroves.

5. Conclusion

This study developed and tested five species-specific and four genus-specific allometric models for the nine most important species in the Sundarbans. All developed models explained a high percentage of the variance in tree AGB (R^2 = 0.97–0.99) using measured DBH and total height (H) data. At the individual tree level, the generic allometric models overestimated AGB between 22% and 167% compared to the species-specific models and at the plot level, they showed statistically significant AGB differences compared to the species-specific models ($p < 0.05$). Measured WD showed 5%–10% less biomass than WD from databases and other sources and AGB was overestimated by up to 20% when using plot top height and underestimated by 8% using plot average height data rather than individual tree heights. The study concludes that biomass estimation in mangroves forests always benefit from species-specific models and individual tree measurements when appropriate input data are available. Tree level measurements from inventory plots play an important role for the improved estimation of forest biomass while scaling from individual trees up to the ecosystem level. Improved estimates of AGB will improve support our understanding of the productivity of mangrove forests, information that is needed for the long-term conservation of these fragile ecosystems that face many natural and anthropogenic pressures.

Data availability statement

The primary inventory data from the Bangladesh Sundarbans are available in TRY database (www.try-db.org/TryWeb/Home.php). The used semi-destructive sampling data for the Sundarbans is publicly available in the supplementary files of Mahmood *et al* (2019). The data that support the findings of this study are openly available at the following URL/DOI: 10.5281/zenodo.5544398 . Data will be available from 30 June 2022.

Acknowledgments

We are grateful to Commonwealth Scholarship Commission in the UK for the PhD scholarship to the first author. We want to extend our gratitude to the Bangladesh Forest Department for giving permission for fieldwork in the Sundarbans and Forestry and Wood Technology Discipline, Khulna University for allowing study leave to the first author. We are also grateful to Institute of Hazard, Risk and Resilience for research grants and Department of Geography, Durham University for allowing laboratory analysis and to Ustinov College, Durham University for a travel grant. We acknowledge the important contribution to all field assistants and forest officials involving in the tree inventory in the Sundarbans.

Funding

The study was funded by Commonwealth Scholarship Commission in the UK (Grant Number BDCS-2017-55).

Conflict of interest

The authors agreed that they have no conflict of interest.

Credit authorship contribution statement

Md Saidur Rahman: conceptualization, data curation, formal analysis, investigation, methodology, visualization, writing—original draft, writing—review and editing.

Daniel N M Donoghue, Louise J Bracken: conceptualization, investigation, supervision, funding acquisition, writing—review and editing.

Hossain Mahmood: data curation, writing—review and editing.

ORCID iDs

Md Saidur Rahman https://orcid.org/0000-0001-6849-4105
Daniel N M Donoghue https://orcid.org/0000-0002-9931-9083
Louise J Bracken https://orcid.org/0000-0002-1268-5516
Hossain Mahmood https://orcid.org/0000-0002-9174-005X

References

Aabeyir R, Adu-Bredu S, Agyare W A and Weir M J C 2020 Allometric models for estimating aboveground biomass in the tropical woodlands of Ghana, West Africa *For. Ecosyst.* **7** 41

Azad M S, Kamruzzaman M and Osawa A 2020 Quantification and understanding of above and belowground biomass in medium saline zone of the Sundarbans, Bangladesh: the relationships with forest attributes *J. Sustain. For.* **39** 331–45

Aziz A and Paul A R 2015 Bangladesh Sundarbans: present status of the environment and biota *Diversity* **7** 242–69

Baccini A, Walker W, Carvalho L, Farina M, Sulla-Menashe D and Houghton R A 2017 Tropical forests are a net carbon source based on aboveground measurements of gain and loss *Science* **358** 230–4

Ball M C and Pidsley S M 1995 Growth responses to salinity in relation to distribution of two mangrove species, *Sonneratia alba* and *S. lanceolata*, in northern Australia *Funct. Ecol.* **9** 77–85

Banerjee K, Sengupta K, Raha A and Mitra A 2013 Salinity based allometric equations for biomass estimation of Sundarban mangroves *Biomass Bioenergy* **56** 382–91

Bartoń K 2020 MuMIn: multi-model inference. R package version 1.43.17 (available at: https://CRAN.R-project.org/package=MuMIn) (Accessed 01 March 2020)

Barua S K, Boscolo M and Animon I 2020 Valuing forest-based ecosystem services in Bangladesh: implications for research and policies *Ecosyst. Serv.* **42** 101069

Basuki T M, van Laake P E, Skidmore A K and Hussin Y A 2009 Allometric equations for estimating the above-ground

biomass in tropical lowland Dipterocarp forests *For. Ecol. Manage.* **257** 1684–94
BFD 2010 *Integrated Resources Management Plans for the Sundarbans (2010–2020)* **I** (Dhaka: Nishorgo Network, Forest Department, Government of Bangladesh)
Brown S 1997 Estimating biomass and biomass change of tropical forests: a primer (Rome: FAO Forestry Paper 134)
Burnham K P and Anderson D R 2002 Information and Likelihood Theory: A Basis for Model Selection and Inference *A practical information-theoretic approach. Model Selection and Multimodel Inference* 2nd edn vol 2 K P Burnham and D R Anderson (Berlin: Springer) pp 49–97
Chanda A *et al* 2016 Blue carbon stock of the Bangladesh Sundarban mangroves: what could be the scenario after a century? *Wetlands* **36** 1033–45
Chave J *et al* 2005 Tree allometry and improved estimation of carbon stocks and balance in tropical forests *Oecologia* **145** 87–99
Chave J *et al* 2014 Improved allometric models to estimate the aboveground biomass of tropical trees *Glob. Change Biol.* **20** 3177–90
Chave J *et al* 2019 Ground data are essential for biomass remote sensing missions *Surv. Geophys.* **40** 863–80
Chave J, Coomes D, Jansen S, Lewis S L, Swenson N G and Zanne A E 2009 Towards a worldwide wood economics spectrum *Ecol. Lett.* **12** 351–66
Chowdhury M Q, de Ridder M and Beeckman H 2016 Climatic signals in tree rings of *Heritiera fomes* Buch.-Ham. in the Sundarbans, Bangladesh *PLoS One* **11** e0149788
de Souza Pereira F R, Kampel M, Gomes Soares M L, Estrada G C D, Bentz C and Vincent G 2018 Reducing uncertainty in mapping of mangrove aboveground biomass using airborne discrete return lidar data *Remote Sens.* **10** 637
Edwards D P, Socolar J B, Mills S C, Burivalova Z, Koh L P and Wilcove D S 2019 Conservation of tropical forests in the anthropocene *Curr. Biol.* **29** R1008–R20
Fatoyinbo T *et al* 2021 The NASA AfriSAR campaign: airborne SAR and lidar measurements of tropical forest structure and biomass in support of current and future space missions *Remote Sens. Environ.* **264** 112533
Feldpausch T R *et al* 2011 Height-diameter allometry of tropical forest trees *Biogeosciences* **8** 1081–106
Feldpausch T R *et al* 2012 Tree height integrated into pantropical forest biomass estimates *Biogeosciences* **9** 3381–403
Fox J and Weisberg S 2019 *An {R} Companion to Applied Regression* (Thousand Oaks, CA: Sage)
Gibbs H K, Brown S, Niles J O and Foley J A 2007 Monitoring and estimating tropical forest carbon stocks: making REDD a reality *Environ. Res. Lett.* **2** 045023
Giri C, Ochieng E, Tieszen L L, Zhu Z, Singh A, Loveland T, Masek J and Duke N 2011 Status and distribution of mangrove forests of the world using earth observation satellite data *Glob. Ecol. Biogeogr.* **20** 154–9
GOB 2019 *Tree and forest resources of Bangladesh: report on the Bangladesh forest inventory* Forest Department, Ministry of Environment, Forest and Climate Change, Government of the People's Republic of Bangladesh, Dhaka, Bangladesh.
Henry M *et al* 2021 A multi-purpose National Forest Inventory in Bangladesh: design, operationalisation and key results *For. Ecosyst.* **8** 12
Henry M, Besnard A, Asante W A, Eshun J, Adu-Bredu S, Valentini R, Bernoux M and Saint-André L 2010 Wood density, phytomass variations within and among trees, and allometric equations in a tropical rainforest of Africa *For. Ecol. Manage.* **260** 1375–88
Hickey S M, Callow N J, Phinn S, Lovelock C E and Duarte C M 2018 Spatial complexities in aboveground carbon stocks of a semi-arid mangrove community: a remote sensing height-biomass-carbon approach *Estuar. Coast. Shelf Sci.* **200** 194–201
Hossain M, Saha C, Rubaiot Abdullah S M, Saha S and Siddique M R H 2016a Allometric biomass, nutrient and carbon stock models for Kandelia candel of the Sundarbans, Bangladesh *Trees* **30** 709–17
Hossain M, Shaikh M A A, Saha C, Abdullah S M R, Saha S and Siddique M R H 2016b Above-ground biomass, nutrients and carbon in *Aegiceras corniculatum* of the Sundarbans *Open J. For.* **6** 72–81
Hossain M, Siddique M R H, Bose A, Limon S H, Chowdhury M R K and Saha S 2012 Allometry, above-ground biomass and nutrient distribution in *Ceriops decandra* (Griffith) Ding Hou dominated forest types of the Sundarbans mangrove forest, Bangladesh *Wetlands Ecol. Manage.* **20** 539–48
Hunter M O, Keller M, Victoria D and Morton D C 2013 Tree height and tropical forest biomass estimation *Biogeosciences* **10** 8385–99
Hutchison J, Manica A, Swetnam R, Balmford A and Spalding M 2014 Predicting global patterns in mangrove forest biomass *Conserv. Lett.* **7** 233–40
ICRAF 2016 *Tree Functional attributes and Ecological Databases: Wood density* (available at: http://db.worldagroforestry.org//wd) (Accessed 25 March 2020)
Iftekhar M and Saenger P 2008 Vegetation dynamics in the Bangladesh Sundarbans mangroves: a review of forest inventories *Wetlands Ecol. Manage.* **16** 291–312
James G, Witten D, Hastie T and Tibshirani R 2013 *An Introduction to Statistical Learning* vol 112 (Berlin: Springer)
Kamruzzaman M, Ahmed S and Osawa A 2017 Biomass and net primary productivity of mangrove communities along the Oligohaline zone of Sundarbans, Bangladesh *For. Ecosyst.* **4** 16
Kamruzzaman M, Ahmed S, Paul S, Rahman M M and Osawa A 2018 Stand structure and carbon storage in the oligohaline zone of the Sundarbans mangrove forest, Bangladesh *For. Sci. Technol.* **14** 23–28
Kassambara A 2020 Rstatix: pipe-friendly framework for basic statistical tests (available at: https://cran.r-project.org/web/packages/rstatix/rstatix.pdf) (Accessed 25 March 2020)
Kearsley E *et al* 2013 Conventional tree height–diameter relationships significantly overestimate aboveground carbon stocks in the Central Congo Basin *Nat. Commun.* **4** 2269
Kenzo T *et al* 2009 Development of allometric relationships for accurate estimation of above- and below-ground biomass in tropical secondary forests in Sarawak, Malaysia *J. Trop. Ecol.* **25** 371–86
Khan M N I, Khatun S, Azad M S and Mollick A S 2020 Leaf morphological and anatomical plasticity in Sundri (*Heritiera fomes* Buch.-Ham.) along different canopy light and salinity zones in the Sundarbans mangrove forest, Bangladesh *Glob. Ecol. Conserv.* **23** e01127
Komiyama A, Ong J E and Poungparn S 2008 Allometry, biomass, and productivity of mangrove forests: a review *Aquat. Bot.* **89** 128–37
Komiyama A, Poungparn S and Kato S 2005 Common allometric equations for estimating the tree weight of mangroves *J. Trop. Ecol.* **21** 471–7
Kuhn M 2008 Building predictive models in R using the caret package *J. Stat. Softw.* **28** 1–26
Lagomasino D, Fatoyinbo T, Lee S, Feliciano E, Trettin C, Shapiro A and Mangora M M 2019 Measuring mangrove carbon loss and gain in deltas *Environ. Res. Lett.* **14** 025002
Larjavaara M and Muller-Landau H C 2013 Measuring tree height: a quantitative comparison of two common field methods in a moist tropical forest *Methods Ecol. Evol.* **4** 793–801
Lüdecke D 2018 ggeffects: tidy data frames of marginal effects from regression models *J. Open Source Softw.* **3** 772
Mahmood H, Siddique M R H, Abdullah S M R, Islam S M Z, Matieu H, Iqbal M Z and Akhter M 2020 Semi-destructive method to derive allometric aboveground biomass model for village forest of Bangladesh: comparison of regional and pantropical models *J. Trop. For. Sci.* **32** 246–56

Mahmood H, Siddique M R H, Rubaiot Abdullah S M, Costello L, Matieu H, Iqbal M Z and Akhter M 2019 Which option best estimates the above-ground biomass of mangroves of Bangladesh: pantropical or site- and species-specific models? *Wetlands Ecol. Manage.* **27** 553–69

Martínez-Sánchez J L, Martínez-Garza C, Cámara L and Castillo O 2020 Species-specific or generic allometric equations: which option is better when estimating the biomass of Mexican tropical humid forests? *Carbon Manage.* **11** 241–9

McGill R, Tukey J W and Larsen W A 1978 Variations of box plots *Am. Stat.* **32** 12–16

Mitchard E T, Saatchi S S, Baccini A, Asner G P, Goetz S J, Harris N L and Brown S 2013 Uncertainty in the spatial distribution of tropical forest biomass: a comparison of pan-tropical maps *Carbon Balance Manage.* **8** 10

Mokria M, Mekuria W, Gebrekirstos A, Aynekulu E, Belay B, Gashaw T and Bräuning A 2018 Mixed-species allometric equations and estimation of aboveground biomass and carbon stocks in restoring degraded landscape in northern Ethiopia *Environ. Res. Lett.* **13** 024022

Ngomanda A *et al* 2014 Site-specific versus pantropical allometric equations: which option to estimate the biomass of a moist central African forest? *For. Ecol. Manage.* **312** 1–9

Ni-Meister W 2015 Aboveground terrestrial biomass and carbon stock estimations from multisensor remote sensing *Land Resources Monitoring, Modeling, and Mapping with Remote Sensing* **II** ed P S Thenkabail (Boca Raton, FL: CRC Press) pp 47–67

Njana M A, Meilby H, Eid T, Zahabu E and Malimbwi R E 2016 Importance of tree basic density in biomass estimation and associated uncertainties: a case of three mangrove species in Tanzania *Ann. For. Sci.* **73** 1073–87

Petrokofsky G, Kanamaru H, Achard F, Goetz S J, Joosten H, Holmgren P, Lehtonen A, Menton M C S, Pullin A S and Wattenbach M 2012 Comparison of methods for measuring and assessing carbon stocks and carbon stock changes in terrestrial carbon pools. How do the accuracy and precision of current methods compare? A systematic review protocol *Environ. Evidence* **1** 6

Phillips O L, Sullivan M J P, Baker T R, Monteagudo Mendoza A, Vargas P N and Vásquez R 2019 Species matter: wood density influences tropical forest biomass at multiple scales *Surv. Geophys.* **40** 913–35

Picard N, Saint-André L and Henry M 2012 *Manual for Building Tree Volume and Biomass Allometric Equations: From Field Measurement to Prediction* Food and Agricultural Organization of the United Nations, Rome, and Centre de Coopération Internationale en Recherche Agronomique pour le Développement, Montpellier

R Core Team 2020 *R: A Language and Environment for Statistical Computing* (Vienna: R Foundation for Statistical Computing)

Rahman M M, Khan M N I, Hoque A K F and Ahmed I 2015 Carbon stock in the Sundarbans mangrove forest: spatial variations in vegetation types and salinity zones *Wetlands Ecol. Manage.* **23** 269–83

Rahman M S, Donoghue D N M and Bracken L J 2021 Is soil organic carbon underestimated in the largest mangrove forest ecosystems? Evidence from the Bangladesh Sundarbans *CATENA* **200** 105159

Rahman M S, Sass-Klaassen U, Zuidema P A, Chowdhury M Q and Beeckman H 2020 Salinity drives growth dynamics of the mangrove tree *Sonneratia apetala* Buch.-Ham. in the Sundarbans, Bangladesh *Dendrochronologia* **62** 125711

Réjou-Méchain M *et al* 2019 Upscaling forest biomass from field to satellite measurements: sources of errors and ways to reduce them *Surv. Geophys.* **40** 881–911

Rovai A S *et al* 2016 Scaling mangrove aboveground biomass from site-level to continental-scale *Glob. Ecol. Biogeogr.* **25** 286–98

Rutishauser E, Noor'an F, Laumonier Y, Halperin J, Rufi'ie, Hergoualc'h K and Verchot L 2013 Generic allometric models including height best estimate forest biomass and carbon stocks in Indonesia *For. Ecol. Manage.* **307** 219–25

Sarker S K, Matthiopoulos J, Mitchell S N, Ahmed Z U, Mamun M B A and Reeve R 2019a 1980s–2010s: the world's largest mangrove ecosystem is becoming homogeneous *Biol. Conserv.* **236** 79–91

Sarker S K, Reeve R, Paul N K and Matthiopoulos J 2019b Modelling spatial biodiversity in the world's largest mangrove ecosystem—the Bangladesh Sundarbans: a baseline for conservation *Divers. Distrib.* **25** 729–42

Sarker S K, Reeve R, Thompson J, Paul N K and Matthiopoulos J 2016 Are we failing to protect threatened mangroves in the Sundarbans world heritage ecosystem? *Sci. Rep.* **6** 21234

Sattar M A, Bhattacharjee D K and Sarker S B 1995 Physical, mechanical and seasoning properties of 45 lesser used or unused forest timbers of Bangladesh and their uses *Bangladesh J. For. Sci.* **24** 11–21

Siddiqi N A 2001 *Mangrove Forestry in Bangladesh* (Chittagong: Institute of Forestry & Environmental Sciences, University of Chittagong)

Siddique M R H, Mahmood H and Chowdhury M R K 2012 Allometric relationship for estimating above-ground biomass of *Aegialitis rotundifolia* Roxb. of Sundarbans mangrove forest, in Bangladesh *J. For. Res.* **23** 23–28

Sileshi G W 2014 A critical review of forest biomass estimation models, common mistakes and corrective measures *For. Ecol. Manage.* **329** 237–54

Slik J W F *et al* 2015 An estimate of the number of tropical tree species *Proc. Natl Acad. Sci.* **112** 7472–7

Slik J W F, Bernard C S, Breman F C, van Beek M, Salim A and Sheil D 2008 Wood density as a conservation tool: quantification of disturbance and identification of conservation-priority areas in tropical forests *Conserv. Biol.* **22** 1299–308

Sprugel D 1983 Correcting for bias in log-transformed allometric equations *Ecology* **64** 209–10

Stas S M, Rutishauser E, Chave J, Anten N P R and Laumonier Y 2017 Estimating the aboveground biomass in an old secondary forest on limestone in the Moluccas, Indonesia: comparing locally developed versus existing allometric models *For. Ecol. Manage.* **389** 27–34

Tomlinson P B 2016 *The Botany of Mangroves* (Cambridge: Cambridge University Press)

van Breugel M, Ransijn J, Craven D, Bongers F and Hall J S 2011 Estimating carbon stock in secondary forests: decisions and uncertainties associated with allometric biomass models *For. Ecol. Manage.* **262** 1648–57

Vieilledent G, Vaudry R, Andriamanohisoa S F D, Rakotonarivo O S, Randrianasolo H Z, Razafindrabe H N, Rakotoarivony C B, Ebeling J and Rasamoelina M 2012 A universal approach to estimate biomass and carbon stock in tropical forests using generic allometric models *Ecol. Appl.* **22** 572–83

Virgulino-Júnior P C C, Carneiro D N, Nascimento W R Jr., Cougo M F and Fernandes M E B 2020 Biomass and carbon estimation for scrub mangrove forests and examination of their allometric associated uncertainties *PLoS One* **15** e0230008

Vorster A G, Evangelista P H, Stovall A E L and Ex S 2020 Variability and uncertainty in forest biomass estimates from the tree to landscape scale: the role of allometric equations *Carbon Balance Manage.* **15** 8

Weiskittel A R, MacFarlane D W, Radtke P J, Affleck D L R, Temesgen H, Woodall C W, Westfall J A and Coulston J W 2015 A call to improve methods for estimating tree biomass for regional and national assessments *J. For.* **113** 414–24

Wickham H 2016 *Ggplot2: Elegant Graphics for Data Analysis* (Berlin: Springer)

Wiemann M C and Williamson G B 2013 Biomass determination using wood specific gravity from increment cores *General Technical Report, FPL-GTR-225* Forest Products Laboratory, USDA Forest Service vol 9 p 225

Wilke C O, Wickham H and Wilke M C O 2019 *Streamlined Plot Theme and Plot Annotations for 'ggplot2* (available at: https://wilkelab.org/cowplot/index.html) (Accessed 01 March 2020)

Xiao X, White E P, Hooten M B and Durham S L 2011 On the use of log-transformation vs. nonlinear regression for analyzing biological power laws *Ecology* **92** 1887–94

Yuen J Q, Fung T and Ziegler A D 2016 Review of allometric equations for major land covers in SE Asia: uncertainty and implications for above- and below-ground carbon estimates *For. Ecol. Manage.* **360** 323–40

Zanne A E, Lopez-Gonzalez G, Coomes D A, Ilic J, Jansen S, Lewis S L, Miller R B, Swenson N G, Wiemann M C and Chave J 2009 Data from: towards a worldwide wood economics spectrum, Dryad, dataset (https://doi.org/10.5061/dryad.234)

Zeileis A and Hothorn T 2002 Diagnostic checking in regression relationships *R News* **2** 7–10

Table B.1. The choice of model parameters between log-linear and nonlinear regression.

Species	No. of trees	Nonlinear AICc	Log-linear AICc	ΔAICc	Error type	Proposed method
Aglaia cucullata	19	88.45	82.1	6.35	Multiplicative log-normal error	Loglinear
Avicennia spp.	42	444.13	380.01	64.12	Multiplicative log-normal error	Loglinear
Bruguiera spp.	31	309.35	254.73	54.62	Multiplicative log-normal error	Loglinear
Excoecaria agallocha	35	201.08	141.22	59.86	Multiplicative log-normal error	Loglinear
Heritiera fomes	97	941.98	742.45	199.53	Multiplicative log-normal error	Loglinear
Lumnitzera racemosa	13	71.56	58.66	12.9	Multiplicative log-normal error	Loglinear
Rhizophora spp.	18	160.29	158.19	2.1	Multiplicative log-normal error	Loglinear
Sonneratia apetala	20	259.73	192.52	67.21	Multiplicative log-normal error	Loglinear
Xylocarpus spp.	51	504.67	431.99	72.68	Multiplicative log-normal error	Loglinear

AICc: Second variant of AIC that corrects small sample size, ΔAICc: the difference between AIC of two models.

Table B.2: Eligibility test results for six log-linear regression models for each species.

Species	Model no.	Shapiro-wilk normality test	BP test for heteroscedasticity	Percent relative standard error (PRSE)			Variance inflation factor (VIF)
				a	b	c	
Aglaia cucullata	E1	W = 0.96, *p* = 0.61	BP = 1.68, *p* = 0.20	5.74	2.24		
	E2	W = 0.95, *p* = 0.45	BP = 0.62, *p* = 0.43	16.32	9.97		
	E3	W = 0.94, *p* = 0.24	**BP = 4.55, *p* = 0.03**	6.59	3.44		
	E4	W = 0.97, *p* = 0.78	**BP = 5.21, *p* = 0.02**	4.93	2.37		
	E5	W = 0.92, *p* = 0.17	BP = 3.03, *p* = 0.08	9.04	5.04		
	E6	W = 0.94, *p* = 0.28	BP = 5.18, *p* = 0.07	9.10	5.49	**47.87**	b = **5.89,** c = **5.89**
***Avicennia* spp.**	E1	W = 0.95, *p* = 0.06	BP = 3.37, *p* = 0.07	9.37	2.37		
	E2	**W = 0.87, *p* = 0.00**	BP = 0.24, *p* = 0.63	22.47	12.14		
	E3	**W = 0.92, *p* = 0.01**	BP = 0.09, *p* = 0.76	6.95	3.19		
	E4	W = 0.95, *p* = 0.07	BP = 0.05, *p* = 0.83	6.51	2.45		
	E5	**W = 0.93, *p* = 0.01**	BP = 2.07, *p* = 0.14	9.53	4.72		
	E6	**W = 0.93, *p* = 0.02**	BP = 2.36, *p* = 0.31	14.45	3.84	**49.87**	b = 2.76, c = 2.76
***Bruguiera* spp.**	E1	W = 0.94, *p* = 0.11	BP = 0.00, *p* = 0.98	9.34	2.29		
	E2	**W = 0.93, *p* = 0.03**	BP = 0.39, *p* = 0.53	**29.07**	12.11		
	E3	W = 0.97, *p* = 0.47	BP = 1.07, *p* = 0.30	8.98	3.48		
	E4	**W = 0.91, *p* = 0.01**	BP = 0.87, *p* = 0.35	6.46	2.23		
	E5	W = 0.96, *p* = 0.29	BP = 0.77, *p* = 0.38	13.00	5.46		
	E6	**W = 0.93, *p* = 0.04**	BP = 0.75, *p* = 0.69	8.99	3.53	**27.04**	b = 2.80, c = 2.80
Excoecaria agallocha	**E1**	W = 0.98, *p* = 0.74	**BP = 8.16, *p* = 0.00**	3.45	1.40		
	E2	W = 0.95, *p* = 0.08	BP = 0.00, *p* = 0.97	11.81	7.03		
	E3	W = 0.95, *p* = 0.11	BP = 0.00, *p* = 0.99	4.78	2.44		
	E4	W = 0.96, *p* = 0.22	BP = 1.40, *p* = 0.24	3.56	1.71		
	E5	W = 0.94, *p* = 0.06	BP = 0.14, *p* = 0.71	6.50	3.54		
	E6	W = 0.99, *p* = 0.95	**BP = 9.03, *p* = 0.01**	5.61	3.68	**53.18**	**b = 6.54, c = 6.54**
Heritiera fomes	E1	W = 0.99, *p* = 0.89	BP = 2.42, *p* = 0.12	2.79	0.85		
	E2	W = 0.98, *p* = 0.20	**BP = 24.46, *p* = 0.00**	8.85	4.64		
	E3	W = 0.98, *p* = 0.18	**BP = 15.80, *p* = 0.00**	3.91	1.70		
	E4	W = 0.97, *p* = 0.05	**BP = 9.67, *p* = 0.00**	3.02	1.18		
	E5	W = 0.99, = 0.43	**BP = 21.55, *p* = 0.00**	5.12	2.41		
	E6	W = 0.99, *p* = 0.84	**BP = 7.80, *p* = 0.02**	4.88	2.08	**63.82**	**b = 5.74, c = 5.74**
Lumnitzera racemosa	E1	W = 0.90, *p* = 0.15	BP = 0.59, *p* = 0.44	7.89	3.46		
	E2	W = 0.92, *p* = 0.28	BP = 0.33, *p* = 0.57	**40.57**	**27.69**		
	E3	W = 0.93, *p* = 0.32	BP = 0.14, *p* = 0.71	10.30	6.20		
	E4	W = 0.88, *p* = 0.07	BP = 0.02, *p* = 0.88	7.85	4.30		
	E5	W = 0.93, *p* = 0.33	BP = 0.02, *p* = 0.90	14.76	9.61		
	E6	W = 0.93, *p* = 0.34	BP = 3.25, *p* = 0.20	18.70	5.32	**180.93**	b = 2.13, c = 2.13
***Rhizophora* spp.**	**E1**	W = 0.96, *p* = 0.58	**BP = 6.73, *p* = 0.01**	24.47	6.13		
	E2	W = 0.89, *p* = 0.05	BP = 0.02, *p* = 0.90	**31.41**	14.99		
	E3	W = 0.93, *p* = 0.18	BP = 0.15, *p* = 0.69	16.55	6.53		
	E4	W = 0.94, *p* = 0.37	BP = 3.31, *p* = 0.07	17.01	5.92		
	E5	W = 0.96, *p* = 0.71	BP = 0.42, *p* = 0.52	18.35	8.00		
	E6	W = 0.96, *p* = 0.65	BP = 5.42, *p* = 0.07	**30.21**	13.08	**86.45**	**b = 3.65, c = 3.65**
Sonneratia apetala	**E1**	W = 0.96, *p* = 0.49	**BP = 5.48, *p* = 0.02**	10.40	2.63		
	E2	W = 0.95, *p* = 0.44	BP = 0.70, *p* = 0.40	22.94	12.36		
	E3	W = 0.98, *p* = 0.91	BP = 1.26, *p* = 0.26	6.60	2.80		
	E4	W = 0.97, *p* = 0.68	BP = 0.12, *p* = 0.73	4.91	1.81		
	E5	W = 0.97, *p* = 0.72	BP = 2.32, *p* = 0.13	10.07	4.79		
	E6	W = 0.99, *p* = 1.00	BP = 0.35, *p* = 0.84	9.09	3.91	21.62	b = 3.53, c = 3.53
***Xylocarpus* spp.**	E1	W = 0.98, *p* = 0.52	BP = 0.27, *p* = 0.60	8.02	2.40		
	E2	W = 0.96, *p* = 0.13	**BP = 4.95, *p* = 0.03**	**71.04**	17.49		
	E3	W = 0.95, *p* = 0.05	**BP = 8.68, *p* = 0.00**	9.68	4.17		
	E4	W = 0.98, *p* = 0.54	**BP = 5.79, *p* = 0.02**	7.02	2.77		
	E5	W = 0.96, *p* = 0.11	**BP = 12.43, *p* = 0.00**	14.85	6.58		
	E6	W = 0.99, *p* = 0.97	BP = 0.32, *p* = 0.85	9.09	2.95	**38.74**	b = 1.55, c = 1.55

N.B: Bold and light shaded grey models are not eligible due to results from one or more test.

Table B.3: Detailed validation results for all allometric equation.

Species	Model	RMSE (Ln Kg Tree^{-1})	MAE (Ln Kg Tree^{-1})
Aglaia cucullata	Species-specific	0.09	0.08
	Mahmood_2019_DHW	0.12	0.11
	Mahmood_2019_DH	0.09	0.08
	Mahmood_2019_D	0.12	0.11
	Chave_2014_DHW	0.36	0.33
	Chave_2005_DW	0.17	0.15
	Chave_2005_DHW	0.22	0.19
	Komiyama_2005_DW	0.58	0.57
***Avicennia* spp.**	Species-specific	0.16	0.13
	Mahmood_2019_D	0.22	0.17
	Mahmood_2019_DH	0.22	0.17
	Mahmood_2019_DHW	0.24	0.19
	Chave_2014_DHW	0.40	0.34
	Chave_2005_DW	0.26	0.19
	Chave_2005_DHW	0.31	0.26
	Komiyama_2005_DW	0.39	0.32
***Bruguiera* spp.**	Species-specific	0.19	0.18
	Mahmood_2019_DHW	0.26	0.21
	Mahmood_2019_DH	0.35	0.31
	Mahmood_2019_D	0.37	0.32
	Chave_2014_DHW	0.44	0.39
	Chave_2005_DW	0.24	0.20
	Chave_2005_DHW	0.33	0.28
	Komiyama_2005_DW	0.27	0.22
Excoecaria agallocha	Species-specific	0.14	0.12
	Mahmood_2019_DHW	0.18	0.14
	Mahmood_2019_DH	0.38	0.36
	Mahmood_2019_D	0.43	0.40
	Chave_2014_DHW	0.56	0.49
	Chave_2005_DW	0.22	0.17
	Chave_2005_DHW	0.41	0.34
	Komiyama_2005_DW	1.08	1.06
Heritiera fomes	Species-specific	0.14	0.12
	Mahmood_2019_DHW	0.16	0.12
	Mahmood_2019_DH	0.20	0.16
	Mahmood_2019_D	0.27	0.23
	Chave_2014_DHW	0.21	0.16
	Chave_2005_DW	0.17	0.13
	Chave_2005_DHW	0.21	0.16
	Komiyama_2005_DW	0.17	0.13
Lumnitzera racemosa	Species-specific	0.20	0.20
	Mahmood_2019_DHW	0.15	0.12
	Mahmood_2019_DH	0.16	0.13
	Mahmood_2019_D	0.14	0.11
	Chave_2014_DHW	0.44	0.41
	Chave_2005_DW	0.20	0.16
	Chave_2005_DHW	0.31	0.26
	Komiyama_2005_DW	0.13	0.10
***Rhizophora* spp.**	Species-specific	0.22	0.21
	Mahmood_2019_DHW	0.28	0.25
	Mahmood_2019_DH	0.22	0.18

	Mahmood_2019_D	0.23	0.19
	Chave_2014_DHW	0.23	0.19
	Chave_2005_DW	0.45	0.41
	Chave_2005_DHW	0.25	0.21
	Komiyama_2005_DW	0.49	0.44
Sonneratia apetala	Species-specific	0.24	0.21
	Mahmood_2019_DHW	0.23	0.18
	Mahmood_2019_DH	0.35	0.30
	Mahmood_2019_D	0.34	0.25
	Chave_2014_DHW	0.24	0.20
	Chave_2005_DW	0.33	0.26
	Chave_2005_DHW	0.21	0.17
	Komiyama_2005_DW	0.59	0.50
***Xylocarpus* spp.**	Species-specific	0.19	0.16
	Mahmood_2019_DHW	0.17	0.13
	Mahmood_2019_DH	0.19	0.15
	Mahmood_2019_D	0.22	0.18
	Chave_2014_DHW	0.46	0.41
	Chave_2005_DW	0.30	0.26
	Chave_2005_DHW	0.36	0.31
	Komiyama_2005_DW	0.36	0.29

Table B.4: Pair-wise comparison test for mean absolute error (MAE) between species-specific and other allometric equations.

Model comparison	**Mean difference MAE (Ln Kg tree^{-1})**	**Mean absolute difference MAE (Ln Kg tree^{-1})**	**Mean relative absolute difference MAE (%)**	**Paired t-test (t), *p*-value**
Species-specific – Mahmood_2019_DHW	-00.0004	0.034	21.85	t = -0.03, p = 0.98
Species-specific – Chave_2005_DW	-0.05	0.06	39.89	t= -2.46, p <0.05
Species-specific – Mahmood_2019_DH	-0.04	0.07	44.61	t = -1.40, p =0.20
Species-specific – Mahmood_2019_D	-0.06	0.09	54.04	t = -1.71, p = 0.13
Species-specific – Chave_2014_DHW	-0.08	0.10	61.07	t= -3.03, p <0.05
Species-specific - Chave_2005_DHW	-0.17	0.18	110.93	t= -3.62, p <0.05
Species-specific – Komiyama_2005_DW	-0.24	0.27	167.43	t = -2.37, p <0.05

N.B: (-) negative signs indicates higher MAE than Species-specific model

Table B.5: Summary of individual tree above-ground biomass differences between different allometric equations. Differences are shown for all sizes (All) and by diameter at breast height (DBH) classes. The negative difference indicates higher biomass than the species-specific equations. In all cases, the denominators for calculating relative differences are the species-specific biomass estimates. The bold percentages show mean relative difference of biomass greater than 50%.

Species	Diameter range (cm)	Species-specific-Chave_2005_DW		Species-specific-Komiyama_2005_DW		Species-specific-Mahmood_2019_D		Species-specific-Mahmood_2019_DH		Species-specific-Mahmood_2019_DHW		Species-specific-Chave_2014_DHW		Species-specific-Chave_2005_DHW	
		Mean Difference (Kg)	Mean Relative Difference (%)	Mean Difference (Kg)	Mean Relative Difference (%)	Mean Difference (Kg)	Mean Relative Difference (%)	Mean Difference (Kg)	Mean Relative Difference (%)	Mean Difference (Kg)	Mean Relative Difference (%)	Mean Difference (Kg)	Mean Relative Difference (%)	Mean Difference (Kg)	Mean Relative Difference (%)
Aegialitis rotundifolia	2.5 - 15	-21.22	**-874.23**	-21.35	**-879.65**	-11.35	**-467.86**	-14.86	**-612.12**	-12.09	**-498.37**	-7.27	**-299.54**	-5.95	**-245.28**
Aegiceras corniculatum	2.5 - 15	-11.40	**-137.20**	-12.69	**-152.64**	-3.92	-47.16	-3.78	-45.41	-6.16	**-74.14**	-5.36	**-64.44**	-3.62	**-43.51**
Aglaia cucullata	2.5 - 15	0.85	23.25	0.18	5.04	0.16	4.27	0.08	2.14	0.70	19.21	1.39	37.98	1.77	48.39
Avicennia alba	2.5 - 15	-78.18	**-104.71**	-48.61	**-65.10**	0.15	0.20	-2.21	-2.96	-4.37	-5.86	5.38	7.20	12.51	16.76
Avicennia marina	2.5 - 15	-21.09	-45.38	-10.31	-22.18	-12.70	-27.32	-0.76	-1.63	-2.57	-5.53	-7.67	-16.50	-2.20	-4.74
	All	-1320.16	**-465.52**	-224.80	**-79.27**	-70.74	-24.94	-50.93	-17.96	-39.53	-13.94	-37.86	-13.35	-22.04	-7.77
Avicennia officinalis	2.5 - 15	-17.67	-49.92	-10.90	-30.80	-0.38	-1.06	-0.05	-0.15	2.35	6.64	6.07	17.16	9.34	26.40
	15.1 - 30	-310.15	**-168.26**	-100.36	**-54.45**	-34.29	-18.61	-18.11	-9.83	-13.14	-7.13	-11.15	-6.05	3.85	2.09
	30.1 - 45	-2732.23	**-419.62**	-529.94	**-81.39**	-168.14	-25.82	-123.55	-18.98	-95.24	-14.63	-91.94	-14.12	-56.66	-8.70
	> 45.1	-11010.72	**-760.81**	-1472.09	**-101.72**	-458.73	-31.70	-366.50	-25.32	-301.18	-20.81	-312.66	-21.60	-263.86	-18.23
Bruguiera gymnorrhiza	2.5 - 15	2.84	12.18	0.56	2.42	7.73	33.15	6.47	27.78	7.38	31.67	10.91	46.84	12.65	**54.29**
Bruguiera sexangula	All	-144.98	**-91.39**	-35.72	-22.52	9.72	6.13	36.81	23.21	13.44	8.48	-12.88	-8.12	0.28	0.18
	2.5 - 15	-19.09	-38.09	-6.72	-13.41	5.54	11.06	12.55	25.04	6.37	12.71	0.81	1.61	5.56	11.09
	15.1 - 30	-197.99	**-96.90**	-47.93	-23.46	11.48	5.62	47.03	23.02	16.42	8.04	-18.64	-9.12	-1.94	-0.95
Cerbera manghas	All	-6.47	-29.27	-2.56	-11.57	-10.52	-47.60	-10.80	-48.82	1.24	5.62	6.80	30.76	8.73	39.47
	2.5 - 15	1.25	10.09	0.24	1.93	-4.09	-32.99	-4.42	-35.64	1.67	13.44	4.60	37.07	5.73	46.21
	15.1 - 30	-37.37	**-61.33**	-13.74	-22.55	-36.25	**-59.49**	-36.29	**-59.56**	-0.46	-0.75	15.62	25.63	20.71	33.98
Ceriops decandra	2.5 - 15	-1.29	**-71.65**	-2.09	**-115.82**	-0.74	-41.20	-0.98	**-54.37**	-1.05	**-58.28**	-0.41	-22.61	-0.03	-1.66
Cynometra ramiflora	2.5 - 15	-1.24	-24.78	-2.28	-45.40	-0.22	-4.38	-0.58	-11.47	-0.33	-6.55	0.78	15.60	1.44	28.78

Excoecaria agallocha	All	-9.07	-54.75	-4.84	-29.19	-7.01	-42.32	-6.25	-37.70	-0.77	-4.65	2.30	13.89	4.01	24.17
	2.5 - 15	-2.76	-23.52	-2.48	-21.15	-4.01	-34.24	-3.62	-30.89	-0.08	-0.69	2.19	18.67	3.46	29.49
	15.1 - 30	-95.27	**-110.96**	-37.79	-44.01	-49.50	**-57.65**	-43.48	**-50.65**	-10.24	-11.93	4.39	5.11	12.34	14.37
	30.1 - 45	-864.88	**-303.91**	-225.91	**-79.38**	-222.07	**-78.03**	-187.75	**-65.97**	-87.04	-30.58	-50.51	-17.75	-27.94	-9.82
Excoecaria indica	2.5 - 15	1.20	11.52	-0.22	-2.15	-2.75	-26.29	-2.40	-23.00	0.94	8.98	3.17	30.33	4.27	40.87
Heritiera fomes	All	-69.83	**-117.23**	-21.46	-36.02	6.28	10.54	11.45	19.22	4.14	6.95	-0.27	-0.46	4.62	7.76
	2.5 - 15	-7.20	-43.61	-6.21	-37.64	1.17	7.09	2.18	13.21	0.04	0.26	-0.00	-0.03	1.93	11.70
	15.1 - 30	-255.85	**-121.43**	-75.63	-35.90	20.90	9.92	42.85	20.34	15.02	7.13	-6.83	-3.24	9.37	4.45
	30.1 - 45	-2064.05	**-249.34**	-275.88	-33.33	183.38	22.15	205.81	24.86	167.98	20.29	140.68	16.99	174.62	21.09
Hibiscus tiliaceus	2.5 - 15	-0.43	-13.27	-1.47	-45.33	-0.45	-13.97	-0.49	-15.29	-0.53	-16.39	0.17	5.16	0.69	21.21
Intsia bijuga	2.5 - 15	-1.13	-27.44	-2.46	**-59.73**	-0.89	-21.65	-1.01	-24.55	-0.99	-24.10	-0.03	-0.84	0.64	15.48
Kandelia candel	All	-75.41	**-226.29**	-49.03	**-147.15**	-21.15	**-63.46**	-27.99	**-84.00**	-18.74	**-56.23**	-5.87	-17.60	-1.50	-4.50
	2.5 - 15	-13.14	-77.15	-13.92	**-81.75**	-11.28	**-66.21**	-9.51	**-55.86**	-7.72	**-45.36**	-4.97	-29.19	-2.16	-12.69
	15.1 - 30	-199.95	**-303.36**	-119.26	**-180.94**	-40.89	**-62.04**	-64.95	**-98.54**	-40.76	**-61.84**	-7.65	-11.61	-0.17	-0.26
Lumnitzera racemosa	2.5 - 15	-4.97	**-61.62**	-6.83	**-84.78**	-0.63	-7.83	-0.83	-10.32	-2.27	-28.18	-1.19	-14.82	0.12	1.50
Millettia pinnata	2.5 - 15	-0.74	-9.76	-2.43	-32.04	-1.70	-22.37	-1.51	-19.89	-0.67	-8.85	0.80	10.59	1.84	24.25
Rhizophora apiculata	2.5 - 15	-58.83	**-79.90**	-42.78	**-58.10**	10.08	13.69	18.03	24.49	-5.79	-7.86	-17.83	-24.22	-8.97	-12.19
Rhizophora mucronata	All	-212.15	**-178.00**	-110.80	**-92.97**	4.05	3.40	10.78	9.05	-23.69	-19.88	-34.55	-28.99	-22.13	-18.56
	2.5 - 15	-89.31	**-139.08**	-65.59	**-102.14**	2.29	3.57	2.07	3.22	-15.22	-23.70	-14.76	-22.98	-6.96	-10.84
	15.1 - 30	-335.00	**-192.36**	-156.01	**-89.58**	5.81	3.33	19.50	11.20	-32.16	-18.47	-54.35	-31.21	-37.29	-21.41
Sonneratia apetala	All	-1858.13	**-366.88**	-248.60	-49.09	-171.56	-33.88	-55.58	-10.97	-41.08	-8.11	-108.42	-21.41	-81.82	-16.16
	2.5 - 15	-32.52	**-101.39**	-21.72	**-67.73**	-10.60	-33.06	-14.62	-45.57	-4.22	-13.15	0.24	0.75	3.68	11.47
	15.1 - 30	-266.56	**-118.05**	-49.31	-21.83	-51.65	-22.87	1.26	0.56	6.43	2.85	-19.21	-8.51	-1.62	-0.72
	30.1 - 45	-2425.31	**-333.93**	-371.56	**-51.16**	-243.66	-33.55	-72.99	-10.05	-68.84	-9.48	-176.00	-24.23	-136.99	-18.86
	> 45.1	-8305.17	**-571.50**	-932.80	**-64.19**	-602.35	-41.45	-277.95	-19.13	-197.52	-13.59	-389.51	-26.80	-340.32	-23.42
Xylocarpus granatum	All	-675.34	**-339.03**	-187.10	**-93.92**	1.52	0.76	-33.12	-16.62	-8.94	-4.49	37.90	19.03	49.72	24.96
	2.5 - 15	-4.58	-41.25	-6.23	**-56.20**	0.12	1.12	-1.12	-10.05	-0.62	-5.56	2.17	19.58	3.45	31.11
	15.1 - 30	-411.34	**-226.70**	-157.56	**-86.83**	-5.24	-2.89	-28.02	-15.44	-13.94	-7.68	22.11	12.19	35.50	19.57
	30.1 - 45	-2808.89	**-446.79**	-637.44	**-101.39**	24.62	3.92	-112.42	-17.88	-10.58	-1.68	156.71	24.93	184.88	29.41
Xylocarpus mekongensis	All	-486.22	**-326.97**	-124.10	**-83.45**	-22.86	-15.37	-24.57	-16.52	-18.80	-12.64	-6.27	-4.22	4.00	2.69
	2.5 - 15	-16.39	**-72.14**	-12.97	**-57.08**	-4.78	-21.02	-2.71	-11.93	-3.91	-17.23	-3.55	-15.62	-0.62	-2.74
	15.1 - 30	-382.37	**-210.66**	-135.76	**-74.80**	-25.55	-14.08	-28.13	-15.50	-19.85	-10.93	-2.78	-1.53	11.58	6.38
	30.1 - 45	-2669.08	**-430.48**	-565.32	**-91.18**	-104.26	-16.82	-111.10	-17.92	-83.47	-13.46	-36.65	-5.91	-3.54	-0.57
	>45.1	-9261.24	**-759.12**	-1615.71	**-132.43**	40.68	3.33	-235.47	-19.30	-110.35	-9.04	201.17	16.49	243.67	19.97

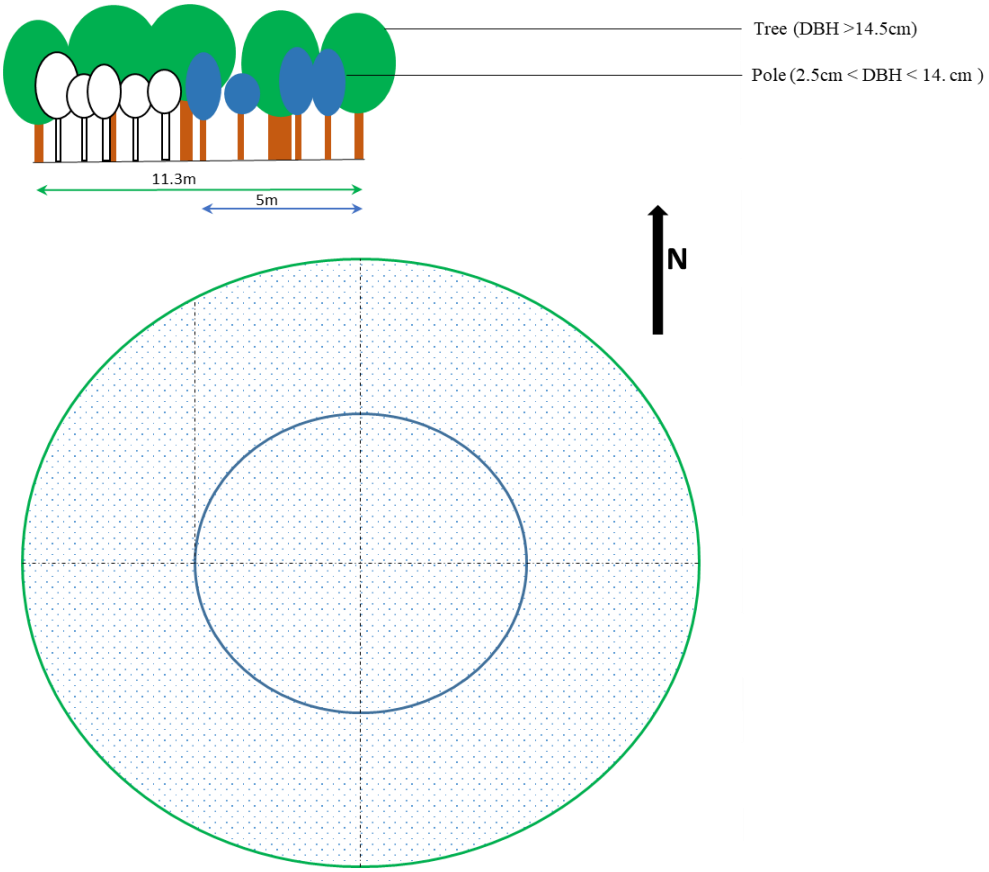

Figure B.1: The nested circular plot and different measured components of vegetation in each segment.

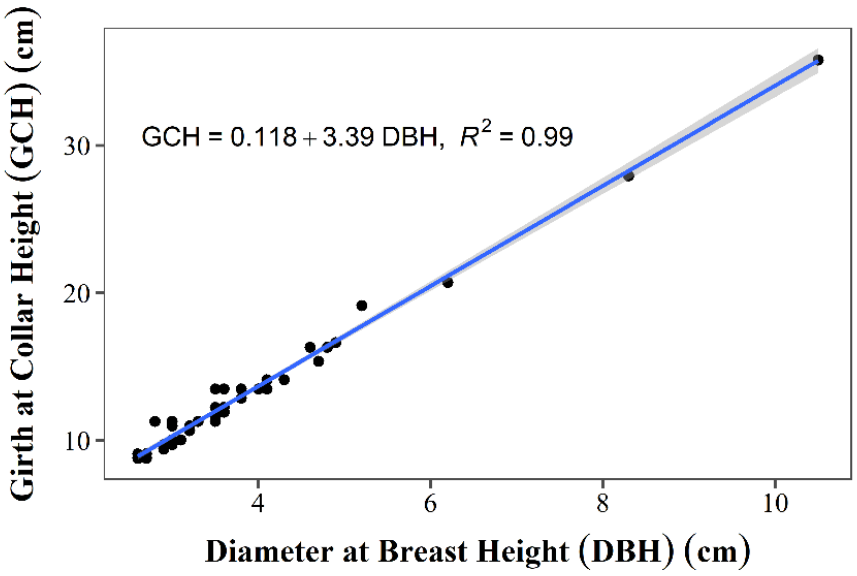

Figure B.2: Relationship between DBH and GCH of *Ceriops decandra*.

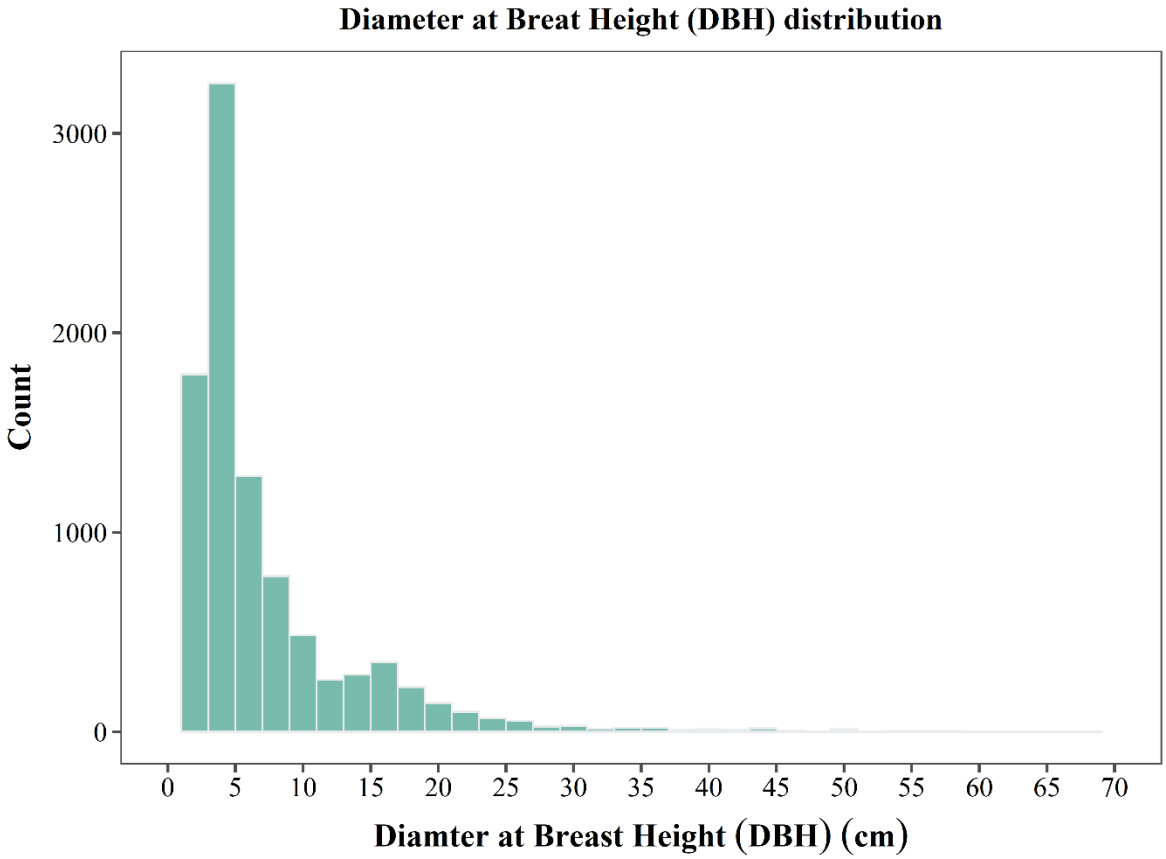

Figure B.3: Histogram of DBH of all trees from tree inventory in the Sundarbans.

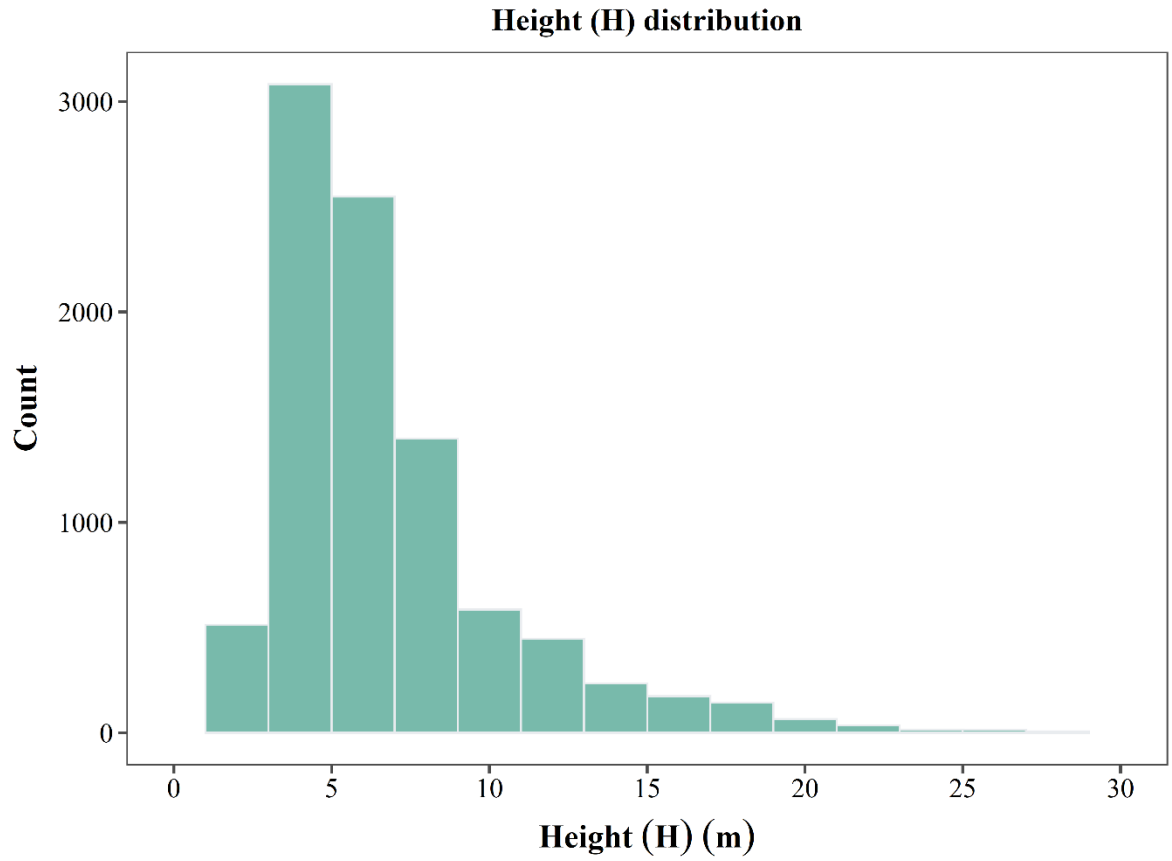

Figure B.4: Histogram of H of all trees from tree inventory in the Sundarbans.

Appendix C

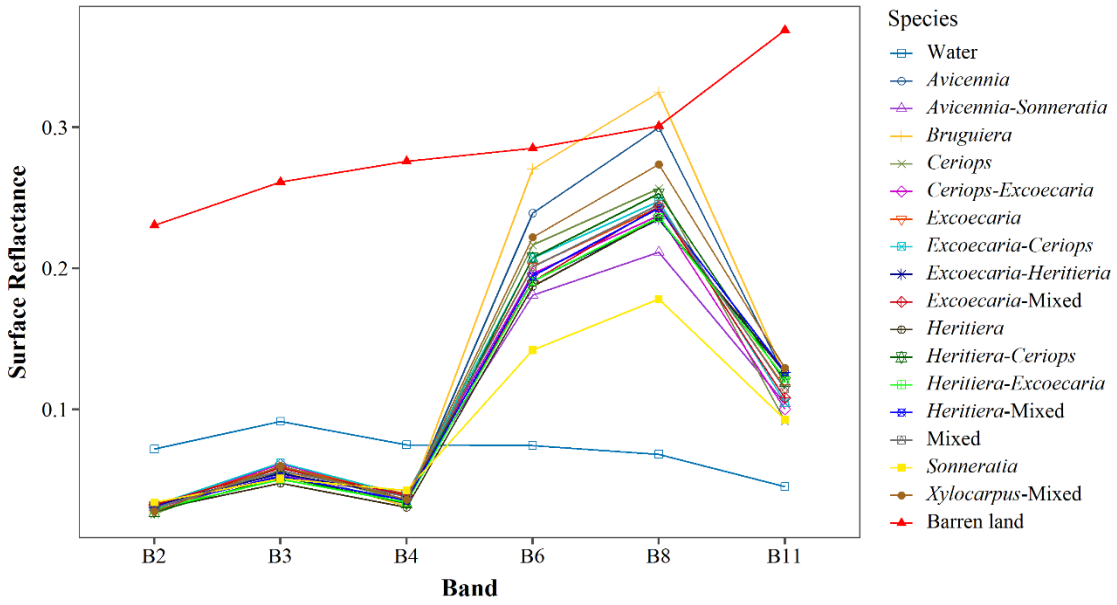

Figure C.1: Surface reflectance of different bands of Sentinel-2 for different forest-type.

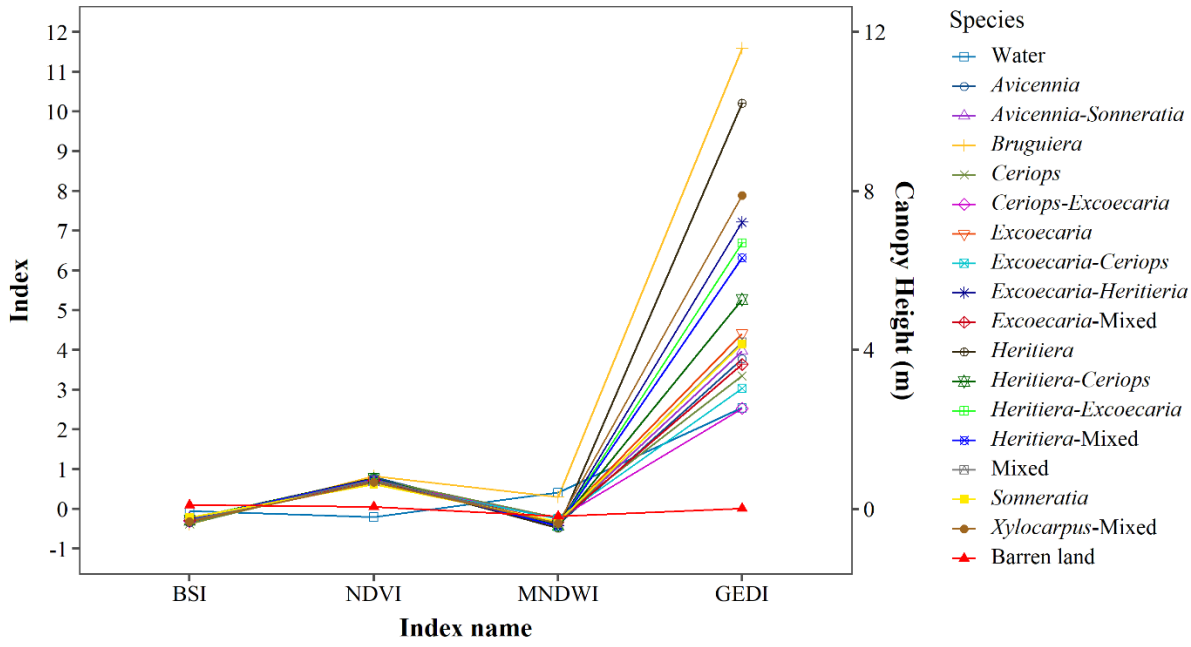

Figure C.2: Spectral indices for Sentinel-2 bands and GEDI forest height map for different forest-type.

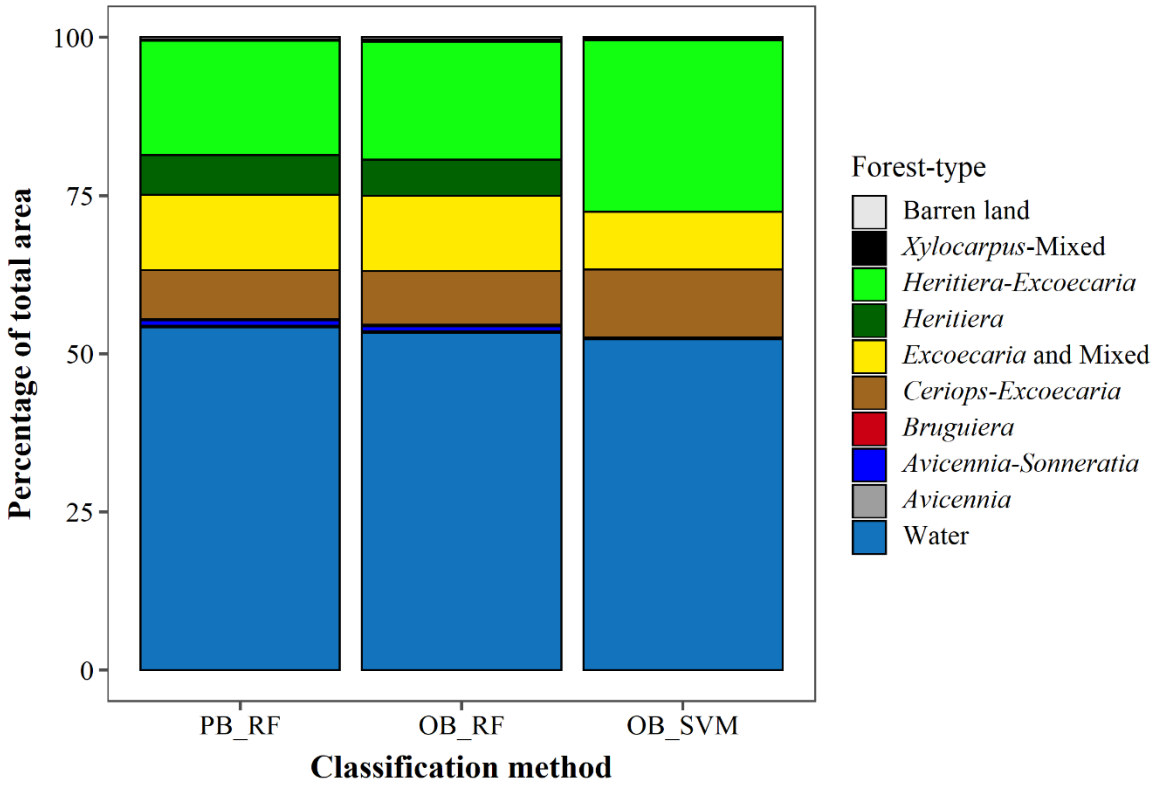

Figure C.3: Spectral indices for Sentinel-2 bands and GEDI forest height map for different forest-type. Here PB_RF: Pixel-based Random Forest, OB_RF: Object-based Random Forest and OB_SVM: Object-based Support Vector Machine classification.

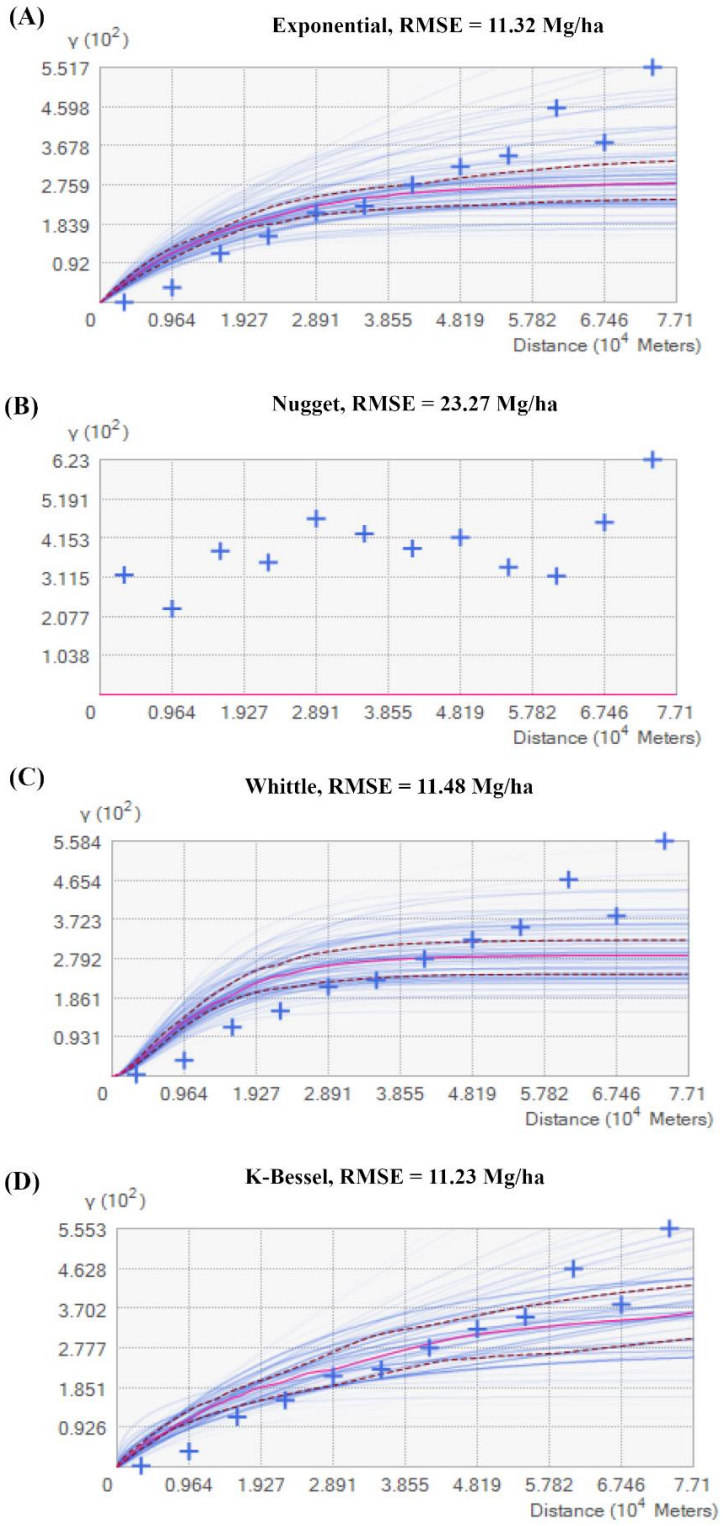

Figure C.4: Spectrum of semivariograms for different models A) Exponential, B) Nugget, C) Whittle and D) K-Bessel for predicting SOC in the Sundarbans using only forest-type. The RMSE of each model is presented on the top of each figure. The solid red line indicates median and red dashed lines indicate the 25th and 75th percentile of the distribution. The cross symbols indicate the average value of predictions. The darkness of each blue line is proportionate to its corresponding weight, where thinner lines indicate lower weights for predictions.

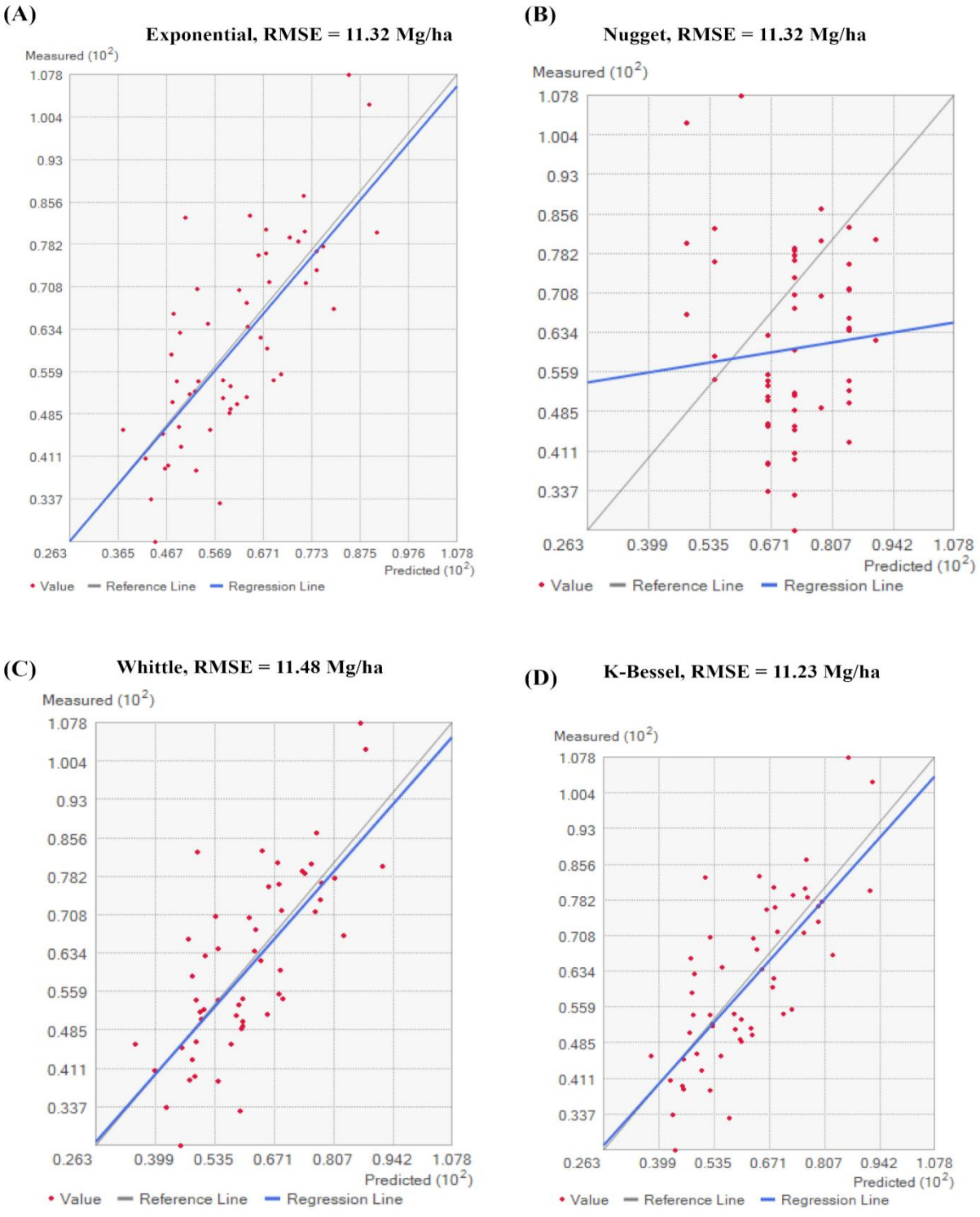

Figure C.5: Scatterplot of predicted values versus true values for all models A) Exponential, B) Nugget, C) Whittle and D) K-Bessel for predicting SOC in the Sundarbans using only forest-type. Red dots indicate the plot level SOC measurement, the grey line indicates 1:1 line, where the predicted values are equal to the true values and the blue line indicates the regression line.

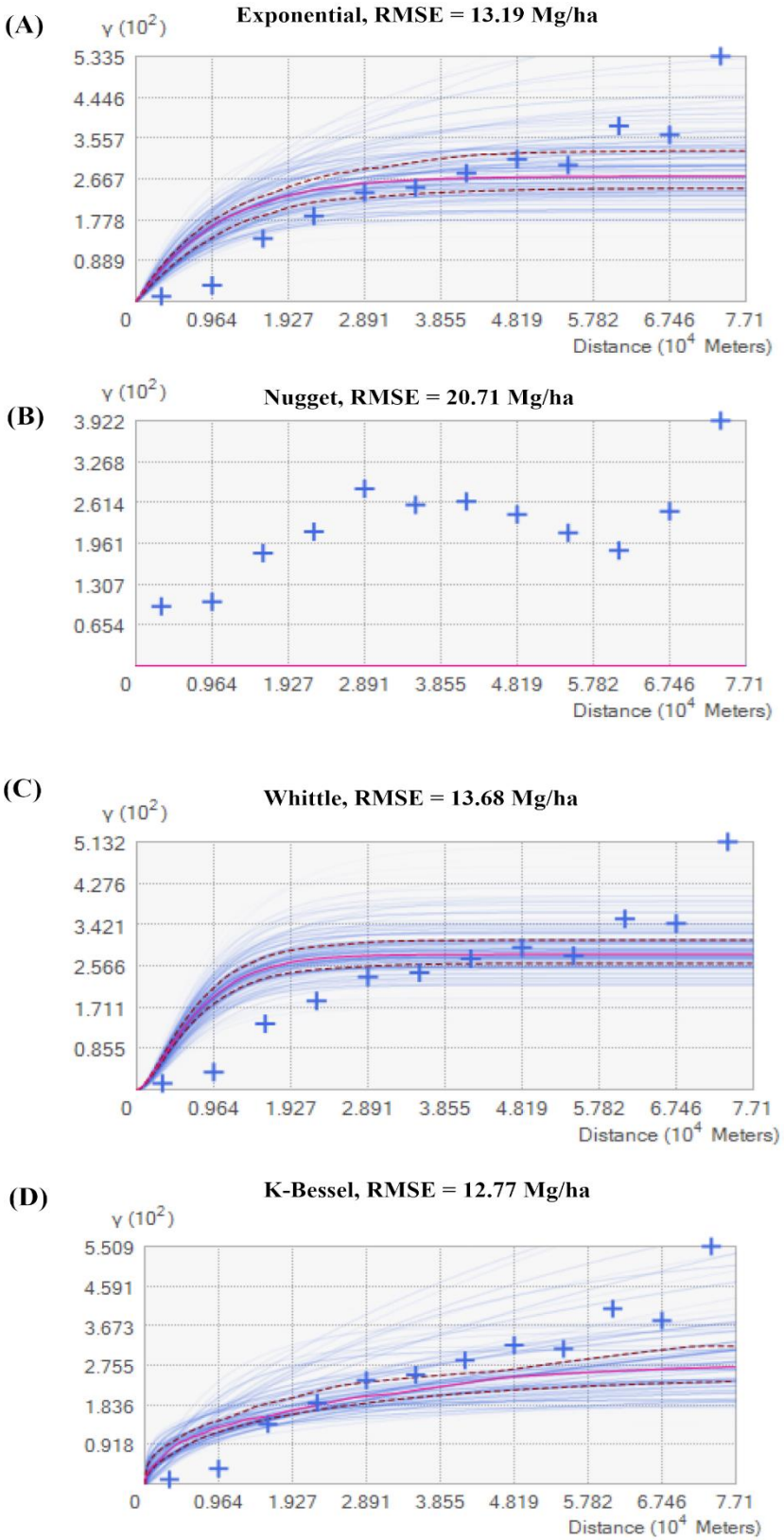

Figure C.6: Spectrum of semivariograms for different models A) Exponential, B) Nugget, C) Whittle and D) K-Bessel for predicting SOC in the Sundarbans using forest-type and DEM. The description of all components is provided in the Figure C.4.

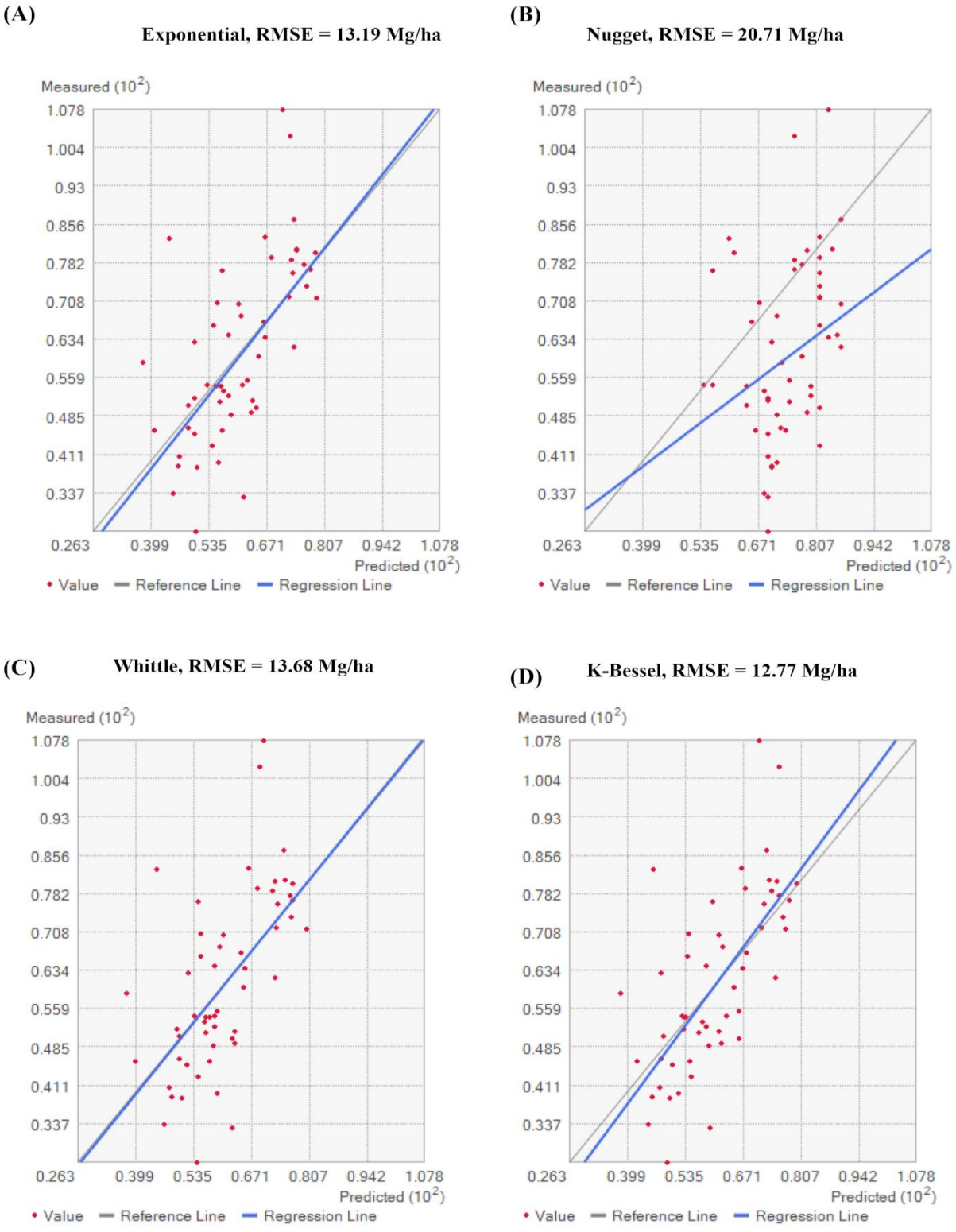

Figure C.7: Scatterplot of predicted values versus true values for all models A) Exponential, B) Nugget, C) Whittle and D) K-Bessel for predicting SOC in the Sundarbans using forest-type and DEM. Detailed figure description is provided in the Figure C.5.

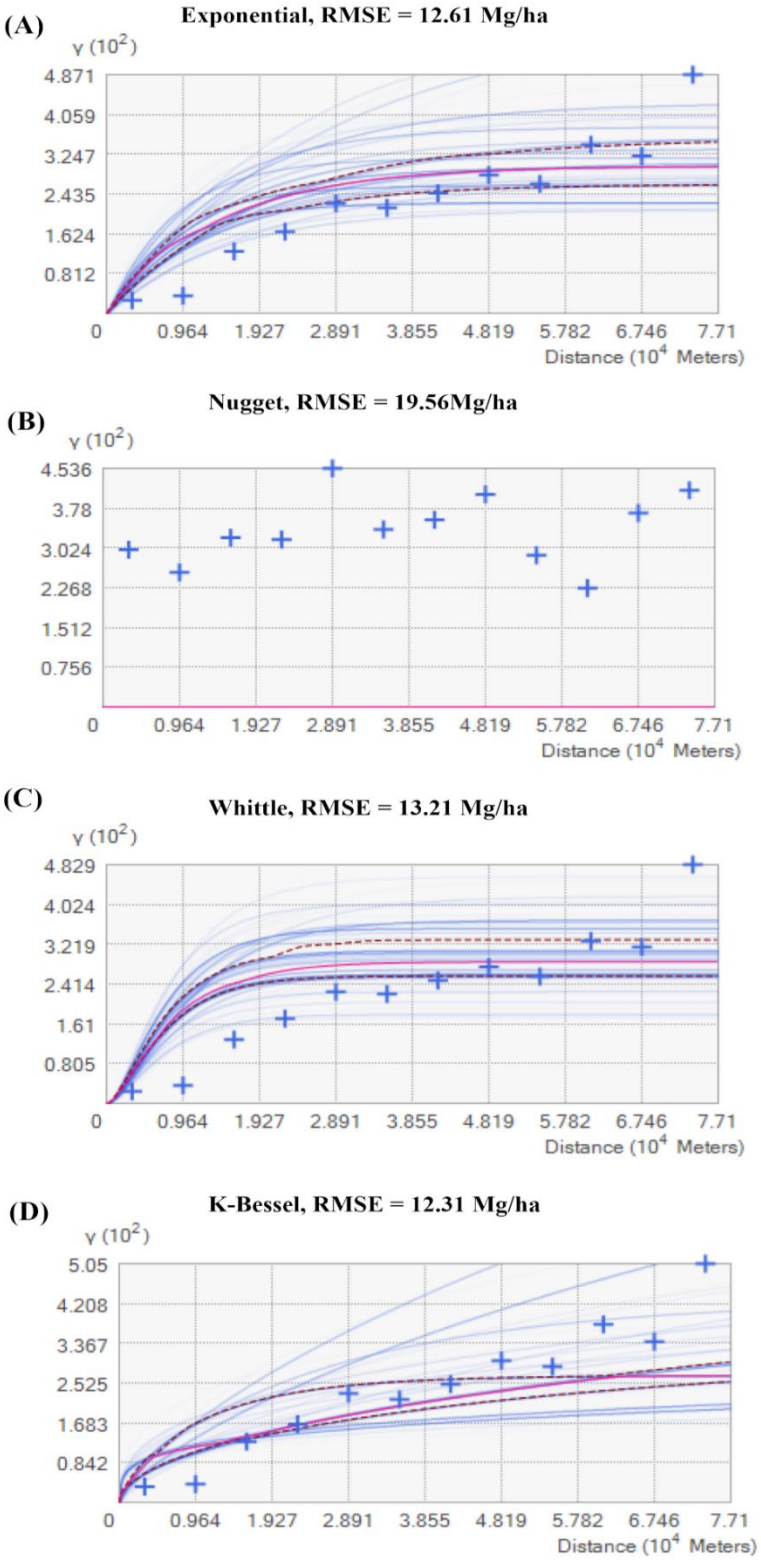

Figure C.8: Spectrum of semivariograms for different models A) Exponential, B) Nugget, C) Whittle and D) K-Bessel for predicting SOC in the Sundarbans using forest-type, DEM, slope and aspect. The description of all components is provided in the Figure C.4.

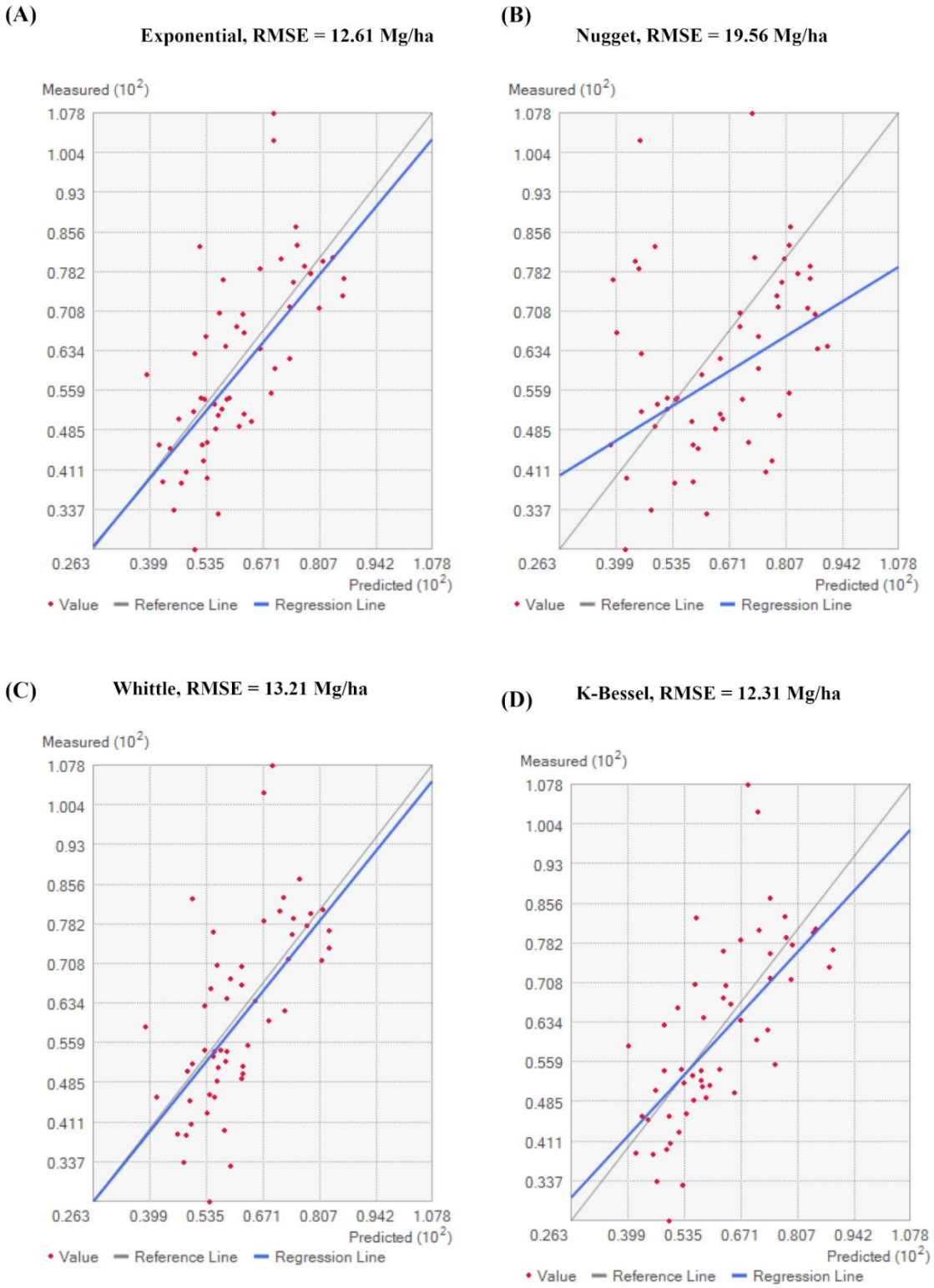

Figure C.9: Scatterplot of predicted values versus true values for all models A) Exponential, B) Nugget, C) Whittle and D) K-Bessel for predicting SOC in the Sundarbans using forest-type, DEM, slope and aspect. Detailed figure description is provided in the Figure C.5.

Table C.1: The average length, diameter, green and dry weight of pneumatophores of different species in the Sundarbans.

Species	**Average length (cm)**	**Average diameter (cm)**	**Average green weight (gm)**	**Average dry weight (gm)**	**Number of samples (n)**
Heritiera fomes	17.87 ± 5.5	3.11 ± 0.6	78.73 ± 49.8	34.59 ± 24.6	41
Xylocarpus moluccensis	15.38 ± 5.0	3.00 ± 0.6	65.40 ± 35.43	30.96 ± 19.5	23
***Bruguiera* spp.**	13.1 ± 2.3	6.22 ± 0.4	168.53 ± 2.9	49.06 ± 1.2	9
Sonneratia apetala	26.65 ± 14.0	2.97 ± 0.9	81.69 ± 60.9	32.64 ± 25.3	15
***Avicennia* spp.**	10.87 ± 2.3	1.77 ± 0.4	21.17 ± 2.9	6.59 ± 1.2	9

Table C.2 One-way ANOVA results for TEC (Mg ha^{-1}) stocks among different components.

Source	DF	SS	MSS	F	p
Carbon components	5	1660.8	332.2	1470	<0.0001
Residuals	756	170.8	0.2		

Table C.3 Two-way ANOVA results for TEC (Mg ha^{-1}) stocks among forest type and salinity zones in the Sundarbans.

Source	DF	SS	MSS	F	p
Salinity zones	2	5.3	2.65	55.6	<0.0001
Forest-type	7	2.2	0.31	6.6	<0.0001
Salinity Zone * Forest-type	7	0.2	0.04	0.7	> 0.05
Residuals	123	5.9	0.05		

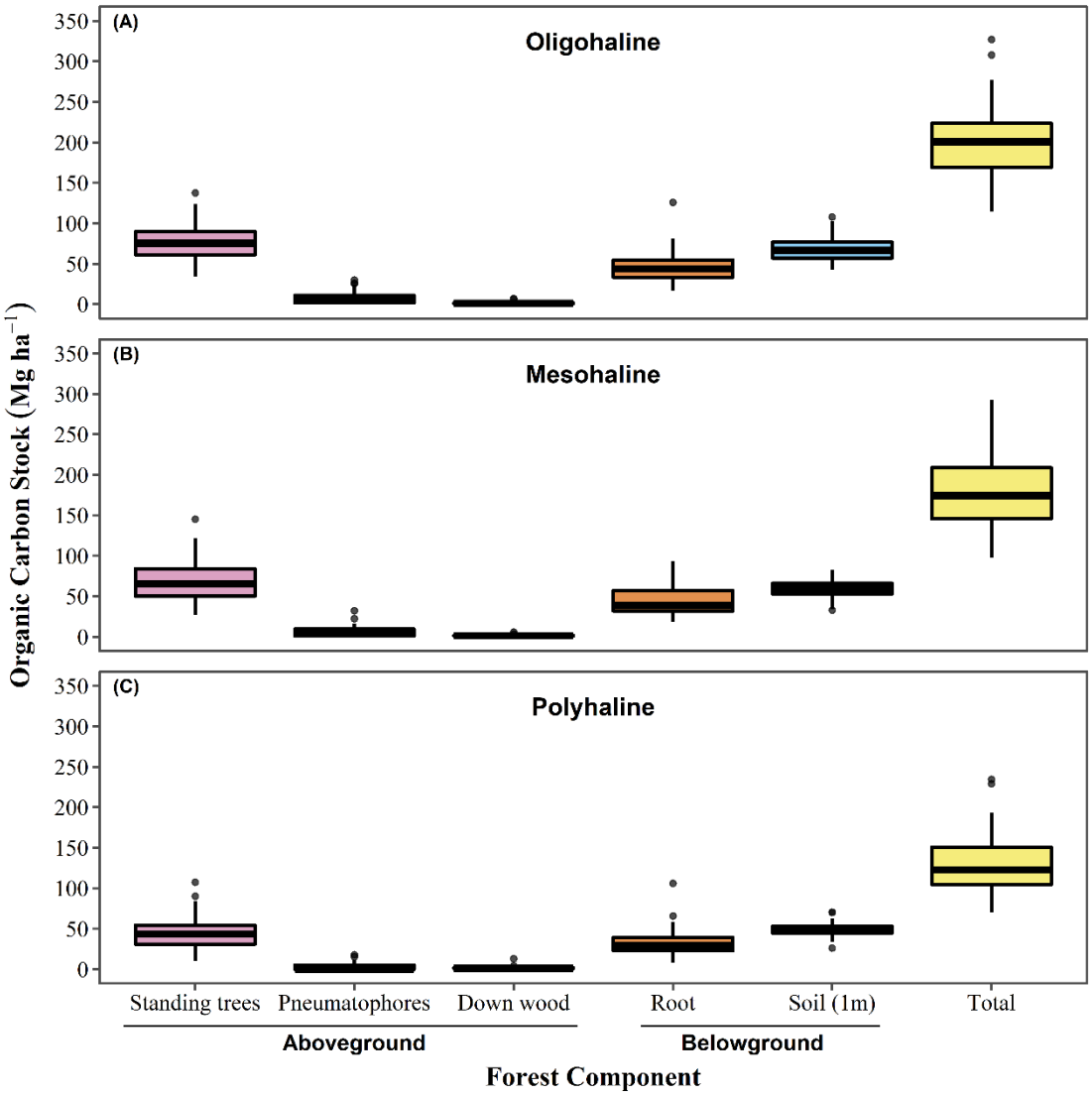

Figure C.10: The total ecosystem carbon stocks (TEC) in the Sundarbans in three salinity zones.

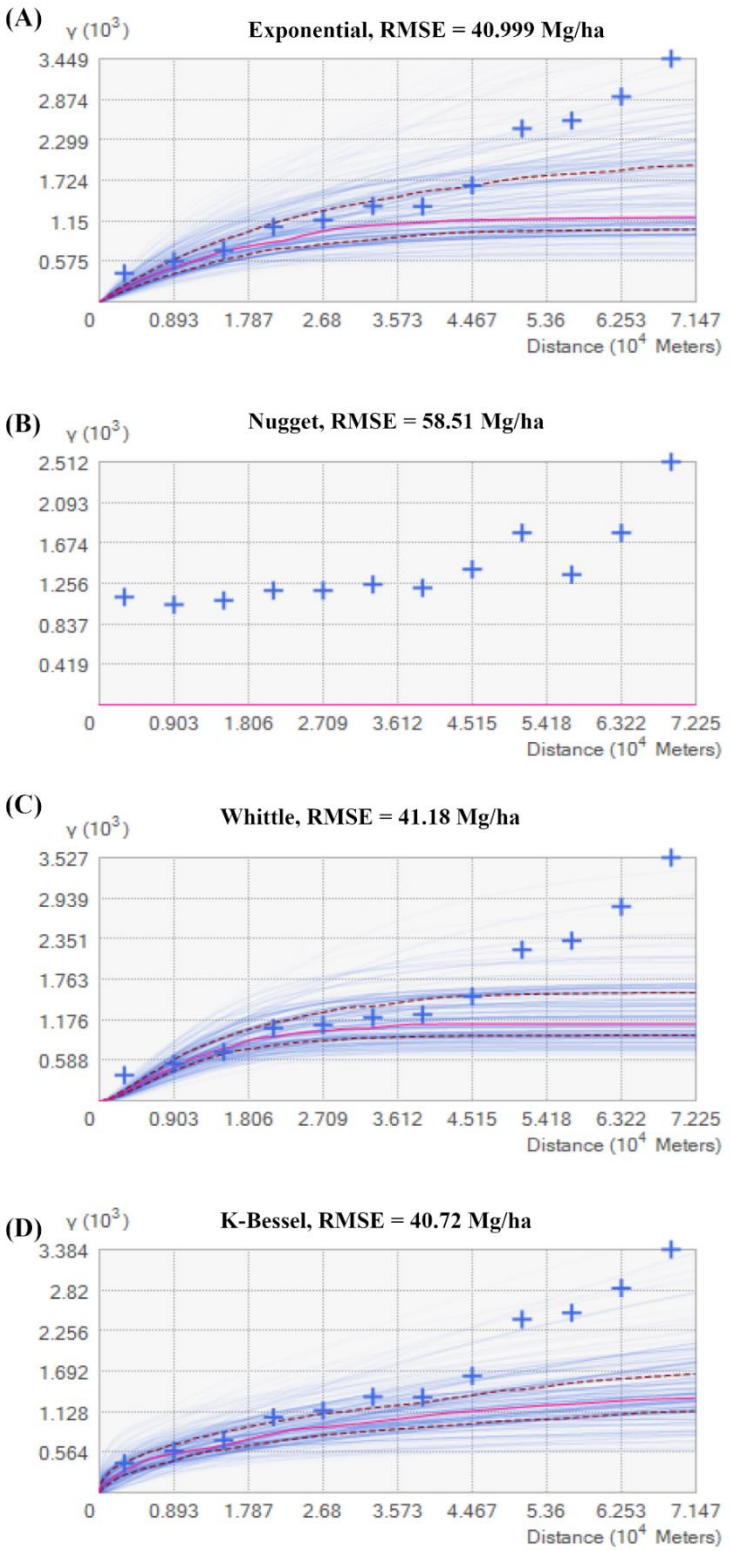

Figure C.11: Spectrum of semivariograms for different models A) Exponential, B) Nugget, C) Whittle and D) K-Bessel for predicting AGC in the Sundarbans using forest-type. The description of all components is provided in the Figure C.4.

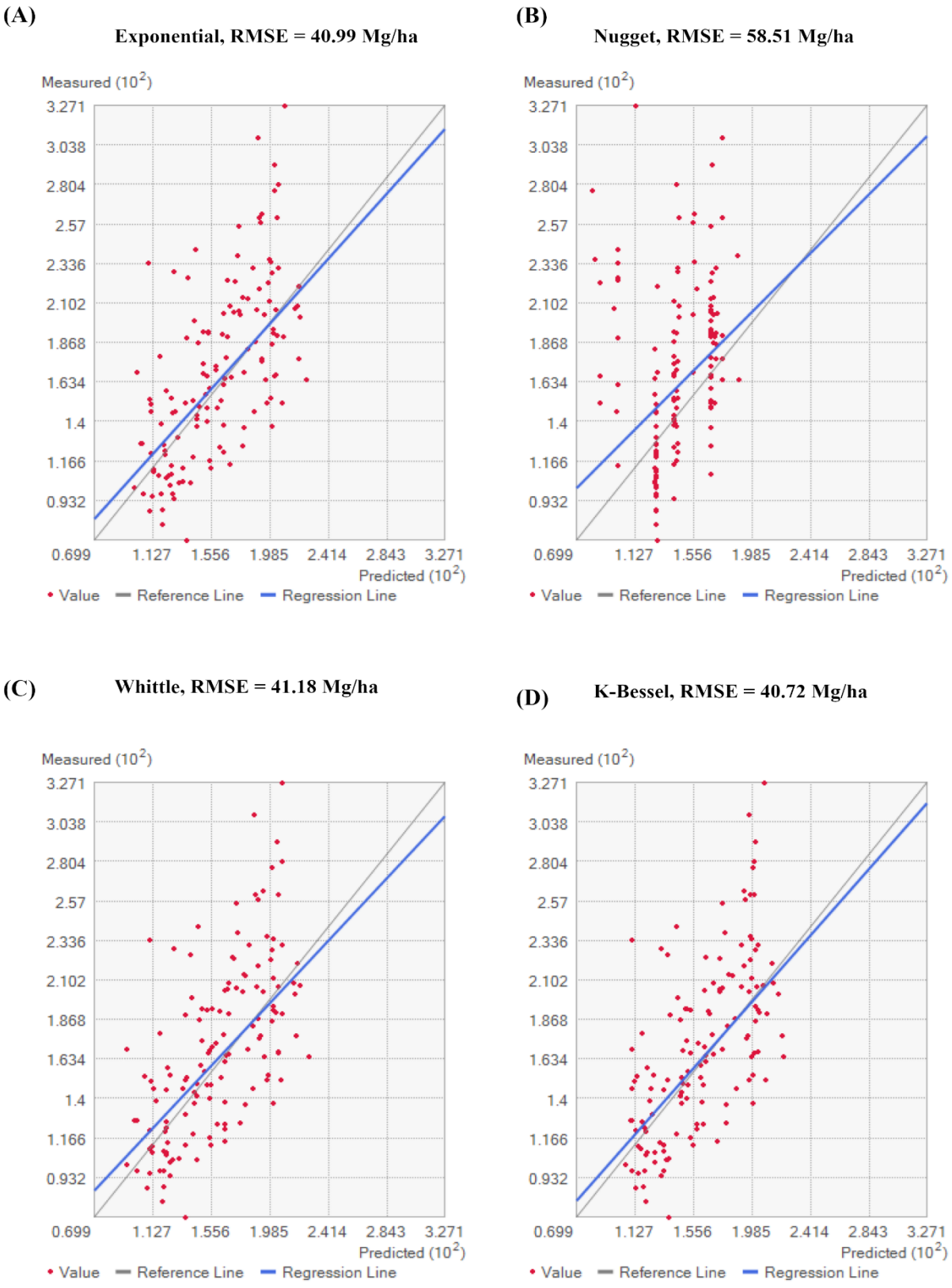

Figure C.12: Scatterplot of predicted values versus true values for all models A) Exponential, B) Nugget, C) Whittle and D) K-Bessel for predicting AGC in the Sundarbans using forest-type. Detailed figure description is provided in the Figure C.5.

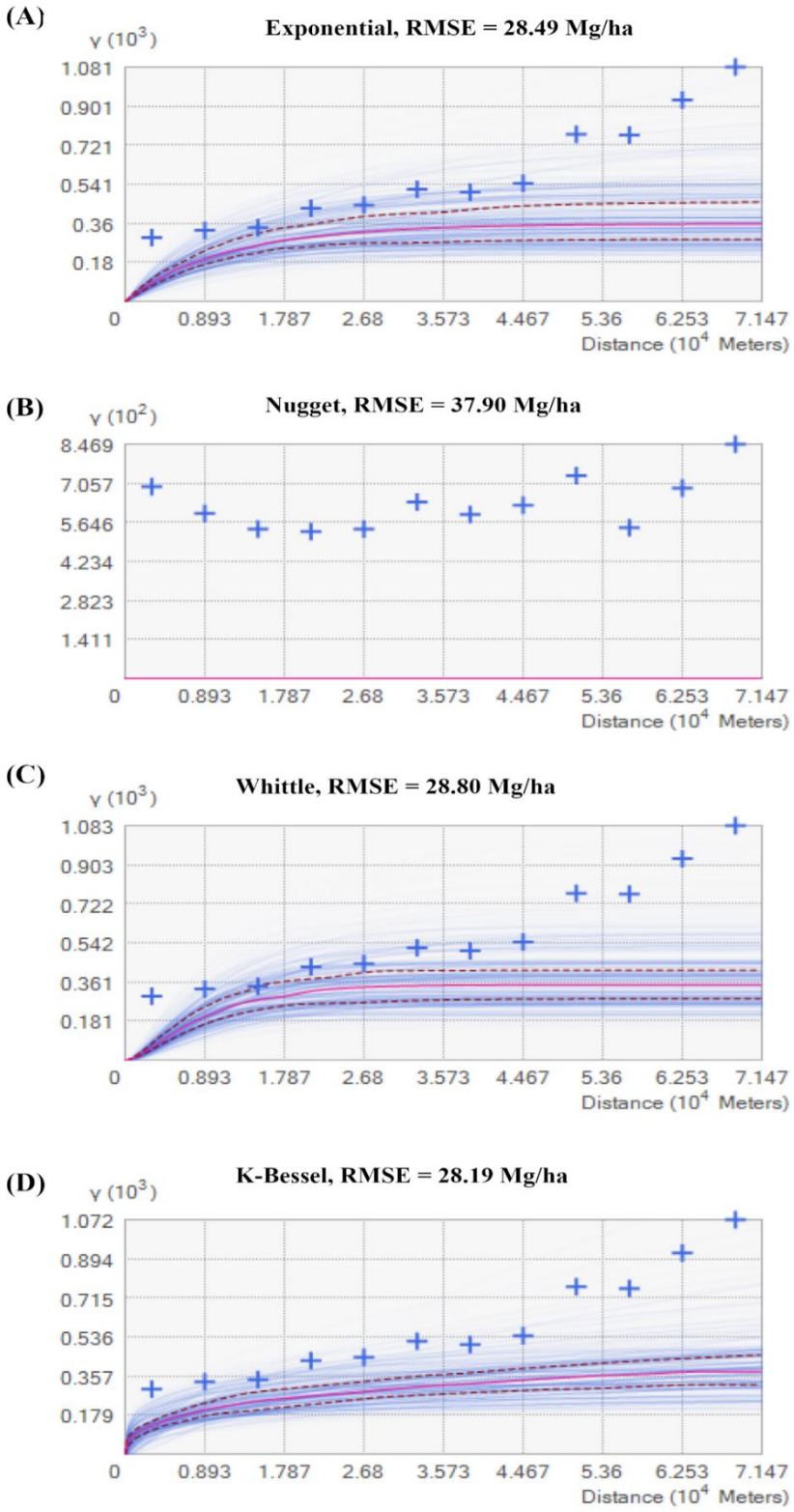

Figure C.13: Spectrum of semivariograms for different models A) Exponential, B) Nugget, C) Whittle and D) K-Bessel for predicting TEC in the Sundarbans using forest-type. The description of all components is provided in the Figure C.4.

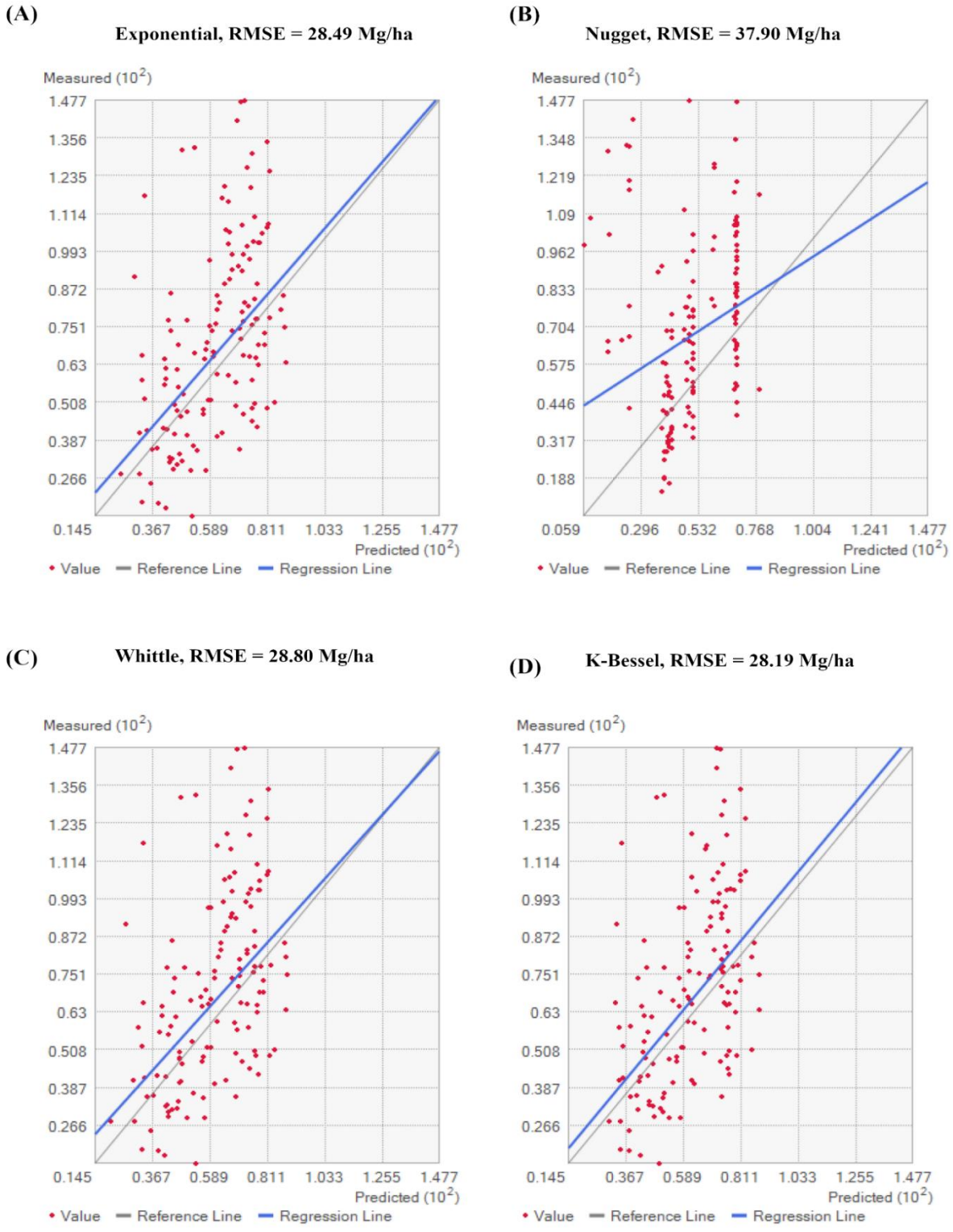

Figure C.14: Scatterplot of predicted values versus true values for all models A) Exponential, B) Nugget, C) Whittle and D) K-Bessel for predicting TEC in the Sundarbans using forest-type. Detailed figure description is provided in the Figure C.5.